methoxy + methane and methoxy + ethane. The measured (IUPAC, 1997) or estimated (NIST, 1994) bond dissociation energies (BDE's) for the C-H bond being attacked are also shown in the Table.

Figure 7 shows plots of the activation energies for the internal or bimolecular alkoxy H-atom abstraction reactions against the relevant bond dissociation energy. [Data for the methoxy + isobutane reaction are inconsistent (NIST 1998), so they are not included.] It can be seen that if the methoxy + acetaldehyde data are not included, then a reasonably good straight line relationship is obtained. The limited data for the isomerization reactions are consistent with the relationship for the bimolecular methoxy reactions, with an offset of 1.6 kcal/mole. Although this offset is probably not outside the uncertainties of the BDE or activation energy determinations, it could also be rationalized as ring strain in the 6-member ring transition state for the isomerization reaction.

The solid line shown on Figure 7 is the least squares line through the data for the methoxy abstraction reactions, with the data for acetaldehyde not being used when determining the fit. The measurement for acetaldehyde is excluded because abstractions from (CO)-H bonds apparently do not have the same correlation with the bond energies as abstractions from hydrocarbon C-H bonds.

The dotted line on Figure 7 shows the line for the methoxy reaction offset by 1.6 kcal/mole to agree with the data for the isomerizations of the butoxy, pentoxy, and hexoxy radicals. Therefore, this can be used as a basis for estimating activation energies for alkoxy radical isomerizations in general, or at least those involving abstractions from alkyl C-H bonds.

The rate constants for any isomerization reaction can be estimated using a generalization of the structure-reactivity approach derived by Atkinson (Atkinson, 1987, Kwok and Atkinson, 1995, Atkinson, 1997a) for estimating OH radical reactions. In this approach, reaction by H-abstraction at each type of group, whether -CH3, -CH2-, -CH<, or -CHO is given by a group rate constant for that group, multiplied by an appropriate correction factor for each substituent other than methyl groups (whose correction factor is 1.0 by definition). Note that the substituting corrections are assumed to be due only to the substituting affecting the activation energy, not the A factor (Kwok and Atkinson, 1995; Atkinson, 1997a).

Obviously a large kinetic database is necessary to derive the substituent correction factors, and this is not available for these alkoxy radical abstraction reactions. However, if we assume that (1) the substituent corrections are due only to the substituent affecting the activation energy and not the A factor, and (2) the activation energy is linearly related to the bond dissociation energy for both the OH and the alkoxy radical abstraction reactions, then one can derive the substituent correction factors for the alkoxy reactions from those for the corresponding OH radical reaction. The latter have been derived by Kwok and Atkinson (1996) using the large kinetic database for OH radical reactions. The first assumption is reasonable, and is already incorporated in the way the Atkinson estimation methods derive temperature dependences. The second assumption is already incorporated in our alkoxy radical estimation methods discussed above, but needs to be examined in the case of OH radical rate constants.

The 298K group rate constants used in estimating OH radical reactions and parameters used by Kwok and Atkinson (1996) to determine their temperature dependences, are given in Table 9. Kwok and Atkinson (1996) gave the temperature dependences in the form $k=C\ T^2\ \exp(-B/T)$, but these can be recast to the Arrhenius activation energy (adjusted to be valid for T around 298K), to place it on the same basis as used for the alkoxy radical reactions. The corresponding activation energies are 1.82, 0.68, -0.20, and -0.62 kcal/mole for -CH3, -CH2-, -CH<, and -CHO, respectively. These activation energies are plotted against the bond dissociation energies associated with the group on Figure 7. It can be seen that the activation energies are reasonably well fit by a linear relationship with the bond dissociation energy for reactions at alkyl C-H bonds, but not for reaction at -CHO groups. In the case of OH radicals, the

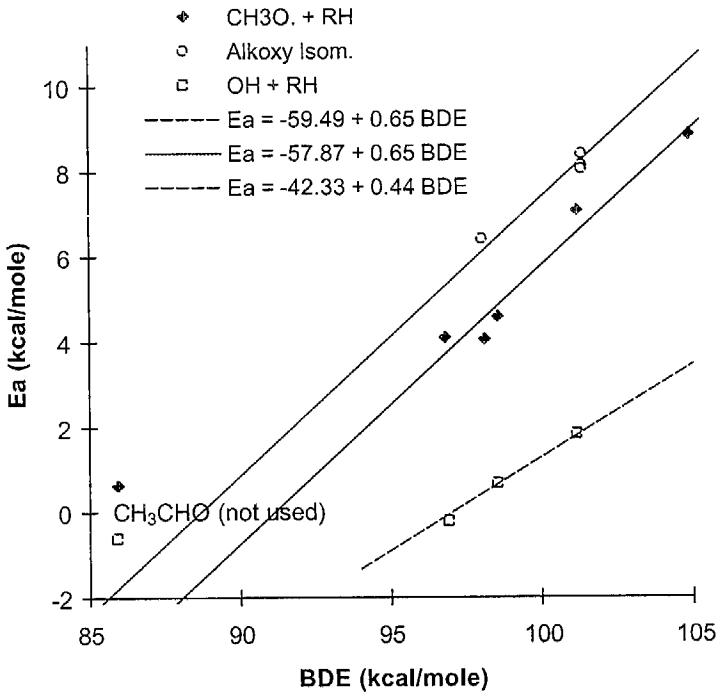

Figure 7. Plot of activation energies vs bond dissociation energies for methoxy abstraction reactions, alkoxy radical isomerizations, and OH abstraction reactions.

correlation breaks down for bond dissociation energies less than ~95 kcal/mole because there is essentially no energy barrier for bonds weaker than that. However, for stronger bonds, the correlation between group activation energy and BDE seems to hold reasonably well.

It is of interest to note that the slope for the line relating Ea to BDE for the alkoxy reactions is somewhat greater than that for the OH reactions, by a factor of ~1.5. This means that the activation energies for the alkoxy reactions would be more sensitive to substituents than is the case for OH reactions, as might be expected given the slower rates of these reactions. If these linear relationships between Ea and BDE are assumed to hold for the substituted species, this suggests that the group correction factors for the alkoxy radical isomerizations (F_{isom}) should be related to those for the OH radical reactions (F_{OH}) by

$$F_{isom} \approx f_{OH}^{1.5} \qquad (X)$$

Thus, the group correction factors given by Kwok and Atkinson (1996) for estimating rate constants for OH radical reactions can be used as a basis for estimating alkoxy radical isomerization reactions.

The dotted line on Figure 7 was derived to fit data primarily for radicals that have a -CH2- attached to the -CH3 group where the reaction is occurring. The OH group correction factor at ~300K for a -CH2- substituent is 1.23, which from Equation (X) corresponds to a correction factor of 1.5 for alkoxy radical reactions. This corresponds to an activation energy reduction of 0.18 kcal/mole. This means that the intercept for the line adjusted to fit the activation energy for these radicals (the dotted line on Figure

7) should be increased by 0.18 for the purpose of estimating group rate constants, which are defined based on -CH_3 substituents. Based on this, the activation energies for group rate constants for alkoxy radical isomerizations involving abstractions from -CH3, -CH2- and -CH< can be estimated from

$$Ea\ (group\ isom) = -57.87 + 0.65\ BDE + 0.18 = 57.69 + 0.65\ BDE \qquad (XI)$$

where BDE is the bond dissociation energy for the breaking bond. To place the BDE's on the same basis as those used to derive the equation, the BDE's for Equation (XII) should be calculated for groups with one -CH2- substituent, with the other substituents, if any, being CH3 groups.

Table 31 shows the activation energies for the various alkyl groups derived using Equation (XI), along with their corresponding A factors and 298K rate constants. In the case of -CHO groups, the activation energy is estimated from the estimated methoxy + acetaldehyde activation energy, plus the estimated 1.6 kcal/mole strain energy, derived as discussed above, plus an additional 3.5 kcal/mole of strain for reactions with -CO- groups in the cyclic transition state, derived as discussed in Section III.J.4, below. These group rate constants, together with the substituent factors derived for Equation (XI) using the substituent factors for estimating OH radical rate constants from Table 9, above, can then be used for estimating isomerization rate constants for any alkoxy radicals where the abstraction is at the given group.

As indicated above, a comparison of the activation energies for the bimolecular methoxy reactions with the estimated activation energies for isomerization of butoxy, pentoxy and hexoxy suggests that the ring strain for these isomerizations is ~1.6 kcal/mole. Note that this is reasonably consistent with the ring strain given by Benson (1976) for a six member ring with one oxygen. However, the strain may be different if the ring in the transition state involves groups other than just -CH2-. We assume that there is no strain difference if the transition state ring also has -CH< or >C< groups, but this does not appear to be the case if the ring also contains -O-, -CO- or -O-CO- groups. In particular, predictions are more consistent with available data if activation energies for isomerization involving -O-, -CO- or -O-CO- in the transition states are increased by an additional ~3.5 kcal/mole. Before giving the basis for this, which is discussed in Section III.J.4, it is necessary to first discuss the rate constant estimates for the competing decomposition reactions. This is given in the following section.

3. Beta Scission Decomposition

The most common unimolecular reactions of alkoxy radicals are β-scission decompositions. These involve breaking the C-C bond next to the alkoxy group, forming a carbonyl compound and a carbon center radical (where the latter will react further, as discussed above). For primary, secondary, and tertiary alkoxy radicals, the respective reactions are:

$$RCH_2O\cdot \rightarrow R\cdot + HCHO$$

$$RCH(O\cdot)R' \rightarrow RCHO + R'\cdot \ \underline{or}\ R'CHO + R\cdot$$

$$RC(O\cdot)(R')R'' \rightarrow R\text{-}CO\text{-}R' + R''\cdot \ \underline{or}\ R\text{-}CO\text{-}R'' + R'\cdot \ \underline{or}\ R'\text{-}CO\text{-}R'' + R\cdot$$

Note that for secondary and tertiary radicals there may be more than one possible reaction route, if the R, R' and/or R" substituents are different.

No direct measurements of absolute rate constants for alkoxy radical decompositions are available, but information is available concerning ratios of these rate constants relative to those for other alkoxy radical reactions. The only information concerning temperature dependent rate constants come from the measurements relative to alkoxy + NO reactions, whose absolute rate constants are known or can

be estimated (Atkinson, 1994, and references therein). Based on these data, Atkinson (1994, 1997b) recommends estimating the Arrhenius A factors using

$$A = 2.0 \times 10^{14} \cdot n \text{ sec-1}, \qquad \text{(XIII)}$$

where n is the reaction path degeneracy. The recommended decomposition rate constants and kinetic parameters are summarized on Table 32. The A factors derived using Equation (XIII) are assumed to be applicable to all alkoxy radical decompositions. Table 32 also gives alkoxy radical decomposition rate constants obtained from rate constant ratios obtained from results of various mechanistic and product studies, and placed on an absolute basis using estimates for the competing decomposition reactions. This is discussed below.

Table 33 lists the various alkoxy radicals for which relevant data are available concerning the branching ratios for their various competing reactions, or at least concerning upper or lower limits for those branching ratios. These are determined from product yields observed in various studies of OH radical + organic + NO_x systems where these alkoxy radicals are expected to be formed, as indicated in the comments on the table. In some cases product yield ratios can be used to derive ratios of rate constants involving an alkoxy radical decomposition; these are indicated in Table 33 and the relevant data are also included in Table 32. (In those cases Table 32 also gives the radical number used on Table 33 to aid the reader in finding the data on that radical.) In many other cases, only upper or lower branching ratios can be derived. For example, lower limits for a reaction route can be based on observing high yields of a product expected from a reaction, and upper limits for another route can be inferred from the failure to observe an expected product from the reaction. Many of the upper or lower limit estimates are subjective and approximate, and probably in many cases they could be refined based on a detailed analysis of the experimental methods. However, these approximate upper and lower limit data are useful for assessing the overall performance of the estimation methods because of the relatively large number and variety of reactions involved.

Table 33 also includes the heats of reaction for the various reactions where relevant and the estimated rate constants and corresponding branching ratios for the competing reactions. (The predictions for the O_2 reactions and the isomerizations are as discussed in the previous section, the predictions for the decompositions are discussed below.) An indication of how well the predicted branching ratios agree with the observed ratios is also shown. Table 34 gives a subset of the information on Table 33, organized by alkoxy reaction type rather than by radical. This is useful for obtaining an indication of how well the estimates are performing for a particular type of reaction. For that reason, Table 34 includes results using several alternative assumptions, which are discussed below.

Based on the approach used by Atkinson (1996), the activation energies for the decomposition reactions are estimated assuming

$$Ea \text{ (decomposition)} = EaA + EaB \cdot \Delta H_r \qquad \text{(XIV)}$$

where EaA and EaB are parameters which are assumed to depend only on the type of radical which is formed in the decomposition. The derivation of these parameters for the various types of decomposition reactions is discussed below.

We will first consider decompositions forming methyl radicals, for which, as shown on Table 32, there are the most extensive and best characterized data. These come in two groups: decompositions of hydrocarbon alkoxy radicals (i.e., alkoxy radicals containing only $-CH_3$, $-CH_2-$, >CH-, or >C< groups) which tend to be endothermic by ~5 to ~13 kcal/mole and relatively slow, and decompositions of alkoxy

Table 32. Summary of measured or estimated rate constants for alkoxy radical decompositions.

Reaction	Rate Parameters [a]				Relative to			Note	Ea (est.)	
	DH_r	A	Ea	k(298)	Type	Ratio	k(ref) [b]		Value	Err
Reactions forming CH3.										
CH3-CH2O. -> CH3. + HCHO	13.04	2.0e+14	20.20	3.1e-1	k(NO)		-	[c]	19.8	-0.4
CH3-CH[O.]-CH3 -> CH3-CHO + CH3.	7.86	4.0e+14	17.60	5.0e+1	k(NO)		-	[c]	17.5	-0.1
CH3-CH2-CH[O.]-CH3 -> CH3-CH2-CHO + CH3.	7.63	2.0e+14	16.60	1.3e+2	k(NO)		-	[c]	17.4	0.8
CH3-C[O.](CH3)-CH3 -> CH3-CO-CH3 + CH3.	4.98	7.5e+14	16.20	9.9e+2	k(NO)		-	[c,d]	16.2	0.0
CH3-C[O.](CH3)CH2-CH3 -> CH3-CH2-CO-CH3 + CH3.	4.82	4.0e+14	18.30	1.5e+1	k(NO)		-	[c,e,f]	16.2	-2.1
CH3-C(CH3)(CH3)-O-CH[O.]-CH3 -> CH3. + CH3-C(CH3)(CH3)-O-CHO	-4.81	2.0e+14	12.30	1.9e+5	k(O2)	4.85	3.9e+4	23 [f]	11.9	-0.4
CH3-CH2-O-CH[O.]-CH3 -> CH3-CH2-O-CHO + CH3.	-4.81	2.0e+14	11.49	7.5e+5	k(O2)	19	3.9e+4	13 [f]	11.9	0.4
CH3-CO-O-CH2-CH2-O-CH[O.]-CH3 -> CH3. + CH3-CO-O-CH2-CH2-O-CHO	-4.81	2.0e+14	11.92	3.6e+5	k(O2)	9.3	3.9e+4	30 [f]	11.9	0.0
CH3-CH[O.]-O-CH2-CH2-OH -> CH3. + HCO-O-CH2-CH2-OH	-4.81	2.0e+14	12.33	1.8e+5	k(O2)	4.62	3.9e+4	16 [f]	11.9	-0.4
Reactions forming CH3-CH2. and CH3-CH2-CH2.										
CH3-CH2-CH[O.]-CH3 -> CH3-CHO + CH3-CH2.	6.94	2.0e+14	13.58	2.2e+4	k(O2)	0.56	3.9e+4	11 [f]	14.3	0.7
CH3-CH2-CH[O.]-CH2-CH3 -> CH3-CH2-CHO + CH3-CH2.	6.71	4.0e+14	13.92	2.5e+4	k(O2)	0.63	3.9e+4	18 [f]	14.2	0.3
CH3-CH2-CH2-CH[O.]-CH3 -> CH3-CH2-CH2. + CH3-CHO	6.13	2.0e+14	14.10	9.1e+3	k(NO)		-	[c]	13.9	-0.2
CH3-C[O.](CH3)-CH2-CH3 -> CH3-CO-CH3 + CH3-CH2.	4.06	2.0e+14	13.90	1.3e+4	k(NO)		-	[c]	13.0	-0.9
Reactions forming CH3-C[.](CH3)-CH3										
CH3-C(CH3)(CH2O.)-CH3 -> HCHO + CH3-C[.](CH3)-CH3	10.40	2.0e+14	11.16	1.3e+6	k(O2)	39	3.4e+4	6 [f]	11.2	0.0
Reactions forming alpha-Hydroxy Alkyl Radicals										
HO-CH2-CH2O. -> HO-CH2. + HCHO	11.79	2.0e+14	12.62	1.1e+5	k(O2)	3.59	3.1e+4	1 [f]	12.6	0.0
CH3-CH(CH3)-CH[O.]-CH2-OH -> CH3-CH(CHO)-CH3 + HO-CH2.	7.15	2.0e+14	11.48	7.6e+5	kd($R_2CH.$)	2.45	3.1e+5	20 [f]	10.6	-0.9
Reactions forming $CH_3C(O)CH_2$. Radicals										
CH3-CO-CH2-CH[O.]-CH3 -> CH3-CHO + CH3-CO-CH2.	3.86	2.0e+14	12.38	1.7e+5	k(O2)	4.26	3.9e+4	19 [f]	12.9	0.6
Reactions forming Alkoxy Radicals										
CH3-C[O.](CH3)-O-CH3 -> CH3-CO-CH3 + CH3O.	9.50	2.0e+14	11.90	3.7e+5	kd(CH3.)	0.15	2.5e+6	36 [f]	12.6	0.7
CH3-CH(CH3)-CH2-O-C[O.](CH3)-CH3 -> CH3-CH(CH2O.)-CH3 + CH3-CO-CH3	9.29	2.0e+14	11.69	5.4e+5	kd(CH3.)	0.21	2.5e+6	46 [f]	12.5	0.8
CH3-C[O.](CH3)-O-CH2-CH3 -> CH3-CH2O. + CH3-CO-CH3	9.28	2.0e+14	11.26	1.1e+6	kd(CH3.)	0.44	2.5e+6	39 [f]	12.5	1.3
Reactions forming R-CO-O. Radicals										
CH3-C[O.](CH3)-O-CO-CH3 -> CH3-CO-CH3 + CH3-CO2.	10.73	2.0e+14	16.72	1.1e+2?	kd(CH3.)	0.32	3.5e+2?	41 [f]	16.7	0.0

[a] Data from Table 33 unless noted otherwise. Rate constants and A factors in units of sec-1, and Ea;s and heats of reaction are in units of kcal/mole. Underlined Ea from references, otherwise Ea's computed from tabiuated k(298) and A. These parameters are explicitly assigned for this radical in the mechanism generation system, unless indicated otherwise.

[b] k(ref) for O_2 reaction is $k(O_2)[O_2]$ for $[O_2] = 5.16 \times 10^{18}$ molec cm^3 at 1 atm and 298K.

[c] Atkinson (1997b). Relative to $k(RO+NO) = 2.3 \times 10^{-11} \exp(150/T)$.

[d] High pressure limit. Batt and Robinson (1987) calculate that rate constant under atmospheric conditions is ~80% of this. However, to fit chamber data, the A factor for atmospheric modeling is increased to from 6.0 to 7.5×10^{14} sec-1.

[e] Not used when computing best fit parameters for reactions forming methyl radicals. No explicit assignments made for this radical.

[f] Number is the radical number on Table 33 from which the data are taken. See footnotes to that table for documentation.

Table 33. Experimental and estimated branching ratios for radicals where relevant data are available.

	Radical [a] Reaction	Type	DH_r (kcal)	Estimated [b] k (s^{-1})	%	Expt. Branching [c] Min	Exp'd	Max	Fit [d]	k Ratios [e] Expt	Calc
1	HO-CH2-CH2O.									kd/kO2	
	HO-CH2-CH2O. + O2 -> HO2. + HCO-CH2-OH	O2	-30.6	3.10e+4	22%	15%	22%	30%	ok		
	HO-CH2-CH2O. -> HO-CH2. + HCHO	D	11.8	1.11e+5	78%	70%	78%	85%	ok	3.59	3.59
	Based on product data for ethene, as recommended by Atkinson (1997a).										
2	CH3-CO-CH2O.										
	CH3-CO-CH2O. + O2 -> CH3-CO-CHO + HO2.	O2	-26.9	1.01e+4	0%	0%		25%	ok		
	CH3-CO-CH2O. -> HCHO + CH3-CO.	D	2.6	1.74e+9	0%	75%	100%	100%	Low		
	Based on data of Jenkin et al (1993) indicating that decomposition dominates.										
3	CH3-CO-O-CH2O.										
	CH3-CO-O-CH2O. + O2 -> CH3-CO-O-CHO + HO2.	O2	-30.1	2.70e+4	65%	55%	65%	75%	ok	k(estr)/kO2	
	CH3-CO-O-CH2O. -> CH3-CO-OH + HCO.	Estr	-3.0	1.46e+4	35%	25%	35%	45%	ok	0.54	0.54
	Based on product yields for OH + methyl acetate (Christensen et al, 2000).										
4	CH3-O-CH2-O-CH2O.										
	CH3-O-CH2-O-CH2O. + O2 -> HO2. + CH3-O-CH2-O-CHO	O2	-46.6	1.58e+5	96%	75%	100%	100%	ok		
	CH3-O-CH2-O-CH2O. -> CH3-O-CH2O. + HCHO	D	13.3	6.50e+3	4%	0%	0%	25%	ok		
	The observed products from OH + dimethoxy methane given by Sidebottom et al (1997), which are consistent with the data of Wallington et al (1997), include CH3-O-CH2-O-CHO, and account for essentially all the reaction. This means that decomposition must not be important.										
5	CH3-CH2-O-CO-CH2O.										
	CH3-CH2-O-CO-CH2O. + O2 -> CH3-CH2-O-CO-CHO + HO2.	O2	-23.3	3.23e+3	14%	30%	75%	100%	Low		
	CH3-CH2-O-CO-CH2O. -> HCHO + CH3-CH2-O-CO.	D	13.5	1.39e+1	0%	0%	0%	70%	ok		
	CH3-CH2-O-CO-CH2O. -> CH3-CH[.]-O-CO-CH2-OH	I(O)		1.99e+4	86%	0%	25%	70%	High		
	The most reasonable explanation for the observation of ~25% of CH3-CH2-O-CO-CHO from ethyl 3-ethoxypropionate (Baxley et al, 1997) is to assume that this radical reacts with O_2 to a significant extent. This radical is predicted to be formed ~33% of the time.										
6	CH3-C(CH3)(CH2O.)-CH3									kd/kO2	
	CH3-C(CH3)(CH2O.)-CH3 + O2 -> CH3-C(CH3)(CHO)-CH3 + HO2.	O2	-30.8	3.35e+4	3%	0%	3%	5%	ok		
	CH3-C(CH3)(CH2O.)-CH3 -> HCHO + CH3-C[.](CH3)-CH3	D	10.4	1.31e+6	98%	75%	98%	100%	ok	39	39
	Based on data summarized by Atkinson (1997b)										
7	CH3-C(CH3)(CH3)-O-CH2O.										
	CH3-C(CH3)(CH3)O-CH2O. + O2 -> CH3-C(CH3)(CH3)O-CHO + HO2.	O2	-46.6	1.58e+5	97%	65%	95%	100%	ok		
	CH3-C(CH3)(CH3)O-CH2O. -> CH3-C[O.](CH3)CH3 + HCHO	D	14.3	3.09e+3	2%	0%	0%	25%	ok		
	CH3-C(CH3)(CH3)O-CH2O. -> CH3-C(CH3)(CH2.)O-CH2-OH	I(O)		1.59e+3	1%	0%	0%	25%	ok		
	Based on observation of t-butyl formate as the major product from MTBE (Tuazon et al, 1991b; Smith et al, 1991).										
8	CH3-CH(CH2O.)-O-CO-CH3										
	CH3-CH(CH2O.)-O-CO-CH3 + O2 -> HO2. + CH3-CH(CHO)-O-CO-CH3	O2	-30.8	3.37e+4	41%	0%	0%	75%	ok		
	CH3-CH(CH2O.)-O-CO-CH3 -> CH3-CO-O-CH[.]-CH3 + HCHO	D	12.8	4.93e+4	59%	25%	100%	100%	ok		
	Necessary to assume decomposition is non-negligible to explain observation of acetic acid as a 9% product from isopropyl acetate (Tuazon et al, 1998b).										
9	CH3-CH[O.]-CH2-OH										
	CH3-CH[O.]-CH2-OH + O2 -> HO2. + CH3-CO-CH2-O	O2	-34.6	2.68e+4	1%						
	CH3-CH[O.]-CH2-OH -> HO-CH2. + CH3-CHO	D	6.6	5.19e+6	99%	85%	100%	100%	ok		
	Based on product data for propene, as discussed by Atkinson (1997a).										

Table 33 (continued)

Radical [a] Reaction	Type	DH_r (kcal)	Estimated [b] k (s^{-1})	%	Expt. Branching [c] Min	Exp'd	Max	Fit [d]	k Ratios [e] Expt	Calc
10 CH3-O-CH[O.]-O-CH3										
CH3-O-CH[O.]-O-CH3 + O2 -> CH3-O-CO-O-CH3 + HO2.	O2	-53.3	3.94e+4	0%	50%	84%	95%	Low	kd/kO2	
CH3-O-CH[O.]-O-CH3 -> CH3-O-CHO + CH3O.	D	-1.7	9.07e+8	100%	0%	16%	50%	High	0.2	2e+4
Based on CH3-O-CHO / CH3-O-CO-O-CH3 yield ratios from dimethoxy methane (Sidebottom et al, 1997), assuming they are both formed from the CH3-O-CH[O.]-CH3 radical.										
11 CH3-CH2-CH[O.]-CH3										
CH3-CH2-CH[O.]-CH3 + O2 -> CH3-CH2-CO-CH3	O2	-36.0	3.94e+4	86%	46%	64%	76%	High	kd/kO2	
CH3-CH2-CH[O.]-CH3 -> CH3-CHO + CH3-CH2.	D	6.9	6.46e+3	14%	24%	36%	54%	Low	0.56	0.16
CH3-CH2-CH[O.]-CH3 -> CH3-CH2-CHO + CH3.	D	7.6	3.43e+1	0%						
Average of rate constant ratios reported by Carter et al (1979) and Cox et al (1981) as given by Atkinson (1997b).										
12 CH3-CH(OH)-CH[O.]-CH3										
CH3-CH(OH)-CH[O.]-CH3 + O2 -> CH3-CH(OH)-CO-CH3 + HO2	O2	-34.8	2.91e+4	0%	0%	0%	0%	ok		
CH3-CH(OH)-CH[O.]-CH3 -> CH3-CHO + CH3-CH[.]-OH	D	2.9	2.56e+9	100%	100%	100%	100%	ok		
CH3-CH(OH)-CH[O.]-CH3 -> CH3-CH(OH)-CHO + CH3.	D	9.1	1.18e+1	0%						
Based on upper limit yields of hydroxy carbonyls from OH + trans-2-butene (Atkinson, personal communication, 1999). Similar results were obtained from OH + trans-3-hexene.										
13 CH3-CH2-O-CH[O.]-CH3										
CH3-CH2-O-CH[O.]-CH3 + O2 -> CH3-CH2-O-CO-CH3 + HO2.	O2	-49.4	3.94e+4	8%	0%	5%	10%	ok		
CH3-CH2-O-CH[O.]-CH3 -> CH3-CH2O. + CH3-CHO	D	10.1	7.44e+4	16%	0%	0%	15%	High	kd/kO2	
CH3-CH2-O-CH[O.]-CH3 -> CH3-CH2-O-CHO + CH3.	D	-4.8	3.54e+5	76%	60%	95%	100%	ok	19.00	8.99
CH3-CH2-O-CH[O.]-CH3 -> CH3-CH(OH)O-CH2-CH2.	I(O)		5.31e+2	0%	0%	0%	25%	ok		
Based on ethyl formate from diethyl ether in 92% (Wallington and Japar, 1991) or 66% (Eberhard et al, 1993) yields and ethyl acetate in 4% yield (Eberhard et al, 1993) Average of yields for ethyl formate used in computing yield ratio. (Acetaldehyde also observed, but could be formed in other ways)										
14 CH3-CO-O-CH[O.]-CH3										
CH3-CO-O-CH[O.]-CH3 + O2 -> CH3-CO-O-CO-CH3 + HO2.	O2	-32.9	1.61e+4	4%	0%	0%	10%	ok		
CH3-CO-O-CH[O.]-CH3 -> CH3-CH(OH)-O-CO-CH2.	I(OCO)		6.72e+1	0%	0%	0%	10%	ok		
CH3-CO-O-CH[O.]-CH3 -> CH3-CO-OH + CH3-CO.	Estr	-8.4	3.54e+5	96%	95%	100%	100%	ok		
Product data from Tuazon et al (1998b) on OH + ethyl acetate indicates that the ester rearrangement must dominate in this reaction.										
15 CH3-CH(OH)-CH[O.]-O-CH3										
CH3-CH(OH)-CH[O.]-O-CH3 + O2 -> HO2. + CH3-CH(OH)-CO-O-CH3	O2	-48.5	3.94e+4	0%	0%	0%	15%	ok		
CH3-CH(OH)-CH[O.]-O-CH3 -> CH3-CH[.]-OH + CH3-O-CHO	D	-9.8	3.14e+13	100%	80%	100%	100%	ok		
CH3-CH(OH)-CH[O.]-O-CH3 -> CH3O. + CH3-CH(OH)-CHO	D	11.5	2.57e+4	0%	0%	0%	15%	ok		
Based on observation of 59% yield of methyl formate and 56% yield of acetaldehyde from 1-methoxy-2-propanol (Tuazon et al, 1998a). This radical is predicted to be formed ~55% of the time, and the observed products account for ~98% of the overall reaction.										
16 CH3-CH[O.]-O-CH2-CH2-OH										
CH3-CH[O.]-O-CH2-CH2-OH + O2 -> HO2. + CH3-CO-O-CH2-CH2-OH	O2	-49.4	3.94e+4	7%	5%	18%	30%	ok	kd/kO2	
CH3-CH[O.]-O-CH2-CH2-OH -> CH3. + HCO-O-CH2-CH2-OH	D	-4.8	3.54e+5	64%	70%	82%	100%	Low	4.62	8.99
CH3-CH[O.]-O-CH2-CH2-OH -> HO-CH2-CH2O. + CH3-CHO	D	10.1	7.39e+4	13%	0%	0%	25%	ok		
CH3-CH[O.]-O-CH2-CH2-OH -> CH3-CH(OH)-O-CH2-CH[.]-OH	I(O)		8.80e+4	16%	0%	0%	25%	ok		

Table 33 (continued)

Radical [a] Reaction	Type	DH_r (kcal)	Estimated [b] k (s^{-1})	%	Expt. Branching [c] Min	Exp'd	Max	Fit [d]	k Ratios [e] Expt	Calc
Based on the observed formation of 36% HO-CH2-CH2-O-CHO and 8% CH3-CO-O-CH2-CH2-OH from 2-ethoxy ethanol (Stemmler et al, 1996). This radical is predicted to be formed ~36% of the time. The observed products account for essentially all the reaction.										
17 CH3-CH2-O-CH[O.]-CH2-OH										
CH3-CH2-O-CH[O.]-CH2-OH + O2 -> HO2. + CH3-CH2-O-CO-CH2-OH	O2	-48.3	3.94e+4	0%	0%	0%	25%	ok		
CH3-CH2-O-CH[O.]-CH2-OH -> CH3-CH2O. + HCO-CH2-OH	D	11.5	2.48e+4	0%	0%	0%	25%	ok		
CH3-CH2-O-CH[O.]-CH2-OH -> HO-CH2. + CH3-CH2-O-CHO	D	-6.1	6.36e+10	100%	75%	100%	100%	ok		
Based on the observed formation of ~43% ethyl formate from 2-ethoxy ethanol (Stemmler et al, 1996). This radical is predicted to be formed ~36% of the time. The observed products account for essentially all the reaction.										
18 CH3-CH2-CH[O.]-CH2-CH3									kd/kO2	
CH3-CH2-CH[O.]-CH2-CH3 + O2 -> CH3-CH2-CO-CH2-CH3 + HO2.	O2	-36.3	3.94e+4	72%	42%	61%	74%	ok		
CH3-CH2-CH[O.]-CH2-CH3 -> CH3-CH2-CHO + CH3-CH2.	D	6.7	1.53e+4	28%	26%	39%	58%	ok	0.63	0.39
Based on data of Atkinson et al (1995).										
19 CH3-CO-CH2-CH[O.]-CH3									kd/kO2	
CH3-CO-CH2-CH[O.]-CH3 + O2 -> CH3-CO-CH2-CO-CH3 + HO2.	O2	-38.1	3.94e+4	38%	10%	19%	30%	High		
CH3-CO-CH2-CH[O.]-CH3 -> CH3-CHO + CH3-CO-CH2.	D	3.9	6.37e+4	62%	70%	81%	90%	Low	4.3	1.6
CH3-CO-CH2-CH[O.]-CH3 -> CH3-CO-CH2-CHO + CH3.	D	5.8	1.35e+2	0%	0%	0%	10%	ok		
CH3-CO-CH2-CH[O.]-CH3 -> CH3-CH(OH)-CH2-CO-CH2.	I(CO)		2.53e+2	0%	0%	0%	10%	ok		
Based on ratios of acetaldehyde to 2,4-pentadione yields from OH + 2-pentanone (Atkinson et al, 2000b).										
20 CH3-CH(CH3)-CH[O.]-CH2-OH									kd/kd(R2CH.)	
CH3-CH(CH3)-CH[O.]-CH2-OH + O2 -> CH3-CH(CH3)-CO-CH2-OH + HO2	O2	-34.4	2.52e+4	1%	0%	0%	10%	ok		
CH3-CH(CH3)-CH[O.]-CH2-OH -> HCO-CH2-OH + CH3-CH[.]-CH3	D	8.1	3.11e+5	8%	15%	29%	50%	Low	2.45	11.26
CH3-CH(CH3)-CH[O.]-CH2-OH -> CH3-CH(CHO)-CH3 + HO-CH2.	D	7.2	3.50e+6	91%	50%	71%	90%	High		
Based on yields of 2-methyl propanal, acetone, and glycolaldehyde from OH + 3-methyl-1-butene (Atkinson et al, 1998), assuming that OH addition occurs an estimated ~65% of the time at the 1-position relative to total OH addition.										
21 CH3-CH2-CH2-CH[O.]-O-CH3										
CH3-CH2-CH2-CH[O.]-O-CH3 + O2 -> HO2. + CH3-CH2-CH2-CO-O-CH3	O2	-49.7	3.94e+4	0%	0%	0%	30%	ok		
CH3-CH2-CH2-CH[O.]-O-CH3 -> CH3-CH2-CH2. + CH3-O-CHO	D	-6.5	1.45e+8	100%	50%	66%	100%	ok		
CH3-CH2-CH2-CH[O.]-O-CH3 -> CH3O. + CH3-CH2-CH2-CHO	D	10.3	6.04e+4	0%	0%	0%	30%	ok		
CH3-CH2-CH2-CH[O.]-O-CH3 -> CH3-O-CH(OH)-CH2-CH2-CH2.	I		1.96e+5	0%	0%	0%	30%	ok		
Based on observations of 43% propionaldehyde and 51% methyl formate from methyl n-butyl ether (Aschmann and Atkinson, 1999). This radical is predicted to be formed ~71% of the time. The observed products account for ~70% of the reaction.										
22 CH3-CH(CH3)-O-CH[O.]-CH2-OH										
CH3-CH(CH3)-O-CH[O.]-CH2-OH + O2 -> HO2. + CH3-CH(CH3)-O-CO-CH2-OH	O2	-48.3	3.94e+4	0%	0%	0%	15%	ok		
CH3-CH(CH3)-O-CH[O.]-CH2-OH -> CH3-CH[O.]-CH3 + HCO-CH2-OH	D	12.4	1.36e+4	0%	0%	0%	15%	ok		
CH3-CH(CH3)-O-CH[O.]-CH2-OH -> HO-CH2. + CH3-CH(CH3)-O-CHO	D	-6.1	6.36e+10	100%	80%	100%	100%	ok		
CH3-CH(CH3)-O-CH[O.]-CH2-OH -> CH3-CH(CH2.)-O-CH(OH)-CH2-OH	I(O)		1.06e+3	0%	0%	0%	15%	ok		
Based on formation of 57% isopropyl formate from 2-isopropoxy ethanol (Aschmann and Atkinson, 1999). This radical is predicted to be formed ~30% of the time, and the observed products account for essentially all the reaction routes.										
23 CH3-C(CH3)(CH3)-O-CH[O.]-CH3										
CH3-C(CH3)(CH3)O-CH[O.]-CH3 + O2 -> CH3-C(CH3)(CH3)O-CO-CH3 + HO2.	O2	-49.4	3.94e+4	9%	0%	17%	25%	ok		

Table 33 (continued)

Radical [a] Reaction	Type	DH$_r$ (kcal)	Estimated [b] k (s^{-1})	%	Expt. Branching [c] Min	Exp'd	Max	Fit [d]	k Ratios [e] Expt	Calc
CH3-C(CH3)(CH3)-O-CH[O.]-CH3 -> CH3-C[O.](CH3)-CH3 + CH3-CHO	D	11.1	3.51e+4	8%	0%	0%	20%	ok	kd/kO2	
CH3-C(CH3)(CH3)-O-CH[O.]-CH3 -> CH3. + CH3-C(CH3)(CH3)-O-CHO	D	-4.8	3.54e+5	82%	70%	83%	100%	ok	3.3	9.0
CH3-C(CH3)(CH3)O-CH[O.]-CH3 -> CH3-C(CH3)(CH2.)O-CH(OH)CH3	I(O)		1.59e+3	0%	0%	0%	20%	ok		
Based on observed t-butyl formate and t-butyl acetate yields from ETBE (Smith et al, 1992).										
24 CH3-CH2-CH[O.]-CH2-O-CO-CH3										
CH3-CH2-CH[O.]-CH2-O-CO-CH3 + O2 -> HO2. + CH3-CH2-CO-CH2-O-CO-CH3	O2	-34.8	2.91e+4	89%	25%	50%	100%	ok		
CH3-CH2-CH[O.]-CH2-O-CO-CH3 -> CH3-CH2. + CH3-CO-O-CH2-CHO	D	8.4	2.15e+3	7%	0%		75%	ok		
CH3-CH2-CH[O.]-CH2-O-CO-CH3 -> CH3-CO-O-CH2. + CH3-CH2-CHO	D	8.8	1.57e+3	5%	0%		75%	ok		
Based on observed formation of ~15% CH3-CH2-CO-CH2-O-CO-CH3 from n-butyl acetate (Veillerot et al. 1995). This radical predicted to be formed ~30% of the time. Only ~30% of the reaction route are accounted for, and the yields are only approximate.										
25 CH3-CO-O-CH2-CH2-CH[O.]-CH3										
CH3-CO-O-CH2-CH2-CH[O.]-CH3 + O2 -> HO2. + CH3-CO-CH2-CH2-O-CO-CH3	O2	-36.0	3.94e+4	62%	25%	65%	100%	ok		
CH3-CO-O-CH2-CH2-CH[O.]-CH3 -> CH3-CO-O-CH2-CH2. + CH3-CHO	D	5.2	2.41e+4	38%	0%	35%	75%	ok		
CH3-CO-O-CH2-CH2-CH[O.]-CH3 -> CH3. + CH3-CO-O-CH2-CH2-CHO	D	7.9	2.76e+1	0%	0%		75%			
Based on observed formation of ~15% CH3-CO-CH2-CH2-O-CO-CH3 from n-butyl acetate (Veillerot et al. 1995). This radical predicted to be formed ~23% of the time. Only ~30% of the reaction route are accounted for, and the yields are only approxmiate.										
26 CH3-CH2-CH2-CH[O.]-O-CO-CH3										
CH3-CH2-CH2-CH[O.]-O-CO-CH3 + O2 -> CH3-CH2-CH2-CO-O-CO-CH3 + HO2.	O2	-33.2	1.75e+4	3%	0%	0%	65%	ok		
CH3-CH2-CH2-CH[O.]-O-CO-CH3 -> CH3-CO-O-CHO + CH3-CH2-CH2.	D [e]	10.0	2.01e+4	4%	0%	0%	65%	ok		
CH3-CH2-CH2-CH[O.]-O-CO-CH3 -> CH3-CH2-CH2-CHO + CH3-CO2.	D	11.6	5.85e+1	0%	0%	0%	65%	ok		
CH3-CH2-CH2-CH[O.]-O-CO-CH3 -> CH3-CO-O-CH(OH)-CH2-CH2-CH2.	I		1.96e+5	36%	35%	100%	100%	ok		
CH3-CH2-CH2-CH[O.]-O-CO-CH3 -> CH3-CO-OH + CH3-CH2-CH2-CO.	Estr	-8.1	3.07e+5	57%	0%	0%	65%	ok		
CH3-CH2-CH2-CH[O.]-O-CO-CH3 -> CH3-CH2-CH2-CH(OH)-O-CO-CH2.	I(OCO)		6.72e+1	0%	0%	0%	65%	ok		
Environmental chamber reactivity data for n-butyl acetate can only be fit by model simulations if it is assumed that the isomerization reaction occurs a significant fraction of the time..										
27 CH3-CH2-CH2-CH[O.]-O-CH2-CH2-OH										
CH3-CH2-CH2-CH[O.]-O-CH2-CH2-OH + O2 -> HO2. + CH3-CH2-CH2-CO-O-CH2-CH2-OH	O2	-49.7	3.94e+4	0%	0%	0%	25%	ok		
CH3-CH2-CH2-CH[O.]-O-CH2-CH2-OH -> CH3-CH2-CH2. + HCO-O-CH2-CH2-OH	D	-6.5	1.45e+8	100%	50%	100%	100%	ok		
CH3-CH2-CH2-CH[O.]-O-CH2-CH2-OH -> HO-CH2-CH2O. + CH3-CH2-CH2-CHO	D	10.1	7.06e+4	0%	0%	0%	25%	ok		
CH3-CH2-CH2-CH[O.]-O-CH2-CH2-OH -> HO-CH2-CH2-O-CH(OH)-CH2-CH2-CH2.	I		1.96e+5	0%	0%	0%	25%	ok		
CH3-CH2-CH2-CH[O.]-O-CH2-CH2-OH -> CH3-CH2-CH2-CH(OH)-O-CH2-CH[.]-OH	I(O)		8.80e+4	0%	0%	0%	25%	ok		
Based on observations of propionaldehyde and HO-CH2-CH2-O-CHO in ~20% yields from 2-butoxy ethanol by Tuazon et al. (1998), with somewhat higher yields observed by Stemmler et al. (1997b). This radical is believed to be formed ~20% of the time.										
28 CH3-CH2-CH2-CH2-O-CH[O.]-CH2-OH										
CH3-CH2-CH2-CH2-O-CH[O.]-CH2-OH + O2 -> HO2. + CH3-CH2-CH2-CH2-O-CO-CH2-OH	O2	-48.3	3.94e+4	0%	0%	0%	25%	ok		
CH3-CH2-CH2-CH2-O-CH[O.]-CH2-OH -> CH3-CH2-CH2-CH2O. + HCO-CH2-OH	D	11.6	2.46e+4	0%	0%	0%	25%	ok		
CH3-CH2-CH2-CH2-O-CH[O.]-CH2-OH -> HO-CH2. + CH3-CH2-CH2-CH2-O-CHO	D	-6.1	6.36e+10	100%	80%	100%	100%	ok		
CH3-CH2-CH2-CH2-O-CH[O.]-CH2-OH -> CH3-CH2-CH[.]-CH2-O-CH(OH)-CH2-OH	I(O)		1.83e+4	0%	0%	0%	25%	ok		

Table 33 (continued)

Radical [a] Reaction	Type	DH_r (kcal)	Estimated [b] k (s^{-1})	%	Expt. Branching [c] Min	Exp'd	Max	Fit [d]	k Ratios [e] Expt	Calc
Based on observations of n-butyl formate from 2-butoxy ethanol with yields of 57% (Tuazon et al, 1998) or ~35% (Stemmler et al., 1997b). This radical is believed to be formed ~50% of the time.										
29 CH3-CH2-O-CH[O.]-CH2-O-CO-CH3										
CH3-CH2-O-CH[O.]-CH2-O-CO-CH3 + O2 -> HO2. + CH3-CH2-O-CO-CH2-O-CO-CH3	O2	-48.3	3.94e+4	0%	0%	0%	30%	ok		
CH3-CH2-O-CH[O.]-CH2-O-CO-CH3 -> CH3-CH2O. + CH3-CO-O-CH2-CHO	D	11.5	2.48e+4	0%	0%	0%	30%	ok		
CH3-CH2-O-CH[O.]-CH2-O-CO-CH3 -> CH3-CO-O-CH2. + CH3-CH2-O-CHO	D	-3.6	1.63e+7	100%	50%	90%	100%	ok		
CH3-CH2-O-CH[O.]-CH2-O-CO-CH3 -> CH3-CO-O-CH2-CH(OH)-O-CH2-CH2.	I(OCO)		5.31e+2	0%	0%	0%	30%	ok		
Based on observed yield of ethyl formate (33%) from 2-ethoxyethyl acetate (Wells et al., 1996). This is somewhat lower than the predicted 44% formation for this radical, but within the uncertainty of the estimate.										
30 CH3-CO-O-CH2-CH2-O-CH[O.]-CH3										
CH3-CO-O-CH2-CH2-O-CH[O.]-CH3 + O2 -> HO2. + CH3-CO-O-CH2-CH2-O-CO-CH3	O2	-49.4	3.94e+4	8%	5%	10%	25%	ok		
CH3-CO-O-CH2-CH2-O-CH[O.]-CH3 -> CH3-CO-O-CH2-CH2O. + CH3-CHO	D	10.1	7.39e+4	15%	0%	0%	25%	ok	kd/kO2	
CH3-CO-O-CH2-CH2-O-CH[O.]-CH3 -> CH3. + CH3-CO-O-CH2-CH2-O-CHO	D	-4.8	3.54e+5	72%	50%	90%	100%	ok	9.3	9.0
CH3-CO-O-CH2-CH2-O-CH[O.]-CH3 -> CH3-CH(OH)-O-CH2-CH[.]-O-CO-CH3	I(O)		2.72e+4	6%	0%	0%	25%	ok		
Based on yields of CH3-CO-O-CH2-CH2-O-CHO (37%) and CH3-CO-O-CH2-CH2-O-CO-CH3 (4%) from 2-ethoxyethyl acetate (Wells et al, 1996). This radical is predicted to be formed ~36% of the time, which is consistent with these product yields.										
31 CH3-CH(CH3)-O-CH[O.]-CH(CH3)-CH3										
CH3-CH(CH3)-O-CH[O.]-CH(CH3)-CH3 + O2 -> HO2. + CH3-CH(CH3)-O-CO-CH(CH3)-CH3	O2	-49.2	3.94e+4	0%	0%	0%	25%	ok		
CH3-CH(CH3)-O-CH[O.]-CH(CH3)-CH3 -> CH3-CH[O.]-CH3 + CH3-CH(CHO)-CH3	D	11.4	2.75e+4	0%	0%	0%	25%	ok		
CH3-CH(CH3)-O-CH[O.]-CH(CH3)-CH3 -> CH3-CH[.]-CH3 + CH3-CH(CH3)-O-CHO	D	-6.1	1.14e+10	100%	50%	100%	100%	ok		
CH3-CH(CH3)-O-CH[O.]-CH(CH3)-CH3 -> CH3-CH(CH3)-CH(OH)-O-CH(CH2.)-CH3	I(O)		5.31e+2	0%	0%	0%	25%	ok		
Based on observation of 48% yield of t-butyl formate from isobutyl isopropyl ether (Stemmler et al, 1997a). This radical is predicted to be formed ~33% of the time.										
32 CH3-CH2-O-CO-CH2-CH[O.]-O-CH2-CH3										
CH3-CH2-O-CO-CH2-CH[O.]-O-CH2-CH3 + O2 -> HO2. + CH3-CH2-O-CO-CH2-CO-O-CH2-CH3	O2	-51.8	3.94e+4	0%	0%	0%	20%	ok		
CH3-CH2-O-CO-CH2-CH[O.]-O-CH2-CH3 -> CH3-CH2-O-CO-CH2. + CH3-CH2-O-CHO	D	-5.8	8.34e+7	100%	50%	84%	100%	ok		
CH3-CH2-O-CO-CH2-CH[O.]-O-CH2-CH3 -> CH3-CH2O. + CH3-CH2-O-CO-CH2-CHO	D	8.0	3.46e+5	0%	0%	16%	20%	ok		
CH3-CH2-O-CO-CH2-CH[O.]-O-CH2-CH3 -> CH3-CH2-O-CO-CH2-CH(OH)-O-CH2-CH2.	I(O)		5.31e+2	0%	0%	0%	20%	ok		
Based on yield ratios for ethyl formate and CH3-CH2-O-CO-CH2-CHO from ethyl 3-ethoxypropionate (Baxley et al, 1997). Total yield is ~42%, while predicted amount of this radical formed is ~50%.										
33 CH3-CH2-O-CO-CH2-CH2-O-CH[O.]-CH3										
CH3-CH2-O-CO-CH2-CH2-O-CH[O.]-CH3 + O2 -> HO2. + CH3-CH2-O-CO-CH2-CH2-O-CO-CH3	O2	-49.4	3.94e+4	8%	0%	0%	50%	ok		
CH3-CH2-O-CO-CH2-CH2-O-CH[O.]-CH3 -> CH3-CH2-O-CO-CH2-CH2O. + CH3-CHO	D	10.1	7.39e+4	16%	0%	0%	50%	ok		
CH3-CH2-O-CO-CH2-CH2-O-CH[O.]-CH3 -> CH3. + CH3-CH2-O-CO-CH2-CH2-O-CHO	D	-4.8	3.54e+5	75%	50%	75%	100%	ok		
CH3-CH2-O-CO-CH2-CH2-O-CH[O.]-CH3 -> CH3-CH(OH)-O-CH2-CH[.]-CO-O-CH2-CH3	I(O)		2.32e+3	0%	0%	0%	50%	ok		
Based on formation of 30% CH3-CH2-O-CO-CH2-CH2-O-CHO from ethyl 3-ethoxypropionate (Baxley et al, 1977). Note that this radical is predicted to be formed 40% of the time, so the observed yield is higher than maximum predicted.										
34 CH3-O-CO-CH2-CH[O.]-CH2-CO-O-CH3										
CH3-O-CO-CH2-CH[O.]-CH2-CO-O-CH3 + O2 -> CH3-O-CO-CH2-CO-CH2-CO-O-CH3 + HO2.	O2	-40.5	3.94e+4	38%	90%	100%	100%	Low		

Table 33 (continued)

Radical [a] Reaction	Type	DH_r (kcal)	Estimated [b] k (s^{-1})	%	Expt. Branching [c] Min	Exp'd	Max	Fit [d]	k Ratios [e] Expt	Calc
CH3-O-CO-CH2-CH[O.]-CH2-CO-O-CH3 -> CH3-O-CO-CH2-CHO + CH3-O-CO-CH2.	D	4.8	6.34e+4	62%	0%	0%	10%	High		
Necessary to assume that reaction with O2 dominates for model simulations of dimethyl glutarate (DBE-5) chamber experiments. The observation of CH3-O-CO-CH2-CO-CH2-CO-O-CH3 as a product of the OH + DBE-5 reaction (Tuazon et al, 1999) also indicates that the O2 reaction is important.										
35 CH3-O-CO-CH2-CH2-CH[O.]-CO-O-CH3										
CH3-O-CO-CH2-CH2-CH[O.]-CO-O-CH3 + O2 -> CH3-O-CO-CH2-CH2-CO-CO-O-CH3 + HO2.	O2	-28.1	3.57e+3	77%	0%	10%	10%	High		
CH3-O-CO-CH2-CH2-CH[O.]-CO-O-CH3 -> CH3-O-CO-CHO + CH3-O-CO-CH2-CH2.	D	15.0	1.67e+1	0%	0%	0%	10%	ok		
CH3-O-CO-CH2-CH2-CH[O.]-CO-O-CH3 -> CH3-O-CO-CH2-CH2-CHO + CH3-O-CO.	D	9.5	2.80e+2	6%	0%	0%	10%	ok		
CH3-O-CO-CH2-CH2-CH[O.]-CO-O-CH3 -> CH3-O-CO-CH2-CH2-CH(OH)-CO-O-CH2.	I(OCO)		7.88e+2	17%	80%	90%	100%	Low		
Isomerization is assumed to dominate by analogy with the assumptions made for CH3-O-CO-CH2-CH[O.]-CO-O-CH3 radicals. This also results in somewhat better fits of model simulations to dimethyl glutarate (DBE-5) reactivity experiments. Reaction with O2, predicted to be the major competing process, is arbitrarily assumed to occur ~10% of the time.										
36 CH3-C[O.](CH3)-O-CH3										
CH3-C[O.](CH3)-O-CH3 -> CH3-O-CO-CH3 + CH3.	D	-6.5	2.51e+6	96%	50%	87%	95%	High	kd/kd(CH_3)	
CH3-C[O.](CH3)-O-CH3 -> CH3-CO-CH3 + CH3O.	D	9.5	1.13e+5	4%	5%	13%	25%	Low	0.15	0.05
Based on ratios of methyl acetate to acetone yields from MTBE (Tuazon et al, 1991, Smith et al, 1991)										
37 CH3-C[O.](CHO)-CH2-OH										
CH3-C[O.](CHO)-CH2-OH -> HCO-CO-CH2-OH + CH3.	D	19.0	7.13e-3	0%	0%	0%	25%	ok		
CH3-C[O.](CHO)-CH2-OH -> CH3-CO-CH2-OH + HCO.	D	-0.7	1.53e+7	94%	75%	100%	100%			
CH3-C[O.](CHO)-CH2-OH -> CH3-CO-CHO + HO-CH2.	D	8.9	9.82e+5	6%	0%	0%	25%	ok		
Based on observations of hydroxyacetone as a major product in the reaction of OH with methacrolein (Tuazon and Atkinson, 1990). This and products from other radicals formed believed to account for all the reaction routes.										
38 *C[O.](CH3)-CH2-O-CO-O-*										
C[O.](CH3)-CH2-O-CO-O- -> *CH2-O-CO-O-CO-* + CH3.	D [e]	11.1	7.40e+1	0%	0%	0%	20%	ok		
C[O.](CH3)-CH2-O-CO-O- -> CH3-CO-O-CO-O-CH2.	D [e]	4.9	8.61e+5	99%	75%	100%	100%	ok		
C[O.](CH3)-CH2-O-CO-O- -> CH3-CO-CH2-O-CO2.	D	5.6	5.12e+3	1%	0%	0%	20%	ok		
Necessary to assume that the decomposition to CH3-CO-O-CO-O-CH2. dominates in order for model to fit results of propylene carbonate reactivity chamber experiments.										
39 CH3-C[O.](CH3)-O-CH2-CH3										
CH3-C[O.](CH3)-O-CH2-CH3 -> CH3. + CH3-CH2-O-CO-CH3	D	-6.5	2.51e+6	95%	0%	69%	100%	ok		
CH3-C[O.](CH3)-O-CH2-CH3 -> CH3-CH2O. + CH3-CO-CH3	D	9.3	1.33e+5	5%	0%	31%	100%	ok	0.44	0.05
CH3-C[O.](CH3)-O-CH2-CH3 -> CH3-C(CH3)(OH)-O-CH2-CH2.	I(O)		5.31e+2	0%						
Based on ratios of acetone and ethyl acetate yields from ETBE (Smith et al, 1992), assuming they are all formed from this radical, which is estimated to be formed 5% of the time. (Total yields of both are ~6%). This is uncertain.										
40 CH3-C[O.](CH3)-CO-O-CH3										
CH3-C[O.](CH3)-CO-O-CH3 -> CH3-O-CO-CO-CH3 + CH3.	D	12.2	1.16e+0	0%	0%	0%	50%	ok		
CH3-C[O.](CH3)-CO-O-CH3 -> CH3-CO-CH3 + CH3-O-CO.	D	5.7	4.62e+3	85%	50%	100%	100%	ok		
CH3-C[O.](CH3)-CO-O-CH3 -> CH3-C(CH3)(OH)-CO-O-CH2.	I(O)		7.88e+2	15%	0%	0%	50%	ok		
It is necessary to assume that the decomposition to CH3-O-CO. is a major route in order for model to simulate results of methyl isobutyrate reactivity experiments (Carter et al, 2000a).										

Table 33 (continued)

Radical [a] Reaction	Type	DH_r (kcal)	Estimated [b] k (s^{-1})	%	Expt. Branching [c] Min	Exp'd	Max	Fit [d]	k Ratios [e] Expt	Calc
41 CH3-C[O.](CH3)-O-CO-CH3										
CH3-C[O.](CH3)-O-CO-CH3 -> CH3-CO-O-CO-CH3 + CH3.	D [e]	10.0	3.48e+2	66%	50%	76%	90%	ok	kd/kd(CH_3)	
CH3-C[O.](CH3)-O-CO-CH3 -> CH3-CO-CH3 + CH3-CO2.	D	10.7	1.09e+2	21%	10%	24%	50%	ok	0.32	0.31
CH3-C[O.](CH3)-O-CO-CH3 -> CH3-C(CH3)(OH)-O-CO-CH2.	I(OCO)		6.72e+1	13%	0%	0%	25%	ok		
Based on yields of acetone and acetic anhydride from isopropyl acetate and t-butyl acetate (Tuazon et al. 1998b).										
42 CH3-C[O.](CH3)-O-CH2-CH2-OH										
CH3-C[O.](CH3)-O-CH2-CH2-OH -> CH3. + CH3-CO-O-CH2-CH2-OH	D	-6.5	2.51e+6	92%	60%	90%	100%	ok		
CH3-C[O.](CH3)-O-CH2-CH2-OH -> HO-CH2-CH2O. + CH3-CO-CH3	D	9.3	1.32e+5	5%	0%	0%	20%	ok		
CH3-C[O.](CH3)-O-CH2-CH2-OH -> CH3-C(CH3)(OH)-O-CH2-CH[.]-OH	I(O)		8.80e+4	3%	0%	0%	20%	ok		
Based on formation of 44% CH3-CO-O-CH2-CH2-OH from 2-isopropoxy ethanol (Aschmann and Atkinson, 1999). This radical is predicted to be formed ~50% of the time, and the observed products account for essentially all the reaction routes.										
43 CH3-C[O.](CH3)-O-CO-O-CH3										
CH3-C[O.](CH3)-O-CO-O-CH3 -> CH3-O-CO-O-CO-CH3 + CH3.	D [e]	10.0	3.48e+2	74%	50%	75%	100%	ok		
CH3-C[O.](CH3)-O-CO-O-CH3 -> CH3-CO-CH3 + CH3-O-CO2.	D	10.6	1.21e+2	26%	0%	25%	50%	ok		
Necessary to assume decomposition forming acetone is slow to be consistent with acetone formation observed in methyl isopropyl carbonate environmental chamber experiments. This also results in somewhat better fits of the model to the data, without having to make large adjustments to the overall nitrate yield.										
44 CH3-CH(CH3)-O-C[O.](CH3)-CH3										
CH3-CH(CH3)-O-C[O.](CH3)-CH3 -> CH3-CH[O.]-CH3 + CH3-CO-CH3	D	10.1	7.28e+4	3%	0%		20%	ok		
CH3-CH(CH3)-O-C[O.](CH3)-CH3 -> CH3. + CH3-CH(CH3)-O-CO-CH3	D	-6.5	2.51e+6	97%	80%	100%	100%	ok		
CH3-CH(CH3)-O-C[O.](CH3)-CH3 -> CH3-C(CH3)(OH)-O-CH(CH2.)-CH3	I(O)		1.06e+3	0%	0%		20%	ok		
Based on observations of isopropyl acetate as major product (nearly 100% yield) from di-isopropyl acetate (Wallington et al, 1993).										
45 CH3-C(CH3)(CH3)-O-C[O.](CH3)-CH3										
CH3-C(CH3)(CH3)-O-C[O.](CH3)-CH3 -> CH3-C[O.](CH3)-CH3 + CH3-CO-CH3	D	10.3	6.27e+4	2%	0%	0%	20%	ok		
CH3-C(CH3)(CH3)-O-C[O.](CH3)-CH3 -> CH3. + CH3-C(CH3)(CH3)-O-CO-CH3	D	-6.5	2.51e+6	97%	75%	100%	100%	ok		
CH3-C(CH3)(CH3)-O-C[O.](CH3)-CH3 -> CH3-C(CH3)(CH2.)-O-C(CH3)(OH)-CH3	I(O)		1.59e+3	0%	0%	0%	20%	ok		
Based on observed 85% yield of isopropyl acetate from di-t-butyl ether (Langer et al, 1996).										
46 CH3-CH(CH3)-CH2-O-C[O.](CH3)-CH3										
CH3-CH(CH3)-CH2-O-C[O.](CH3)-CH3 -> CH3-CH(CH2O.)-CH3 + CH3-CO-CH3	D	9.3	1.32e+5	5%	0%	18%	40%	ok	kd/kd(CH_3)	
CH3-CH(CH3)-CH2-O-C[O.](CH3)-CH3 -> CH3. + CH3-CH(CH3)-CH2-O-CO-CH3	D	-6.5	2.51e+6	94%	40%	82%	100%	ok	0.21	0.05
CH3-CH(CH3)-CH2-O-C[O.](CH3)-CH3 -> CH3-C(CH3)(OH)-O-CH2-C[.](CH3)-CH3	I(O)		2.70e+4	1%	0%	0%	30%	ok		
Based on 6% yields of CH3-CH(CHO)-CH3 and 28% of CH3-CH(CH3)-CH2-O-CO-CH3 from isopropyl isobutyl ether (Stemmler et al, 1997a), assuming that the former is formed from subsequent reactions from this radical. This radical is predicted to be formed ~50% of the time.										
47 CH3-CH(CH3)-O-CH2-C[O.](CH3)-CH3										
CH3-CH(CH3)-O-CH2-C[O.](CH3)-CH3 -> CH3-CH(CH3)-O-CH2. + CH3-CO-CH3	D	3.7	6.96e+4	13%	0%	0%	25%	ok		
CH3-CH(CH3)-O-CH2-C[O.](CH3)-CH3 -> CH3. + CH3-CH(CH3)-O-CH2-CO-CH3	D	6.2	1.93e+2	0%	0%	0%	25%			
CH3-CH(CH3)-O-CH2-C[O.](CH3)-CH3 -> CH3-C(CH3)(OH)-CH2-O-C[.](CH3)-CH3	I(O)		4.81e+5	87%	75%	100%	100%	ok		
Based on observed formation of ~25% of CH3-C(CH3)(OH)-CH2-O-CO-CH3 from isobutyl isopropyl ether (Stemmler et al, 1997a), which can only be formed by the isomerization reaction. However, this radical is predicted to be formed only ~8% of the time.										

Table 33 (continued)

Radical [a] Reaction	Type	DH_r (kcal)	Estimated [b] k (s^{-1})	%	Expt. Branching [c] Min	Exp'd	Max	Fit [d]	k Ratios [e] Expt	Calc
48 CH3-C(CH3)(OH)-CH2-O-C[O.](CH3)-CH3										
CH3-C(CH3)(OH)-CH2-O-C[O.](CH3)-CH3 -> CH3-C(OH)(CH2O.)-CH3 + CH3-CO-CH3	D	9.3	1.32e+5	5%	0%	0%	25%	ok		
CH3-C(CH3)(OH)-CH2-O-C[O.](CH3)-CH3 -> CH3. + CH3-C(CH3)(OH)-CH2-O-CO-CH3	D	-6.5	2.51e+6	95%	75%	100%	100%	ok		
Based on observed formation of ~25% of CH3-C(CH3)(OH)-CH2-O-CO-CH3 from isobutyl isopropyl ether (Stemmler et al, 1997a), which can only be formed by this reaction. However, this radical is predicted to be formed only ~5% of the time.										

[a] Radicals are given in order of primary, secondary, and then tertiary. Within each type, radicals are sorted first by carbon number, then by molecular weight.

[b] Rate constants estimated for T=298K using recommended parameters as discussed in the text. Units are sec-1. Unimolecular rate constants for O2 reaction calculated assuming [O2] = 5.18 x 10-18 molec cm-3. "%" is the estimated percentage of the radical which reacts with this reaction.

[c] Minimum, expected, and maximum fractions for this reaction route relative to all reactions of this radical, based on analysis of the experimental data. Minimum and maximum values are subjective estimates. Underlined branching ratios are used for explicit estimates for this radical -- overriding the temperature-dependent rate constant estimates.

[d] "High" means that the estimated branching ratio is greater than the maximum value estimated from analysis of the experimental data; "Low" means that the estimated ratio is lower than the minimum; "ok" means that the estimated branching ratio lies between the minimum and maximum considered consistent with the experimental data.

[e] Rate constant ratios that can be used for quantitative rate constant estimates.

[f] The activation energy is reduced by 2 kcal/mole for reactions that form products with -CO-O-CO- groups. If this correction were not applied, the estimated rate constant would be a factor of ~30 lower.

radicals with a-O groups such as formed in photooxidations of ethers, which are exothermic by ~5 kcal/mole and tend to be much more rapid. Note that the rate constants for the latter are uncertain because of uncertainty in the estimates for the O_2 reaction used to place the experimental rate constant ratio on an absolute basis. It is possible that the O_2 reaction is significantly faster than estimated in this work, in which case these decompositions will also be faster.

Figure 8 shows plots of the estimated activation energy for selected decompositions reactions vs. the estimated heats of reaction. It can be seen that the data for reactions forming methyl radicals fall reasonably well on a straight line, if the point for the 2-methyl-2-butoxy radical, which seems to be somewhat inconsistent with the other data, is excluded. The least squares line (excluding the point for 2-methyl-2-butoxy) is

$$Ea \text{ (decomp. to CH3.)} = 14.05 + 0.44\ \Delta H_r \qquad \text{(XV)}$$

where Ea is the activation energy and ΔH_r is the estimated heat of reaction, both in kcal/mole. This corresponds to EaA = 14.05 kcal/mole and EaB = 0.44. These are used for estimating activation energies for all the alkoxy radical decompositions forming methyl radicals.

Figure 8 shows that Equation (XV) overpredicts the activation energies for reactions forming ethyl and propyl radicals. However, the data for these decompositions are reasonably well fit if EaB is assumed to be the same as form reactions forming methyl radicals, and EaA is reduced to 11.25 kcal/mole, i.e.,

$$Ea \text{ (decomp. to RCH2.)} = 11.25 + 0.44\ \Delta Hr \qquad \text{(XVI)}$$

Although the data are not sufficient to determine whether the EaB for decompositions forming these radicals is necessarily the same as for those forming methyl, this is assumed for lack of sufficient data to determine otherwise. Likewise, the single measurement for a decomposition forming tertiary radicals is fit

using EaA = 6.58 kcal/mole, and the least uncertain measurement for a decomposition forming $HOCH_2\cong$ is

Table 34. Experimental and estimated branching ratios for radicals where relevant data are available, sorted by type of reaction. Estimated branching ratios derived using alternative mechanistic assumptions are also shown.

Reaction Type and Reaction	Rad. [a]	Hr (kcal)	Estimated k (min^{-1})	%	Expt. Fract React. Min	Exp'd	Max	Estimation vs Experimental
Estimates using Recommended Parameters								
Decomposition Forming CH3.								
CH3-CH2-O-CH[O.]-CH3 -> CH3-CH2-O-CHO + CH3.	13	-4.81	3.54e+5	76%	60%	95%	100%	ok
CH3-CH[O.]-O-CH2-CH2-OH -> CH3. + HCO-O-CH2-CH2-OH	16	-4.81	3.54e+5	64%	70%	82%	100%	Low: 64% vs 70%
CH3-C(CH3)(CH3)-O-CH[O.]-CH3 -> CH3. + CH3-C(CH3)(CH3)-O-CHO	23	-4.81	3.54e+5	82%	70%	83%	100%	ok
CH3-CO-O-CH2-CH2-O-CH[O.]-CH3 -> CH3. + CH3-CO-O-CH2-CH2-O-CHO	30	-4.81	3.54e+5	72%	50%	90%	100%	ok
CH3-CH2-O-CO-CH2-CH2-O-CH[O.]-CH3 -> CH3. + CH3-CH2-O-CO-CH2-CH2-O-CHO	33	-4.81	3.54e+5	75%	50%	75%	100%	ok
CH3-C[O.](CH3)-O-CH3 -> CH3-O-CO-CH3 + CH3.	36	-6.51	2.51e+6	96%	50%	87%	95%	High: 96% vs 95%
CH3-C[O.](CH3)-O-CH2-CH3 -> CH3. + CH3-CH2-O-CO-CH3	39	-6.51	2.51e+6	95%	0%	69%	100%	ok
CH3-C[O.](CH3)-O-CO-CH3 -> CH3-CO-O-CO-CH3 + CH3.	41	9.99	3.48e+2	66%	50%	76%	90%	ok
CH3-C[O.](CH3)-O-CH2-CH2-OH -> CH3. + CH3-CO-O-CH2-CH2-OH	42	-6.51	2.51e+6	92%	60%	90%	100%	ok
CH3-CH(CH3)-O-C[O.](CH3)-CH3 -> CH3. + CH3-CH(CH3)-O-CO-CH3	44	-6.51	2.51e+6	97%	80%	100%	100%	ok
CH3-C(CH3)(CH3)-O-C[O.](CH3)-CH3 -> CH3. + CH3-C(CH3)(CH3)-O-CO-CH3	45	-6.51	2.51e+6	97%	75%	100%	100%	ok
CH3-CH(CH3)-CH2-O-C[O.](CH3)-CH3 -> CH3. + CH3-CH(CH3)-CH2-O-CO-CH3	46	-6.51	2.51e+6	94%	40%	82%	100%	ok
CH3-C(CH3)(OH)-CH2-O-C[O.](CH3)-CH3 -> CH3. + CH3-C(CH3)(OH)-CH2-O-CO-CH3	48	-6.51	2.51e+6	95%	75%	100%	100%	ok
Decomposition Forming RCH2.								
CH3-CH2-CH[O.]-CH3 -> CH3-CHO + CH3-CH2.	11	6.94	6.46e+3	14%	24%	36%	54%	Low: 14% vs 24%
CH3-CH2-CH[O.]-CH2-CH3 -> CH3-CH2-CHO + CH3-CH2.	18	6.71	1.53e+4	28%	26%	39%	58%	ok
CH3-CH2-CH2-CH[O.]-O-CH3 -> CH3-CH2-CH2. + CH3-O-CHO	21	-6.54	1.45e+8	100%	50%	66%	100%	ok
CH3-CO-O-CH2-CH2-CH[O.]-CH3 -> CH3-CO-O-CH2-CH2. + CH3-CHO	25	5.17	2.41e+4	38%	0%	35%	75%	ok
CH3-CH2-CH2-CH[O.]-O-CH2-CH2-OH -> CH3-CH2-CH2. + HCO-O-CH2-CH2-OH	27	-6.54	1.45e+8	100%	50%	100%	100%	ok
Decomposition Forming R2CH.								
CH3-CH(CH3)-O-CH[O.]-CH(CH3)-CH3 -> CH3-CH[.]-CH3 + CH3-CH(CH3)-O-CHO	31	-6.09	1.14e+10	100%	50%	100%	100%	ok
Decomposition Forming R3C.								
CH3-C(CH3)(CH2O.)-CH3 -> HCHO + CH3-C[.](CH3)-CH3	6	10.40	1.31e+6	98%	75%	98%	100%	ok
Decomposition Forming RO. (Rate constants estimated to minimize bias [Equation (XX)].								
CH3-O-CH2-O-CH2O. -> CH3-O-CH2O. + HCHO	4	13.34	6.50e+3	4%	0%	0%	25%	ok
CH3-C(CH3)(CH3)O-CH2O. -> CH3-C[O.](CH3)CH3 + HCHO	7	14.34	3.09e+3	2%	0%	0%	25%	ok
CH3-O-CH[O.]-O-CH3 -> CH3-O-CHO + CH3O.	10	-1.67	9.07e+8	100%	0%	16%	50%	High: 100% vs 50%
CH3-CH2-O-CH[O.]-CH3 -> CH3-CH2O. + CH3-CHO	13	10.06	7.44e+4	16%	0%	0%	15%	High: 16% vs 15%
CH3-CH(OH)-CH[O.]-O-CH3 -> CH3O. + CH3-CH(OH)-CHO	15	11.49	2.57e+4	0%	0%	0%	15%	ok
CH3-CH[O.]-O-CH2-CH2-OH -> HO-CH2-CH2O. + CH3-CHO	16	10.07	7.39e+4	13%	0%	0%	25%	ok
CH3-CH2-O-CH[O.]-CH2-OH -> CH3-CH2O. + HCO-CH2-OH	17	11.54	2.48e+4	0%	0%	0%	25%	ok

Table 34 (continued)

Reaction Type and Reaction	Rad. [a]	Hr (kcal)	Estimated k (min^{-1})	%	Expt. Fract React. Min	Exp'd	Max	Estimation vs Experimental
CH3-CH2-CH2-CH[O.]-O-CH3 -> CH3O. + CH3-CH2-CH2-CHO	21	10.34	6.04e+4	0%	0%	0%	30%	ok
CH3-CH(CH3)-O-CH[O.]-CH2-OH -> CH3-CH[O.]-CH3 + HCO-CH2-OH	22	12.35	1.36e+4	0%	0%	0%	15%	ok
CH3-C(CH3)(CH3)-O-CH[O.]-CH3 -> CH3-C[O.](CH3)-CH3 + CH3-CHO	23	11.07	3.51e+4	8%	0%	0%	20%	ok
CH3-CH2-CH2-CH[O.]-O-CH2-CH2-OH -> HO-CH2-CH2O. + CH3-CH2-CH2-CHO	27	10.13	7.06e+4	0%	0%	0%	25%	ok
CH3-CH2-CH2-CH2-O-CH[O.]-CH2-OH -> CH3-CH2-CH2-CH2O. + HCO-CH2-OH	28	11.55	2.46e+4	0%	0%	0%	25%	ok
CH3-CH2-O-CH[O.]-CH2-O-CO-CH3 -> CH3-CH2O. + CH3-CO-O-CH2-CHO	29	11.54	2.48e+4	0%	0%	0%	30%	ok
CH3-CO-O-CH2-CH2-O-CH[O.]-CH3 -> CH3-CO-O-CH2-CH2O. + CH3-CHO	30	10.07	7.39e+4	15%	0%	0%	25%	ok
CH3-CH2-O-CO-CH2-CH[O.]-O-CH2-CH3 -> CH3-CH2O. + CH3-CH2-O-CO-CH2-CHO	32	7.99	3.46e+5	0%	0%	16%	20%	ok
CH3-CH2-O-CO-CH2-CH2-O-CH[O.]-CH3 -> CH3-CH2-O-CO-CH2-CH2O. + CH3-CHO	33	10.07	7.39e+4	16%	0%	0%	50%	ok
CH3-C[O.](CH3)-O-CH3 -> CH3-CO-CH3 + CH3O.	36	9.50	1.13e+5	4%	5%	13%	25%	Low: 4% vs 5%
CH3-C[O.](CH3)-O-CH2-CH3 -> CH3-CH2O. + CH3-CO-CH3	39	9.28	1.33e+5	5%	0%	31%	100%	ok
CH3-C[O.](CH3)-O-CO-CH3 -> CH3-CO-CH3 + CH3-CO2.	41	10.73	1.09e+2	21%	10%	24%	50%	ok
CH3-C[O.](CH3)-O-CH2-CH2-OH -> HO-CH2-CH2O. + CH3-CO-CH3	42	9.29	1.32e+5	5%	0%	0%	20%	ok
CH3-CH(CH3)-O-C[O.](CH3)-CH3 -> CH3-CH[O.]-CH3 + CH3-CO-CH3	44	10.09	7.28e+4	3%	0%	0%	20%	ok
CH3-C(CH3)(CH3)-O-C[O.](CH3)-CH3 -> CH3-C[O.](CH3)-CH3 + CH3-CO-CH3	45	10.29	6.27e+4	2%	0%	0%	20%	ok
CH3-CH(CH3)-CH2-O-C[O.](CH3)-CH3 -> CH3-CH(CH2O.)-CH3 + CH3-CO-CH3	46	9.29	1.32e+5	5%	0%	18%	40%	ok
CH3-C(CH3)(OH)-CH2-O-C[O.](CH3)-CH3 -> CH3-C(OH)(CH2O.)-CH3 + CH3-CO-CH3	48	9.29	1.32e+5	5%	0%	0%	25%	ok
Decomposition Forming RCO.								
CH3-CO-CH2O. -> HCHO + CH3-CO.	2	2.59	1.74e+9	0%	75%	100%	100%	Low: 0% vs 75%
CH3-CH2-O-CO-CH2O. -> HCHO + CH3-CH2-O-CO.	5	13.50	1.39e+1	0%	0%	0%	70%	ok
Decomposition forming HCO.								
CH3-C[O.](CHO)-CH2-OH -> CH3-CO-CH2-OH + HCO.	37	-0.66	1.53e+7	94%	75%	100%	100%	ok
Decomposition Forming a-Hydroxy Radicals								
HO-CH2-CH2O. -> HO-CH2. + HCHO	1	11.79	1.11e+5	78%	70%	78%	85%	ok
CH3-CH[O.]-CH2-OH -> HO-CH2. + CH3-CHO	9	6.62	5.19e+6	99%	85%	100%	100%	ok
CH3-CH(OH)-CH[O.]-CH3 -> CH3-CHO + CH3-CH[.]-OH	12	2.87	2.56e+9	100%	100%	100%	100%	ok
CH3-CH(OH)-CH[O.]-O-CH3 -> CH3-CH[.]-OH + CH3-O-CHO	15	-9.80	3.14e+13	100%	80%	100%	100%	ok
CH3-CH2-O-CH[O.]-CH2-OH -> HO-CH2. + CH3-CH2-O-CHO	17	-6.05	6.36e+10	100%	75%	100%	100%	ok
CH3-CH(CH3)-CH[O.]-CH2-OH -> CH3-CH(CHO)-CH3 + HO-CH2.	20	7.15	3.50e+6	91%	50%	71%	90%	High: 91% vs 90%
CH3-CH(CH3)-O-CH[O.]-CH2-OH -> HO-CH2. + CH3-CH(CH3)-O-CHO	22	-6.05	6.36e+10	100%	80%	100%	100%	ok
CH3-CH2-CH2-CH2-O-CH[O.]-CH2-OH -> HO-CH2. + CH3-CH2-CH2-CH2-O-CHO	28	-6.05	6.36e+10	100%	80%	100%	100%	ok
Decompositions Forming ROCH2.								
CH3-CH2-CH[O.]-CH2-O-CO-CH3 -> CH3-CO-O-CH2. + CH3-CH2-CHO	24	8.84	1.57e+3	5%	0%		75%	ok
CH3-CH(CH3)-O-CH2-C[O.](CH3)-CH3 -> CH3-CH(CH3)-O-CH2. + CH3-CO-CH3	47	3.74	6.96e+4	13%	0%	0%	25%	ok
Decompositions Forming ROCH[.]R								

Table 34 (continued)

Reaction Type and Reaction	Rad. [a]	Hr (kcal)	Estimated k (min^{-1})	%	Expt. Fract React. Min	Exp'd	Max	Estimation vs Experimental
CH3-CH(CH2O.)-O-CO-CH3 -> CH3-CO-O-CH[.]-CH3 + HCHO	8	12.81	4.93e+4	59%	25%	100%	100%	ok
								ok
Decomposition Forming RO-CO-CH2. or R-CO-O-CH2.								
CH3-CH2-O-CH[O.]-CH2-O-CO-CH3 -> CH3-CO-O-CH2. + CH3-CH2-O-CHO	29	-3.60	1.63e+7	100%	50%	90%	100%	ok
CH3-CH2-O-CO-CH2-CH[O.]-O-CH2-CH3 -> CH3-CH2-O-CO-CH2. + CH3-CH2-O-CHO	32	-5.80	8.34e+7	100%	50%	84%	100%	ok
Decompositions forming RO-CO.								
CH3-CH2-O-CO-CH2O. -> HCHO + CH3-CH2-O-CO.	5	13.50	1.39e+1	0%	0%	0%	70%	ok
CH3-C[O.](CH3)-CO-O-CH3 -> CH3-CO-CH3 + CH3-O-CO.	40	5.69	4.62e+3	85%	50%	100%	100%	ok
Isomerizations (no -O- or -CO- in transition state ring)								
CH3-CH2-CH2-CH[O.]-O-CH2-CH2-OH -> HO-CH2-CH2-O-CH(OH)-CH2-CH2-CH2.	27		1.96e+5	0%	0%	0%	25%	ok
Isomerizations with -O- or -CO- in transition state ring (3.5 kcal/mole strain energy assumed)								
CH3-C(CH3)(CH3)O-CH2O. -> CH3-C(CH3)(CH2.)O-CH2-OH	7		1.59e+3	1%	0%	0%	25%	ok
CH3-CH2-O-CH[O.]-CH3 -> CH3-CH(OH)O-CH2-CH2.	13		5.31e+2	0%	0%	0%	25%	ok
CH3-CH[O.]-O-CH2-CH2-OH -> CH3-CH(OH)-O-CH2-CH[.]-OH	16		8.80e+4	16%	0%	0%	25%	ok
CH3-CO-CH2-CH[O.]-CH3 -> CH3-CH(OH)-CH2-CO-CH2.	19		2.53e+2	0%	0%	0%	10%	ok
CH3-CH2-CH2-CH[O.]-O-CH3 -> CH3-O-CH(OH)-CH2-CH2-CH2.	21		1.96e+5	0%	0%	0%	30%	ok
CH3-C(CH3)(CH3)O-CH[O.]-CH3 -> CH3-C(CH3)(CH2.)O-CH(OH)CH3	23		1.59e+3	0%	0%	0%	20%	ok
CH3-CH2-CH2-CH[O.]-O-CH2-CH2-OH -> CH3-CH2-CH2-CH(OH)-O-CH2-CH[.]-OH	27		8.80e+4	0%	0%	0%	25%	ok
CH3-CH2-CH2-CH2-O-CH[O.]-CH2-OH -> CH3-CH2-CH[.]-CH2-O-CH(OH)-CH2-OH	28		1.83e+4	0%	0%	0%	25%	ok
CH3-CO-O-CH2-CH2-O-CH[O.]-CH3 -> CH3-CH(OH)-O-CH2-CH[.]-O-CO-CH3	30		2.72e+4	6%	0%	0%	25%	ok
CH3-CH2-O-CO-CH2-CH[O.]-O-CH2-CH3 -> CH3-CH2-O-CO-CH2-CH(OH)-O-CH2-CH2.	32		5.31e+2	0%	0%	0%	20%	ok
CH3-CH2-O-CO-CH2-CH2-O-CH[O.]-CH3 -> CH3-CH(OH)-O-CH2-CH[.]-CO-O-CH2-CH3	33		2.32e+3	0%	0%	0%	50%	ok
CH3-C[O.](CH3)-O-CO-CH3 -> CH3-C(CH3)(OH)-O-CO-CH2.	41		6.72e+1	13%	0%	0%	25%	ok
CH3-C[O.](CH3)-O-CH2-CH2-OH -> CH3-C(CH3)(OH)-O-CH2-CH[.]-OH	42		8.80e+4	3%	0%	0%	20%	ok
CH3-CH(CH3)-O-C[O.](CH3)-CH3 -> CH3-C(CH3)(OH)-O-CH(CH2.)-CH3	44		1.06e+3	0%	0%	0%	20%	ok
CH3-C(CH3)(CH3)-O-C[O.](CH3)-CH3 -> CH3-C(CH3)(CH2.)-O-C(CH3)(OH)-CH3	45		1.59e+3	0%	0%	0%	20%	ok
CH3-CH(CH3)-CH2-O-C[O.](CH3)-CH3 -> CH3-C(CH3)(OH)-O-CH2-C[.](CH3)-CH3	46		2.70e+4	1%	0%	0%	30%	ok
CH3-CH(CH3)-O-CH2-C[O.](CH3)-CH3 -> CH3-C(CH3)(OH)-CH2-O-C[.](CH3)-CH3	47		4.81e+5	87%	75%	100%	100%	ok
Estimates using alternative assumptions (see text)								
Decomposition Forming RO. (Rate constants estimated to best fit data on Table 32 [Equation (XIX)].)								
CH3-O-CH2-O-CH2O. -> CH3-O-CH2O. + HCHO	4	13.34	1.49e+4	9%	0%	0%	25%	ok
CH3-C(CH3)(CH3)O-CH2O. -> CH3-C[O.](CH3)CH3 + HCHO	7	14.34	3.14e+4	17%	0%	0%	25%	ok
CH3-O-CH[O.]-O-CH3 -> CH3-O-CHO + CH3O.	10	-1.67	6.55e+4	0%	0%	16%	50%	ok
CH3-CH2-O-CH[O.]-CH3 -> CH3-CH2O. + CH3-CHO	13	10.06	1.19e+5	0%	0%	0%	15%	ok
CH3-CH(OH)-CH[O.]-O-CH3 -> CH3O. + CH3-CH(OH)-CHO	15	11.49	1.20e+5	1%	0%	0%	15%	ok

Table 34 (continued)

Reaction Type and Reaction	Rad. [a]	Hr (kcal)	Estimated k (min^{-1})	%	Expt. Fract React. Min	Exp'd	Max	Estimation vs Experimental
CH3-CH[O.]-O-CH2-CH2-OH -> HO-CH2-CH2O. + CH3-CHO	16	10.07	1.20e+5	0%	0%	0%	25%	ok
CH3-CH2-O-CH[O.]-CH2-OH -> CH3-CH2O. + HCO-CH2-OH	17	11.54	1.24e+5	0%	0%	0%	25%	ok
CH3-CH2-CH2-CH[O.]-O-CH3 -> CH3O. + CH3-CH2-CH2-CHO	21	10.34	1.70e+5	30%	0%	0%	30%	High: 30% vs 30%
CH3-CH(CH3)-O-CH[O.]-CH2-OH -> CH3-CH[O.]-CH3 + HCO-CH2-OH	22	12.35	2.18e+5	100%	0%	0%	15%	High: 100% vs 15%
CH3-C(CH3)(CH3)-O-CH[O.]-CH3 -> CH3-C[O.](CH3)-CH3 + CH3-CHO	23	11.07	2.92e+5	0%	0%	0%	20%	ok
CH3-CH2-CH2-CH[O.]-O-CH2-CH2-OH -> HO-CH2-CH2O. + CH3-CH2-CH2-CHO	27	10.13	3.03e+5	11%	0%	0%	25%	ok
CH3-CH2-CH2-CH2-O-CH[O.]-CH2-OH -> CH3-CH2-CH2-CH2O. + HCO-CH2-OH	28	11.55	3.41e+5	0%	0%	0%	25%	ok
CH3-CH2-O-CH[O.]-CH2-O-CO-CH3 -> CH3-CH2O. + CH3-CO-O-CH2-CHO	29	11.54	3.51e+5	12%	0%	0%	30%	ok
CH3-CO-O-CH2-CH2-O-CH[O.]-CH3 -> CH3-CO-O-CH2-CH2O. + CH3-CHO	30	10.07	3.57e+5	47%	0%	0%	25%	High: 47% vs 25%
CH3-CH2-O-CO-CH2-CH[O.]-O-CH2-CH3 -> CH3-CH2O. + CH3-CH2-O-CO-CH2-CHO	32	7.99	3.57e+5	46%	0%	16%	20%	High: 46% vs 20%
CH3-CH2-O-CO-CH2-CH2-O-CH[O.]-CH3 -> CH3-CH2-O-CO-CH2-CH2O. + CH3-CHO	33	10.07	3.57e+5	43%	0%	0%	50%	ok
CH3-C[O.](CH3)-O-CH3 -> CH3-CO-CH3 + CH3O.	36	9.50	3.59e+5	48%	5%	13%	25%	High: 48% vs 25%
CH3-C[O.](CH3)-O-CH2-CH3 -> CH3-CH2O. + CH3-CO-CH3	39	9.28	5.45e+5	0%	0%	31%	100%	ok
CH3-C[O.](CH3)-O-CO-CH3 -> CH3-CO-CH3 + CH3-CO2.	41	10.73	6.37e+5	20%	10%	24%	50%	ok
CH3-C[O.](CH3)-O-CH2-CH2-OH -> HO-CH2-CH2O. + CH3-CO-CH3	42	9.29	6.37e+5	20%	0%	0%	20%	ok
CH3-CH(CH3)-O-C[O.](CH3)-CH3 -> CH3-CH[O.]-CH3 + CH3-CO-CH3	44	10.09	6.37e+5	20%	0%	0%	20%	High: 20% vs 20%
CH3-C(CH3)(CH3)-O-C[O.](CH3)-CH3 -> CH3-C[O.](CH3)-CH3 + CH3-CO-CH3	45	10.29	6.41e+5	20%	0%	0%	20%	High: 20% vs 20%
CH3-CH(CH3)-CH2-O-C[O.](CH3)-CH3 -> CH3-CH(CH2O.)-CH3 + CH3-CO-CH3	46	9.29	1.67e+6	2%	0%	18%	40%	ok
CH3-C(CH3)(OH)-CH2-O-C[O.](CH3)-CH3 -> CH3-C(OH)(CH2O.)-CH3 + CH3-CO-CH3	48	9.29	4.38e+9	100%	0%	0%	25%	High: 100% vs 25%
Isomerizations with -O- in transition state ring (Estimates assuming no excess ring strain energy)								
CH3-C(CH3)(CH3)O-CH2O. -> CH3-C(CH3)(CH2.)O-CH2-OH	7		2.15e+5	29%	0%	0%	25%	High: 29% vs 25%
CH3-CH2-O-CH[O.]-CH3 -> CH3-CH(OH)O-CH2-CH2.	13		6.46e+5	80%	0%	0%	25%	High: 80% vs 25%
CH3-CH[O.]-O-CH2-CH2-OH -> CH3-CH(OH)-O-CH2-CH[.]-OH	16		6.46e+5	57%	0%	0%	25%	High: 57% vs 25%
CH3-CO-CH2-CH[O.]-CH3 -> CH3-CH(OH)-CH2-CO-CH2.	19		4.31e+5	13%	0%	0%	10%	High: 13% vs 10%
CH3-CO-CH2-CH[O.]-CH3 -> CH3-CH(OH)-CH2-CO-CH2.	19		9.32e+4	47%	0%	0%	10%	High: 47% vs 10%
CH3-C(CH3)(CH3)O-CH[O.]-CH3 -> CH3-C(CH3)(CH2.)O-CH(OH)CH3	23		6.46e+5	18%	0%	0%	20%	ok
CH3-CH2-CH2-CH[O.]-O-CH2-CH2-OH -> CH3-CH2-CH2-CH(OH)-O-CH2-CH[.]-OH	27		2.15e+5	0%	0%	0%	25%	ok
CH3-CH2-CH2-CH2-O-CH[O.]-CH2-OH -> CH3-CH2-CH[.]-CH2-O-CH(OH)-CH2-OH	28		9.19e+5	63%	0%	0%	25%	High: 63% vs 25%
CH3-CO-O-CH2-CH2-O-CH[O.]-CH3 -> CH3-CH(OH)-O-CH2-CH[.]-O-CO-CH3	30		1.08e+7	95%	0%	0%	25%	High: 95% vs 25%
CH3-CH2-O-CO-CH2-CH[O.]-O-CH2-CH3 -> CH3-CH2-O-CO-CH2-CH(OH)-O-CH2-CH2.	32		3.49e+7	18%	0%	0%	20%	ok
CH3-CH2-O-CO-CH2-CH2-O-CH[O.]-CH3 -> CH3-CH(OH)-O-CH2-CH[.]-CO-O-CH2-CH3	33		7.26e+6	0%	0%	0%	50%	ok
CH3-C[O.](CH3)-O-CO-CH3 -> CH3-C(CH3)(OH)-O-CO-CH2.	41		2.15e+5	0%	0%	0%	25%	ok
CH3-C[O.](CH3)-O-CH2-CH2-OH -> CH3-C(CH3)(OH)-O-CH2-CH[.]-OH	42		1.06e+7	78%	0%	0%	20%	High: 78% vs 20%

Table 34 (continued)

Reaction Type and Reaction	Rad. [a]	Hr (kcal)	Estimated k (min^{-1})	%	Expt. Fract React. Min	Exp'd	Max	Estimation vs Experimental
CH3-CH(CH3)-O-C[O.](CH3)-CH3 -> CH3-C(CH3)(OH)-O-CH(CH2.)-CH3	44		1.89e+8	100%	0%	0%	20%	High: 100% vs 20%
CH3-C(CH3)(CH3)-O-C[O.](CH3)-CH3 -> CH3-C(CH3)(CH2.)-O-C(CH3)(OH)-CH3	45		3.49e+7	92%	0%	0%	20%	High: 92% vs 20%
CH3-CH(CH3)-CH2-O-C[O.](CH3)-CH3 -> CH3-C(CH3)(OH)-O-CH2-C[.](CH3)-CH3	46		3.49e+7	99%	0%	0%	30%	High: 99% vs 30%

[a] Radical number on Table 33

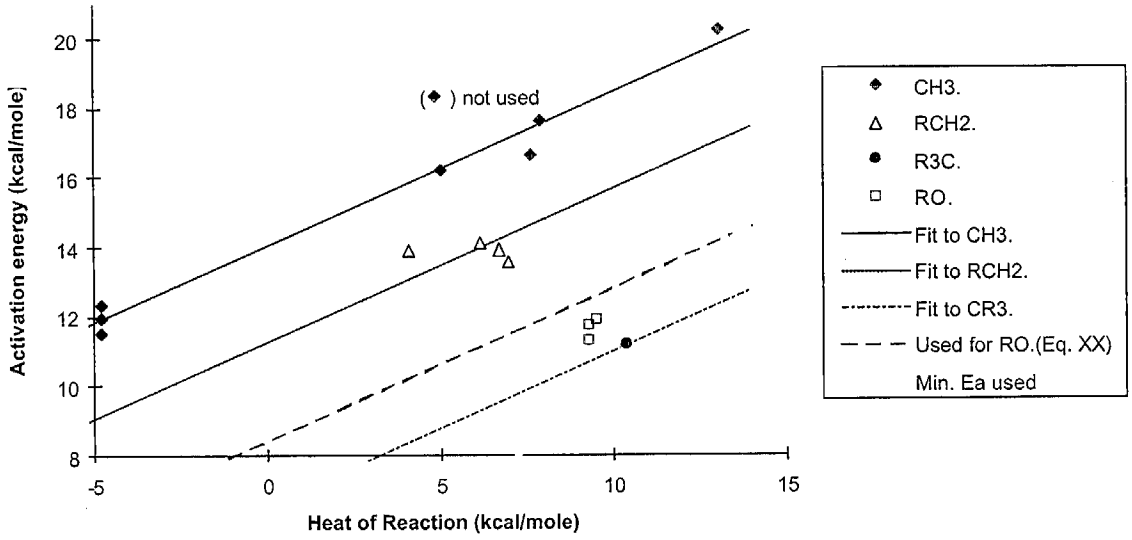

Figure 8. Plots of estimated or measured activation energies vs. heats of reaction for various alkoxy radical decompositions.

fit using EaA = 7.42 kcal/mole, if it is assumed that the same EaB is applicable for reactions assuming these radicals as well. Thus,

$$Ea \text{ (decomp. to } R_3C.) = 6.58 + 0.44\ \Delta H_r \qquad \text{(XVII)}$$

$$Ea \text{ (decomp. to } HOCH_2\cong) = 7.43 + 0.44\ \Delta Hr \qquad \text{(XVIII)}$$

can be used to estimate activation energies for these types of decompositions.

Quantitative information concerning decompositions forming alkoxy radicals is sparse, though as shown on Table 33 and Table 34 there are a number of cases where upper or lower limit estimates can be obtained. As shown on Table 32, the only quantitative information concerns two radicals where decomposition to an alkoxy radical competes with a decomposition forming a methyl radical. If equation (XIII) and (XV) are used to estimate the Arrhenius parameters and thus the rate constants for these competing decompositions to methyl radicals, then the rate constants forming alkoxy radicals can be placed on an absolute basis. If this is assumed, and if the same EaB is used as assumed for the reactions forming alkyl or $HOCH_2\cong$ radicals, then a value of EaA = 7.42 kcal/mole can be derived, i.e.,

$$Ea \text{ (decomp to RO. - initial estimate)} = 7.50 + 0.44\ \Delta H_r \qquad \text{(XIX)}$$

Note that using Equation (XIX) gives a reasonably good fit to the data for the decomposition determined relative to the O_2 reaction, even though this was not used in the derivation of Equation (XIX).

However, although use of Equation (XIX) to predict alkoxy-forming decomposition activation energies gives good fits to the limited quantitative product yield data, Table 34 shows that there are many cases where it results in predictions which are inconsistent with upper limit data concerning the relative importance of this reaction (see "rate constants estimated to best fit data on Table 32" in the "alternative assumptions" section of the table). In particular, use of Equation (XIX) appears to be biased towards overpredicting the relative importance of this reaction. Such a bias is not acceptable as a basis for deriving a general methodology for deriving estimated VOC reaction mechanisms, and if uniformly good predictions cannot be obtained, at a minimum the prediction method should be as likely to underpredict as overpredict.

To obtain unbiased estimates for the relative importances of these decompositions, an optimization was performed to minimize the cases where the estimates were outside of the estimated upper and lower limit ranges, as well as to minimize the discrepancies between estimated and experimental quantitative yield ratios[16]. This optimization was done in two ways: one where EaA was adjusted and EaB was held fixed at the 0.44 value as assumed for the reactions forming alkyl radicals, and the other where both EaA and EaB were optimized. However, the qualities of the fits were not significantly different in either case, so for consistency with the estimates for the other reactions we will only use the data where we assumed EaB = 0.44. The results of this optimization yielded EaA = 8.44 kcal/mole, i.e.,

$$Ea \text{ (decomp to RO. - recommended)} = 8.43 + 0.44\ \Delta H_r \qquad \text{(XX)}$$

This resulted in overpredicting the apparent activation energies for the three alkoxy-forming decompositions on Table 32 by ~1 kcal/mole each, which corresponds to an underprediction of the 298K rate

[16] The data for the $CH_3OCH(O\cdot)OCH_3$ radical, where the estimates appear to fail by orders of magnitude more than was the case for any other radicals, were not used in the optimization.

constant by a factor of ~6. However, use of Equation (XX) for predicting activation energies for alkoxy-forming decompositions is preferred over Equation (XIX) because the latter removes the apparent bias towards overpredicting upper limit rate constants. In particular, this gives only three cases (as opposed to six for Equation XIX) where the prediction is outside the estimation is outside the estimated uncertainty range of the experimental data.

The estimates discussed above do not cover all the types of radicals that may be formed in alkoxy radical decompositions, and methods are needed to estimate EaA values for cases where there are no data. Atkinson (1997b) observed that there is an apparent correlation between the EaA and the ionization potential of the radical formed, and used this to derive a general estimation method for all alkoxy radical decompositions. Plots of the EaA values obtained as discussed above against ionization potential of the radical formed is shown on Figure 9. The IP's used are given in Table 35 and are from the NIST (1994) database. It can be seen that the three points for the alkyl (methyl, ethyl, propyl and t-butyl) radicals are reasonably well fit by a straight line, which is given by

$$\text{EaA (decomp. to hydrocarbon radicals)} = -8.73 + 2.35\ \text{IP} \qquad \text{(XXI)}$$

where EaA is in kcal/mole and IP is the ionization potential of the radical formed in eV. When combined with Equation (XIV), and using EaB = 0.44 as discussed above, this yields

$$\text{Ea (decomp. to hydrocarbon radicals)} = -8.73 + 2.35\ \text{IP} + 0.44\ \Delta H_r \qquad \text{(XXII)}$$

where IP is in eV and Ea and ΔH_r is in kcal/mole. This is close to the general relationship derived by Atkinson (1997a), which is

$$\text{Ea (general decompositions)} = -8.1 + 2.4\ \text{IP} + 0.36\ \Delta H_r. \qquad \text{(XXIII)}$$

The small differences between these equations are due to the fact that in this work the EaB parameter is determined using only the reactions forming methyl radicals, and that Atkinson (1996) did not include the exothermic decompositions of the radicals from the ether systems in his analysis, but did include the reaction forming $HOCH_2\cong$.

Figure 9 shows that Equation (XXI) overpredicts the EaA for the reaction forming $HOCH_2\cong$ by 1.65 kcal/mole, resulting in an underprediction of the 298K rate constant by a factor of ~16. However, it can be argued that the discrepancy is not large considering the data and the assumptions behind the empirical correlations. Equation (XXI) clearly fails in the case of reactions forming alkoxy radicals, overpredicting activation energies by over 4.5 kcal/mole and the decomposition rate constants by three orders of magnitude. For that reason, we conclude that Equations (XXI) should only be used for reactions forming carbon-centered radicals. For substituted radicals the actual data should be used to derive EaA estimates whenever possible.

Based on these considerations, together with the availability of IP data, Equation (XXI) can therefore be used to derive the EaA parameters for decompositions forming secondary alkyl radicals ($R_2CH\cong$), and a modified version of Equation (XXI), where the EaA is reduced by 1.65 kcal/mole so its predictions are consistent with the data for the reaction forming $HOCH_2O\cong$, can be used to estimate EaA for reactions forming $CH_3C(.)OH$. In the case of reactions forming HCO and $RC(O)\cdot$ radicals, predictions that are reasonably consistent with the limited upper and lower limit data (see Table 34) if the EaA predicted using Equation (XXI) is reduced by ~2 kcal/mole. These estimates are given on Table 35, together with the EaA values derived for the decompositions discussed above, and the associated ionization potentials. Obviously, these EaA estimates are the least uncertain for secondary alkyl radicals, are highly uncertain for formyl and acetyl radicals.

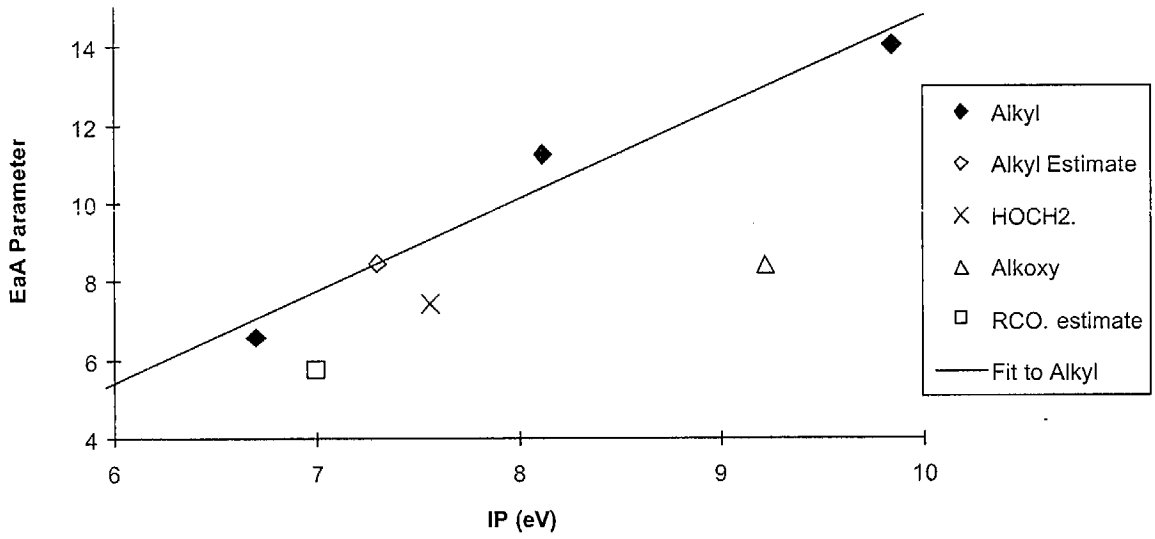

Figure 9. Plots of the EaA parameter used in Equation (XIV) to predict activation energies from heats of reactions for various types of alkoxy radical decompositions vs. the ionization potential of the radical formed. These are based on assuming all lines have the same slope as fits the data for reactions forming methyl radicals.

Available IP data and Equation (XXI) (or the modified version of it) can also be used to derive an EaA for reactions forming $CH_3OCH_2\cong$ radicals, which presumably could also be applied to reactions forming other radicals of the type $ROCH_2\cong$. However, applying this approach to reactions forming these radicals predict that this type of reaction is extremely rapid (having rate constants > 10^9 sec^{-1}) in at least two cases where available data are inconsistent with this reaction dominating (see Table 34 and radicals 24 and 48 on Table 33). Predictions are more consistent with the data if the activation energies are derived assuming the same EaA as employed for reactions forming alkyl $RCH_2\cong$ radicals. For other radicals, Equation (XII) is either not applicable or cannot be used because of lack of available IP data.

For reactions forming substituted alkyl radicals (i.e., reactions forming radicals with non-alkyl substituents) we assume that ß- or further substituents on the radical formed have no effect, and make various estimates concerning the effects of various types of a-substituents, based on highly uncertain assumptions or fits to a very limited data base. In several cases, adjustments were made so the predictions would be consistent with product data or with environmental chamber reactivity data for several compounds. For example, it was initially assumed that decompositions forming $RC(O)O\cong$ radicals have the same parameters as those forming simple alkoxy ($RO\cong$) radicals, but,, as indicated on Table 35, better fits to product and environmental chamber data for several compounds were obtained if a much higher EaA value was used. These estimates, which are obviously very uncertain, are summarized on Table 35.

Although this is not the case with any of the radicals listed on Table 33, there may be cases where Equation (XIV) and the recommended EaA and EaB values may predict unreasonably low or negative

activation energies. For general estimation purposes, we assume a minimum decomposition energy of ~0.75 kcal/mole. Thus if Equation (XIV) predicts a lower activation energy lower than that, 0.75

Table 35. Summary of ionization potentials and EaA parameters used to estimate activation energies for alkoxy radical decompositions from the heats of reactions.

Type of radical Formed [a]	IP [b] (eV)	EaA (kcal $mole^{-1}$)	Derivation of EaA
CH_3.	9.84	14.05	Derived from least squares fits of Ea vs Hr as discussed in the text (Equation (XV). The EaB derived from these data are assumed to be applicable for all alkoxy radical decompositions.
RCH_2.	8.12	11.25	Derived to by adjusting EaA to fit the data as discussed in the text (Equation (XVI).
RCH[.]R	7.30	8.46	EaA is estimated from the IP using Equation (XXI). See text.
R_2C[.]R	6.70	6.58	Derived to by adjusting EaA to fit the data as discussed in the text (Equation (XVII).
RO.	9.22	8.43	Derived to minimize errors and biases in predictions of relative product yield data as discussed in the text (Equation XX).
OH	13.00	8.43	EaA assumed to be the same as derived for decompositions forming alkoxy radicals. This is highly uncertain.
HCO.	~8.8? [c]	9.99	Estimated from the IP using Equation (XXI), with the intercept reduced by 2.0 kcal/mole to give predictions which are more consistent with the limited available upper and lower limit data. Highly uncertain and may be upper limit.
R'C(O).	7.00	5.76	(see above)
R'C(O)O.		12.00	Necessary to assume that decompositions forming RCO2. radicals are slow to be consistent with product data from reaction of OH with isopropyl and t-butyl acetates, and for model simulations to fit chamber data for propylene carbonate. The EaA value used is the lowest value that is consistent with the data for propylene carbonate.
$HOCH_2$.	7.56	7.43	Derived to by adjusting EaA to fit the data as discussed in the text (Equation (XVIII).
RCH[.]OH	6.70	5.41	Estimated from the IP using Equation (XXI), with the intercept reduced by 1.65 kcal/mole to correctly predict the data for the decomposition of HOCH2CH2O. to HOCH2.
R_2C[.]OH		4.21	Ratio of EaA for R_2C[.]OH to R2C[.]R assumed to be the same as ratio of EaA's for RCH[.]OH to RCH[.]R.
R'OCH_2.	6.94	11.25	Better fits to available data are obtained if reactions forming $ROCH_2$. Radicals have the same activation energies as those forming RCH_2 radicals.
RCH[.]OR'		7.46	R'O- substitution assumed to reduce EaA by 1 kcal/mole relative to alkyl substitution to fit data for a minor product from isopropyl acetate. This is highly uncertain, and the data are also consistent with reducing EaA even further.
R_2C[.]OR'		5.58	R'O- substitution assumed to reduce EaA by 1 kcal/mole to be consistent with assumption made when estimating EaA for RCH[.]OR'. This is highly uncertain.
ROC(O).		12.00	Derived to be such that this decomposition is predicted to be minor for CH3-O-CO-CH2-CH[O.]-CO-O-CH3 radicals, but is the dominant process for CH3-C[O.](CH3)-CO-O-CH3, for model predictions to be consistent with environmental chamber reactivity data for dimethyl succinate (DBE-4) and methyl isobutyrate, respectively.
$XC(O)CH_2$.		11.25	For lack of available data, R'C(O)- and HC(O)- substitution is assumed to have no effect on EaA.
RCH[.]C(O)X		8.46	(see above)
R_2C[.]C(O)X		6.58	(see above)

[a] "R" is any substituent where the radical center is bonded to a non-carbonyl carbon. "R'" is any substituent other than H. "X" is any substituent, including H.

Table 35 (continued)

[b] IP data from NIST (1994) and is given for the methyl substituted species except where indicated.

[c] Not in NIST database. Entry of "8.8?" given in Lange's handbook of chemistry (1985).

kcal/mole is used. Although the possibility of a lower minimum cannot be ruled out, the data for the decomposition of neopentoxy and $HOCH_2CH_2O\cong$ radicals tend to rule out the minimum being higher than this.

The above discussion, based on the use of Equation (XIV), incorporates the assumption that the activation energy for the decomposition only depends on the nature of the radical formed and the overall heat of reaction. With appropriate choices of EaA, as shown on Table 35, this gives predictions which, though not always consistent with the data to within the experimental uncertainty, are at least good to within an order of magnitude in most cases. Note that this assumption implies that the activation energy does not depend on the nature of the carbonyl compound that is formed. This appears to work in the case of reactions forming aldehydes, ketones, or esters, which includes most of the reactions listed on Table 33.

However, this assumption appears to fail in the case of reactions where the carbonyl group formed is in an anhydride or carbonate anhydride, i.e., is contained in a -C(O)OC(O)- structure. The data of Tuazon et al (1989b) indicate that the $CH_3C[O.](CH_3)OC(O)CH_3$ radical formed in the reactions of OH radicals with t-butyl and isopropyl acetates (radical 41 on Table 33) decomposes to a significant extent to form acetic anhydride and methyl radicals, while Equation (XIV) and the parameters that fit the data for most of the other methyl radical-forming reactions predict that this reaction is sufficiently slow that the competing isomerization pathway, which is not observed, would dominate[17]. In addition, reactivity and product data recently obtained from a methyl isopropyl carbonate can only be explained if an analogous reaction of a carbonate-containing radical (Radical 43 on Table 33) is much more rapid than predicted by these estimates (Carter et al, 2000d). The data of Tuazon et al (1998b), together with the estimated rate constant for the competing decomposition of $CH_3C[O.](CH_3)OC(O)CH_3$ to acetone and $CH_3CO_2\cdot$, can be predicted if the reactions forming anhydride products have a 2 kcal/mole lower reaction energy than predicted using Equation (XIV), and the methyl isopropyl carbonate environmental chamber data are also better fit if this is assumed.

Therefore, for estimating activation energies for β-scission decompositions that form carbonyl compounds with -C(O)OC(O)- structures, the following modified version of Equation (XIV) is employed:

$$Ea \text{ (decomposition forming } R\cdot + \text{-CO-O-CO-}) = EaA - 2 \text{ kcal/mole} + EaB \cdot \Delta H_r \qquad \text{(XXIV)}$$

where EaA is derived based on the radical, R·, that is formed as shown on Table 35, and the same EaB value is used as assumed for all other reactions. This is obviously uncertain because it is derived based on highly uncertain estimates for competing rate constants, and is based on only a limited number of reactions. However, employing this correction means that the mechanism estimation system gives branching ratio predictions that are consistent with the limited data that are currently available.

[17] The decomposition is predicted to dominate even after the ring strain correction of 3.5 kcal/mole for transition states containing -O- or -CO- groups is added, as discussed in Section III.J.4.

One area where the estimation methods discussed above clearly fails is the predictions of the branching ratios of the $CH_3OCH(O\cdot)OCH_3$ radical (radical 10 on Table 33). The data of Sidebottom et al (1997) indicate that decomposition and O_2 reaction occur at competitive rates (with O_2 reaction being somewhat more important), while the estimation methods derived in this work predict that decomposition will dominate by orders of magnitude. It is unclear whether the problem is with the estimation of the O_2 reaction, the estimates of the decomposition rates, the thermochemical estimates, or (least likely) the experimental data or its interpretation. Until data are available for other similar radicals with similar discrepancies between the estimates and the data, it is unclear what, if any, adjustments may be appropriate. Therefore, estimates for reactions of alkoxy radicals with two alkoxy substituents near the radical center must be considered suspect. However, dimethoxy methane is the only compound of this structure in the current detailed mechanism, and because of the experimental data of Sidebottom et al (1997) it is not necessary to use estimates to determine its mechanism.

The decomposition activation energy and rate constant estimates discussed in this section are obviously highly uncertain in many (if not most) cases, being based in many cases on very uncertain alkoxy + O_2 rate constants, employing many highly uncertain and untested assumptions, and not giving satisfactory predictions in all cases. Clearly, additional data are needed, particularly for reactions of oxygen-containing alkoxy radicals, to test, refine, and improve these estimates and the many assumptions they incorporate. Indeed, it may not be possible to develop a totally satisfactory estimation method that can accurately predict rate constants for the full variety of these reactions, without carrying out detailed theoretical calculations for each system. Thus, rate constants or branching ratios derived from experimental data should always be used whenever possible when developing reaction mechanisms for atmospheric reactivity predictions. However, when no data are available, we have no choice but to use estimates such as those discussed in this section.

4. Isomerization Corrections

As discussed above, when estimating alkoxy radical isomerization rate constants, an additional 3.5 kcal/mole is added to the activation energy if the cyclic transition state contains -O-, -C(O)- or -OC(O)- groups. The need for this correction is shown on Table 34, which compares the experimental and predicted upper and lower limit branching ratios for these isomerizations with and without this correction. It can be seen that if the additional 3.5 kcal/mole is not added to the activation energy, there are 8 cases where isomerization is predicted to be important where the experimental data indicate it is not. This overprediction of the importance of isomerization is removed when the additional 3.5 kcal/mole activation energy is assumed. On the other hand, if a strain energy of greater than that is assumed, then the estimation becomes inconsistent with the observation that the $CH_3CH(CH_3)$-$OCH_2C(O\cong)(CH_3)CH_3$ reacts primarily by isomerization (Stemmler et al, 1997a).

Note that if it is assumed that the reactions of O_2 with the O-substituted alkoxy radicals are much more rapid than estimated in this work, as predicted, for example, by the estimation method of Atkinson (1997a), then many of the competing decompositions would also be predicted to be faster, and this isomerization strain correction may not be necessary. Obviously this isomerization correction, as well as all our estimates concerning the decomposition reactions, would need to be revisited if new data indicate that our estimates concerning these alkoxy + O_2 reactions are incorrect.

5. Ester Rearrangement

Tuazon et al (1998b) and Christensen et al (2000) recently reported data indicating that α-ester-substituted alkoxy radicals undergo a second type of hydrogen shift isomerization, where the hydrogen α

to the alkoxy center shifts, via a 5-member ring transition state, to the ester carbonyl oxygen atom, forming an acid and an acyl radical, e.g.,

$$RCH(O\cdot)\text{-}O\text{-}CO\text{-}R' \rightarrow RC(O)\cdot + O{=}C(OH)\text{-}R'.$$

In order to account for the product data in the reactions of OH + methyl (Christensen et al, 2000) and ethyl (Tuazon et al, 1998b) acetates, it is necessary to assume that this "ester rearrangement" reaction occurs at a non-negligible or rapid rate. Therefore, this reaction must be taken into account when generating mechanisms for esters.

The available data give some limited information upon which to base quantitative estimates for the rate constants for these reactions. In the case of the alkoxy radical formed from methyl acetate [CH_3-CO-O-$CH_2O\cdot$], the product data reported by Christensen et al (2000) indicated that the ester rearrangement occurs at a rate that is about 0.54 times that of the competing reaction with O_2 under ambient conditions. Based on the 298K rate constant for the reaction of O_2 with this radical estimated as discussed in Section III.J.1, this gives a 298K rate constant for the ester rearrangement to be 1.5×10^{-4} sec^{-1}. In the case of the radical formed from ethyl acetate [$CH_3CH(O\cdot)O$-CO-CH_3], the data of Tuazon et al (1998b) indicate that the ester rearrangement dominates over the competing reactions of this alkoxy radical (primarily reaction with O_2 and decomposition to CH_3CHO and $CH_3CO_2\cdot$), which are estimated to have a total rate constant of $\sim 5 \times 10^4$ sec^{-1} under atmospheric conditions. This means that the ester rearrangement for this radical must have a rate constant of at least $\sim 3 \times 10^5$ sec^{-1} under ambient conditions. The differences in these two rate constants can be explained if it is assumed that the ester rearrangement rate constant depends on the heat of reaction. In particular, the ester rearrangement for the radical formed from methyl acetate is estimated to be endothermic by ~3 kcal/mole, while the more rapid ester rearrangement of the radical formed from ethyl acetate is estimated to be endothermic by ~8.4 kcal/mole.

To obtain a rough estimate of temperature dependence, we assume that these ester rearrangements have an A factor of 8×10^{10} sec^{-1}, which is approximately the same as that used for 1,4-H shift isomerizations, based on expected similarities in the structure of the transition states. As with the decomposition reactions discussed above, the activation energy is assumed to linearly dependent on the heat of reaction, i.e.,

$$Ea(\text{ester rearrangement}) = EaA^{cstr} + EaB^{cstr} \cdot \Delta H_r \qquad (XXV)$$

where ΔH_r is the heat of reaction of the rearrangement. Obviously, the one quantitative rate constant derived from the methyl acetate data and the lower limit from the ethyl acetate data are insufficient to uniquely determine EaA^{cstr} and EaB^{cstr}. However, the results of the environmental chamber reactivity experiments for n-butyl acetate (Carter et al, 2000a; see also Section V.B) can only be fit by model simulations if the ester rearrangement for $CH_3CH_2CH_2CH(O\cdot)$-O-CO-CH_3 (radical 26 on Table 33) is of comparable rate or slower than the competing isomerization to $\cdot CH_2CH_2CH_2CH(OH)$-O-CO-CH_3, which means that this ester rearrangement, with an estimated ΔH_r of -8.1 kcal/mole, should have an estimated 298K rate constant of $\sim 3 \times 10^5$ sec-1 or less. To be consistent with this as well as the methyl and ethyl acetate product data discussed above, we assume that

$$EaA^{cstr} = 10.23 \text{ kcal/mole}$$

and

$$EaB^{cstr} = 0.35,$$

which yields

$$k(\text{ester rearrangement}) = 8 \times 10^{10}\ e^{-(10.23+0.35\Delta Hr)/RT} \qquad \text{(XXVI)}$$

Obviously, this is highly uncertain, and more quantitative information concerning relative rates of competing reactions involving this rearrangement, or at least more upper or lower limit data, would significantly reduce the uncertainty of these estimates.

Tuazon et al (1998b) saw no evidence that the analogous ester rearrangement reaction involving a 6-member ring transition state that might be expected to occur in the t-butyl acetate system, e.g.,

$$\cdot OCH_2C(CH_3)_2O\text{-}CO\text{-}CH_3 \rightarrow HC(O)C(\cdot)(CH_3)CH_3 + O{=}C(OH)\text{-}CH_3$$

in fact occurs to any significant extent. Of course, this could be because the competing decomposition to HCHO + $CH_3C(\cdot)(CH3)$-O-CO-CH_3 is predicted to be very fast, with an estimated rate constant of ~3 x 10^7 sec^{-1}. Nevertheless, we tentatively assume that these reactions are not important, and the possibility that they may occur is not presently incorporated in the mechanism generation system. However, the possibility that this occurs needs to be investigated.

6. Acyloxy Radicals

Acyloxy radicals are radicals of the form RC(O)O· or HC(O)O·. It is expected that the decomposition of RC(O)O· to R· and CO_2,

$$RC(O)O\cdot \rightarrow R\cdot + CO_2$$

should be rapid, based on thermochemical considerations, so this is assumed to be its major fate when it is generated in the mechanisms. In the case of HC(O)O·, the it is assumed to be consumed by rapid reaction with O_2.

$$HC(O)O\cdot + O_2 \rightarrow HO_2 + CO_2$$

Although it is also possible that it may primarily decompose to H· + CO_2, under atmospheric conditions the net effect would be the same because the major fate of H· atoms is reaction with O_2, forming HO_2.

7. Explicit Alkoxy Reaction Assignments

Because of the uncertainties in estimating alkoxy radical rate constants, explicit assignments of alkoxy radical rate constants or branching ratios are used rather than estimates whenever there are sufficient data available to make such assignments. These are shown on Table 30 through Table 33, above, where Table 30 contains the explicit assignments for the three measured alkoxy + O_2 reactions, Table 31 shows the assignments used for the butoxy and pentoxy isomerizations, Table 32 shows the assignments for those decompositions where quantitative rate constant assignments could be made, and Table 33 shows the assignments where the available data are appropriate for assigning branching ratios only. Note that many of these are quite uncertain, in most cases being based on highly indirect determinations or adjustments in complex mechanisms to fit reactivity data in chamber experiments, and having highly uncertain, usually estimated, reference rate constants. Note also that the system does not incorporate temperature dependence estimates for those reactions on Table 33 where only branching ratio assignments could be made, so the estimates may not be applicable for temperatures much different from ~300K. Nevertheless, these are less uncertain than the rate constants or branching ratios that have to be based entirely on estimates.

The reactions of isoprene, isoprene products and alkynes involve the formation of radicals whose mechanisms cannot be estimated because of lack of available thermochemical data, so explicit assignments have to be made in those cases so reactions of those compounds could be generated. These assignments are listed on Table 36, along with footnotes indicating the basis for the assignments. Note that those for radicals formed from isoprene and its products are based on estimates incorporated in the isoprene and isoprene products mechanism of Carter and Atkinson (1996), and those for other radicals are based on analogy for reactions of similar radicals for which estimates could be made.

8. Thermochemical Assignments Used in Estimates

Many of the estimates of alkoxy radical rate constants discussed above require a knowledge or estimate of the heats of reaction for the reactions being considered. These are estimated using the group additivity methods of Benson (1976), using updated group additivity data that were obtained primarily from the NIST (1994) thermochemical database. Although that database is extensive, it is not sufficient for many of the reactions that need to be considered, and assignments or estimates for additional groups had to be added. Table 37 and Table 38 give a complete listing of the thermochemical group assignments currently incorporated in the database. Table 37 gives the data obtained from the NIST (1994) database,and Table 38 gives the thermochemical assignments that were added for this work, indicating the source of the assignments.

Note that there were insufficient resources in this project to comprehensively review the available and most up-to-date thermochemical group data, so some of the assignments shown on Table 38 may not necessarily represent the state of the art, and they probably can be improved significantly in some cases. However, given the other uncertainties of the estimation methods discussed above, it is suspected that this probably does not represent the largest source of uncertainty involved, at least in most cases.

The more significant problem with the thermochemical assignment database in the current mechanism generation system is a lack of assignments for certain groups, which limits the overall scope of the mechanism generation system. In particular, the limited number of assignments for halogenated groups (particularly those containing radicals) means that mechanisms cannot be generated for most halogenated compounds. Also, the lack of assignments for unsaturated radicals means the system cannot automatically generate mechanisms for abstraction reactions from alkenes [which are believed to be non-negligible for longer chain alkenes (Atkinson, 1997a)] or reactions of OH or NO_3 radicals with dialkenes. Lack of thermochemical group estimates also prevents mechanisms from being generated for certain highly substituted groups as well. Because of this, improving the thermochemical database must be a priority when this system is updated.

K. Reactions of Crigiee Biradicals

Crigiee biradicals, i.e., species of the type >C[·]OO·, are assumed to be formed in the reactions of O_3 with alkenes or alkynes, and by the reactions of carbenes (which are assumed to be formed in the photolyses of some unsaturated compounds) with O_2. These radicals are believed to be formed with initial vibrational excitation, and can undergo various unimolecular decompositions or be collisionally stabilized. The ranges of excitation energies of the biradicals formed from the reactions of carbenes with O_2 or O_3 with alkynes are almost certainly different from those formed in the reactions of O_3 with alkenes, so in general one might expect the branching ratios for the decomposition and stabilization routes to differ depending on the source of the biradicals. However, because of lack of information concerning the former reactions we assume that they react with the same mechanism as determined from O_3 + alkene systems.

Table 36. Explicit assignments for reactions of alkoxy radicals whose mechanisms could not be estimated.

Radical	Products	Ratio	Notes
Isoprene Intermediates			
HO-CH2-C(CH3)=CH-CH2O.	HO-CH2-CH=C(CH3)-CH[.]-OH		1
HO-CH2-C(CH3)=CH(CH2O.)	HO-CH2-C(CH2.)=CH(CH2-OH)		1
CH2=C(CH2-OH)-CH[O.]-CH2-OH	CH2=C(CHO)-CH2-OH + HO-CH2.		1
CH2=CH-C[O.](CH3)-CH2-OH	CH2=CH-CO-CH3 + HO-CH2.		1
CH3-C(CH2O.)=CH(CH2-OH)	HO-CH2-C(CH3)=CH-CH[.]-OH		1
CH3-C(CH2O.)=CH-CH2-OH	CH3-C(CHO)=CH-CH2-OH + HO2.		1
CH2=C(CH3)-CH[O.]-CH2-OH	CH2=C(CHO)-CH3 + HO-CH2.		1
CH2=CH-C(OH)(CH2O.)-CH3	*C(CH3)(OH)-CH2-O-CH2-CH[.]-*		1
CH2=C(CH3)-CH(CH2O.)-OH	*CH(OH)-C[.](CH3)-CH2-O-CH2-*		1
CH2=CH-CO-CH2O.	HCHO + CH2=CH-CO.		1
Isoprene Product Intermediates			
HCO-CO-CH2O.	HCHO + HCO-CO.		1
.OCH2-CH=C(CH3)-CH2-ONO2	HCO-CH=C(CH3)-CH2-ONO2 + HO2.	80%	1
	HO-CH2-CH=C(CH3)-CH[.]-ONO2	20%	
Alkyne and Diene Intermediates			
CH3-CH[O.]-CO-CHO	CH3-CHO + HCO-CO.		2
CH3-CO-CO-CH2O.	HCHO + CH3-CO-CO.		3
CH2=CH-CH[O.]-CH2-OH	CH2=CH-CHO + HO-CH2.		4
HO-CH2-CH=CH(CH2O.)	HCO-CH=CH(CH2-OH) + HO2.		5
HO-CH2-CH=CH-CH2O.	HO-CH2-CH=CH-CH[.]-OH		6
CH2=CH-CH[O.]-CHO	CH2=CH-CHO + HCO.		7
.OCH2-CH=CH(CH2-ONO2)	HCO-CH=CH(CH2-ONO2) + HO2.		5
.OCH2-CH=CH-CH2-ONO2	HO-CH2-CH=CH-CH[.]-ONO2		6
CH2=CH-CH[O.]-CH2-ONO2	CH2=CH-CO-CH2-ONO2 + HO2.		8

Notes

1 As assumed by Carter and Atkinson (1996).

2 Assumed to be fast by analogy with estimated reactions for CH_3-CH[O.]-CO-R radicals.

3 Assumed to be fast by analogy with estimated reactions for CH_3-CO-CH_2O. radicals.

4 Assumed to be fast by analogy with estimated reactions for R-CH[O.]-CH_2-OH radicals.

5 Assumed to be fast based on lack of facile decomposition routes, and the fact that isomerization would involve a trans cyclic transition state.

6 Isomerization, which is permitted by the cis configuration, is expected to dominate.

7 Assumed to be fast by analogy with estimated reactions for R-CH[O.]-CHO radicals.

8 Reaction with O_2 estimated to be the major route based on the estimated mechanism for CH_3-CH2-CH[O.]-CH_2-ONO_2.

Table 37. Thermochemical group assignments used for estimating heats of reaction for rate constant estimation purposes that were obtained from the NIST (1994) database, or assigned as zero. Estimation methods and notation based on Benson (1976).

Group	kcal/mole	Group	kcal/mole	Group	kcal/mole
		From NIST (1994)			
C*_(C)	39.10	C_(C)(Cd)	-4.76	Cd_(Cd)(Cd)(Cd)	4.60
C*_(C)(C)	40.95	C_(C)(Cd)(O)	-6.50	Cd_(Cd)(Cd)(O)	8.90
C*_(C)(C)(C)	42.60	C_(C)(Cl)	-15.60	Cd_(Cd)(CO)	5.00
C*_(C)(O)	35.10	C_(C)(Cl)(Cl)	-18.90	Cd_(Cd)(CO)(O)	11.60
C*_(CO)	37.90	C_(C)(Cl)(Cl)(Cl)	-24.90	Cd_(Cd)(O)	8.60
C_(*CO)	-5.40	C_(C)(Cl)(F)(F)	-106.30	CO_(C)	-29.10
C_(*CO)(C)	-0.30	C_(C)(Cl)(O)	-21.60	CO_(C)(C)	-31.40
C_(*CO)(C)(C)	2.60	C_(C)(CO)	-5.20	CO_(C)(C*)	-31.40
C_(Br)(Br)(Br)(C)	3.90	C_(C)(CO)(Cl)	-22.00	CO_(C)(Cl)	-47.92
C_(Br)(C)	-5.40	C_(C)(F)	-51.50	CO_(C)(CO)	-29.20
C_(Br)(C)(C)	-3.40	C_(C)(F)(F)	-102.30	CO_(C)(F)	-95.50
C_(Br)(C)(C)(C)	-0.40	C_(C)(F)(F)(F)	-158.00	CO_(C)(I)	-20.00
C_(Br)(C)(Cl)	-10.10	C_(C)(I)	8.00	CO_(C)(O)	-35.10
C_(C)	-10.20	C_(C)(I)(I)	26.00	CO_(Cd)	-29.10
C_(C)(C)	-4.93	C_(C)(NO2)	-14.40	CO_(Cd)(O)	-32.00
C_(C)(C)(C)	-1.90	C_(C)(O)	-8.10	CO_(Cl)(O)	-49.20
C_(C)(C)(C)(C)	0.50	C_(C)(O)(O)	-16.30	CO_(CO)	-25.30
C_(C)(C)(C)(Cd)	1.68	C_(C)(O)(O)(O)	-29.60	CO_(CO)(Cl)	-40.15
C_(C)(C)(C)(Cl)	-12.80	C_(C)(O*)	6.10	CO_(CO)(O)	-29.30
C_(C)(C)(C)(CO)	1.40	C_(C)(O*)	6.10	CO_(O)	-32.10
C_(C)(C)(C)(F)	-48.50	C_(C*)	-10.08	CO_(O)(O)	-29.70
C_(C)(C)(C)(I)	13.00	C_(Cd)	-10.20	N_(C)(F)(F)	-7.80
C_(C)(C)(C)(NO2)	-11.70	C_(Cd)(Cd)	-4.29	O_(C)	-37.90
C_(C)(C)(C)(O)	-6.60	C_(Cd)(CO)	-3.80	O_(C)(C)	-23.20
C_(C)(C)(C)(O*)	8.60	C_(CO)	-10.20	O_(C)(C*)	-23.20
C_(C)(C)(Cd)	-1.48	C_(CO)(Cl)	-10.20	O_(C)(Cd)	-30.50
C_(C)(C)(Cl)	-14.80	C_(CO)(Cl)(Cl)	-12.00	O_(C)(CO)	-43.10
C_(C)(C)(Cl)(Cl)	-22.00	C_(CO)(Cl)(Cl)(Cl)	-11.80	O_(C)(NO2)	-19.40
C_(C)(C)(CO)	-1.70	C_(CO)(CO)	-7.60	O_(C)(O)	-4.50
C_(C)(C)(F)	-49.00	C_(I)(O)	3.80	O_(C*)	-37.90
C_(C)(C)(F)(F)	-97.00	C_(O)	-10.20	O_(Cd)(Cd)	-33.00
C_(C)(C)(I)	10.50	C_(O)(O)	-16.10	O_(Cd)(CO)	-45.20
C_(C)(C)(NO2)	-13.60	Cd_(C)(C)(Cd)	10.34	O_(CO)	-58.10
C_(C)(C)(O)	-7.20	Cd_(C)(Cd)	8.59	O_(CO)(CO)	-46.50
C_(C)(C)(O)(O)	-18.60	Cd_(C)(Cd)(Cd)	8.88	O_(CO)(O)	-19.00
C_(C)(C)(O*)	7.80	Cd_(C)(Cd)(CO)	7.50	O_(NO2)(O)	4.00
C_(C)(C*)	-4.95	Cd_(C)(Cd)(O)	10.30	O_(O)	-16.30
C_(C)(C*)(C)	-1.90	Cd_(Cd)	6.26	O_(O)(O)	14.70
C_(C)(C*)(C)(C)	1.50	Cd_(Cd)(Cd)	6.78		
		Assigned to Zero			
*CO_(C)	0.00	Cl_(C)	0.00	I_(CO)	0.00
*CO_(CO)	0.00	Cl_(CO)	0.00	NO2_(C)	0.00
Br_(C)	0.00	F_(C)	0.00	NO2_(O)	0.00
Br_(C*)	0.00	F_(CO)	0.00	ONO2_(C)	0.00
Br_(CO)	0.00	I_(C)	0.00		

Table 38. Thermochemical group assignments used for estimating heats of reaction for rate constant estimation purposes that were derived for this work. Estimation methods and notation based on Benson (1976).

Group	ΔH_f (kcal/mole)	Documentation
*CO_(O)	-4.20	The C-H bond energy in formates is estimated to be 95 kcal/mole or higher based on an assumed correlation between bond the dissociation energy and CO-H + OH rate constants.
*CO_(ONO2)	-19.40	Calculated from O_(C)(NO2) + *CO_(O), *CO_(O).
C*_(Br)(C)	41.78	Estimated using an assumed correlation between the OH radical rate constants and the bond dissociation energies for alkanes and methanol, and the OH radical rate constant estimated using group additivity.
C*_(C)(C)(CO)	42.25	Estimated assuming that the heat of reaction of CH3-C[.](CH3)-CHO + CH3-CH2-CHO = CH3-CH(CH3)-CHO + CH3-CH[.]-CHO is zero.
C*_(C)(C)(O)	31.50	Estimated assuming that the heat of reaction of CH3-C[.](CH3)OH + CH3-CH(CH3)CH3 + CH3-CH2-OH + CH3-CH[.]-CH3 = CH3-CH(CH3)OH + CH3-C[.](CH3)CH3 + CH3-CH[.]-OH + CH3-CH2-CH3 is zero.
C*_(C)(C)(ONO2)	12.10	Estimated assuming that the heat of reaction of CH3-C[.](ONO2)-CH3 = CH3-C[.](O-NO2)-CH3 is zero.
C*_(C)(CO)	38.58	Estimated assuming that the heat of reaction of CH3-CO-CH2. + CH3-CH2-CO-CH3 + CH3-CH2-CH3 + CH3-CH2-CH[.]-CH3 = CH3-CO-CH3 + CH3-CH[.]-CO-CH3 + CH3-CH2-CH2. + CH3-CH2-CH2-CH3 is zero.
C*_(C)(CO)(O)	32.46	Assumed that the carbonyl group does not affect the C..H bond dissociation energy.
C*_(C)(O)(O)	24.50	Estimated assuming that the heat of reaction of HO-CH(CH3)-OH + HO-CH[.]-CH3 = HO-C[.](CH3)-OH + HO-CH2-CH3 is zero.
C*_(C)(ONO2)	15.70	Calculated from O_(C)(NO2) + C*_(C)(O).
C*_(CO)(O)	34.95	Assumed to be the same as normal primary alcohols, i.e., that carbonyl group does not affect bond dissociation energy.
C*_(CO)(ONO2)	15.55	Estimated assuming that the heat of reaction of HCO-CH[.]-ONO2 = HCO-CH[.]-O-NO2 is zero.
C*_(O)	35.75	This was 33.7 kca/mole in the NIST database. Adjusted to agree with the heat of formation of .CH2OH given by IUPAC (1996)
C*_(O)(O)	29.93	Estimated assuming that the heat of reaction of HO-CH2-OH + HO-CH2. = HO-CH[.]-OH + HO-CH3 is zero.
C*_(ONO2)	16.35	Calculated from O_(C)(NO2) + C*_(O).
C_(*CO)(C)(C)(C)	5.70	CH3-C(CH3)(CH3)-CHO is assumed to have the same CO..H bond dissociation energy as CH3-CH(CH3)-CHO.
C_(*CO)(C)(C)(CO)	3.25	CH3-C(CH3)(CHO)-CO..H is assumed to have the same bond dissociation energy as CH3-CO..H.
C_(*CO)(C)(C)(O)	-0.98	CH3-C(CH3)(OH)CO..H is assumed to have the same bond dissociation energy as CH3-CO..H.
C_(*CO)(C)(CO)	0.15	CH3-CH(CHO)-CO..H is assumed to have the same bond dissociation energy as CH3-CO..H.
C_(*CO)(C)(CO)(O)	-3.85	CH3-C(OH)(CHO)-CO..H is assumed to have the same bond dissociation energy as CH3-CO..H.
C_(*CO)(C)(O)	-1.60	CH3-CH(CHO)-CO..H is assumed to have the same bond dissociation energy as CH3-CO..H.
C_(*CO)(C)(ONO2)	-20.53	CH3-CH(ONO2)-CHO is assumed to have the same (CO)..H bond dissociation energy as CH3-CH2-CHO.

Table 38 (continued)

Group	ΔH_f (kcal/mole)	Documentation
C_(*CO)(CO)	-2.41	HCO-CH2-CHO is assumed to have the same (CO)..H bond dissociation energy as CH3-CH2-CHO.
C_(*CO)(CO)(O)	-4.47	CH3-CH(CHO)-CO..H is assumed to have the same bond dissociation energy as CH3-CO..H.
C_(*CO)(CO)(ONO2)	-23.87	CH3-CH(CHO)-CO..H is assumed to have the same bond dissociation energy as CH3-CO..H.
C_(*CO)(O)	-1.76	CH3-O-CH2-CHO is assumed to have the same (CO)..H bond dissociation energy as CH3-CH2-CHO.
C_(*CO)(O)(O)	-10.70	HO-CH(OH)-CO..H is assumed to have the same bond dissociation energy as CH3-CO..H.
C_(*CO)(ONO2)	-21.17	HCO-CH2-ONO2 is assumed to have same (CO)..H bond dissociation energy as CH3-CH2-CHO.
C_(Br)(C)(CO)	4.00	The heat of reaction for CH3-CH(CHO)-Br + CH3. = CH3-CH(CHO)-CH3 + Br. is assumed to be the same as that for analogous reactions of CH3-CH(Cl)-Br.
C_(Br)(C)(O)	-2.50	The heat of reaction for CH3-CH(OH)-Br + CH3. = CH3-CH(OH)-CH3 + Br. is assumed to be the same as that for analogous reactions of CH3-CH(Cl)-Br.
C_(Br)(C)(O*)	12.50	The heat of reaction for CH3-CH[O.]-Br + CH3. = CH3-CH[O.]-CH3 + Br. is assumed to be the same as that for analogous reactions of CH3-CH(Cl)-Br.
C_(Br)(C*)	-6.67	The heat of reaction for .CH2-CH2-Br + CH3. = .CH2-CH2-CH3 + Br. is assumed to be the same as that for analogous reactions for alkyl groups.
C_(Br)(CO)	-6.27	The heat of reaction for CH3-CO-CH2-Br + CH3. = CH3-CO-CH2-CH3 + Br. is assumed to be the same as that for analogous reactions for alkyl groups.
C_(Br)(O)	-3.70	Estimated assuming that the heat of reaction of Br-CH2O. + CH3-OH = Br-CH2-OH + CH3O. is zero.
C_(Br)(O*)	10.79	The heat of reaction for .OCH2-Br + CH3. = .OCH2-CH3 + Br. is assumed to be the same as that for analogous reactions of CH3-CH(Cl)-Br.
C_(Br)(OO*)	9.30	Estimated assuming that the heat of reaction of Br-CH2OO. + CH3-O-OH = Br-CH2-O-OH + CH3OO. Is zero.
C_(C)(C)(C)(C*)	-1.20	Estimated assuming that the heat of reaction of CH3-C(CH3)(CH3)-CH3 = CH3-C(CH3)(CH3)CH2. + H. is 99.7.
C_(C)(C)(C)(NO2)	-11.70	Note in NIST database: "Benson's value -15.8"
C_(C)(C)(C)(ONO2)	-26.00	Calculated from O_(C)(NO2) + C_(C)(C)(C)(O).
C_(C)(C)(C)(OO*)	5.50	The bond dissociation energy for ROO..H is assumed to be 85.0 based on IUPAC heats of formation for CH3OO. and C2H5OO.
C_(C)(C)(C*)	-3.60	Estimated assuming that the heat of reaction of CH3-CH(CH3)CH3 = CH3-CH(CH3)CH2. + H. is 99.7
C_(C)(C)(C*)(CO)	-0.30	The bond dissociation energy for HO-CH(..H)-C(CH3)(CH3)-CHO is assumed to be the same as that for HO-CH[..H]-CH2-CHO.
C_(C)(C)(C*)(O)	-8.90	Estimated assuming that the heat of reaction of CH3-C(CH3)(OH)-CH2. + CH3-CH(OH)-CH3 = CH3-C(CH3)(OH)-CH3 + CH3-CH(OH)-CH2. Is zero.
C_(C)(C)(C*)(ONO2)	-28.30	Estimated assuming that the heat of reaction of .CH2-C(CH3)(CH3)-ONO2 = .CH2-C(CH3)(CH3)-O-NO2 is zero.
C_(C)(C)(CO)(CO)	-1.47	Estimated assuming that the heat of reaction of HCO-CH(CH3)-CHO + CH3-C(CH3)(CH3)-CHO = HCO-C(CH3)(CH3)-CHO + CH3-CH(CH3)-CHO is zero.
C_(C)(C)(CO)(O)	-5.70	Estimated assuming that the heat of reaction of CH3-C(OH)(CH3)-CHO + CH3-C(CH3)(CH3)CH3 = CH3-C(CH3)(CH3)CHO + CH3-C(OH)(CH3)-CH3 is zero.

Table 38 (continued)

Group	ΔH_f (kcal/mole)	Documentation
C_(C)(C)(CO)(O*)	9.50	Estimated assuming that the heat of reaction of CH3-C(OH)(CH3)CHO + CH3-C[O.](CH3)CH3 = CH3-C[O.](CH3)CHO + CH3-C(OH)(CH3)CH3 is zero.
C_(C)(C)(CO)(ONO2)	-25.10	Estimated assuming that the heat of reaction of CH3-C(CH3)(ONO2)-CO-CH3 = CH3-C(CH3)(O-NO2)-CO-CH3 is zero.
C_(C)(C)(NO2)	-13.60	Notation in NIST database: "Benson's value -15.1"
C_(C)(C)(O)(O*)	-3.40	Assumed to have same O..H bond dissociation energy as that for t-butanol.
C_(C)(C)(O)(ONO2)	-38.00	Calculated from O_(C)(NO2) + C_(C)(C)(O)(O).
C_(C)(C)(O)(OO*)	-6.50	The bond dissociation energy for ROO..H is assumed to be 85.0 based on IUPAC heats of formation for CH3OO. and C2H5OO.
C_(C)(C)(O*)(ONO2)	-23.80	Calculated from O_(C)(NO2) + C_(C)(C)(O)(O*).
C_(C)(C)(ONO2)	-26.60	Calculated from O_(C)(NO2) + C_(C)(C)(O).
C_(C)(C)(OO*)	4.90	The bond dissociation energy for ROO..H is assumed to be 85.0 based on IUPAC heats of formation for CH3OO. and C2H5OO.
C_(C)(C*)(CO)	-3.40	Estimated assuming that the heat of reaction of CH3-CO-CH(CH3)-CH2. + CH3-CH(CH3)-CH3 = CH3-CO-CH(CH3)-CH3 + CH3-CH(CH3)-CH2. is zero.
C_(C)(C*)(CO)(O)	-8.00	Estimated assuming that the heat of reaction of CH3-O-C(CH3)(CHO)-CH2. + CH3-O-C(CH3)(CH3)-CH3 = CH3-O-C(CH3)(CHO)-CH3 + CH3-O-C(CH3)(CH3)-CH2. is zero.
C_(C)(C*)(CO)(ONO2)	-27.40	HCO-C(CH3)(ONO2)-CH3 is assumed to have the same CH2..H bond dissociation energy as HCO-C(CH3)(OH)-CH3.
C_(C)(C*)(O)	-9.50	Assumed to have a C..H bond dissociation energy of 100.
C_(C)(C*)(O)(O)	-21.50	Difference between bond dissociation energy for CH3-C(OH)(OH)-CH(CH3)..H and CH3-C(CH3)(OH)-CH(CH3)..H is assumed to be the same as the difference between bond dissociation energy for CH3-C(CH3)(OH)-CH(CH3)..H and CH3-C(CH3)(CH3)-CH(CH3)..H.
C_(C)(C*)(ONO2)	-28.90	Calculated from O_(C)(NO2) + C_(C)(C*)(O).
C_(C)(Cd)(ONO2)	-25.90	Calculated from O_(C)(NO2) + C_(C)(Cd)(O).
C_(C)(Cl)(O*)	-6.60	The heat of reaction for CH3-CH[O.]-Cl + CH3. = CH3-CH[O.]-CH3 + Cl. is assumed to be the same as those for analogous reactions of compounds with the C_ClHO group.
C_(C)(Cl)(ONO2)	-41.00	Calculated from O_(C)(NO2) + C_(C)(Cl)(O).
C_(C)(CO)(CO)	-4.57	Estimated assuming that the heat of reaction of CH3-CO-CH2-CO-CH3 + CH3-CH2-CH(CH3)-CH2-CH3 = CH3-CO-CH(CH3)-CO-CH3 + CH3-CH2-CH2-CH2-CH3 is zero.
C_(C)(CO)(CO)(O)	-8.57	Estimated assuming that the heat of reaction of HCO-C(CH3)(OH)-CHO + HCO-C(CH3)(CH3)-CH3 = HCO-C(CH3)(CH3)-CHO + HCO-C(CH3)(OH)-CH3 is zero.
C_(C)(CO)(CO)(O*)	6.63	CH3-C[O..H](CHO)-CHO is assumed to have the same bond dissociation energy as CH3-C[O..H](CH3)-CH3.
C_(C)(CO)(O)	-6.32	Estimated assuming that the heat of reaction for CH3-CH2-OH + CH3-CHO = CH3-CH3 + HOCH2-CHO is the same as the heat of reaction for CH3-CH(OH)-CH3 + CH3-CH2-CHO -> CH3-CH(OH)-CHO + CH3-CH2-CH3.
C_(C)(CO)(O)(O)	-17.70	Estimated assuming that the heat of reaction of CH3-O-C(CHO)(CH3)-O-CH3 + CH3-O-C(CH3)(CH3)-CH3 = CH3-O-C(CH3)(CH3)-O-CH3 + CH3-O-C(CHO)(CH3)-CH3 is zero.
C_(C)(CO)(O)(O*)	-2.50	Radicals with this group are assumed to have the same O..H bond dissociation energy as analogous radicals formed from other tertiary alcohols.
C_(C)(CO)(O*)	7.87	An H-O bond dissociation energy of 104.2 is assumed.

Table 38 (continued)

Group	ΔH_f (kcal/mole)	Documentation
C_(C)(CO)(ONO2)	-25.72	Estimated assuming that the heat of reaction of CH3-CH(ONO2)-CO-CH3 = CH3-CH(O-NO2)-CO-CH3 is zero.
C_(C)(NO2)(NO2)	-9.90	Note in NIST database: "DIPPR value -16.5, No Benson H-value, this from iiterature".
C_(C)(O)(O)(ONO2)	-49.00	Calculated from O_(C)(NO2) + C_(C)(O)(O)(O).
C_(C)(O)(O*)	-2.10	The O..H bond dissociation energy is assumed to be the same as that for CH3-CH2-CH2-O..H.
C_(C)(O)(ONO2)	-35.70	Calculated from O_(C)(NO2) + C_(C)(O)(O).
C_(C)(O)(OO*)	-4.20	The bond dissociation energy for ROO..H is assumed to be 85.0 based on IUPAC heats of formation for CH3OO. and C2H5OO.
C_(C)(O*)(ONO2)	-21.50	Calculated from O_(C)(NO2) + C_(C)(O)(O*).
C_(C)(ONO2)	-27.50	Calculated from O_(C)(NO2) + C_(C)(O).
C_(C)(OO*)	3.34	Based on IUPAC heats of formation for CH3-CH2OO.
C_(C*)(Cl)	-18.01	The heat of reaction for .CH2-CH2-Cl + CH3. = .CH2-CH2-CH3 + Cl. is assumed to be the same as for analogous reactions of chloroalkanes.
C_(C*)(CO)	-6.90	The bond dissociation energy for H..CH2-CH2-CHO is assumed to be the same as that for H..CH2-CH2-CH3.
C_(C*)(CO)(O)	-8.02	Estimated assuming that the heat of reaction of HCO-CH(CH2.)OH + CH3-CH(CH3)CH3 = HCO-CH(CH3)OH + CH3-CH(CH2.)CH3 is zero.
C_(C*)(CO)(ONO2)	-27.42	HCO-CH(ONO2)-CH3 is assumed to have same CH2..H bond dissociation energy as HCO-CH(OH)-CH3.
C_(C*)(O)	-9.73	Estimated using heat of formation of n-propyl.
C_(C*)(O)(O)	-18.60	The bond dissociation energy for CH3-O-CH(OH)-CH2..H is assumed to be the same as for CH3-CH(OH)-CH2...H.
C_(C*)(ONO2)	-29.13	Calculated from O_(C)(NO2) + C_(C*)(O).
C_(Cd)(O)	-8.05	Set to give same estimated heat of formation for CH2=CH-CH2-OH as as tabulated by NIST at http://webbook.nist.gov/
C_(Cd)(O*)	5.25	CH2=CH-CH2-OH is assumed to have the same O..H bond dissociation energy as other primary alcohols.
C_(Cd)(OO*)	3.39	The O..H bond dissociation energy in allylic hydroperoxides is assumed to be the same as in alkyl hydroperoxides.
C_(Cl)(Cl)(O*)	-10.10	The heat of reaction of Cl-CH[O.]-Cl + CH3. = Cl-CH[O.]-CH3 + Cl. is assumed to be the same as for analogous reactions for dichlroralkanes.
C_(CO)(CO)(O)	-9.19	Estimated assuming that the heat of reaction of HCO-CH(OH)-CHO + HCO-CH(CH3)-CH3 = HCO-CH(CH3)-CHO + HCO-CH(OH)-CH3 is zero.
C_(CO)(CO)(O*)	5.81	Alcohols forming radicals with this group are assumed to have same O..H bond dissociation energy as other secondary alcohols.
C_(CO)(CO)(ONO2)	-28.59	Derived from the heat of formation of HCO-CH(O-NO2)-CHO.
C_(CO)(O)	-6.95	Estimated assuming Heat of reaction of -CO-CH2-CO- + CH2Cl2 = 2 -CO-CH2-Cl is the same as that for -CO-CH2-CO- + -O-CH2-O- = 2 -CO-CH2-O-.
C_(CO)(O)(O)	-15.42	Estimated assuming that the heat of reaction of HCO-CH(OH)-O-CH3 + CH3-CH(OH)-CH3 = HCO-CH(OH)-CH3 + CH3-CH(OH)-O-CH3 is zero.
C_(CO)(O)(O*)	-1.22	CH3-O-CH(OH)-CO-CH3 is assumed to have the same O..H bond dissociation energy as CH3-CH2-CH2-OH.
C_(CO)(O*)	7.24	Alcohols forming this radical are assumed to have the same O..H bond dissociation energy as CH3-CH2-CH2-O..H Note that this depends on highly uncertain assignment for C_(CO)O.
C_(CO)(ONO2)	-26.36	Calculated from O_(C)(NO2) + C_(CO)(O).
C_(CO)(OO*)	6.05	Estimated assuming that the heat of reaction of CH3-CO-CH2-O-OH + CH3OO. = CH3-CO-CH2OO. + CH3-O-OH is zero.

Table 38 (continued)

Group	ΔH_f (kcal/mole)	Documentation
C_(I)(ONO2)	-15.60	Calculated from O_(C)(NO2) + C_(I)(O).
C_(O)(O)(O)	-26.92	Based on average of the heats of formation of trimethoxy methane as tabulated by NIST at http://webbook.nist.gov/.
C_(O)(O)(O)(O)	-40.25	Based on average of the heats of formation of tetramethoxy methane tabulated by NIST at http://webbook.nist.gov/.
C_(O)(O)(O)(O*)	-25.05	Alcohols forming radicals with this group are assumed to have same O..H bond dissociation energy as other tertiary alcohols.
C_(O)(O)(O*)	-12.72	CH3-O-CH(OH)-O-CH3 is assumed to have the same O..H bond dissociation energy as CH3-O-CH(OH)-CH3.
C_(O)(O*)	-1.90	Alcohols forming radicals with this group are assumed to have same bond dissociation energy as CH3-CH2-CH2-O..H.
C_(O)(ONO2)	-35.50	Calculated from O_(C)(NO2) + C_(O)(O).
C_(O)(OO*)	-4.00	The bond dissociation energy for ROO..H is assumed to be 85.0 based on IUPAC heats of formation for CH3OO. and C2H5OO.
C_(O*)(ONO2)	-21.30	Calculated from O_(C)(NO2) + C_(O)(O*).
C_(ONO2)	-29.60	Calculated from O_(C)(NO2) + C_(O).
C_(OO*)	2.49	Estimated using IUPAC (1996) heats of formation for CH3OOH and CH3OO.
CO_(*CO)	-16.78	RCO-CO..H is assumed to have same bond dissociation energy as R-CO..H.
CO_(*CO)(C)	-20.77	CH3-CO-CO..H is assumed to have the same bond dissociation energy as CH3-CO..H.
CO_(*CO)(O)	-20.78	ROCO-CO..H is assumed to have same bond dissociation energy as RCO..H
CO_(Br)	-25.73	The heat of reaction of HCO-Br + CH3. = HCO-CH3 + Br. is assumed to be the same as analogous reactions of CH3-CH(Cl)-Br.
CO_(Br)(C)	-27.81	The heat of reaction of CH3-CO-BR + CH3. = CH3-CO-CH3 + Br. is assumed to be the same as analogous reactions of CH3-CH(Cl)-Br.
CO_(C)(Cd)	-34.06	Derived to fit the heats of formation for CH2=CH-CO-CH3 in the NIST database at http://webbook.nist.gov/.
CO_(C)(O*)	-39.36	Derived from the IUPAC heat of formation for CH3COOH, and the CRC O..H bond dissociation energy.
CO_(C)(OO*)	-30.91	Derived using the IUPAC heat of formation for CH3-C(O)OO.
CO_(C*)	-29.10	The C..H bond dissociation energy forming radicals with this group is assumed to be the same as CH3-CO-CH2..H.
CO_(C*)(CO)	-31.10	Estimated assuming that the heat of reaction of CH3-CO-CO-CH3 + CH3-CO-CH2. = CH3-CO-CO-CH2. + CH3-CO-CH3 is zero.
CO_(C*)(O)	-34.10	Estimated using correlation between the OH radical rate constants and bond dissociation energies for alkanes and methanol, and the OH radical rate constant estimated using group additivity.
CO_(Cl)	-45.84	The heat of reaction for HCO-Cl + CH3. = HCO-CH3 + Cl. is assumed to be the same as for analogous reaction of R-CO-Cl.
CO_(Cl)(ONO2)	-68.60	Calculated from O_(C)(NO2) + CO_(Cl)(O).
CO_(CO)(CO)	-26.89	The heat of reaction for elimination of CO from CH3-CO-CO-CO-CH3 is assumed to be the same as for elimination of CO from biacetyl.
CO_(CO)(O*)	-33.70	bond dissociation energy for HCO-CO-O..H assumed to be the same as for CH3-CO-O..H and HCO-O..H
CO_(O)(O*)	-34.10	Estimated assuming that the heat of reaction of CH3-CO-OH + CH3-O-CO2. = CH3-CO2. + CH3-O-CO-OH is zero.
CO_(O)(OO*)	-25.51	The bond dissociation energy for CH3-O-CO-OO..H is assumed to be same as for CH3-CO-OO..H.

Table 38 (continued)

Group	ΔH_f (kcal/mole)	Documentation
CO_(O*)	-36.84	Estimated assuming that the heat of reaction of CH3-CO-OH + HCO2. = CH3-CO2. + HCO-OH is zero.
O_(*CO)	-42.64	HCO-OH is assumed to have same (CO)..H bond dissociation energy as CH3-O-CHO.
O_(*CO)(C)	-27.30	The bond dissociation energy for H-CO-O-R is estimated to be relatively high (~100) based on low OH radical rate constants for formates. Highly uncertain.
O_(*CO)(CO)	-30.70	The bond dissociation energy for HCO-O-CO..H is assumed to be the same as that for CH3-O-CO..H.
O_(C)(NO2)	-19.40	Notation in NIST database: "Benson value = -14.9".
O_(C*)(CO)	-40.65	The bond dissociation energy for H...CH2-O-CO- is assumed to be the same as for CH3-CH2..H.
O_(C*)(NO2)	-12.45	Estimated using correlation between the OH radical rate constants and bond dissociation energies for alkanes and methanol, and the OH radical rate constant estimated using group additivity.
O_(C*)(O)	-4.50	Estimated assuming that the heat of reaction of *CH(CH3)-O-C[.](CH3)-O-O-O-* + HO-CH2-CH3 = *CH(CH3)-O-CH(CH3)-O-O-O-* + HO-CH[.]-CH3 is zero.
O_(Cd)	-44.86	Derived to fit the heat of formation of CH2=CH-OH in the NIST database at http://webbook.nist.gov/.
O_(NO2)(O)	4.00	Notation in the NIST database: "Alan Baldwin's value".
O_(O)(O*)	17.50	Estimated assuming that the heat of reaction of CH3-O-O-OH + CH3OO. = CH3-O-O-O. + CH3-O-OH is zero.
O_(O*)(ONO2)	14.00	Calculated from O_(C)(NO2) + O_(O)(O*).
ONO2_(C*)	6.95	Derived from the heat of reaction derived for .CH2-O-NO2.

1. $HCHO_2$ Biradicals

Atkinson (1997a) reviewed available information concerning reactions of O_3 with alkenes, and recommended the following mechanisms for the reactions of excited $HCHO_2$ biradicals:

$$HCHO_2(\text{excited}) + M \rightarrow HCHO_2(\text{stabilized}) \quad (37\%)$$

$$HCHO_2(\text{excited}) \rightarrow HCO + OH \quad (12\%)$$

$$HCHO_2(\text{excited}) \rightarrow CO_2 + H_2 \quad (13\%)$$

$$HCHO_2(\text{excited}) \rightarrow CO + H_2O \quad (38\%)$$

These branching ratios are used in the current mechanism. As indicated in Section II.B.2, the stabilized biradicals are assumed to react primarily with H_2O, forming the corresponding acid, i.e.,

$$HCHO_2(\text{stabilized}) + H_2O \rightarrow HC(O)OH + H_2O$$

2. $RCHO_2$ Biradicals

The reactions of substituted Crigiee biradicals are more uncertain. In the case of excited CH_3CHO_2, the following routes, discussed by Atkinson (1997a), appear to be the most reasonable to consider[18]:

$$CH_3CHOO(excited) + M \rightarrow CH_3CHOO(stabilized) + M \quad (A)$$

$$CH_3CHO_2(excited) \rightarrow CH_3\cdot + CO + OH \quad (B)$$

$$CH_3CHO_2(excited) \rightarrow CH_3\cdot + CO_2 + H\cdot \quad (C)$$

$$CH_3CHO_2(excited) \rightarrow CH_4 + CO_2 \quad (D)$$

Based on examination of the available literature, Atkinson (1997a) recommends assuming branching ratios of 15%, 54%, 17%, and 14% for pathways A-D, respectively. In the case of other substituted biradicals, this scheme can be generalized to

$$RCHOO(excited) + M \rightarrow RCHOO(stabilized) + M \quad (A')$$

$$RCHO_2(excited) \rightarrow R\cdot + CO + OH \quad (B')$$

$$RCHO_2(excited) \rightarrow R\cdot + CO_2 + H\cdot \quad (C')$$

$$RCHO_2(excited) \rightarrow RH + CO_2 \quad (D')$$

Note that Pathway B can account for much of the OH radical formation observed in the reactions of O_3 with 1-alkenes. The measured yields of OH radicals from the reactions of O_3 with 1-butene through 1-octene, as summarized by Atkinson (1997a) (see also Table 18, above), do not appear to be greatly different from that for the reaction of O_3 with propene, suggesting that the branching ratios may not change as the size of the biradical increases.

However, assuming the relatively high branching ratios recommended by Atkinson (1997a) for Pathways B and C results in positive biases in model simulations of the large data base of propene - NO_x environmental chamber experiments, and in significant overpredictions of O_3 formation rates in 1-butene - NO_x and (especially) 1-hexene - NO_x environmental chamber experiments. Although there are other uncertainties in the mechanisms that could be causing these discrepancies, reasonably consistent fits to the data cannot be obtained unless it is assumed that (1) somewhat lower radical yields (i.e., lower yields of Pathways B and C) are assumed for the excited CH_3CHOO reactions than recommended by Atkinson (1997a), and (2) the radical yields (i.e., the yields of Pathways B' and C') decrease as the size of the molecule increases. Note that both assumptions are inconsistent with the observed OH yields in the reactions of O_3 with 1-alkenes (Atkinson, 1997a – see also Table 18, above), so there is an apparent inconsistency between the laboratory measurements of the OH yields in the O_3 + alkene reactions and the results of modeling the 1-alkene - NO_x chamber experiments used to evaluate the mechanism.

The reason for this apparent inconsistency is unknown, and it might be due in part to the fact that NO_x is present in the environmental chamber experiments but not in the laboratory systems used to measure the OH yields. However, the possibility that the problems with modeling the 1-alkene chamber experiments using the Atkinson (1997a)-recommended branching ratios are due to other problems with

[18] Two other routes, involving formation of $CH_3O\cdot$ + HCO and CH_3OH + CO, are also given by Atkinson (1997a), but are not considered here because they do not involve chemically reasonable transition states for vibrationally excited molecules.

the mechanism certainly cannot be ruled out. Nevertheless, satisfactory fits to the available data cannot be obtained even after adjusting or making reasonable modifications in the other uncertain aspects of the alkene photooxidation mechanisms. Because the objective of this project is to develop a mechanism that correctly predicts O_3 reactivities and other impacts of VOCs in simulated smog systems, it is necessary to use branching ratios that give predictions that are consistent with the large environmental chamber data.

The adjusted branching ratios for the reactions of excited $RCHO_2$ biradicals that are used in the current version of the mechanism are summarized on Table 39. As shown there, to fit the chamber data the biradicals are assumed to be increasingly likely to be stabilized as the size of the "R" substituent on the radical is increased. For this purpose, the "size" of the substituent is defined as the number of groups used by the mechanism generation system to define the substituent, as indicated in Table 5, above. Note that for biradicals formed from unsubstituted alkenes the number of groups is the same as the number of carbons. Footnotes to the table indicate the rationalizations for the particular sets of branching ratios used.

3. R_2COO Biradicals

Available information on OH yields from reactions of O_3 with alkenes such as isobutene, 2-methyl-2-butene, 2,3-dimethyl-2-butene and other compounds (Atkinson, 1997a – see also Table 18, above) are most easily rationalized if it is assumed that most excited R_2COO react forming OH radicals in near-unit yields. In contrast with the case with 1-alkenes, model simulations assuming high radical yields in the reactions of O_3 with such alkenes are also reasonably consistent with the available chamber data, at least in the case of isobutene and several of the terpenes that are expected to form this type of biradical (see Section V and Appendix B). If one of the R groups has an α hydrogen, the reaction is assumed to proceed via rearrangement to an unsaturated hydroperoxide, which subsequently decomposes (Atkinson, 1997a):

$$>CH\text{-}C(\cdot)(OO\cdot)R \rightarrow >C=C(OOH)R \rightarrow >C=C(O\cdot)R + OH$$

$$>C=C(O\cdot)R \leftrightarrow >C(\cdot)C(O)R$$

Although other reactions probably occur to some extent, this is assumed to be the dominant reaction pathway for R_2COO biradicals which have the necessary α hydrogen. It may be that this reaction also occurs with the stabilized biradical, which may explain why there is no indication of decreased OH yield as the size of the molecule increases.

If the two substituents on the biradical are different and both have abstractable α hydrogens, then two possible OH-forming reactions can occur. In these cases, we estimate that the branching ratio is roughly proportional to the ratio of OH radical abstraction from the abstracted α hydrogens involved. This is uncertain because there is no experimental basis for this estimate.

The above mechanism cannot occur for those disubstituted Crigiee biradicals that do not have substituents with α hydrogens. It is also considered to be unlikely if the only substituent(s) with α hydrogens are -CHO groups, since it is expected that formation of a ketene hydroperoxide intermediate would involve a strained transition state. In those cases (which probably do not occur in many cases for the VOCs currently considered in the mechanism), we arbitrarily assume that 90% is stabilized and 10% decomposes to $CO_2 + 2\ R\cdot$.

Table 39. Adjusted branching ratios used for the reactions of excited $RCHO_2$ biradicals..

Pathway		Branching Ratio				
Number of Groups in R.		1	2	3	4	5+
Stabilization -> RC(O)OH	(A)	34%	89%	92%	95%	100%
R. + CO + OH	(B)	52%	11%	8%	5%	0%
R. + CO2 + H	(C)	0%	0%	0%	0%	0%
RH + CO2	(D)	14%	0%	0%	0%	0%
Notes		1	2	3	4	5

Notes

1 OH yield and methane formation (Pathways B and D) approximately as recommended by Atkinson (1997a). Radical formation from Pathway C is assumed to be negligible to improve fits of model simulation to propene - NOx chamber experiments, and fraction of stabilization (Pathway A) is increased accordingly.

2 Radical formation from Pathway (C) is assumed to be negligible and OH formation from Pathway (B) is reduced to improve fits of model simulations to 1-butene - NOx chamber experiments. Rest of reaction is assumed to be stabilization.

3 Branching ratios intermediate between those derived for the 1-butene and 1-hexene systems.

4 Model simulations are most consistent with results of 1-hexene - NOx chamber experiments if radical formation from the reactions of this biradical is assumed to involve no more than ~5% radical formation routes. The rest of the reaction is assumed to involve stabilization.

5 100% stabilization is assumed by extrapolation from the mechanisms assumed for the smaller biradicals.

4. Assigned Reactions of α-Carbonyl or Unsaturated Crigiee Biradicals

Carter and Atkinson (1996) gave estimated mechanisms for several α-carbonyl or unsaturated Crigiee biradicals that are different from the general mechanisms discussed above. In most cases, these are adopted in this work. These are summarized on Table 40. Note that the reactions shown for HC(O)CHOO, CH_2=CHCHOO, and CH_2=C(CH_3)CHOO are assigned mechanisms applicable for those biradicals only, while that shown for RC(O)CHOO is a general mechanism that is derived based on the mechanism assumed by Carter and Atkinson (1996) for $CH_3C(O)CHOO$, but is assumed to be applicable for all radicals of this type, regardless of the nature of the "R" group.

5. Stabilized Crigiee Biradicals

As discussed above, the major fate of stabilized Crigiee biradicals with α-hydrogens is assumed to be reaction with H_2O, forming the corresponding acid. This is consistent with the rate constant ratios cited by Atkinson (1997a) for the reactions of $HCHO_2$ with H_2O, HCHO, CO, and NO_2. The mechanism for the reactions of stabilized $HCHO_2$ with water appear to be complex and may involve some formation of H_2O_2 or other peroxides, but based on the discussion of Atkinson (2000) we assume that these competing processes are relatively minor compared to acid formation.

Table 40. Assigned mechanisms for the reactions of excited α-carbonyl or unsaturated Crigiee biradicals.

Reactant and Products	Factor	Documentation
R-CO-CHOO[excited]		
R-COO[excited]-CHO	100.0%	O-shifts of alpha-carbonyl biradicals, via a primary ozonide transition state, are assumed to be rapid if they form a more substituted biradical (Carter and Atkinson, 1996)
CH2=C(CH3)-CHOO[excited]		
CO2 + CH2=CH-CH3	25.0%	As assumed by Carter and Atkinson (1996).
CH2=C(CHOO[stab])-CH3	75.0%	See above.
CH2=CH-CHOO[excited]		
CO2 + CH2=CH2	25.0%	Assumed to be analogous to mechanism assumed for methyl-substituted radical formed from O3 + isoprene (Carter and Atkinson, 1996).
CH2=CH-CHOO[stab]	75.0%	See above.
HCO-CHOO[excited]		
CO + HCO. + OH	50.0%	Assumed that decomposition is much more facile than in the CH3-CHOO[excited] case because of the weaker H..CO and C..CO bonds. The two most likely decomposition routes are arbitrarily assumed to have equal probability.
HCO2. + HCO.	50.0%	See above.

The current mechanism does not predict significant formation of stabilized Crigiee biradicals that lack α hydrogens because as discussed in III.K.3 the excited precursor biradicals are assumed to primarily decompose. The only exceptions are R_2COO biradicals that lack the β-hydrogens needed to undergo the hydroperoxide rearrangement, which are rarely formed. The subsequent reactions of the stabilized biradicals of this type are ignored in the current mechanism.

L. Lumping Assignments

Once the reactions of a given VOC with OH, NO_3, O_3, etc. have been fully generated, the system summarizes the overall yields of all products (including the $NO \rightarrow NO_2$ conversion operator), so that each initial reaction of the VOC in the presence of NO_x can be represented by one overall process

$$X + VOC \rightarrow p_1\ HO_2 + p_2\ (NO \rightarrow NO_2\ \text{conversions}) + \Sigma_i\ p_i\ \text{Product}_i$$

Here X refers to the species reacting with the VOC (OH, hν, etc.), product_i represents each of the products that are formed, and p_i represents its overall yield. Since many hundreds and even thousands of products might be formed in the reactions of larger molecules, it is clearly not possible that they all be represented explicitly in the model simulations. As discussed in Section II.C, above, the current mechanism represents most oxidation products using a limited number of model species based on various "lumped molecule" assignments.

These assignments, which provide the interface between the mechanism generation system discussed above and the base mechanism discussed in Section II, are summarized on Table 41. For each product that is formed in the overall reaction, the system checks the "lumping rules" associated with each model species in the order they are given on this table, and assigns the product to the first model species on the list whose associated rules describe the products being considered. Note that the last model species on the list is "INERT", which means that if the product satisfies none of the other criteria, it is treated as unreactive in the model. The total yield of each of the model species formed in the overall reaction are then summed up, and the overall reaction is then recast into the form

$$X. + VOC \rightarrow m_1\ HO2. + m_2\ RO2\text{-}R. + m_3\ R2O2. + \sum_i m_i\ ModSpe_i$$

where HO2., RO2-R., R2O2., or $ModSpe_i$ are model species in the base mechanism (see Table A-1 in Appendix A), and m_1, ..., m_i are their corresponding yields. Reactions expressed in this way can be inserted directly into the mechanism, or the values of the overall rate constant and product yield parameters (the set of m_i's) can serve as a basis for deriving parameters for lumped parameter species used to represent the compound in complex mixtures (see Section VI).

Although most of Table 41 is reasonably self-explanatory, some explanation is needed concerning how overall yields of HO2., RO2-R., R2O2., and RO2-N. are determined. In the case of RO2-N., just determining if the product contains a nitrate (-ONO2) group is not always appropriate, since the starting reactant itself may contain nitrate groups, and nitrate-containing species are formed when NO_3 reacts with double bonds. Because of this, the system stores a flag with the product log whenever a RO_2+NO reaction forming a nitrate is generated, which can be used to determine if it is appropriate to represent the product by RO2-N. In the case of HO2., RO2-R., and RO2-N., the total yields are computed from the total HO_2 and total $NO \rightarrow NO_2$ counts as follows:

Condition:	[Total HO_2] ≥ [Total $NO \rightarrow NO_2$]	[Total $NO \rightarrow NO_2$] > [Total HO_2]
HO2. Yield =	[Total HO_2] - [Total $NO \rightarrow NO_2$]	0
RO2-R. yield =	[Total $NO \rightarrow NO_2$]	[Total HO_2]
R2O2. Yield =	0	[Total $NO \rightarrow NO_2$] - [Total HO_2]

Note that this is an approximate treatment, since the system lumps HO_2 that is formed with no NO to NO_2 conversions (e.g., in reactions of alcohols forming α-hydroxy alkyl groups) with extra NO to NO_2 conversions from another reaction pathway. However, the effect of this approximation should be small, and would only be non-negligible under low NO_x conditions where peroxy + peroxy reactions convert with NO to NO_2 conversion processes.

M. Generation of Mechanisms of Major Reactive Products

The representation of the major reactions of the oxidation products formed when a VOC reacts can have a significant impact on the calculated atmospheric impacts of the VOC if these products are sufficiently reactive. As discussed above, the standard method for representing the VOC's reactive oxidation products is to use the set of explicit or lumped product model species as discussed above. This obviously introduces inaccuracies in cases where the reactivities of the actual products formed are different than those of the model species used to represent them. These inaccuracies are minimized if a sufficiently comprehensive set of model species are used to represent the variety of types of organic products that can be formed, but they can never be completely eliminated unless fully explicit mechanisms are used.

Table 41. Summary of lumping assignments used to determine how individual explicit product species are represented in the base mechanism.

Model Species	Structure or Lumping Criteria
Radical Operators (see text)	
RO2-N.	Any organic nitrate that is formed in a RO2 + NO reaction
Total HO2	HO2.
Total NO → NO2	NO → NO2 conversion operator
Explicit Radicals	
CCO-O2.	CH3-CO[OO.]
C-O2.	CH3OO.
HO.	OH
Cl.	Cl.
TBU-O.	CH3-C[O.](CH3)-CH3
Lumped Radicals	
MA-RCO3.	Any compound containing a C=C double-bonded group next to a CO[OO.] group.
RCO-O2.	Any other compound containing a CO[OO.] group.
Explicit Products	
HNO3	HNO3
NO2	NO2
CO	CO
CO2	CO2
HCHO	HCHO
ACET	CH3-CO-CH3
GLY	HCO-CHO
HCOOH	HCO-OH
CCO-OH	CH3-CO-OH
Lumped Products	
CCHO	CH3-CHO or HO-CH2-CHO
RCHO	Any other compound containing a -CH2-, >CH- or >C< group next to a -CHO group.
MGLY	Any compound containing a -CO- next to a -CHO group.
BACL	Any compound containing a -CO- next to another -CO- group.
METHACRO	CH2=C(CHO)-CH3 or CH2=CH-CHO
MVK	Any compound containing CH2=CH-CO- groups except as indicated above.
ISOPROD	Any compound containing a C=C double-bonded group next to a -CHO or -CO- group except as indicated above, or 3-methyl furan.
RNO3	Any compound containing a -ONO2 group that reacts with OH faster than 5×10^{-13} cm^3 $molec^{-1}$ s^{-1}, that is not formed in a peroxy + NO reaction.
XN	Any other compound containing a -ONO2 group except as indicated above.
PROD2	Anything that reacts with OH faster than 5×10^{-12} cm^3 $molec^{-1}$ s^{-1}, except as indicated above.
RCO-OH	Any compound other than those listed above containing a -CO- group next to a -OH group. (Note that acids with $kOH > 5 \times 10^{-12}$ cm^3 $molec^{-1}$ s^{-1} are lumped with PROD2.)
MEK	Anything that reacts with OH faster than 5×10^{-13} cm^3 $molec^{-1}$ s^{-1}, except as indicated above.
INERT	Anything not satisfying any of the above criteria.

The ideal situation would be to represent all the major reactive products explicitly, but this is not practical because of the thousands of types of oxidation products that can be formed from the hundreds of types of VOCs emitted into actual atmospheres. A more practical solution is to derive the kinetic and mechanistic parameters of the lumped model species used to represent the particular set of products that they are being represented in any particular model application. As discussed in Section II.C.2, above, this approach is in fact used to derive the parameters for the PROD2 and RNO3 model species, *based on the assumption that the mixture of VOCs in the model simulation is reasonably well represented by the* "Base ROG mixture" used in the atmospheric reactivity calculations (Carter 1994a,b). In principle, the methods discussed in Section II.C.2 can be used to derive the appropriate PROD2 or RNO3 parameters for any mixture of VOCs, though the software to do this routinely has not yet been developed.

Adjusting the parameters for the lumped product species to be appropriate for modeling particular ambient mixtures does not necessarily solve the problem of inaccuracy in representing the products formed from individual VOCs when assessing their reactivities. This is because at least some types of individual VOCs whose reactivities are of interest may in some cases form quite different types of products than the mixture of VOCs that dominate current atmospheres. Therefore, use of standard mechanisms for lumped reactive products such as PROD2 or RCHO may not be the optimum representation of the reactions of the major products from such VOCs.

One approach to address this problem is to use the mechanism estimation and generation system to derive the mechanisms for the major products formed from any VOC whose reactivity is being assessed, and then represent the reactions of these products explicitly in the model. This is obviously not practical for representing all reacting VOCs in a model simulation, but may be feasible if only one VOC is of particular interest, such as in reactivity assessment calculations. This approach can be used if the VOC and its major product reactions can be processed using the current mechanism generation system, and if the VOC forms a manageable number of major reactive products. Furthermore, the latter requirement can be eliminated if products of similar reactivity ranges are lumped together and represented by lumped product model species whose parameters are derived based on the specific mixture of products from the VOC.

To address these issues, two separate mechanisms are derived for VOCs whose product reactions can be processed using the mechanism generation system. The "standard" or "lumped product" (LP) mechanisms are those derived as discussed in the previous sections, where all the VOC products are represented only using the standard set of model species described in Section II.C, as shown on Table 41. In the "adjusted product" (AP) mechanisms, the more reactive VOC products are represented using separate model species whose mechanisms are derived to represent the specific set of products predicted to be formed. Because of the large number of products predicted to be formed from some VOCs, the individual products are not all represented separately, but are used as the basis for deriving adjusted kinetic and mechanistic parameters for the lumped model species used to represent these products. Note that these adjusted mechanism lumped products are associated with the specific individual VOCs forming them, and are distinct from the lumped model species used to represent the products from the mixtures of other VOCs present in the simulation. Models that use adjusted product mechanisms for a VOC must include model species not only for the VOC itself, but also for the adjusted lumped product species used to represent their major reactive products.

The VOC mechanism listing in Table A-6 in Appendix A gives each of these mechanisms for all VOCs where this is applicable, as well as the mechanisms used for the major products in the adjusted product versions. The adjusted product (AP) mechanism is used in the reactivity assessment calculations for the individual VOCs (discussed in Section VII) and also in the simulations of the chamber

experiments for evaluating individual VOC mechanisms, as discussed in Section V. The lumped product (LP) mechanism is used in all other applications, such as representing the VOC when present in mixtures as discussed in Section VI. If no separate AP or LP mechanism is given for a VOC, it means that either an adjusted product mechanism could not be generated, or that the mechanism generation system determined that the major reactive products are adequately represented by the standard set of organic product model species. In these cases the same mechanism is used in reactivity or mechanism evaluation calculations as are used when representing the VOC in mixtures.

The mechanism generation system employs the following procedure to derive the adjusted product mechanisms for reactivity assessment of VOCs. Note that the first step is the same as employed when generating the lumped product version of the mechanism.

- The fully explicit mechanisms for the NO_x-air reactions of the subject VOC is generated, as discussed in Section III.A, and the lumped product model species corresponding to each of the explicit products that are predicted to be formed are determined.
- The products that are already adequately represented by the existing set of model species, or that are judged to have relatively low reactivity and thus not significantly affect the overall reactivity of the parent VOC, are represented in the same way as in the lumped product mechanism. The former includes compounds that are already represented explicitly (e.g., formaldehyde) or that are used as the basis for deriving the mechanism of the lumped model species used to represent them (e.g., propionaldehyde and methyl glyoxal). The latter include products that are represented by MEK, RCO-OH, RNO3, or INERT in lumped product mechanisms.
- The products that are represented by "reactive" lumped product model species (i.e., PROD2, RCHO, MGLY, BACL, METHACRO, ISO-PROD or MVK) are used to derive the mechanisms for adjusted versions of those model species that are specific to the individual VOC. If the VOC reacts in more than one way (e.g., reacts with O_3, NO_3, etc. as well as with OH), then separate model species are used to represent products from the different reactions, unless the products are exactly the same. These separate model species are given the name PRD1, PRD2, etc., starting with the reactive products formed in the OH reaction.
- The mechanisms of these VOC-specific product model species are derived by generating the mechanisms of all the individual compounds that they represent, deriving the lumped product representations of these mechanisms as discussed in Section III.L, and then determining the average kinetic and product yield parameters, weighted by the relative yields of the products. To minimize unnecessary processing for VOCs that form large numbers of products in very low yields, products with total yields of less than 2.5% are not used when computing the parameters for the VOC-specific lumped products. If all the products represented by a given type of model species are formed in less than 2.5% yield, then the standard lumped parameter model species is used, i.e., no separate VOC-specific product model species is created.
- The overall reaction mechanism of the VOC is then given in terms of yields of the standard lumped products representing the low reactivity VOCs and yields of the VOC-specific adjusted product model species derived as discussed above. Since the mechanisms of these adjusted product model species are in general different for each VOC, the mechanisms for these must also be specified as part of the overall adjusted product mechanism of the VOC. These are shown in Table A-6 in Appendix A for all VOCs for which explicit product mechanisms can be derived.

An illustrative example can be shown in the case of 2-hexanone, which can react with OH and by photolysis. The reactive products formed when generating the mechanism for this compound are as follows:

OH Products Represented by PROD2	Yield
$CH_3C(O)CH_2C(O)CH_2CH_2CH_2OH$	22.6%
$CH_3CH_2C(O)CH_2CH_2C(O)CH_3$	7.2%
$CH_3CH_2CH_2C(O)CH_2C(O)CH_3$	4.8%
$CH_3C(O)CH_2CH_2CH_2C(O)CH_3$	0.1%
OH Products Represented by RCHO	**Yield**
CH_3CH_2CHO	14.0%
$CH_3C(O)CH_2CHO$	13.8%
$CH_3CH(OH)CH_2CH_2CHO$	10.4%
$CH_3CH_2CH_2CH_2CHO$	9.2%
$CH_3CH_2CH_2CHO$	8.6%
$CH_3C(O)CH_2CH(OH)CH_2CH_2CHO$	1.6%
$CH_3C(O)CH_2CH_2CHO$	1.3%
Photolysis Products Represented by RCHO	**Yield**
$CH_3CH(OH)CH_2CH_2CHO$	87.4%

It can be seen that three adjusted product model species need to be used in the 2-hexanone adjusted product mechanism, one each to represent the PROD2 and RCHO products of the OH reaction and one to represent the RCHO product from the photolysis. These are as follows:

- The PRD1 model species is created to represent the PROD2 products from the OH reaction, with its yield set at 34.7%, and its mechanism is derived by generating those for $CH_3C(O)$-$CH_2C(O)CH_2CH_2CH_2OH$, $CH_3CH_2C(O)CH_2CH2C(O)CH_3$, and $CH_3CH_2CH_2C(O)CH_2C(O)CH_3$, with using weighting factors of 65.3%, 20.8%, and 13.9%, respectively. The contribution by $CH_3C(O)CH_2CH_2CH_2C(O)CH_3$ being ignored because its yield is less than 2.5%.
- The propionaldehyde (CH_3CH_2CHO) formed in 14% yield in the OH reaction is already well represented by the standard RCHO model species, since its mechanism is derived based on that of propionaldehyde (see Section II.C.2). Therefore, this product is represented by the formation of the standard RCHO model species in 14% yield. The PRD2 model species is created to represent the other OH products represented by RCHO, with a yield set at 44.9%. Its mechanism is derived based on the generated mechanisms for $CH_3C(O)CH_2CHO$, $CH_3CH(OH)CH_2CH_2CHO$, CH_3CH_2-CH_2CH_2CHO, and $CH_3CH_2CH_2CHO$ with weighting factors determined by their relative yields. The mechanisms for the other two products are not used because their yields are less than 2.5%.
- The PRD3 model species is created to represent the formed in the photolysis reaction that would otherwise be represented by RCHO, with a yield of 87.4% and a with the mechanism generated for $CH_3CH(OH)CH_2CH_2CHO$.

These mechanisms are shown on Table A-6 in Appendix A as the "AP" mechanism for 2-hexanone. Analogous procedures are used to generate the adjusted product mechanisms for the other VOCs whose product reactions can be processed using the mechanism generation system.

IV. PARAMETERIZED MECHANISMS

The mechanism generation system discussed in the previous system cannot be used for VOCs where the nature of the radical intermediates are unknown, or that involve formation of intermediates that cannot be processed by the present system. These include the aromatics (whose intermediates are highly uncertain and almost certainly involve highly unsaturated radicals for which thermochemical estimates cannot be made), terpenes (whose polycyclic structure cannot be represented by the current system), halogenated compounds (for which insufficient thermochemical information is available on the current database implemented with the system), and compounds containing groups, such as amins, for which general estimation methods have not been developed.

These VOCs must continue to be represented by parameterized or highly simplified mechanisms, as is the case in other mechanisms and previous versions of this mechanism. The representation and mechanisms used in these cases are discussed in this section.

A. Representation of Aromatics

Aromatic hydrocarbons are believed to react in the atmosphere primarily with OH radicals, forming a variety of ring-containing and fragmentation products (Atkinson, 1990, 2000, and references therein). Despite progress in recent years towards improving our understanding of the atmospheric chemistry of aromatic hydrocarbons (e.g., see Atkinson, 2000, and references therein), there is still insufficient understanding of the details of these mechanisms to derive, or even estimate, predictive mechanisms. Therefore, it is still necessary to use parameterized mechanisms, with yields of model species representing reactive uncharacterized products adjusted to fit chamber data, in order to represent the atmospheric reactions of this important class of compounds.

All current photochemical mechanisms are based on assuming that the reactions of OH radicals with aromatics involve two initial processes. The first, which is applicable only for aromatics with substituents about the ring, involves H-atom abstraction from the side group, ultimately forming primarily aromatic aldehydes and ketones, and possibly small yields of aromatic nitrates as well:

$$\text{OH + aromatic} \rightarrow H_2O + \text{(benzyl type radical, e.g., } \Phi CH_2\cdot)$$

$$\text{(benzyl type radical)} + O_2 \rightarrow \text{(benzyl peroxy type radical, e.g., } \Phi CH_2OO\cdot)$$

$$\text{(benzyl peroxy type radical) + NO} \rightarrow \text{aromatic nitrate, e.g., } \Phi CH_2ONO_2$$

$$\text{(benzyl peroxy type radical) + NO} \rightarrow NO_2 + \text{(benzyl oxy type radical, e.g., } \Phi CH_2O\cdot)$$

$$\text{(benzyl oxy type radical)} + O_2 \rightarrow HO_2 + \text{aromatic aldehyde or ketone, e.g., } \Phi CHO$$

The other reaction route, which is generally the more important (and also the most uncertain), involves addition of OH to the aromatic ring, ultimately forming phenols or cresols to some extent, but primarily forming various ring fragmentation products:

$$\text{OH + aromatic} \rightarrow \text{(OH-aromatic adduct)}$$

$$\text{(OH-aromatic adduct)} + O_2 \rightarrow HO_2 + \text{phenol or cresol}$$

$$\text{(OH-aromatic adduct)} + O_2 \rightarrow \text{(OH-aromatic-}O_2\text{ adduct)}$$

$$\text{(OH-aromatic-}O_2\text{ adduct) + NO} \rightarrow \text{uncharacterized nitrate products}$$

(OH-aromatic-O_2 adduct) + NO $\rightarrow$ NO_2 + (uncharacterized radical intermediates)

(uncharacterized radical intermediates) $\rightarrow \rightarrow$ HO_2 + α-dicarbonyls and other fragmentation products

Alternative mechanism formulations, e.g., assuming the OH-aromatic reacts with NO_2 at a rate competing with or exceeding its reaction with O_2, assuming radical intermediates react with NO_2 to form stable products, or assuming that additional NO to NO_2 conversions are involved in the formation of α-dicarbonyls or other fragmentation products, can also be considered. However, except for the naphthalenes and tetralin (discussed below), experience has shown that parameterizations based on these alternative mechanisms do not fit the available environmental chamber data as well as those based on the general reaction schemes shown above.

The exception to this general scheme is that as discussed below improved fits of model simulations to chamber data for naphthalene, 2,3-dimethyl naphthalene, and tetralin are obtained if it is assumed that at least some of the uncharacterized radical intermediates react in a manner analogous to a PAN precursor (e.g., acyl peroxy) radicals. This involves radicals where the reaction with NO_2 forming a relatively stable termination product, e.g.,

(uncharacterized radical intermediates) + NO_2 $\rightarrow$ (uncharacterized PAN analogue)

competes with the reaction with NO forming radical propagation products (shown above). Model calculations do not fit the chamber data for these compounds if it is assumed that there is no significant radical termination process, nor are the chamber data well fit if it is assumed that the extent of termination is not strongly affected by reaction conditions. The latter would be the case if the termination were due to organic nitrate formation from the reactions of peroxy radicals with NO, or to the formation of some intermediate, such as phenoxy radicals, that only reacts by a termination process.

Therefore, the parameterization used to represent the reactions of the aromatics in this version is similar to that employed previously (Carter et al, 1997a), except that, as discussed above in Sections II.C.1 and II.C.3, a larger number of model species are used to represent the reactions of the various known and uncharacterized aromatic ring fragmentation projects. In this version, all three of the α-dicarbonyl products from the methylbenzenes are represented explicitly, and three different model species are used to represent the non-photoreactive (DCB1) and the two types of photoreactive (DCB2 and DCB3) uncharacterized ring fragmentation products. In addition, the mechanisms for the DCB's are are estimated based roughly on those estimated for unsaturated dicarbonyls (see Section II.C.3), unlike the previous mechanism where they were based on reactions of α-dicarbonyls (Carter, 1990). In addition, to at least approximately fit chamber data for the naphthalenes and tetralin, the possibility for the formation of PAN precursor radicals, represented by the RCO-O2· model species, is also included in the parameterization.

In terms of model species used in the current mechanism, the overall reactions of the aromatics are represented as follows:

OH + aromatic $\rightarrow$ y_{RH} HO2. + y_{RR} RO2-R. + y_{NR} RO2-N. + y_{Q2} RCO-O2. +
y_{PH} PHEN + y_{CR} CRES + y_{BL} BALD + y_{K6} PROD2 +
y_{GL} GLY + y_{MG} MGLY + y_{BA} BACL + y_{D1} DCB1 + y_{D2} DCB2 + y_{D3} DCB3.

Here the y_{PH}, ..., y_{D3} are the stoichiometric parameters that must be specified to define the mechanism. Note that the products shown in the first line represents the formation of various radical products and their effects of NO to NO_2 or organic nitrate formation from reactions of peroxy radicals, those shown in the second line represent the aromatic ring-retaining products (with PROD2 being used to represent aromatic

ketones such as methyl phenyl ketone that may be formed from ethylbenzene), and those in the third line represent the various known or uncharacterized ring fragmentation products.

Note that based on the reaction mechanism formulation discussed above, and considerations of factors such as radical conservation, relationships between some of the parameters can be derived, to reduce the number of parameters that have to be estimated or optimized. Radical conservation requires that

$$y_{RH} + y_{RR} + y_{RN} + y_{Q2} = 1.$$

If it is assumed that cresol or phenol formation occurs as shown above and that all the other processes involve a NO to NO_2 conversion, then

$$y_{RH} = y_{PH} + y_{CR}$$

This means that y_{RR} can be derived given the y_{Q2} value that best fits the data and the assigned phenol and cresol yields and the assigned nitrate yield (y_{RN}) parameter.

$$y_{RR} = 1 - (y_{PH} + y_{CR} + y_{Q2} + y_{RN}) \qquad \text{(XXVII)}$$

In addition, we assume that all the ring fragmentation processes, including those that form α-dicarbonyls, but probably excluding those involving involve formation of radicals represented by RCO-O2·, involve formation of some type of reactive dicarbonyl product. This implies that

$$\text{Total DCB Yield} = y_{D1} + y_{D2} + y_{D3} = 1 - (y_{Q2} + y_{NR} + y_{PH} + y_{CR} + y_{BL} + y_{K6}) \qquad \text{(XXVIII)}$$

This is used to derive y_{D1} given the optimized yields of y_{D1}, y_{D3}, and y_{Q2} and the assigned yields of the other parameters.

The stoichiometric yield parameters that were assigned or derived for the various aromatic compounds currently incorporated in the mechanism are summarized on Table 42. Footnotes to that table indicating the sources of the derivations are given on Table 43. As indicated in the footnotes, some of the product yield parameters are based on experimental data, some are estimated, and some are adjusted to fit chamber data. The adjustments were done by using a non-linear optimization method to minimize the sum of squares error between experimental and calculated values of the data indicated on the footnotes, with the errors normalized relative to the maximum values of the measurements for each experiment.

The following points are noted concerning these assignments and the resulting mechanisms for the various types of compounds.

1. Benzene

The glyoxal and phenol yields used were based on experimental data summarized by Atkinson (1997). Contrary to the previous version of the mechanisms (Carter, 1990; Carter et al, 1997a), the data are best fit if it is assumed that the uncharacterized ring fragmentation product does not photolyze to a significant extent. This change can be attributed to the fact that the photoreactivity of glyoxal is increased significantly in the present mechanism. This is based on results of modeling chamber studies of acetylene, where the reactivity of this compound could not be simulated unless significantly higher photoreactivity for glyoxal, its major photoreactive product, is assumed (Carter et al, 1997c; see also footnotes to Table A-2 in Table A-4). Therefore, only DCB1 is used to represent the uncharacterized fragmentation products from this compound.

Table 42. Summary of assigned and optimized stoichiometric yield parameters used to represent the reactions of the aromatics.

Parameters and Products		Benzene	Toluene	Ethyl Benzene	o-Xylene	m-Xylene	p-Xylene
OH abstraction pathway							
yBL	BALD		0.000		0.000	0.000	0.085
yK6	PROD2			0.000			
yNR	RO2-N.		0.129	0.000	0.000	0.000	0.008
Notes [b]		1	6,7	10	6,14	6,14	6,14
Phenol/Cresol patheay							
yPH	PHEN	0.000					
yCR	CRES		0.000	0.000	0.000	0.000	0.234
Notes		2,3	6	11	15	15	15
α-Dicarbonyl products							
yGL	GLY	0.084	0.084	0.207	0.207	0.207	0.116
yMG	MGLY		0.000	0.000	0.000	0.000	0.135
yBA	BACL				0.000		
Notes		4,3	8	11,12	8	8	8
Optimized Fragmentation Products							
yD2	DCB2		0.046		0.000	0.000	0.156
yD3	DCB3		0.046	0.000	0.000	0.000	0.057
Notes		5	9	13	16	17	18,19
Derived Yields [a]							
yRH	HO2.	0.236	0.600	0.236	0.236	0.236	0.234
yRR	RO2-R.	0.094	0.108	0.764	0.764	0.764	0.758
yD1	DCB1	0.000	0.016	0.764	0.764	0.764	0.460

Parameters and Products		1,2,3-Trimethyl Benzene	1,2,4-Trimethyl Benzene	1,3,5 Trimethyl Benzene	Naphthalene	Methyl Naphthalene	2,3-Dimethyl Naphthalene	Tetralin
OH abstraction pathway								
yBL	BALD	0.044	0.044	0.025				
yNR	RO2-N.	0.010	0.010	0.010	0.070	0.070	0.070	0.129
Notes [b]		20	20	20	24	29	24	31
Phenol/Cresol patheay								
yPH	PHEN				0.236			0.600
yCR	CRES	0.186	0.186	0.186		0.236	0.236	
Notes [b]		20	20	20	24	29	24	
α-Dicarbonyl products								
yGL	GLY	0.065	0.063	0.000	0.084	0.084	0.084	0.084
yMG	MGLY	0.166	0.364	0.621		0.038	0.076	
yBA	BACL		0.079		25	29	25,30	25
Notes [b]		8	8	8				
Optimized Fragmentation Products								
yD2	DCB2	0.077	0.000	0.097	0.049	0.076	0.103	0.046
yD3	DCB3	0.149	0.027	0.114	0.049	0.076	0.103	0.046
yQ2	RCO-O2.				0.479	0.539	0.600	0.163
Notes [b]		21	22	23	26,27,28	29	26,27,30	26,31
Derived Yields [a]								
yRH	HO2.	0.186	0.186	0.186	0.236	0.236	0.236	0.600
yRR	RO2-R.	0.804	0.804	0.804	0.215	0.155	0.094	0.108
yD1	DCB1	0.533	0.733	0.569	0.117	0.003	0 [c]	0.016

[a] Parameters calculated using Equations (XXVI) and (XXVII).

[b] Documentation notes are given on Table 43.

[c] Equation (XXVII) predicts a slightly negative DCB1 yield for this compound. Zero yield assumed.

Table 43. Documentation notes for the assigned and optimized stoichiometric yield parameters used to represent the reactions of the aromatics.

No.	Note
1	Organic nitrate yields from reaction of NO to OH - aromatic - O_2 adducts is assumed not to be significant
2	Glyoxal yields from Tuazon et al (1986).
3	See also yield data summarized by Atkinson (1994).
4	Phenol yield from Atkinson et al (1989).
5	Best fits to the D([O_3]-[NO]) data in benzene - NOx runs ITC560, ITC561, ITC562, ITC710, CTC159A, CTC159B, CTC160A, and CTC160B are obtained if yields of photoreactive DCB products are assumed to be negligible..
6	Aromatic aldehyde and and total phenolic product yields are averages of data tabulated by Atkinson (1994), except that the benzaldehyde and tolualdehyde yields of Gery et al (1987) are not used because they are substantially higher than the other measurements.
7	The approximate yield of organic nitrates in the RO_2+NO reaction are estimated from the benzyl nitrate yields tabulated by Atkinson (1994). Note that this corresponds to an approximately 9.5% yield from benzyl peroxy radicals, which is in the expected range for a molecule of this size.
8	Alpha-dicarbonyl yields are averages of data tabulated by Atkinson (1994), with low values from Shepson et al (1984) and the high values of Tagkagi et al (1980) excluded from the averages.
9	The DCB2 and DCB3 yields were adjusted to fit the concentration-time data for D([O_3]-[NO]) and toluene in toluene - NOx - air runs CTC079, CTC048, CTC026, CTC034, CTC065, DTC042B, DTC155A, DTC151A, DTC170A, and DTC042A.
10	The fraction reacted by abstraction from -CH_2- group is estimated from the rate constants for ethylbenzene and toluene, and from the benzaldehyde yield form toluene, assuming OH addition to the aromatic ring occurs with the same rate constant as with toluene. The expected abstraction product is benzophenone, which is very approximately represented in the mechanism by the lumped higher oxygenate product PROD2. The organic nitrate yield is estimated to be 10% of reaction of peroxy radical formed after abstraction from the -CH_2- group. Since abstraction is estimated to occur ~24% of the time and nitrate formation from the OH-aromatic-O_2 adducts is assumed to be negligible, this gives a 2.4% overall nitrate yield.
11	The phenolic product and alpha-dicarbonyl yields, relative to OH addition to aromatic ring, are assumed to be the same as for toluene
12	Methyl glyoxal is used to represent ethyl glyoxal.
13	The DCB2 and DCB3 yields were adjusted to fit the concentration-time data for D([O_3]-[NO]) and ethylbenzene in ethylbenzene - NOx - air runs CTC057, CTC092A, CTC092B, CTC098B, DTC223A, DTC223B, DTC224A, and DTC224B.
14	Nitrate yields for the xylenes are based approximately on the methylbenzyl nitrate yields tabulated by Atkinson (1994). The yields are consistent with 10-20% nitrate formation from reaction of NO with methylbenzyl peroxy radicals.
15	Phenolic product yields from Atkinson et al (1991).
16	The DCB2 and DCB3 yields were adjusted to fit the concentration-time data for D([O_3]-[NO]) and o-xylene in o-xylene - NOx - air runs CTC038, CTC039, CTC046, CTC068, CTC081, CTC091A, DTC207A, DTC207B, DTC208A, DTC208B, DTC209A, and DTC209B.
17	The DCB2 and DCB3 yields were adjusted to fit the concentration-time data for D([O_3]-[NO]) and and m-xylene in m-xylene - NOx - air runs CTC029, CTC035, CTC036, CTC094A, DTC193B, DTC192B, DTC206B, DTC295A, DTC188B, and DTC191B.
18	The DCB2 and DCB3 yields were adjusted to fit the concentration-time data for D([O_3]-[NO]) and p-xylene in p-xylene - NOx - air runs CTC041, CTC043, CTC044, CTC047, CTC070, DTC198A, DTC198B, and DTC199A.

Table 43 (continued)

No.	Note
19	Note that the apparent low photoreactive DCB yields from p-xylene and 1,2,4-trimethylbenzene can be attributed to the expected formation of diketone as well as dialdehyde products, where the diketones apparently do not photolyze as rapidly as dialdehydes.
20	The extent of reaction via abstraction from CH_3 groups is estimated from average rate constant per CH_3 group derived for toluene and the xylenes, which is 4.7×10^{-13} cm^3 $molec^{-1}$ s^{-1}. The overall yields of organic nitrates and phenolic products are estimated to be comparable to those for the xylenes, and to be similar for all isomers.
21	The DCB2 and DCB3 yields were adjusted to fit the concentration-time data for D([O_3]-[NO]) and the reactant aromatic in the 1,2,3-trimethylbenzene - NOx - air runs CTC054, CTC075, CTC076, DTC211A, DTC211B, DTC212A, DTC212B, DTC213A, and DTC213B.
22	The DCB2 and DCB3 yields were adjusted to fit the concentration-time data for D([O_3]-[NO]) and the reactant aromatic in the 1,2,4-trimethylbenzene - NOx - air runs CTC056, CTC091B, CTC093A, CTC093B, DTC201A, DTC201B, DTC203A, DTC203B, DTC204A, and DTC204B.
23	The DCB2 and DCB3 yields were adjusted to fit the concentration-time data for D([O_3]-[NO]) and the reactant aromatic in the 1,3,5-trimethylbenzene - NOx - air runs CTC030, CTC050, CTC071, CTC073, DTC194A, DTC194B, DTC195A, DTC195B, DTC196A, DTC196B, and DTC206A.
24	The naphthalenes are assumed to have the same yield of phenol-like products as benzene. Abstraction from the methyl group in the methyl naphthalenes is assumed to be relatively unimportant. However, model simulations of naphthalene - NOx and 2,3-dimethyl naphthalene runs are best fit by assuming relatively high nitrate yields of 12% and 7%, respectively, though assuming 7% overall yields for both compounds gives satisfactory fits to the data. Note that the actual reactions that this "nitrate formation" parameterization represents may be something other than nitrate formation from peroxy + NO.
25	The glyoxal yield from the naphthalenes and tetralin is assumed to be approximately the same as the glyoxal yield from o-xylene.
26	Since the only difference between DCB2 and DCB3 is the action spectrum of the photolysis reaction and since the available naphthalene, 2,3-dimethyl naphthalene and tetralin chamber experiments were all carried out using the same light source, the data are not sufficient to determine the yield ratio for these products. Based on the optimization results for the alkylbenzenes, where the optimized DCB2/DCB3 yield ratios varied from 0 to 3 with an average of about 1, we assume that the best fit yields for these two should be roughly equal for the naphthalenes and tetralins.
27	Satisfactory fits to the chamber data could not be obtained unless it was assumed that the ring fragmentation process included substantial formation of a peroxynitrate precursor, which was represented by the model species RCO-O2., the precursor of PAN2. See text.
28	The yields of RCO-O2. and DCB2 + DCB3 were optimized to fit D([O3]-[NO]) data for the naphthalene - NOx runs ITC751, ITC755, ITC756, ITC798, and ITC802.
29	No chamber data are available to derive a best fit mechanism for this compound. All its mechanistic parameters were derived by averaging those estimated or optimized for naphthalene and 2,3-dimethylnaphthalene.
30	The yields of RCO-O2. DCB2 + DCB3 and MGLY were optimized to fit D([O3]-[NO]) and PAN data for the 2,3-DMN - NOx runs ITC771, ITC774, ITC775, and ITC806. Best fits were obtained when the yield of the PAN precursor species was ~0.8, but using a value of 0.6, which is more consistent with the expected upper limit for ring opening, gave similar results. The DCB1 yield calculated using Equation XXIX was slightly negative, so a zero DCB1 yield is used.

Table 43 (continued)

No.	Note
31	Best fits to the chamber data are obtained if relatively high organic nitrate yields and high yields of phenol-like products are assumed. Higher nitrate yields could result if significant abstraction from -CH2- groups occurred, forming alkane-like peroxy radicals. It is also necessary to assume some formation of peroxynitrate precursors, represented by RCO-O2., to obtain satisfactory fits to the data, though the optimum yield for tetralin is less than derived for that for the naphthalenes. The total yield of phenol-like products was set at 0.6, which is reasonably consistent with the maximum value assuming that DCB, nitrate and peroxynitrate precursor formation account for the other pathways. The total alkyl nitrate yields, and yields of RCO-O2. and DCB2 + DCB3 from ring fragmentation were optimized to fit D([O3]-[NO]) data for the tetralin - NOx runs ITC739, ITC747, ITC748, ITC750, and ITC832.

Figure 10 shows plots of the $\Delta([O_3]-[NO])$ data for the benzene - NO_x experiments that were used for evaluating and deriving the mechanism for this compound. (See Section V for a summary of the model simulation methods and a more complete discussion of the evaluation results for all experiments used.) The results of model simulations using the assigned mechanism are also shown. It can be seen that the mechanism does not perform particularly well in simulating some of the data, tending to overpredict the rate of O_3 formation and NO oxidation in some of the xenon arc chamber runs and significantly underpredicting it in some of the blacklight chamber runs. However, no reasonable alternative parameterization that was examined resulted in a mechanism that better fit the data. Assuming any additional radical source from photolysis of uncharacterized products (or their reaction with O_3 for that matter) exacerbated the overprediction of the reactivity of the xenon arc chamber runs. Assuming higher radicals sources and countering them by increasing termination processes, such as using higher nitrate yield or assuming formation of products represented by PAN precursors (as found to improve simulations of data for the naphthalenes) did not solve the problem. Assuming alternative mechanisms such as formation of radicals that react with NO_2 also did not improve the fits.

More data are needed concerning the products formed in the photooxidation of benzene and their reactivities, including *direct* studies on the photoreactivity of glyoxal, before the uncertainties in the benzene photooxidation mechanism can be reduced. In addition, the possibility that there are experimental problems with some of the older ITC experiments, where the results appear to be inconsistent, cannot be ruled out. More comprehensive chamber data are needed to more unambiguously evaluate the mechanism for benzene. Although the model performs much better in simulating the data for the alkylbenzenes, and benzene is relatively unimportant in affecting atmospheric O_3 formation (because of its low reactivity and relatively low emissions amounts), the problems with the mechanism for what is presumably the simplest aromatic suggests fundamental problems with all aromatics mechanisms.

2. Methylbenzenes

The methylbenzenes (toluene, the xylenes and the trimethylbenzenes) are representative of the most important class of aromatic hydrocarbons in terms of both emissions and reactivity, and for that reason have the most extensive database of environmental chamber experiments for mechanism evaluation, as well information concerning yields of known products. The yields of phenolic products, benzaldehyde or tolualdehydes, and the α-dicarbonyls are based on experimental data summarized by Atkinson (1994). Averages of the reported data were used in those cases where more than one measurement is listed, though in some cases, measurements that appeared to fall outside the distribution of data from other studies were not used when computing the averages. The nitrate yields are somewhat

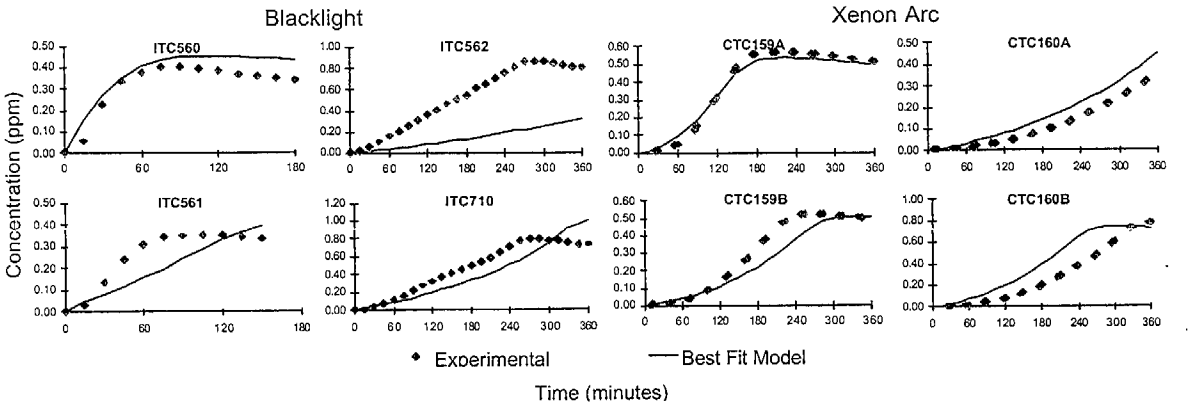

Figure 10. Plots of experimental and calculated $\Delta([O_3]-[NO])$ data for the experiments used to evaluate the benzene mechanism.

uncertain, but they appear to be relatively low and not highly important in affecting alkylbenzene reactivity.

As discussed above, the yields of model species DCB2 and DCB3, used to represent the uncharacterized photoreactive products, were optimized to fit the chamber data (see the footnotes to Table 42 in Table 43 for the specific data used). As discussed previously (Carter et al, 1997a) it is necessary to assume varying action spectra to fit the data in chambers with different light sources with data from chambers with both blacklight and xenon arc light source being used to determine their yields. Such data are available for all the methylbenzenes through the trimethylbenzenes, permitting their mechanisms to be optimized.

In contrast with benzene, the adjusted mechanism generally performs reasonably well in simulating the available chamber data, with no large or consistent differences in model performance in chambers with differing light sources. The performance of the model in simulating the individual alkylbenzene - NO_x chamber experiments is similar to that observed with previous versions of the mechanism (Carter et al, 1997a) and is presented in Section V.

3. Ethylbenzene

The mechanism for ethylbenzene is important because it is used as a surrogate (or surrogate species) for all the higher monoalkylbenzenes, such as propylbenzene or cumene. No product data for this compound is given by Atkinson (1994), and thus yields of all products had to be estimated. It is estimated that OH abstraction from the side group is more important than in the case of methylbenzenes because of the more reactive $-CH_2-$ group, as indicated in the footnotes to Table 42 in Table 43. Other than that, the phenolic and α-dicarbonyl products are estimated based on those for toluene, reduced by the appropriate factor to correspond to the relatively lower fraction of reaction by OH addition to the aromatic ring.

As with the methylbenzenes, the DCB2 and DCB3 yields were adjusted to optimize the fit of model calculation to the chamber data, which also included experiments with both blacklight and xenon arc light sources. The model fit the data reasonably well (see Section V), performing comparably as the model for the methyl benzenes. However, it is interesting to note that the best fit DCB2 yield for

ethylbenzene is zero, while the yield for toluene is relatively high, being larger than that for DCB3 (see Table 42). On the other hand, the DCB3 yields for ethylbenzene and toluene are not greatly different. There is no obvious explanation for the large difference in DCB2 yields, which will have a significant effect on predicted reactivity, and suggests that estimates of comparable reactivity for aromatics with "comparable" structure may not always be reliable.

4. Naphthalenes and Tetralin

Relatively little is known about the details of the atmospheric reactions of naphthalenes and tetralins, except that appears that there are probably significant differences between the mechanisms for the alkylbenzenes and the naphthalenes (e.g., Atkinson, 2000, and references therein). The limited environmental chamber data for these compounds indicate that the naphthalenes and tetralin are considerably less reactive than the alkylbenzenes, despite their relatively high OH rate constants (Carter et al, 1981, 1987). Therefore, it is not appropriate to represent the naphthalenes and tetralins using general aromatic model species, and separate mechanisms are necessary to appropriately predict the reactivities of these compounds.

There was insufficient time and resources in this project to evaluate all available data for the naphthalenes (or tetralins) to determine the most appropriate parameterization for their mechanisms, so the parameterization used for the alkylbenzenes was used as the starting point. The yields of the phenolic products, organic nitrates, and α-dicarbonyls were very approximately estimated as discussed in the footnotes to Table 42 in Table 43, and optimizations were carried out to determine the best fit DCB2 + DCB3 yields. Because naphthalene and tetralin environmental chamber data are only available with a blacklight light source, it was not possible to separately optimize both products, so their yields were assumed to be the same (see footnotes to the table).

Although adjusting DCB2 and DCB3 yields was found to be sufficient to fit the chamber data for the alkylbenzene runs, this was found not to be the case when attempting to fit the mechanism to the data for the naphthalenes and tetralins. This is shown, for example, on Figure 11, which shows experimental and calculated $\Delta([O_3]-[NO])$ data for the naphthalene experiments. The calculated lines labeled "Optimize $y_{D2}=y_{D3}$" show the results of optimizing the photoreactive DCB yields only, using the initial estimates for the other parameters. It can be seen that the O_3 formation and NO oxidation rates in some runs are overpredicted and some are underpredicted, depending on the initial reactant concentrations. The results for 2,3-dimethyl naphthalene and tetralin are similar. In an attempt to improve the fits, a second set of optimizations were carried out where the nitrate yields, y_{NR}, were optimized along with the photoreactive DCB yields. This also did not result in acceptable fits to the data, as shown on the curves labeled "Optimize $y_{D2}=y_{D3}$, y_{NR}" on Figure 11. Reparameterizing mechanism to represent the possible formation of radicals that react with NO_2 to form termination products (such as phenoxy) and adjusting the yields of those radicals along with the photoreactive DCB yields gives similar results as adjusting the nitrate yields. Using alternative parameterizations where the product yields depend on the absolute NO_2 concentration (as would occur if radicals which react with both NO_2 and O_2 were involved) also did not yield acceptable fits to the data.

Improved fits of the parameterized model to the naphthalene, dimethylnaphthalene, and tetralin data were only obtained when it was assumed that the reactions involved the formation of radicals that in a manner to PAN precursors, which were represented in the model by RCO-O2·. The simulations of the naphthalene experiments using the best fit mechanism with the optimized PAN precursor and photoreactive DCB yields given on Table 42 are shown on Figure 11, where it can be seen that reasonably good performance in simulating the data is obtained. The results are similar for 2,3-dimethylnaphthalene

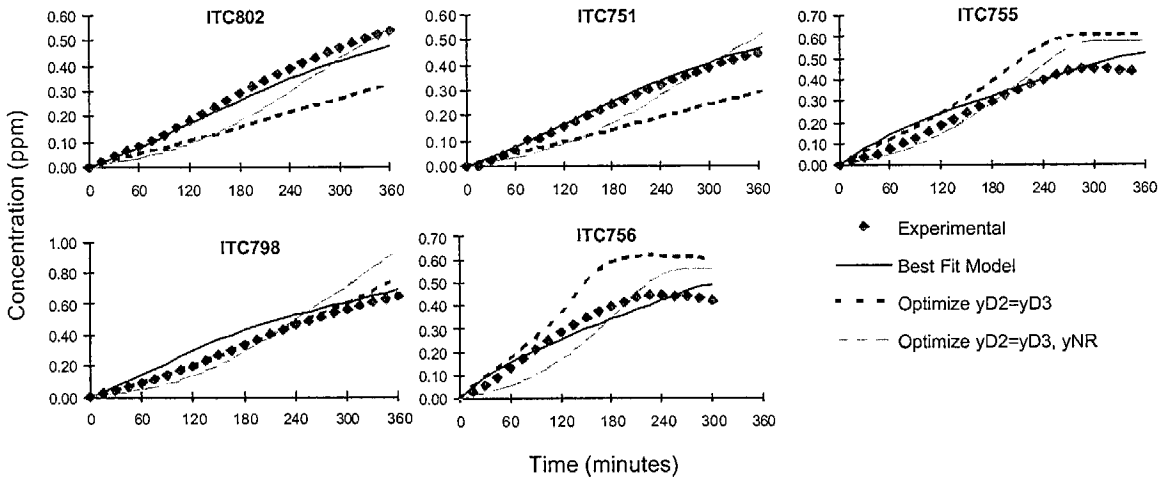

Figure 11. Plots of experimental and calculated $\Delta([O_3]-[NO])$ data for the naphthalene - NO_x used to derive the naphthalene mechanism.

and tetralin. However, in the case of 2,3-dimethylnaphthalene the yields of MGLY were also adjusted to optimize fits to the PAN data for these experiments, while for tetralin it was found that it was necessary also to adjust the overall nitrate yield for the model to satisfactorily simulate the data. The higher apparent nitrate yields in the case of tetralin could be due to reactions of radicals formed from OH abstractions from the non-aromatic ring.

These parameterized mechanisms for the naphthalenes and tetralin are clearly highly uncertain. Since the only currently available chamber data came from using a blacklight light source, the mechanism may not be correctly predicting the reactivity contributions of the photoreactive products in sunlight, where the spectrum is more similar to the xenon arc light sources. Perhaps more significantly, if the parameterizations employed do not correspond sufficiently well to the underlying chemistry of these compounds, the model may not be correctly extrapolating from the conditions of these experiments to the conditions of the atmosphere. However, these mechanisms represent our current best estimates at the present time.

5. Estimated Mechanisms for Other Aromatics

Table 8, above, shows that there are several other aromatic compounds whose OH rate constants are known, but for which no environmental chamber data are available for deriving mechanistic product yield parameters. These compounds are represented in the mechanism with model species using the appropriate measured rate constant, but with product yield parameters that are estimated based on those for most structurally similar compound(s) whose parameters are given in Table 42. These are as follows:

- Chlorobenzene (CL-BEN), dichlorobenzene (CL2-BEN) and nitrobenzene (NO2-BENZ) are assumed to have the same product yield parameters as derived for benzene.
- Parachlorobenzyltrifluoride (PCBTF) and trifluromethyl benzene (CF3-BEN) are assumed to have the same product yield parameters as derived for toluene.

- Isopropyl benzene (I-C3-BEN), n-propyl benzene (N-C3-BEN) and s-butyl benzene (S-C4-BEN) are assumed to have the same product yield parameters as derived for ethylbenzene.
- Monomethylnaphthalene (ME-NAPH) is assumed to have parameters that are averages of the corresponding parameters for naphthalene and 2,3-dimethylnaphthalene. The parameters so derived are shown on Table 42.

Obviously these estimates are uncertain, especially in view of the differences for the parameters for toluene and ethylbenzene, as discussed above. However, these provide the best available estimates concerning the mechanisms for these compounds, and at least incorporate their known OH rate constants. In this respect, their representation is presumed to be somewhat less uncertain than those aromatics that are not incorporated in the mechanism, but are represented by other aromatics using the "lumped molecule" approach (see Table C-1 in Appendix C).

B. Representation of Other Compounds

Table 44 shows the representation used for the reactions of the other compounds or classes of compounds that are incorporated in the present mechanism and that do not fall into the categories discussed above. The assignments for the various types of compounds are discussed in more detail below.

1. Terpenes

Terpenes are bicyclic alkenes or dialkenes or cyclic alkenes, and as such their reactions cannot be processed by the current mechanism generation system. The rate constants for their initial reactions are given above in Table 8 (for OH radicals), Table 13 (for NO_3 radicals) Table 16 (for O_3) and Table 22 (for O^3P atoms). Although some product data are available for their reactions with OH radicals and O_3 (see Atkinson, 1997a), the available information is not sufficient to completely determine their mechanisms. Their representation is therefore estimated based on simplified or parameterized mechanisms, or using mechanisms generated for similar monocyclic, monoalkene structures.

The terpenes whose reactions are represented in this mechanism are α- and β-pinenes, Δ^3-carene, d-limonene, and sabinene, the only terpenes for which environmental chamber data are available. The mechanisms used for these compounds, given in terms of model species in the base mechanism, are given in Table 44. The considerations used when deriving mechanisms for the terpenes are discussed below. The performance of these mechanisms in simulating the chamber data for these compounds is summarized in Section V.

Reaction with OH radicals. In the case of the reaction with OH radicals, the simplest mechanism would involve OH adding to the double bond, forming a β-hydroxy radical which will react with O_2 to form the corresponding peroxy radical. This then reacts with NO to form either the corresponding nitrate or alkoxy radical, and where the alkoxy radical can react in various ways, including decomposing to ultimately forming HO_2 and carbonyl compounds.

Table 44 Assigned mechanisms for terpenes and other non-aromatic compounds or groups of compounds that are not processed using the mechanism generation system.

Compound	Kinetic Parameters [a,b] A	Ea	B	Reaction [c] Reaction
				Assigned Mechanisms
α-Pinene	1.21e-11	0.882		A-PINENE + HO. = #.75 RO2-R. + #.25 RO2-N. + #.5 R2O2. + #.75 RCHO + #6.5 XC
	1.01e-15	1.455		A-PINENE + O3 = #.7 HO. + #.081 RO2-R. + #.321 RO2-N. + #1.375 R2O2. + #.298 RCO-O2. + #.051 CO + #.339 HCHO + #.218 RCHO + #.345 ACET + #.002 GLY + #.081 BACL + #.3 RCO-OH + #3.875 XC
	1.19e-12	0.974		A-PINENE + NO3 = #.75 NO2 + #.25 RO2-N. + #.75 R2O2. + #.75 RCHO + #6.25 XC + #.25 XN
	3.20e-11			A-PINENE + O3P = PROD2 + #4 XC
β-Pinene	2.38e-11	0.709		B-PINENE + HO. = #.75 RO2-R. + #.25 RO2-N. + #.5 R2O2. + #.75 HCHO + #.75 PROD2 + #3.25 XC
	1.01e-15	2.493		B-PINENE + O3 = #.34 HO. + #.09 HO2. + #.05 RO2-N. + #.2 R2O2. + #.2 RCO-O2. + #.375 CO + #.1 CO2 + #.25 HCHO + #.75 PROD2 + #.28 HCOOH + #3.595 XC
	2.51e-12			B-PINENE + NO3 = #.75 RO2-R. + #.25 RO2-N. + #.75 R2O2. + #.75 RNO3 + #4 XC + #.25 XN
	2.70e-11			B-PINENE + O3P = #.4 RCHO + #.6 PROD2 + #5.2 XC
3-Carene	1.64e-11	0.994		3-CARENE + HO. = #.75 RO2-R. + #.25 RO2-N. + #.5 R2O2. + #.75 RCHO + #6.25 XC
	1.01e-15	1.958		3-CARENE + O3 = #.7 HO. + #.161 RO2-N. + #.539 R2O2. + #.482 CCO-O2. + #.058 RCO-O2. + #.058 HCHO + #.482 RCHO + #.3 RCO-OH + #5.492 XC
	9.10e-12			3-CARENE + NO3 = #.75 NO2 + #.25 RO2-N. + #.75 R2O2. + #.75 RCHO + #6.25 XC + #.25 XN
	3.20e-11			3-CARENE + O3P = PROD2 + #4 XC
d-Limonene	3.19e-11	0.994		D-LIMONE + HO. = #.75 RO2-R. + #.25 RO2-N. + #.5 R2O2. + #.75 RCHO + #6.25 XC
	3.71e-15	1.729		D-LIMONE + O3 = #.7 HO. + #.161 RO2-N. + #.539 R2O2. + #.482 CCO-O2. + #.058 RCO-O2. + #.058 HCHO + #.482 RCHO + #.3 RCO-OH + #5.492 XC
	1.22e-11			D-LIMONE + NO3 = #.75 NO2 + #.25 RO2-N. + #.75 R2O2. + #.75 RCHO + #6.25 XC + #.25 XN
	7.20e-11			D-LIMONE + O3P = PROD2 + #4 XC
Sabinene	2.19e-11	0.994		SABINENE + HO. = #.75 RO2-R. + #.25 RO2-N. + #.5 R2O2. + #.75 HCHO + #.75 PROD2 + #3.25 XC
	1.01e-15	1.459		SABINENE + O3 = #.34 HO. + #.09 HO2. + #.05 RO2-N. + #.2 R2O2. + #.2 RCO-O2. + #.375 CO + #.1 CO2 + #.25 HCHO + #.75 PROD2 + #.28 HCOOH + #3.595 XC
	1.00e-11			SABINENE + NO3 = #.75 RO2-R. + #.25 RO2-N. + #.75 R2O2. + #.75 RNO3 + #4 XC + #.25 XN
	1.69e-11			SABINENE + O3P = #.4 RCHO + #.6 PROD2 + #5.2 XC

Table 44 (continued)

Compound	Kinetic Parameters [a,b] A	Ea	B	Reaction [c] Reaction
Styrene	5.80e-11			STYRENE + HO. = #.87 RO2-R. + #.13 RO2-N. + #.87 HCHO + #.87 BALD + #.26 XC
	1.71e-17			STYRENE + O3 = #.4 HCHO + #.6 BALD + #.6 HCOOH + #.4 RCO-OH + #1.6 XC
	1.51e-13			STYRENE + NO3 = #.22 NO2 + #.65 RO2-R. + #.13 RO2-N. + #.22 R2O2. + #.22 HCHO + #.22 BALD + #.65 RNO3 + #1.56 XC + #.13 XN
	1.76e-11			STYRENE + O3P = PROD2 + #2 XC
N-Methyl-2-Pyrrolidone	2.15e-11			NMP + HO. = #.92 HO2. + #.08 RO2-N. + #.46 RCHO + #.46 PROD2 + #.38 XC + XN
	1.26e-13			NMP + NO3 = #.92 HO2. + #.08 RO2-N. + #.92 PROD2 + #-1 XC + XN
				Adjusted Parameterized Mechanisms
Para Toluene Isocyanate	5.90e-12			P-TI + HO. = #.2 HO. + #.7 HO2. + #.15 MGLY + CRES
Toluene Diisocyanate	7.40e-12			TDI + HO. = #.5 HO. + CRES
Diphenylene Diisocyanate	1.18e-11			MDI + HO. = #.2 HO. + #.7 HO2. + #.15 MGLY + CRES
				"Placeholder" Mechanisms for Approximate Estimates [c]
Trichloro-ethylene	5.63e-13	-0.849		CL3-ETHE + HO. = RO2-R. + #.5 HCHO + #.5 RCHO
n-Propyl Bromide	1.18e-12			C3-BR + HO. = RO2-R. + #.5 HCHO + #.5 RCHO
n-Butyl Bromide	2.46e-12			C4-BR + HO. = RO2-R. + #.5 HCHO + #.5 RCHO
Methyl Chloride	3.15e-13	1.163	2	CH3-CL + HO. = RO2-R. + #.5 HCHO + #.5 RCHO
Dichloro-methane	7.69e-13	0.994	2	CL2-ME + HO. = RO2-R. + #.5 HCHO + #.5 RCHO
Methyl Bromide	2.34e-13	1.035	2	ME-BR + HO. = RO2-R. + #.5 HCHO + #.5 RCHO
Chloroform	5.67e-13	1.002	2	CHCL3 + HO. = RO2-R. + #.5 HCHO + #.5 RCHO
Ethyl Chloride	6.94e-13	0.302	2	C2-CL + HO. = RO2-R. + #.5 HCHO + #.5 RCHO
1,2-Dichloro-ethane	9.90e-13	0.813	2	12CL2-C2 + HO. = RO2-R. + #.5 HCHO + #.5 RCHO
1,1-Dichloro-ethane	2.60e-13			11CL2-C2 + HO. = RO2-R. + #.5 HCHO + #.5 RCHO
1,1,2-Trichloro-ethane	4.00e-13	0.413	2	112CL3C2 + HO. = RO2-R. + #.5 HCHO + #.5 RCHO
1,1,1-Trichloro-ethane	5.33e-13	2.244	2	111-TCE + HO. = RO2-R. + #.5 HCHO + #.5 RCHO
Ethyl Bromide	2.72e-11	2.671		C2-BR + HO. = RO2-R. + #.5 HCHO + #.5 RCHO
1,2-Dibromo-ethane	9.27e-13	0.839	2	11BR2-C2 + HO. = RO2-R. + #.5 HCHO + #.5 RCHO
Vinyl Chloride	1.69e-12	-0.839		CL-ETHE + HO. = RO2-R. + #.5 HCHO + #.5 RCHO
t-1,2-Dichloro-ethene	1.01e-12	-0.497		T-12-DCE + HO. = RO2-R. + #.5 HCHO + #.5 RCHO
Perchloro-ethylene	9.64e-12	2.403		CL4-ETHE + HO. = RO2-R. + #.5 HCHO + #.5 RCHO
Ethyl Amine	1.47e-11	-0.376		ET-AMINE + HO. = RO2-R. + #.5 HCHO + #.5 RCHO

Table 44 (continued)

Compound	Kinetic Parameters [a,b] A	Ea	B	Reaction [c] Reaction
Dimethyl Amine	2.89e-11	-0.491		DM-AMINE + HO. = RO2-R. + #.5 HCHO + #.5 RCHO
Trimethyl Amine	2.62e-11	-0.501		TM-AMINE + HO. = RO2-R. + #.5 HCHO + #.5 RCHO
Ethanolamine	3.15e-11			ETOH-NH2 + HO. = RO2-R. + #.5 HCHO + #.5 RCHO
Diethanol Amine	9.37e-11			ETOH2-NH + HO. = #.96 RO2-R. + #.04 RO2-N. + #.5 HCHO + #.5 RCHO
Triethanolamine	1.16e-10			ETOH3-N + HO. = #.905 RO2-R. + #.095 RO2-N. + #.5 HCHO + #.5 RCHO

[a] Rate constant given by A exp(-Ea/RT) $(T/300)^B$, where the rate constant and A factor are in cm^3 $molec^{-1}$ s^{-1} and the activation energy is in kcal/mole.

[b] See Table 8 for the derivation of the OH radical rate constants used.

[c] See text for a discussion of how the mechanisms were derived.

[d] These mechanisms are for approximate estimates only, and are based on assuming formation of relatively reactive products. They are not based on any evaluation of the chemistry of the compounds, and may not accurately predict their ozone impacts. See text.

$$\text{Terpene} + OH \rightarrow >C(\cdot)\text{-}C(OH)<$$

$$>C(\cdot)\text{-}C(OH)< + O_2 \rightarrow >C(OO\cdot)\text{-}C(OH)<$$

$$>C(OO\cdot)\text{-}C(OH)< + NO \rightarrow >C(ONO_2)\text{-}C(OH)<$$

$$>C(OO\cdot)\text{-}C(OH)< + NO \rightarrow NO_2 + >C(O\cdot)\text{-}C(OH)<$$

$$>C(O\cdot)\text{-}C(OH)< \rightarrow >C{=}O + \text{-}C(\cdot)(OH)\text{-}$$

$$\text{-}C(\cdot)(OH)\text{-} + O_2 \rightarrow HO_2 + >C{=}O$$

$$>C(O\cdot)\text{-}C(OH)< \rightarrow \text{other radicals (additional NO to } NO_2 \text{ conversions)}$$

If the decomposition involves breaking what was the double bond to form an α-hydroxy radical, which is the dominant process for most of the simpler alkenes, then no additional NO to NO_2 conversions would be involved. However, additional NO to NO_2 conversions may occur if other decompositions can compete, which are estimated to be non-negligible for compounds with similar structures as the terpenes. If the reacting double bond is in the ring, the carbonyl products would be expected to be bifunctional compounds with at least one aldehyde group, which is represented in the model by the RCHO model species. If the reacting double bond is a $=CH_2$ group outside the ring, then the products would be formaldehyde + a ketone, the latter represented by PROD2 in the model.

Therefore, for compounds with the double bond in the ring, such as α-pinene, Δ^3-carene, and d-limonene, the following parameterized mechanism is employed:

$$OH + \text{Terpene(ring d.bond)} \rightarrow y_N\ \text{RO2-N}\cdot + (1\text{-}y_N)\ \{\text{RO2-R}\cdot + \text{RCHO}\} + y_{R2O2}\ \text{R2O2}\cdot$$

where the nitrate yield, y_N, and the amount of extra NO to NO_2 conversions, y_{R2O2}, are determined based on model simulations of the available terpene - NO_x chamber data. For compounds with $=CH_2$ groups, such as β-pinene and sabinene, the parameterized mechanism is

$$OH + Terpene(=CH_2) \rightarrow y_N\ RO2\text{-}N\cdot + (1\text{-}y_N)\ \{RO2\text{-}R\cdot + HCHO + PROD2\} + y_{R2O2}\ R2O2\cdot$$

Best fits to most of the chamber data are obtained using $y_N = 0.25$ and $y_{R2O2} = 0.5$, and as indicated on Table 44 this is assumed for all the terpenes.

Reaction with O_3 The Crigiee biradicals expected to be formed in the reactions of O_3 with α-pinene, Δ^3-carene and d-limonene could all be represented in the mechanism generation system, so the overall O_3 reactions could be generated in the same way as used for the other alkenes, if the mechanism for the initial reaction is assigned. This is the approach used for these compounds. All three of these compounds have trisubstituted double bond in the ring, and as discussed above in Section III.E.3, it is assumed that the formation of -CO- + -CHOO[excited] and -CHO + -COO[excited]- occur respectively 30% and 70% of the time, based on ketone yields from acyclic trisubstituted alkenes. Although d-limonene has a second double bond outside the ring, it is assumed that most of the reaction occurs at the more substituted bond in the ring, and reactions at the second double bond is ignored when estimating the overall mechanism. Note that this procedure results in predicted OH yields of 70% for these compounds, which is reasonably close to the experimentally-determined values of 0.76-0.85 for α-pinene and 86% for d-limonene (Atkinson, 1997b). The overall processes generated in this way are shown in Table 44.

The mechanism generation system cannot be used as readily to estimate the reactions of O_3 with β-pinene and sabinene, since reaction to form formaldehyde + a Crigiee biradical with a bicyclic structure is expected to be formed to a non-negligible extent. However, the expected overall reactions of these biradicals are not expected to differ greatly with the structure, at least in terms of model species in the base mechanism. This is expected to be as follows,

$$\text{ring-COO[excited]-ring} \rightarrow \text{ring-C=C(OOH)-ring} \rightarrow OH + \text{ring-C(}\cdot\text{)-CO-ring}$$
$$\text{ring-C(}\cdot\text{)-CO-ring} + O_2 \rightarrow \text{ring-C(OO}\cdot\text{)-CO-ring}$$
$$\text{ring-C(OO}\cdot\text{)-CO-ring} + NO \rightarrow 0.2\ \text{ring-C}(ONO_2)\text{-ring} + 0.8\ \text{ring-C(O}\cdot\text{)-CO-ring}$$
$$\text{ring-C(O}\cdot\text{)-CO-ring} \rightarrow \text{-CO-chain-CO}\cdot$$

where the 20% nitrate yield is the value derived by the mechanism generation system for a substituted C_9 peroxy radical, such as expected to be formed in this case. Therefore, in terms of model species in the base mechanism, reaction of the terpene with O_3 to form this biradical yields the following overall process:

$$O_3 + Terpene(=CH_2) \rightarrow HCHO + OH + 0.2\ RO2\text{-}N\cdot + 0.8\ \{R2O2\cdot + RCO\text{-}O2\cdot\} \qquad (A)$$

Of course, part of the time the reaction would also involve formation of the cyclic ketone + HCHO2[excited], whose subsequent reactions are as discussed above. In this case, the overall process is

$$O_3 + Terpene(=CH_2) \rightarrow PROD2 + 0.12\ HO2 + 0.12\ OH + 0.5\ CO + 0.13\ CO2 + 0.37\ HCOOH \qquad (B)$$

The branching ratio for these two routes is derived based on assuming an overall OH yield of ~35%, which is the measured value for β-pinene and close to the measured values of 26% and 33% for sabinene (Atkinson, 1997a and references therein). This is predicted if Pathways (A) and (B) are assumed to occur respectively 25% and 75% of the time, which gives the following overall process:

$$O_3 + Terpene(=CH_2) \rightarrow 0.25\ HCHO + 0.75\ PROD2 + 0.34\ OH + 0.05\ RO2\text{-}N\cdot + 0.2\ R2O2\cdot$$
$$+ 0.2\ RCO\text{-}O2\cdot + 0.09\ HO2. + 0.375\ CO + 0.1\ CO2 + 0.28\ HCOOH$$

Note, however, that assuming ~75% ketone + HCHO2[excited] formation is not consistent with the observed yields of only 22-23% nopinone from β-pinene and 50% ketone from sabinene (Atkinson, 1997a, and references therein), so this is clearly an oversimplification of the actual mechanisms for these terpenes.

Reaction with NO_3 Radicals. The mechanisms for the terpene + NO_3 reactions are represented in a manner similar to that used for the OH reactions as discussed above, being based on assuming the following set of reactions:

$$\text{Terpene} + NO_3 \rightarrow >C(\cdot)\text{-}C(ONO_2)<$$

$$>C(\cdot)\text{-}C(ONO_2)< + O_2 \rightarrow >C(OO\cdot)\text{-}C(ONO_2)<$$

$$>C(OO\cdot)\text{-}C(ONO_2)< + NO \rightarrow >C(ONO_2)\text{-}C(ONO_2)<$$

$$>C(OO\cdot)\text{-}C(ONO_2)< + NO \rightarrow NO_2 + >C(O\cdot)\text{-}C(ONO_2)<$$

$$>C(O\cdot)\text{-}C(ONO_2)< \rightarrow >C{=}O + \text{-}C(\cdot)(ONO_2)\text{-}$$

$$\text{-}C(\cdot)(ONO_2)\text{-} \rightarrow >C{=}O + NO_2$$

The alkoxy radical estimation methods discussed above predict that the $>C(O\cdot)\text{-}C(ONO_2)<$ radicals of the types formed in these reactions should primarily decompose, so the possible competing reactions are not considered. As with the OH reaction, the carbonyls formed would either be a bifunctional aldehyde (represented by the RCHO model species) in the case of terpenes with double bonds in the ring, or formaldehyde + a ketone (represented by PROD2) in the case of terpenes with $=CH_2$ groups. If a the same overall nitrate yield is assumed as is used in the OH reaction (~25%), then the overall process is:

$$NO_3 + \text{Terpene(ring d.bond)} \rightarrow 0.25\ \{RO2\text{-}N\cdot + XN\} + 0.75\ \{RCHO + R2O2\cdot + NO2\}$$

for terpenes with the double bond in the ring, and

$$NO_3 + \text{Terpene}(=CH_2) \rightarrow 0.25\ \{RO2\text{-}N\cdot + XN\} + 0.75\ \{HCHO + PROD2 + R2O2\cdot + NO2\}$$

for terpenes with $=CH_2$ groups.

Reaction with O^3P. As discussed above in Section III.F.3, it is assumed that the reactions of O^3P with the higher alkenes involve formation of ~60% of the corresponding oxide, and ~40% formation of a carbonyl compound. The oxide formed in the reactions of O^3P with the terpenes are represented by the PROD2 model species For terpenes with the double bond in the ring, the carbonyl product is expected to be primarily a ketone, which is also represented in the model by PROD2, while if the terpene has a $=CH_2$ group, the predicted product is an aldehyde, whose formation is represented by RCHO. Thus, the overall reactions are

$$O^3P + \text{Terpene(ring double bond)} \rightarrow PROD2$$

for terpenes with the double bond in the ring, and

$$O^3P + \text{Terpene}(=CH_2) \rightarrow 0.6\ PROD2 + 0.4\ RCHO$$

for terpenes with $=CH_2$ groups.

2. Styrene

The mechanism used for the reactions of styrene is based on that derived by Carter et al (1999b) based on environmental chamber experiments employing that compound. Note that to fit the environmental chamber reactivity data it is necessary to assume that essentially no radical formation occurs in the O_3 reaction. The only modification to the mechanism of Carter et al (1999b) is that the nitrate yield for the OH reaction was increased from 10% to 13% to reduce biases in the model simulations of the mini-surrogate incremental reactivity experiments. The nitrate yield in the NO_3 reaction was also increased from 10% to 13%, since it is assumed to be the same in the OH reaction.

3. N-Methyl-2-Pyrrolidone

The mechanism for the reactions of N-methyl-2-pyrrolidone (NMP) is based on that derived by Carter et al (1996c), based on environmental chamber experiments employing that compound. The main differences are that the products 1-formyl-2-pyrrolidinone and N-methyl succimide were represented by PROD2 and RCHO, respectively, rather than by separate model species with parameterized mechanisms. In addition, the nitrate yields used in the mechanism had to be reduced from 15% to 8% for the model to give reasonably good simulations of the data. The fits of the model simulations to the chamber data are given in Appendix B (see also Section V).

4. Aromatic Isocyanates

Environmental chamber reactivity experiments have been carried out for toluene diisocyanate (TDI) (Carter et al, 1997i) and para-toluene isocyanate (P-TI) (Carter et al, 1999a), allowing simplified parameterized mechanisms for these compounds to be developed. Based on the P-TI mechanism, a simplified estimated mechanism for the structurally similar (and commercially more important) compound methylene diphenylene diisocyanate (MDI) was also derived (Carter et al, 1999a). Although the details of the atmospheric reactions of these compounds are unknown, highly simplified mechanisms, such as those shown on Table 44, were shown to simulate the data reasonably well (Carter et al, 1997i, 1999a).

These parameterized aromatic isocyanate mechanisms were incorporated in the updated mechanism and reoptimized to fit the chamber data. In the case of TDI, the OH yield in had to be increased from 0.3 to 0.6 in order to simulate the data approximately as well as the mechanism reported by Carter et al (1997i). In other words, with the updated base mechanism the chamber data are fit with a parameterized model with considerably less radical termination than the model used with the SAPRC-97 mechanism. In the case of P-TI, the extent of radical termination (which in any case is considerably less than for TDI) did not have to be readjusted, but the yield of product compounds represented by methyl glyoxal was reduced from 0.3 to 0.15. The reoptimized mechanisms are shown on Table 44, along with the estimated MDI mechanism, which was derived from the P-TI mechanism as discussed by Carter et al (1999a).

5. Halogenated Compounds

Although we have previously carried out experimental studies of the ozone reactivities of chloropicrin (CCl_3ONO_2) (Carter et al, 1997h), n-propyl and n-butyl bromides (Carter et al, 1997d) and trichloroethylene (Carter et al, 1996d), and developed mechanisms for those compounds that were evaluated using the data obtained, satisfactory fits of the model to chamber data were obtained only for chloropicrin. In particular, no reasonable adjustments of uncertain portions of the mechanisms would result in satisfactory fits to the data for the alkyl bromides (Carter et al, 1997d) or trichloroethylene

(Carter et al, 1996d), especially after the times in the experiment when O_3 formation began. Additional data are needed, with chemically simpler systems, before mechanisms can be developed that can reliably predict ozone impacts of halogenated compounds.

Because the explicit mechanisms with the ClO_x or BrO_x chemistry did not adequately fit the data for two of the three compounds studied, it was decided that our knowledge of these systems is not sufficient to include this chemistry in the base mechanism. Instead, a highly simplified and parameterized "placeholder" mechanism is used in the current mechanism to provide very rough estimates of the approximate range of reactivities of halogenated compounds under MIR conditions, given their OH radical rate constants. This parameterized mechanism, which is shown on Table 44, is based on the assumption that the overall reactions involve at least one NO to NO_2 conversion, form relatively reactive products (which are represented by formaldehyde and the lumped higher aldehyde), and do not involve any significant radical termination processes such as nitrate formation. The appropriate OH rate constant for the compound, given on Table 8 is used in conjunction with the placeholder mechanism given on Table 44.

Note that this mechanism is not appropriate for chloropicrin because it does not represent VOCs that are photoreactive. The reactions of chloropicrin are not represented in the current version of the mechanism, since the necessary ClO_x chemistry has not yet been incorporated in the base mechanism.

The performance of the placeholder mechanisms in simulating the reactivities of the two other halogenated compounds that were studied was evaluated by simulating the results of the incremental reactivity experiments. The results, which are given in Appendix B (see also Section V), indicate that the simplified mechanism performs remarkably well in simulating the experiments with trichloroethylene, especially in the higher NO_x experiments that are more representative of MIR conditions. The simulations of the higher NO_x reactivity experiments with the alkyl bromides were variable, with some experiments being reasonably well simulated, and others with the O_3 reactivity being overestimated by about a factor of 1.5-2. The parameterized mechanism performed very poorly in simulating the reactivities of these compounds under low NO_x conditions, with the model predicting they enhance O_3 in all cases, while O_3 was not enhanced in the low NO_x trichloroethylene runs, and inhibited in the low NO_x runs with the bromides.

Based on the results of this evaluation with a very limited number of compounds, it is possible that the parameterized mechanism may give at least rough estimates of reactivities under MIR (i.e., relatively high NO_x) conditions, but would likely significantly overestimate ozone impacts of such compounds under low NO_x conditions, where many may actually be O_3 inhibitors. Appropriately representing reactivities of these compounds under low NO_x conditions would require incorporating ClO_x or BrO_x reactions into the mechanism, and a better understanding of how they interact with the VOCs and NO_x species under ambient conditions, as well as how they interact with the chamber walls.

6. Amines

There are a number of amines and alcohol amines in the emissions inventories, and an ability to estimate at least their approximate ranges of reactivities, at least under MIR conditions, would be desirable. However, there is insufficient information available to derive or estimate atmospheric reaction mechanisms for amines, and no environmental chamber data available that are suitable for deriving parameterized mechanisms. For that reason, no attempt was made to derive or estimate mechanisms for these compounds. Instead, as with halogenated compounds, simplified and parameterized "placeholder" mechanisms were used for this purpose. These are given on Table 44. As with the amines, the placeholder mechanisms are based on the assumption that there is at least one NO to NO_2 conversion, that relatively

reactive products, represented by formaldehyde and the lumped higher aldehyde, are formed, and that no significant radical termination occurs for C_1-C_3 compounds. For the higher molecular weight alcohol amines, the nitrate yield is estimated based on that for a substituted, non-secondary peroxy radical with the same number of carbons (see Section III.I).

Since it assumes relatively reactive products and no inhibition other than the expected nitrate formation for the higher molecular weight compounds, the mechanism may be biased towards overpredicting the reactivities of these compounds. However, until more data are available this cannot be adequately assessed. In any case, reactivities estimated using these mechanisms must be considered to be highly uncertain.

C. Unrepresented Compounds

Although Table 8 includes OH radical rate constants for the atmospheric reactions of representatives of other classes of organic compounds, including several sulfur- and silicon-containing compounds, these are not represented in the current version of the mechanism. With the exception of several volatile siloxanes (Carter et al, 1992), which were shown to be ozone inhibitors under all conditions, there is insufficient information available to develop or evaluate mechanisms for these compounds. Although highly approximate estimated mechanisms could be developed in some cases, there was insufficient time and resources available to carry this out for this version of the mechanism.

V. MECHANISM EVALUATION

The base mechanism and the mechanisms for the individual VOCs were evaluated by comparing results of model simulations of with results of primarily indoor environmental chamber experiments carried out at the University of California at Riverside. These include not only experiments from the large data base of UCR chamber experiments through 1993 (Carter et al, 1995d), but also the large number of experiments carried out subsequently at CE-CERT. These include the experiments used in the development and evaluation of the SAPRC-97 mechanism (Carter et al, 1997a), and reactivity studies of a wide variety of individual VOCs (Carter et al, 1996a-d, 1997b-g,i, 1999a,b, 2000b-g), and studies of representative consumer product VOCs (Carter et al, 2000a). The experiments used in the evaluation, and references to the reports documenting the experiments, are summarized on Table B-1 in Appendix B. These consisted of the following:

- 76 characterization runs, including 3 pure air runs, 8 acetaldehyde - air runs to determine NO_x offgasing effects, and 65 CO - NO_x or n-butane - NO_x experiments to measure the chamber radical source.
- 481 single VOC runs involving 37 types of VOCs.
- 447 incremental reactivity experiments involving 87 types of VOCs or mineral spirits or solvent samples. These experiments consisted of determining the effect of adding the VOC or sample to a "base case" reactive organic gas (ROG) - NO_x "surrogate" mixture simulating ambient mixtures. The types of incremental reactivity experiments used in this evaluation, and the codes used to identify them in the tables and figures in Appendix B, are indicated on Table 45.
- 673 mixture runs involving various types of simple or complex mixtures or ambient ROG surrogates. Most of these (556 runs) were "base case" surrogate - NO_x runs carried out in conjunction with the incremental reactivity experiments. The types of mixtures or surrogates employed, and the codes used to identify them in Appendix B, are indicated on Table 45.

The environmental chambers used to generate the data used in this evaluation are summarized on Table 46. Note that a two- or three-letter code is used to designate each chamber. The individual experiments in any given chamber are numbered sequentially, and as shown on Table B-1, the runs are designated by the chamber code followed by the run number. Note that the DTC, OTC, and (for most runs) the CTC had dual reactors where two mixtures could be irradiated simultaneously. In those cases, the suffix "A" or "B" is used to indicate the reactor used to obtain the data. For incremental reactivity experiments, the designation refers to the reactor where the test VOC was added, with the understanding that the other reactor contained the same mixture without the added VOC.

There is also a large database of outdoor environmental chamber experiments that were carried out at the University of North Carolina that can be used for mechanism evaluation. These have been used for evaluations of the SAPRC-90 (Carter and Lurmann, 1991) and other (e.g., Carter and Lurmann, 1990; Gery et al, 1988) mechanisms, as well as for evaluation of the detailed isoprene mechanism of Carter and Atkinson (1996). Unfortunately, there was insufficient time to conduct a comprehensive evaluation of this mechanism using the UNC chamber data base, because of the need to update and re-evaluate the chamber model for that chamber. However, results of previous evaluation studies have shown that mechanisms that perform reasonably well in simulating the UCR indoor chamber data base also perform reasonably well in simulating the UNC chamber data (Carter and Lurmann, 1990, 1991; Carter and Atkinson, 1996).

Table 45. Designations used for types of incremental reactivity experiments and complex mixtures in the summaries of the evaluation experiments and results.

Designation	Description
	Types of Incremental Reactivity Experiments
MR3	Experiments using the 3-component "mini-surrogate" at relatively high NO_x levels. This type of experiment was used in our first major experimental incremental reactivity study (Carter et al, 1993a), and is still used as part of our experimental protocol to evaluate VOC reactivity. This employs relatively high NOx levels and uses an ethene, n-hexane, and m-xylene mixture as a simple representation of ambient VOCs. As discussed by Carter et al (1995b), experiments using this surrogate are very sensitive to effects of VOCs on radical levels (e.g., aspects of the mechanism that affect radical initiation or inhibition).
MR8	Experiments using the 8-component "full surrogate" at relatively high NO_x levels. This type of experiment was first employed by Carter et al (1995b) as a more realistic representation of maximum incremental reactivity (MIR) conditions than the mini-surrogate system, and that is also used as part of our standard experimental protocol to evaluate reactivity. Like the mini-surrogate, this also employs relatively high NOx conditions, but uses a mixture as of of n-butane, n-octane, ethene, propene, trans-2-butene, toluene, m-xylene, and formaldehyde as a more realistic representation of ambient conditions. Incremental reactivities measured using these experiments have been shown to give the best correlation to atmospheric MIR's than the other types of surrogate - NOx systems we employ for reactivity studies (Carter et al, 1995b).
R8	Experiments using the 8-component "full surrogate" at lower NO_x levels. This uses the same surrogate mixture as the "MR8" experiments, but with NO_x levels reduced by a factor of ~2. This type of experiment was also developed by Carter et al (1995b) and is also used as part of our standard experimental protocol to evaluate reactivity. These experiments evaluate the effects of VOCs on O3 formation under conditions where NOx is limited.
MRE	Experiments using ethene alone as the ROG surrogate, at relatively high NO_x levels. This was used in the study of Carter et al (1995b) when evaluating the effects of using simplified surrogate systems, and in some experiments to evaluate reactivities of terpenes. It has not been used subsequently because evaluation results are highly sensitive to the ability of the model to simulate the base case experiment, which tend to be variable.
MR4	Similar to "MR3" except that toluene and 1,3,5-trimethylbenzene is used in place of m-xylene. This was used in some recent experiments as an alternative to the standard mini-surrogate because the more rapidly reacting 1,3,5-trimethylbenzene gives a somewhat better measure of the effects of the VOC on radical levels. It is not widely used because the results are similar to those using the standard mini-surrogate, and use of the standard surrogate gives better comparability to the large existing data base.
R3	Experiments using the standard "MR3" mini-surrogate, but at lower NOx levels than the standard mini-surrogate. This was used in a few cases as part of specialized studies, or because of errors in reactant injections.
RE	Experiments using ethene as the surrogate and carried out under NOx limited conditions. This was used in a few experiments with terpenes (i.e., ethene + terpene experiments were carried out to evaluate terpene mechanisms).
RX	Experiments using other miscellaneous or non-standard surrogate - NO_x mixtures for the base case. These were used either for special studies, because gas chromatographic interferences prevented use of the standard surrogate, or because of injection errors.

Table 45 (continued)

Designation	Description
	Types of Simple Mixtures
MIX-A	Mixture of alkanes
MIX-E	Mixture of alkenes
MIX-AE	Mixture of alkanes and alkenes
MIX-AO	Mixtures of alkanes and oxygenates (generally aldehydes)
MIX-RO	Mixtures of aromatics and oxygenates (generally aldehydes)
MIX-AR	Mixtures of alkanes and aromatics
MIX-ER	Mixtures of alkenes and aromatics
	Ambient Surrogate Mixtures used in Base Case Incremental Reactivity Experiments.
SURG-3M	Base case for the "MR3" incremental reactivity experiments. Employed the standard 3-component "mini-surrogate" at relatively high NO_x concentrations.
SURG-8M	Base case for the "MR8" incremental reactivity experiments. Employed the standard 8-component "full surrogate" at relatively high NO_x concentrations.
SURG-8	Base case for the "R8" incremental reactivity experiments. Employed the standard 8-component "full surrogate" at lower NO_x concentrations.
SURG-3	Base case for the "R3" incremental reactivity experiments. Employed the standard 3-component "mini-surrogate" at lower NO_x concentrations.
SURG-4M	Base case for the "MR4" incremental reactivity experiments. Employed the modified version of the 3-component "mini-surrogate" at relatively high NO_x concentrations.
SURG-X	Base case for the "MRX" incremental reactivity experiments. Employed various miscellaneous surrogates, usually (but not always) at relatively high NO_x concentrations.
	Ambient Surrogate Mixtures used in Various Complex Mixture Experiments.
SURG-4	Experiments in the ITC chamber using a 4-component surrogate, low NO_x mixture used in the early incremental reactivity study of Carter and Atkinson (1987).
SURG-4R	Modified versions of the "SURG-4" mixture used in the study of Carter and Atkinson (1987).
SURG-7	A surrogate mixture of seven hydrocarbons used in several runs in the SAPRC EC (Pitts et al, 1979).
SURG-8S	A surrogate mixture of 8 hydrocarbons used in the "multi-day effects" study of Carter et al (1984b).

Table 46. Summary of environmental chambers used to obtain the data used for mechanism evaluation.

Chamber ID	Light Source	Type	Volume (liters)	Surface	RH	Period for Runs	Additional Information
ITC	Blacklight	Single	~6400	Semi-collapsible 2 mil FTP Teflon bag held by frame	~50%	1982-86	See Carter et al (1995d)
ETC	Blacklight	Single	~3000	Semi-collapsible 2 mil FTP Teflon bag held by frame	Dry	1989-93	See Carter et al (1995d)
DTC	Blacklight	Dual	2 x ~5000	Two semi-collapsible 2 mil FTP Teflon bags held by frames	Dry	1993-99	See Carter et al (1995d)
EC	25 KW Xenon Arc	Single	5774	Teflon coated aluminum, evacuable cylinder	~50%	1975-84	See Carter et al (1995d)
XTC	4 x 6 KW Xenon Arc	Single	~5000	Semi-collapsible 2 mil FTP Teflon bag held by frame	Dry	1993	See Carter et al (1995d)
CTC (11-82)	4 x 6 KW Xenon Arc	Single	~5000	Semi-collapsible 2 mil FTP Teflon bag held by frame	Dry	1994-95	Very similar to XTC.
CTC (83+)	4 x 6 KW Xenon Arc	Dual	2 x ~2500	Two semi-collapsible 2 mil FTP Teflon bags held by frames	Dry	1995-99	Similar to XTC except dual bags.
OTC	Sunlight	Dual	2 x ~20,000	Dividable and completely collapsible 2 mil FEP Teflon bag.	Dry	1992-93	See Carter et al (1995c,d)

Data from seven different chambers were used in these evaluations, and their major characteristics are summarized in Table 46. As indicated on the table, most of these chambers are described in detail by Carter et al (1995d), or references therein. The only exception is the CTC, which is the most recently constructed of these chambers. This is essentially the XTC after it was moved from SAPRC to CT-CERT, and employed the same light source and general design.

A. Chamber Simulation Methods

Evaluations of mechanisms using chamber data require an appropriate representation of the conditions of the chamber experiments that affect the simulation results. These include initial reactant concentrations, physical conditions such as temperature and dilution, light intensity and spectrum, and the major wall effects such as the chamber radical source, O_3 decays, NO_x offgasing, etc. These considerations are discussed in detail elsewhere (e.g., Carter and Atkinson, 1990, 1991; Carter et al, 1995c,d, 1997a), and generally the approach employed in this work was similar. This is summarized briefly in the following sections.

1. Light Characterization

Light characterization requires specification of both the intensity and the spectrum of the light source used in the experiments. As discussed by Carter et al (1995c,d) for indoor chamber runs, this is determined by the NO_2 photolysis rate (usually derived from results of NO_2 actinometry experiments), and the relative spectral distribution of the light source. For blacklight chambers the spectrum is assumed to be constant and the spectrum recommended by Carter et al (1995d) is used. For xenon arc chambers, the spectrum tends to vary with time, and the spectrum used for modeling is based on measurements made during or around the time of the experiment as discussed by Carter et al (1995d). For the outdoor

chamber, the spectrum was calculated as a function of solar zenith angle as described by Carter et al. (1995c).

For the blacklight chambers and the EC, the NO_2 photolysis rates were determined by carrying out periodic NO_2 actinometry experiments, with the values assigned to individual runs being based on the trends or averages of the measurements carried out around the time of the experiment (Carter et al, 1995d, 1997a). For the XTC and CTC, the relative trends in light intensity with time were determined primarily using absolute spectral intensity measurements, whose data were placed on an absolute basis using occasional in-chamber steady-state or Cl_2 actinometry measurements (Carter et al, 1995d, 1997a). For the outdoor chamber, the absolute light intensities were obtained using continuous UV radiometer and total solar radiometer (TSR) data. These were used to derive absolute spectra for calculating photolysis rates by fitting outputs of a solar radiation model to these measurements (Carter et al, 1995c).

For the DTC and CTC experiments carried out since 1994, a check on the accuracy of the light intensity assignments can be obtained from the trends of the results of the many replicate "base case" experiments carried out in conjunction with the incremental reactivity experiments. As the light intensity gradually decreases over time, the rate of O_3 formation and NO oxidation also decrease accordingly, and these rates take step increases when the changes are made that increase the light intensity. There are two periods when the trends of the results of these experiments were not consistent with the photolysis rates as indicated by the NO_2 actinometry or spectral intensity results. One case involved DTC runs 624-647 that were carried out using 75% lights (Carter et al, 1999c), but no runs in this group were used in this evaluation. The other case consisted of the CTC runs after CTC170, which includes a number of runs used in this evaluation. For these experiments, the rates of decrease in the rates of NO oxidation and O_3 formation in the base case runs decreased more rapidly with time than did the light intensity as measured by NO_2 actinometry or spectral measurements made outside the chamber (Carter et al, 1999b). On the other hand, the Cl_2 actinometry measurements made inside the chamber, though less precise than the other measurement methods, were consistent with the trend in base case surrogate reactivity results. This suggests that the chamber walls may be contributing to the decreasing intensity trend. For these CTC runs, the method for assigning NO_2 photolysis rates was adjusted to be consistent with the trend in replicate base case surrogate results (Carter et al, 1999b).

2. Representation of Chamber Wall Effects

The chamber wall effects that were represented in the simulations of these experiments were the chamber radical source (Carter et al, 1982), NO_x offgasing, heterogeneous formation of HONO from NO_2, N_2O_5 hydrolysis, O_3 dark decay, and background effects causing excess NO to NO_2 conversions. These are represented by the following psuedo-reactions:

$$\text{Walls} + h\nu \rightarrow \text{HONO} \qquad \text{(RN)}$$

$$\text{Walls} + NO_2 + h\nu \rightarrow 0.5\ \{\text{HONO} + \text{Wall-NO}_x\} \qquad \text{(RS)}$$

$$\text{Walls} + NO_2 \rightarrow y_{HONO}\ \text{HONO} + (1\text{-}y_{HONO})\ \text{Wall-NO}_x \qquad \text{(NO}_2\text{W)}$$

$$N_2O_5 + \text{walls} \rightarrow 2\ \text{Wall-NO}_x \qquad \text{(N}_{25}\text{I)}$$

$$N_2O_5 + H_2O + \text{walls} \rightarrow 2\ \text{Wall-NO}_x \qquad \text{(N}_{25}\text{S)}$$

$$\text{Walls} + O_3 \rightarrow (\text{loss of } O_3) \qquad \text{(O}_3\text{W)}$$

Note that "Wall-NO_x" in the above reactions is an inert counter species that was used to account for nitrogen balance only, since it undergoes no subsequent reaction in the model. The rate constants for

these processes, and the stoichiometric parameter y_{HONO} were assigned based on the results of appropriate characterization runs or estimates as indicated on Table 47. See Carter and Lurmann (1990, 1991) and Carter et al (1995d) for a more detailed discussion of how these processes are represented in chamber models and how their rate parameters are derived.

The formation of HONO from the walls (Reaction RN) was used to represent both the chamber radical source and NO_x offgasing, because the HONO so formed would photolyze rapidly to form both OH radicals and NO

$$HONO + h\nu \rightarrow OH + NO$$

Previously, the radical source and NO_x offgasing were represented as separate processes, as

$$Walls + h\nu \rightarrow OH \qquad (RS)$$

$$Walls + h\nu \rightarrow NO_2 \qquad (ENO_2)$$

with the rates of each being assigned independently based on appropriate characterization runs (n-butane - NO_x or CO - NO_x runs for the radical source, and pure air or acetaldehyde-air runs for NO_x offgasing) (Carter and Lurmann, 1990, 1991; Carter et al, 1995d, 1997a). However, in most cases the rates of these two reactions tended to be the same to within the uncertainty of the determination, suggesting that they may be due to the same process. For that reason, the revised representation, using Reactions (RN) and (RS), is used in this work. Note that the NO_2 dependence of the radical source, represented by Reaction (RS), appears to be significant only in the case of the EC, so that reaction is assigned a nonzero rate constant only for runs in that chamber. If there is an NO_2 dependence for the radical source in the other chambers, it is much less than the run-to-run variability of the radical source.

Table 47 gives the rate constants and other wall-dependent parameters that were assigned to the experiments used in this evaluation. Note that the "Set(s)" column on the table indicates the "characterization set" (Carter et al, 1995d), which refers to a group of runs that are all assumed to have the same characterization parameters. The characterization set assigned to each experiment is given with the run listing in Table B-1 in Appendix B. In most cases, this refers to runs in a given reaction bag, though sometimes the characterization set changes if the results of characterization runs indicate that the wall effects parameters have changed. For the CTC, characterization sets are also used to refer to runs that are assumed to have the same spectral distribution. Since the spectral distribution changes more rapidly then the reactor characteristics, for that chamber there are many characterization sets where the same wall effects parameters are assigned.

3. Other Reaction Conditions

The other reaction conditions that need to be represented in the simulations are the initial reactant concentrations, temperature, humidity and dilution. In most cases the initial reactant concentrations are determined from measurements made prior to the start of the irradiation, but in some reactivity experiments with missing data for a "base case" reactant the average concentration measured in similar experiments is used. The one exception to this is the initial HONO that may be introduced as a contaminant with the NO_x injections; this is represented by the parameter "HONO-F", whose value is derived based on results of radical source characterization runs as indicated on Table 47. The humidity used in the simulations is also indicated on Table 47.

Table 47. Chamber wall effect and background characterization parameters used in the environmental chamber model simulations for mechanism evaluation.

Cham.	Set(s)	Value	Discussion
RN-I (ppb)			Ratio of the rate of **wall + hν -> HONO** to the NO_2 photolysis rate.
ITC	All	0.045	Average of value of RS-I which gave best fits to n-butane - NOx chamber experiments carried out in this chamber. The initial HONO was optimized at the same time. Temperature does not vary significantly in the ITC runs used for evaluation.
ETC	2-3	9.00e+9 exp(-9712/T) 0.078 @ 300K	The few n-butane - NOx experiments in this chamber appear to be anomalous. The preexponential factor is derived to minimize biases in model simulations of the large number of mini-surrogate - NOx chamber experiments carried out in this chamber. The activation energy is based on the value that gives best fits to temperature dependences of RN-I values which fit n-butane - NOx and CO - NOx experiments in the OTC and other Teflon bag chambers.
DTC	1	0.058	Average of value of RS-I which gave best fits to n-butane - NOx chamber experiments carried out in this chamber. The initial HONO was optimized at the same time. If a temperature dependence is shown, it was derived from the temperature dependence of the RN-I values that best fit characterization data in outdoor chamber experiments, with the same activation energy used in all cases. If a temperature dependence is not shown, then the temperature variation for experiments in this set is small compared to the run-to-run variability in the best fit RN-I values. Note that the radical source in Sets 3, 12, 13, and 16 runs was anomalously high.
	3	2.16e+10 exp(-9712/T) 0.188 @ 300K	
	10	8.14e+9 exp(-9712/T) 0.071 @ 300K	
	11	0.080	
	12	0.277	
	13	0.146	
	14	0.082	
	15	0.057	
	16	0.212	
	17	0.073	
	18	0.066	
XTC	1	5.25e+9 exp(-9712/T) 0.0457 @ 300K	Same procedure as DTC
CTC	1-8	0.064	Same procedure as DTC
	9	0.097	
	10	0.064	
OTC		6.04e+9 exp(-9712/T) 0.053 @ 300K	Same procedure as DTC
EC	1	0.308	Based on the NO2 dependence radical source derived by Carter et al (1981), adjusted downward by 20% to reduce biases in simulations of n-butane - NOx experiments carried out in this chamber. The NO2-dependent radical source term, RS-S, was reduced by an equal factor.
RS-S (unitless)			Ratio of the rate of **NO2 + hν -> 0.5 HONO + 0.5 wall NOx** to the NO_2 photolysis rate.
EC	1	0.17%	Based on the NO2 dependence radical source derived by Carter et al (1981), adjusted downward by 20% to reduce biases in simulations of n-butane - NOx experiments carried out in this chamber. The NO2-independent radical source term, RN-I, was reduced by an equal factor.
All others		0	Any dependence of apparent radical source on initial NOx levels in Teflon bag chambers was found to be much less than the run-to-run variability.

Table 47 (continued)

Cham.	Set(s)	Value	Discussion
HONO-I (ppb)			Initial HONO in experiment, assumed to be independent of other reactants.
ITC	All	1.7	Average of initial HONO value which gave best fits to n-butane - NOx chamber experiments carried out in this chamber. The RN-I parameter was optimized at the same time. The best fit initial HONO values appear to be approximately independent of the initial NO2.
HONO-F (unitless)			Ratio of the initial HONO concentration to the measured initial NO2. [The initial NO2 in the experiment is reduced by a factor of 1 - (HONO-F)]. Unless the characterization data indicate otherwise, it is assumed that the initial HONO is introduced with the NO2 injection, so is it is assumed to be proportional to the initial NO2 concentration.
ETC	2-3	0	Initial HONO assumed to be small for these experiments, where special procedures were employed to minimize HONO contamination. See Carter et al (1993a).
DTC	1	0.1%	Average of value of initial HONO to initial NO2 which gave best fits to n-butane - NOx chamber experiments carried out in this chamber. The RN-I parameter was optimized at the same time.
	3	0.4%	
	10	0.8%	
	11	0.6%	
	12	0.5%	
	13	0.9%	
	14	0.6%	
	15	0.7%	
	16	0.5%	
	17	0.3%	
	18	0.8%	
XTC	1	1.2%	Same procedure as DTC
CTC	1-8,10	0.8%	Same procedure as DTC
	9	0.8%	
OTC	10-12	0	Apparently not significant compared to RN-I.
E-NO2/K1 (ppb)			Ratio of rate of NO2 offgasing from the walls to the NO2 photolysis rate.
EC	1	0.10	Adjusted to fit O3 formation in acetaldehyde/air run EC-253.
All Teflon Bag Chambers		0	The NOx offgasing caused by representing the radical source by HONO offgasing appears to be sufficient for accounting for NOx offgasing effects in most cases. RN-I parameters adjusted to fit experiments sensitive to the radical source are consistent with NOx offgasing rates adjusted to fit pure air or aldehyde - air runs, to within the uncertainty and variability.
k(NO2W) (min^{-1})			Rate of unimolecular loss (or hydrolysis) of NO2 to the walls.
All Teflon Bag Chambers		1.6e-4	Based on dark NO2 decay and HONO formation measured in the ETC by Pitts et al. (1984). Assumed to be the same in all Teflon bag chambers, regardless of volume.
EC	1	2.8e-4	Based on dark NO2 decay and HONO formation measured in the EC by Pitts et al. (1984).
YHONO			Yield of HONO in the unimolecular reaction (hydrolysis) of NO2 on the walls.

Table 47 (continued)

Cham.	Set(s)	Value	Discussion
All Teflon Bag Chambers		0.2	Based on dark NO2 decay and HONO formation measured in the ETC by Pitts et al. (1984). Assumed to be the same in all Teflon bag chambers, regardless of volume.
EC	1	0.5	Based on dark NO2 decay and HONO formation measured in the EC by Pitts et al. (1984).
k(O3W) (min^{-1})			Unimolecular loss rate of O3 to the walls.
ITC	All	1.5e-4	Based on results of O_3 decay in Teflon bag chambers experiments as discussed by Carter et al (1995d).
ETC	All	1.5e-4	Same as ITC
DTC	All	1.5e-4	Same as ITC
XTC	All	1.5e-4	Same as ITC
CTC	All	8.5e-5	Based on results of O_3 decay experiments in this chamber
OTC	All	1.7e-4	Based on results of O_3 decay experiments in this chamber
EC	All	1.1e-3	Based on results of O_3 decay in Teflon bag chambers experiments as discussed by Carter et al (1995d).
k(N26I) (min^{-1})			Rate constant for **N2O5 -> 2 Wall-NOx**. This represents the humidity-independent portion of the wall loss of N_2O_5, or the intercept of plots of rates of N_2O_5 loss against humidity.
All Teflon Bag Chambers		2.8e-3	Based on N_2O_5 decay rate measurements made by Tuazon et al (1983) for the ETC. Assumed to be independent of chamber size (Carter et al, 1995d).
EC	1	4.7e-3	Based on N_2O_5 decay rate measurements made by Tuazon et al (1983) for the EC. See also Carter et al (1995d).
k(N26S) (ppm^{-1} min^{-1})			Rate constant for **N2O5 + H2O -> 2 Wall-NOx.** This represents the humidity dependent portion of the wall loss of N_2O_5, or the slope of plots of rates of N_2O_5 loss against humidity.
All Teflon Bag Chambers		1.1e-6	Based on N_2O_5 decay rate measurements made by Tuazon et al (1983) for the ETC. Assumed to be independent of chamber size (Carter et al, 1995d).
EC	1	1.8e-6	Based on N_2O_5 decay rate measurements made by Tuazon et al (1983) for the EC. See also Carter et al (1995d).
k(XSHC) (min^{-1})			Rate constant for **OH -> HO2**. This represents the effects of reaction of OH with reactive VOCs in the background air or offgased from the chamber walls. This parameter does not significantly affect model simulations of experiments other than pure air runs.
All Teflon Bag Chambers		250	Estimated from modeling several pure air in the ITC (Carter et al, 1996d), and also consistent with simulations of pure air runs in the ETC (Carter et al, 1997a).
EC	1	0	Assumed to be negligible because the EC is generally evacuated overnight between experiments (Carter et al, 1995d).
H2O (ppm)			Default water vapor concentration for runs where no humidity data are available.
ITC	all	2.0e+4	This corresponds to ~50% RH at 303K, which is the condition for most experiments in this chamber.

Table 47 (continued)

Cham.	Set(s)	Value	Discussion
All Other Teflon Bag Chambers		1.0e+3	Experiments in these chambers were carried out using dried purified air. The limited humidity data for such runs indicate that the humidity was less than 5%, probably no more than ~2.5%, and possibly much less than that. The default value corresponds to ~2.5 - 3% RH for the conditions of most experiments.
EC	1	2.0e+4	This corresponds to ~50% RH at 303K, which is the condition for most experiments in this chamber. Humidity data are available for most EC runs, so the default is usually not used.

The temperature used in the simulations is derived from the measurements made during the experiments, as discussed by Carter et al (1995d). The dilution varies depending on the chamber, and is derived as also discussed by Carter et al (1995d). The dilution is relatively small for all experiments used for mechanism evaluation in this work, being about 2% per hour in the EC, and generally less than 1% per hour in the Teflon bag chambers, which can collapse as samples are withdrawn.

Most experiments used in this evaluation were 6-hour runs. A few multi-day runs were included in the evaluation set, but only the simulation results for the first day are shown. Except for the few outdoor runs, most of the experiments were carried out with constant light intensity and approximately constant temperature.

4. Incremental Reactivity Simulations

Most incremental reactivity experiments consisted of simultaneous irradiations of two mixtures in the two reactors (or "sides") of the chamber, one with and one without the added test compound. Those were simulated by separately simulating the experiment on each side, using the reactant concentrations and conditions measured for that side. The incremental reactivity data (i.e., change in measured quantities caused by adding the VOC, divided by the amount added) were then calculated from the results of these two simulations in exactly the same way the experimental reactivity data were calculated from the experimental measurements.

This procedure could not be used when simulating incremental reactivity experiments carried out in the ECT, where base case and added test VOC irradiations were carried out as separate experiments, and temperature and some other conditions tended to vary from run to run (Carter et al, 1993a). In those cases, the base case conditions used to derive the experimental incremental reactivity measurement was derived using correlations between experimental conditions and results of the separate base case experiments (Carter et al, 1993a). In the model simulations, the base case was simulated by simulating the test VOC experiment without the test compound added, and the incremental reactivities were calculated from the differences in the results of that simulation and the simulation of the actual experiment.

5. Chemical Mechanism Employed

The chemical mechanism employed in the chamber simulations consisted of the base mechanism with reactions added as needed to represent the VOCs present, together with the reactions used to represent the chamber effects. The base mechanism used is listed in Table A-2 in Appendix A. The

reactions used to represent the individual VOCs not in the base mechanism, which were derived as discussed in previous sections, are listed in Table A-6 in Appendix A[19]. No lumping of initially present VOCs was employed except when simulating the components of the mineral spirits samples (MS-A through MS-D), where lumped species with averaged parameters were used to represent the alkanes and (for MS-A) aromatics and alkenes present. The reactions and parameters added to represent chamber effects are as discussed above in Section V.A.2.

B. Chamber Simulation Results

The results of the simulation of the chamber experiments are summarized in Table B-1 and in the various figures in Appendix B. Table B-1 gives the experimental and calculated values of the quantity $\Delta(O_3\text{-}NO)$[20] for 2, 4, and 6-hours into the experiments for all experiments used in the evaluation except for the pure air and acetaldehyde-air runs. The quantity $\Delta\ (O_3\text{-}NO)$ is defined as

$$\Delta\ (O_3\text{-}NO)_t = [O_3]_t - [NO]_t - ([O_3]_0 - [NO]_0) \qquad \text{(XXX)}$$

where $[O_3]_0$, $[NO]_0$, $[O_3]_t$, and $[NO]_t$ are the initial and time=t concentrations of ozone, and NO, respectively. As discussed previously (e.g., Carter and Lurmann, 1990, 1991); Carter and Atkinson, 1984), this gives a measure of the ability of the model to simulate the chemical processes that cause ozone formation that gives a useful measure even where ozone is suppressed by the presence of excess NO. Table B-1 also shows the percentage error in the calculation for each experiment where $\Delta(O_3\text{-}NO)$ is greater than 1 pphm (0.01 ppm). This is defined as

$$\Delta\% = 100 \text{ x (Calculated value - Experimental value) / Calculated value} \qquad \text{(XXXI)}$$

This gives a measure of the performance of the model in simulating the rates of O_3 formation and NO oxidation at various times in the individual experiments.

Because of the large number of experiments, Table B-1 is not very useful for giving a sense of the overall model performance in simulating the various types of experiments. For that reason, most of Appendix B consists of various figures displaying the model performance in graphical form. Depending on the types and numbers of runs involved, these can consist of concentration - time plots of $\Delta(O_3\text{-}NO)$ or (in a few cases) of other species; distribution plots of percentage errors in model simulations of $\Delta(O_3\text{-}NO)$ (calculated using Equation XXXI), or plots of incremental reactivity data.

The incremental reactivity data plots include plots of experimental and calculated $\Delta(O_3\text{-}NO)$ for the base case and added VOC ("test") experiment, and plots of experimental and calculated incremental reactivities (IR)'s for $\Delta(O_3\text{-}NO)$ and IntOH. These quantities are defined as follows:

$$\text{IR } \Delta(O_3\text{-}NO)_t = \{\Delta(O_3\text{-}NO)_t^{\text{Added VOC Experiment}} - \Delta(O_3\text{-}NO)_t^{\text{Base Case Experiment}}\} / [\text{VOC added}]$$

$$\text{IR IntOH}_t = \{\text{IntOH}_t^{\text{Added VOC Experiment}} - \text{IntOH}_t^{\text{Base Case Experiment}}\} / [\text{VOC added}]$$

---

[19] The VOCs were actually represented in the software using generalized reactions with variable parameters, whose values were assigned depending on the particular VOC being represented. However, the effect is the same as explicitly incorporating the reactions as shown in Table A-6.

[20] Note that $\Delta(O_3\text{-}NO)$ is sometimes referred to as d(O3-NO) or D(O3-NO) on some of the tabulations of the results.

and IntOH is the integrated OH radical levels, calculated from the rates of consumption of the most reactive VOC in the base case mixture that reacts only with OH radicals (usually m-xylene) (Carter et al, 1993a). Note that there are no "base case" data shown for incremental reactivity experiments carried out in the ETC, since there is no single base case experiment associated with those runs (see above).

As observed in previous mechanism evaluation studies, although there were runs that were not particularly well simulated by the model, overall the model fit most of $\Delta(O_3\text{-NO})$ data to within ±30% or better. The overall performance of the model in simulating all the runs listed in Table B-1 is shown on Figure 12. The model simulated the 6-hour $\Delta(O_3\text{-NO})$ to within ±5% for ~1/3 of the experiments, to within ±15% for ~3/4 of the runs, and to within ±25% for almost 90% of the experiments. The model has a slight bias (average Δ% of 9%) towards overpredicting the t=1 hour $\Delta(O_3\text{-NO})$ data, but this bias decreases to ~4% for the later periods of the runs. This is a somewhat better model performance than the simulations of the previous versions of the SAPRC mechanism (e.g., Carter and Lurmann, 1991). However, this better overall performance may be more a result of eliminating poorly characterized experiments or more difficult to characterize outdoor runs from the evaluation set than to changes or improvements in the mechanism.

Table 48 gives a summary of the results of the evaluations of the mechanisms for the various types of experiments, and indicates the figures in Appendix B where the various evaluation results are shown. The table also gives codes indicating the overall mechanism performance. These include

1. Fits the data to within the experimental uncertainty or with biases that are not considered to be significant. For mixtures, this is used to indicate that there is no overall bias in the distribution of fits to $\Delta([O_3]\text{-}[NO])$.
2. Poor fits for some runs or non-negligible overall biases indicate possible problems with the mechanism for this compound, or there are insufficient data for satisfactory mechanism evaluation. For mixtures, this is used to indicate that there is a non-negligible bias in the distribution of fits to $\Delta([O_3]\text{-}[NO])$.
3. The mechanism either does not satisfactorily fit the data, or is considered to be too unrepresentative of the chemistry involved to give reliable atmospheric reactivity predictions. For mixtures, this is used to indicate that there is a large bias in the distribution of fits to $\Delta([O_3]\text{-}[NO])$.

The compounds where the evaluation results indicated possible adjustments to the mechanism may be appropriate or where there was insufficient data for satisfactory evaluation included the following: Cresols, naphthalene, dimethyl naphthalene, and tetralin are included because the data are considered insufficient for satisfactory mechanism development; 4-diethyl hexane, cyclohexanone, t-butyl alcohol, and dimethyl glutarate, because there are non-negligible biases in simulations of full surrogate experiments after adjusting the nitrate yields to fit the mini-surrogate runs; β-pinene is included because of poor fits to the data for some runs; and benzene is included because of poor fits to the data in some runs and for some measures of reactivity. Reactivity predictions for these compounds are therefore considered to be somewhat uncertain, though not as uncertain as those for compounds for which no data are available for mechanism evaluation.

The compounds where the mechanism does not satisfactorily fit the data or is considered to be too uncertain for reliable reactivity predictions are the alkyl bromides and trichloroethylene. As discussed in Section IV.B.5, halogen chemistry is not included in this version of the mechanism, and highly simplified "placeholder" mechanisms are used to make approximate estimates of likely reactivity ranges.

Figure 12. Distribution plots of model simulations of the hourly $\Delta(O_3\text{-NO})$ data for all the experiments used for mechanism evaluation.

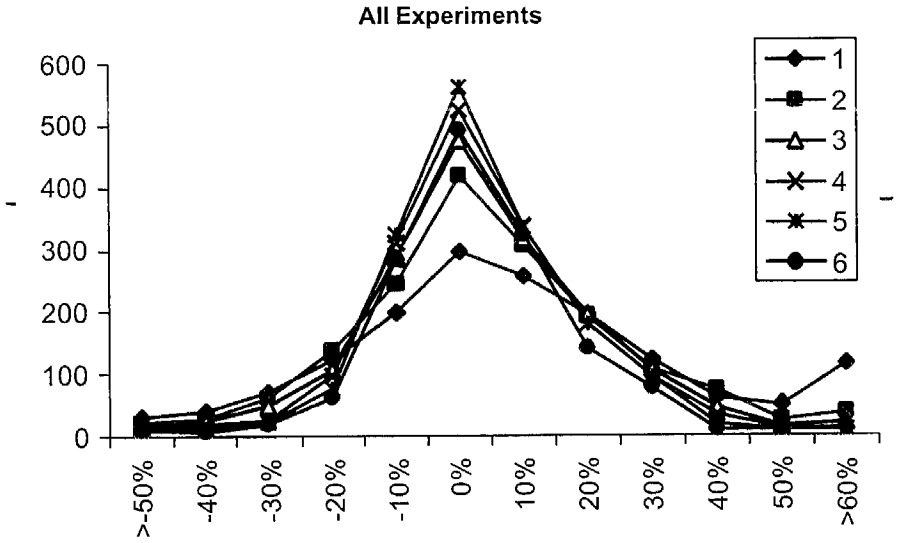

The reactivity predictions for these compounds should be considered to be almost as uncertain as those for compounds where no data are available.

However, as indicated on the table, the evaluation results for most VOCs are given code "1", indicating acceptable fits to the data. Of course, as also indicated on the table, this is often a result of adjusting uncertain aspects of the mechanism to fit the data. For the aromatics this consisted of the various adjustments to the parameterized mechanisms as discussed in Section IV.A, while in most other cases this consisted of adjusting the nitrate yield in the OH reaction (see Section III.I).

Table 48. Summary of results of mechanism evaluation for the various types of experiments, and figures in Appendix B where the evaluation results are shown.

Run Type	Figure no. [a] C	D	R	P	Fit [c]	Comments [d,e]
NOx Offgasing Characterization Runs.	1					NOx offgasing parameter adjusted to fit data for various characterization sets. Ozone fit in most runs, but overpredicted in some cases.
Radical Source Characterization Runs		2				Radical source parameter adjusted to fit data for each characterization set. Scatter indicates run-to-run variability, with most of the data being fit to within +/- 40%. No consistent biases.
Carbon Monoxide			3		1	Slight tendency to underpredict d(O3-NO) reactivity in some experiments, but generally good fits. No adjustments. (MRE, MR3, MR8, R8) (B)
Formaldehyde	4		8		1	Tendency to somewhat overpredict initial NO oxidation rates in most (but not all) blacklight chamber runs. Good fits to the xenon arc chamber runs. No adjustments. (S, MRE, MR3, MR8, R8) (B, X)
Acetaldehyde	5		9		1	Reasonably good fits with no consistent biases. No adjustments. (S, MR3, MR8, R8) (B, X)
Acetone	6		10		1	Reasonably good fits to most data. May be slightly biased towards overpredicting d(O3-NO). No adjustments for this evaluation. (S, MRE, MR3, MR8, R8) (B, X, O)
Methyl Ethyl Ketone	7		11	7	1	Necessary to increase the overall quantum yield to 0.15 to remove biases in simulations.. Good fits to d(O3-NO), and formaldehyde data. Underpredicts acetaldehyde in two runs, fits it in two others. (S, MR3, MRX, MR8) (B, X)
Benzaldehyde			12		1	Reasonably good fit for one experiment and fair fit to the other, where the model does not simulate the base case well. No adjustments. (MR4, R8) (B)
Cresols	13				2	Mechanism adjusted to fit d(O3-NO) data in o-cresol run. Reasonably good fit to d(O3-NO) in p-cresol run, but d(O3-NO) underpredicted in run with m-cresol. (S) (X)
Methacrolein	14				1	Overall quantum yield optimized to fit d(O3-NO) data. Quality of fits similar to that reported by Carter and Atkinson (1996). (S) (B, X, O)
Methylvinyl ketone	14				1	Overall quantum yield optimized to fit d(O3-NO) data. Quality of fits similar to that reported by Carter and Atkinson (1996). (S) (B, X)
Ethane			15		1	Fits most data to within experimental uncertainty. No adjustments. (MRE, MR3) (B)
Propane			16		1	Good fits to data in two MR3 runs; underpredicts d(O3-NO) reactivity in the third. No adjustments. (MR3) (B)

Table 48 (continued)

Run Type	Figure no. [a] C	D	R	P	Fit [c]	Comments [d,e]
n-Butane			17		1	Significantly underpredicts d(O3-NO) reactivity in MRE experiments, but base case is not particularly well simulated. Good fits to MR3, R3, MR8, and R8 reactivity data. No adjustments. (MRE, MR3, R3, MR8, R8) (B) [e]
n-Hexane			18		1	Significantly overpredicts d(O3-NO) inhibition in the MRE run, but good fits to MR3 reactivity data. No adjustments. (MR3) (B)
n-Octane			18		1	Good fits to data in most runs, but somewhat underpredicts d(O3-NO) reactivity in some runs. No adjustments. (MR3, MR8, R8) (B, X)
n-Dodecane			19		1	Slight bias towards overpredicting inhibition in MR3 runs, but reasonably good fits for full surrogate runs. No adjustments. MR3, MR8, R8) (B)
n-Tetradecane			20		1	Similar bias towards overpredicting d(O3-NO) reactivity as in n-dodecane runs, but slight bias towards underpredicting d(O3-NO) inhibition in some (but not all) MR8 runs. No adjustments. (MR3, MR8) (B)
n-Pentadecane			21		1	No consistent biases. Somewhat overpredicts inhibition in MR3 run, underpredicts in MR8 run. (MR3, MR8) (B).
n-Hexadecane			21		1	No consistent biases for MR3 runs. Fair fits for MR8 runs. (MR3, MR8) (B, X)
Isobutane			22		1	Rate of decomposition of t-butoxy radicals adjusted in part based on simulations of these experiments. No consistent biases after adjustment. Generally fits within experimental uncertainty and variability. (MR3) (B)
2,2,4-Trimethyl Pentane			22		1	Nitrate yields from C7 and C8 peroxy radicals adjusted to fit data. Good fits after adjustment. (MR3) (B)
2,6-Dimethyl Octane			22		1	Slight tendency to overpredict d(O3-NO) reactivities in MR4 and MR8 runs may indicate need to adjust nitrate yield slightly, but no adjustments made. Good fit to d(O3-NO) reactivity in R8 run. (MR4, MR8, R8) (B)
2-Methyl Nonane			23		1	Very slight tendency to overpredict d(O3-NO) reactivities in MR3 and MR8 runs may indicate a need to slightly adjust nitrate yield slightly, but no adjustments made. (MR3, MR8, R8) (B)
3,4-Diethyl Hexane			23		2	Non-negligible tendency to overpredict d(O3-NO) inhibition in MR4 experiments and to overpredict d(O3-NO) reactivity in low NOx (R8) runs indicate that adjustments need to be made to the mechanism, but no adjustments made. (MR3, MR8, R8) (B).
Cyclohexane			24		1	Slight bias towards underpredicting inhibition in MR3 runs but good fits for full surrogate runs. No adjustments (MR3, MR8, R8) (B)

Table 48 (continued)

Run Type	Figure no. [a] C	D	R	P	Fit [c]	Comments [d,e]
Hexyl Cyclohexane			24		1	Fits most data to within experimental uncertainty. No adjustments. (MR3, MR8, R8) (B)
Octyl Cyclohexane			25		1	Fits data to within uncertainty for all but one MR3 run, where d(O3-NO) inhibition is slightly overpredicted. No adjustments. (MR3, MR8, R8) (B)
Ethene	27	26	28		1	Variable fits to the large number of ethene - NOx experiments, but overall bias in d(O3-NO) predictions is small (may be slightly high). Tends to underpredict O3 in the outdoor chamber ethene - NOx runs. Good fits to reactivity experiments. No adjustments (S, MR3, MR8, R8) (B, O)
Propene	29	30	31		1	Radical yields in O3P reaction had to be assumed to be low and radical yields in O3 reaction had to be reduced in order to remove bias in simulations of the large number of propene - NOx runs. No bias in d(O3-NO) simulations of propene - NOx runs in blacklight chambers, negative bias for XTC, CTC, and OTC runs and positive bias for EC runs. Fits reactivity data to within experimental uncertainty and variability. (S, MRE, MR3, MR8, R8) (B, X, O)
1-Butene	32				1	Radical yields in both O3P and O3 reaction had to be assumed to be low to approximately fit data, even though assuming low OH yield in O3 reaction is inconsistent with laboratory data. Some variability in fits to data, but no consistent biases after adjustment. (S) (B,X)
1-Hexene	32					Radical yields in both O3P and O3 reaction had to be assumed to be low to approximately fit data, even though assuming low OH yield in O3 reaction is inconsistent with laboratory data. Reasonably good fits to the data after adjustment. (S) (B)
Isobutene	32		33		1	Nitrate yield in OH reaction adjusted upwards to fit data. Somewhat overpredicts maximum O3 in isobutene - NOx runs. Good fits to reactivity data. (S, MR3) (B)
trans-2-Butene	32		33		1	Good fits to data for most runs without adjustments. (S, MRE, MR3, MR8, R8, RE) (B, X)
Isoprene	34		35		1	Reasonably good fits to most (but not all) isoprene - NOx runs; similar to the fits reported by Carter and Atkinson (1996). Bias towards underpredicting O3 reactivity at end of MRE and RE runs, but good fits to MR3 reactivity data. (S, MRE, MR3, RE) (B, X, O)
2-Pentanone	36		37		1	Overall quantum yield for photodecomposition had to be reduced to 0.1 to fit data. Good fits to MPK - NOx and reactivity data after this adjustment. (S, MR3, MR8, R8) (X)

Table 48 (continued)

Run Type	Figure no. [a] C	D	R	P	Fit [c]	Comments [d,e]
Cyclohexanone	36		38		2	Branching ratio for reactions of OH radicals at different positions and overall nitrate yield in OH reaction had to be adjusted to improve model simulations to reactivity data. Photolysis is assumed not to form radicals, so overall quantum yield not adjusted. Fair fits to reactivity data after adjustment, but d(O3-NO) reactivity is still overpredicted in some full surrogate experiments. Model underpredicts d(O3-NO) in the cyclohexanone - NOx experiments in the DTC runs, but gives reasonably good fits to the d(O3-NO) data in the CTC runs. (S, MR3, MR8, R8) (B, X)
4-Methyl-2-Pentanone	39		40		1	Need to adjust quantum yield to 0.04 to fit reactivity data. Reasonably good fits for ketone - NOx, mini-surrogate and high NOx full surrogate runs. Also gives good fits to formaldehyde data in the ketone - NOx runs. Somewhat overpredicts reactivity at end of low NOx full surrogate runs. (S, MR3, MR8, R8) (B, X)
2-Heptanone	36		40		1	Overall quantum yield for photodecomposition had to be reduced to 0.02 to fit data. Good fits to MPK - NOx and reactivity data after this adjustment. (S, MR3, MR8, R8) (X)
Methanol			41		1	Fits data to within experimental uncertainty without adjustments. (MR3) (B)
Ethanol			41		1	Fits data to within experimental uncertainty without adjustments. (MR3) (B)
Isopropyl Alcohol			43		1	Variable fits. Good fits to some mini-surrogate runs, some where d(O3-NO) reactivity underpredicted. No consistent biases for full surrogate runs. No adjustments. (MR3, MR8, R8) (B)
t-Butyl Alcohol			42		2	Nitrate yields adjusted to fit data in the MR3 experiments. The resulting mechanism overpredicts d(O3-NO) reactivities by about 30-50%, but is more consistent with the data for the R8 experiments. Data are somewhat better fit if the rate constant is reduced by about a factor of 1.6 to the estimated value, but the rate constant was not adjusted in the mechanism used. (MR3, MR8, R8) (B)
1-Octanol			44		1	Good fits to two experiments and tendency to overpredict d(O3-NO) reactivity in two others. No adjustments (MR3, MR8, R8) (B)
2-Octanol			44		1	Fits data to within experimental uncertainty and variability. No adjustments (MR3, MR8, R8) (B)
3-Octanol			44		1	Slight bias towards overpredicting d(O3-NO) reactivity. No adjustments. (MR3, MR8, R8) (B)
Propylene Glycol			45		1	Mechanism fits data to within experimental uncertainty. No adjustments (MR3, MR8, R8) (B)

Table 48 (continued)

Run Type	Figure no. [a] C	D	R	P	Fit [c]	Comments [d,e]
Dimethyl Ether			47		1	Mechanism fits data to within experimental uncertainty. No adjustments (MR3) (B)
Diethyl Ether			47		1	Mechanism may be slightly biased towards overpredicting d(O3-NO) reactivity. No adjustments. (MR3, MR8, R8) (B)
Methyl t-Butyl Ether			46		1	Fits data to within experimental uncertainty after adjusting overall nitrate yield (MR3) (B)
1-Methoxy-2-Propanol			48		1	Fits data to within experimental uncertainty after adjusting overall nitrate yield (MR3, MR8, R8) (B)
2-Ethoxyethanol			49		1	Fits data to within experimental uncertainty after adjusting overall nitrate yield (MR3) (B)
2-(2-Ethoxy-ethoxy) Ethanol			49		1	Fits data to within experimental uncertainty after adjusting overall nitrate yield (MR3) (B)
2-Butoxyethanol			50		1	Fits most data to within experimental uncertainty after adjusting overall nitrate yield (MR3, MR8, R8) (B)
Methyl Acetate			51		1	Chamber data are somewhat better fit is it is assumed that reaction at the acetate group is assumed to be negligible. Also necessary to adjust overall nitrate yield somewhat. Adjusted mechanism fits data without consistent biases. (MR3, MR8, R8) (B)
Ethyl Acetate			52		1	Nitrate yield adjusted to improve fits to data. Model fits data for all but one MR8 experiment within experimental uncertainty. (MR3, MR8, R3, R8) (B, X)
Isopropyl Acetate			53	54	1	Reactivity data fit to within experimental uncertainty. Formaldehyde and acetone yields may be slightly underpredicted. No adjustments. (MR3, MR8) (B).
t-Butyl Acetate			53	54	1	Overall nitrate yield adjusted to fit data, but these is still a slight bias towards overpredicting d(O3-NO) reactivity. Model gives good fits to formaldehyde data but may slightly underpredict acetone yields. (MR3, MR8, R8) (X)
Methyl Pivalate			55	56	1	Overall nitrate yields adjusted upwards to fit data. Model gives reasonably good fits to reactivity, formaldehyde, and acetone data, though there may be a slight bias towards underpredicting formaldehyde and acetone yields. (MR3, MR8, R8) (B)
Methyl Isobutyrate			57	58	1	In order to even approximately fit the reactivity data for this compound, it is necessary to assume that radicals such as CH3-O-CO. react with NO2 to form a PAN analogue rather than decompose. Overall nitrate yields and initial OH reaction branching ratios adjusted to improve fits to chamber data. (MR3, MR8, R8) (B)

Table 48 (continued)

Run Type	Figure no. [a] C	D	R	P	Fit [c]	Comments [d,e]
n-Butyl Acetate			59		1	Nitrate yield adjusted to fit data. Fits most data to within experimental uncertainty, though may be slight bias towards overpredicting d(O3-NO) reactivity in the MR8 runs. (MR3, MR8, R8) (B)
Dimethyl Carbonate			60		1	Model gives good fits to data without adjustment. (MR3, MR8, R8) (B)
Methyl Isopropyl Carbonate			61	63	1	Nitrate yields had to be adjusted downwards slightly to fit data. Good fits to d(O3-NO) reactivity data and formaldehyde and acetone yields, though estimation method for reactions of carbonate-derived alkoxy radicals was derived in part based on fits to data for this compound. Model has a bias towards underpredicting IntOH reactivity. (MR3, MR8, R8) (B)
Propylene Carbonate			62		1	Nitrate yields reduced to by relatively large factor to fit mini-surrogate (MR3) runs, and branching ratio for initial OH reaction had to be adjusted also to reduce biases in simulations of full surrogate reactivity runs. Adjusted model still slightly overpredicted reactivity in full surrogate runs. Run DTC243 appears to be anomalous and wasn't used in judging fits. (MR3, MR8, R8) (B)
1-Methoxy-2-Propyl Acetate			64		1	Model gives reasonably good fits to the data without adjustments. May be slight bias towards overpredicting d(O3-NO) reactivity in the MR8 experiments. (MR3, MR8) (B)
Dimethyl Succinate			65		2	Mechanism needed a number of adjustments to yield acceptable fits to the data. Isomerization of the CH3-O-CO-C[O.]-R radical had to be assumed to dominate, which is within the uncertainty of the estimates. Adjusted model fits data to within experimental uncertainty except that it tends to underpredict the d(O3-NO) reactivity in the R8 experiments. (MR3, MR8, R8) (X)
Dimethyl Glutarate			65		2	Had to adjust branching ratio for initial OH reaction, overall nitrate yield, and an alkoxy intermediate branching ratio in order for model to be consistent with the chamber data and available product data. Adjusted model somewhat overpredicts d(O3-NO) reactivity in MR8 experiments, but gives good fits to the data for the MR3 and R8 runs. (MR3, MR8, R8) (X)
Acetylene	66		67		1	Quantum yields for radical formation from the photolysis of glyoxal had to be assumed to be much higher than estimated previously in order to even approximately fit reactivity data for acetylene (see documentation of base mechanism). Model gives reasonably good fits to data from acetylene - NOx runs and reactivity runs, but there may be a slight bias towards underpredicting d(O3-NO) reactivity in the MR3 runs. (S, MR3, MR8, R8) (B, X)

Table 48 (continued)

Run Type	Figure no. [a] C	D	R	P	Fit [c]	Comments [d,e]
Acrolein	68				2	Overall quantum yield adjusted to fit data for acrolein - NOx runs. Good fits for runs at lower acrolein / NOx ratios, but initial NO oxidation rate underpredicted in higher acrolein / NOx run ITC946. (S) (B)
a-Pinene	69		70		1	Overall nitrate yield and number of NO to NO2 conversions in OH reaction adjusted to fit chamber data. Very good fits to a-pinene - NOx runs, reactivity runs fit to within experimental variability and uncertainty. (S, MRE, R8, RE) (B, X, O)
b-Pinene	69		70		2	Overall nitrate yield and numbers of NO to NO2 conversions assumed to be the same as best fits a-pinene data since using significantly different values did not improve fits for this compound. Although initial NO oxidation rates reasonably well fit in the b-pinene - NOx runs, the maximum ozone yield is consistently overpredicted. Fair fits to the incremental reactivity data. (S, MRE, RE) (B, X, O)
3-Carene	69				1	Overall nitrate yield and numbers of NO to NO2 conversions assumed to be the same as best fits a-pinene data since using significantly different values did not improve fits for this compound. Although initial NO oxidation rates reasonably well fit, the maximum ozone yield was underpredicted in three of the four runs. (S) (B)
Sabinene	69				1	Overall nitrate yield and numbers of NO to NO2 conversions assumed to be the same as best fits a-pinene data since using significantly different values did not improve fits for this compound. Slight tendency to overpredict O3 formation rate in middle of run, but maximum O3 concentration reasonably well simulated in most cases. (S) (B)
d-Limonene	69				1	Overall nitrate yield and numbers of NO to NO2 conversions assumed to be the same as best fits a-pinene data since using significantly different values did not improve fits for this compound. Slight tendency to overpredict O3 formation rate in middle of run (though not as much as for sabinene) but maximum O3 concentration reasonably well simulated in most cases. (S) (B)
Benzene	71		79		2	Representation of reactive products adjusted to fit benzene - NOx experiments as discussed in the aromatic mechanism documentation section. Tendency of model to overpredict peak O3 yields in some benzene - NOx runs, and very poor fits to data for one run (ITC562). Reasonably good fits to d(O3-NO) reactivity in reactivity runs, but tendency to underpredict IntOH reactivity. (S, MR3, R8) (B)

Table 48 (continued)

Run Type	Figure no. [a] C	D	R	P	Fit [c]	Comments [d,e]
Toluene	72		79		1	Representation of reactive products adjusted to fit aromatic - NOx experiments as discussed with aromatic mechanism documentation. Reasonably good fits to most toluene - NOx runs. Fits d(O3-NO) reactivity in reactivity experiments within experimental uncertainty and variability, but tends to somewhat underpredict IntOH reactivity. (S, MR3, MR8, R8) (B, X)
Ethyl Benzene	73		79		1	Representation of reactive products adjusted to fit aromatic - NOx experiments as discussed with aromatic mechanism documentation. Reasonably good fits to most ethylbenzene - NOx runs. Fits reactivity runs to within the uncertainty of the data, but effect of added ethylbenzene too small for good mechanism evaluation. (S, MR3) (B, X)
m-Xylene	74		80		1	Representation of reactive products adjusted to fit aromatic - NOx experiments as discussed with aromatic mechanism documentation. Reasonably good fits to most m-xylene - NOx runs. Fits most reactivity runs to within the uncertainty of the data. (S, MR3, MR8, R8) (B, X)
o-Xylene	75				1	Representation of reactive products adjusted to fit aromatic - NOx experiments as discussed with aromatic mechanism documentation. Fair fits to most o-xylene - NOx runs. (S) (B, X)
p-Xylene	76		80		1	Representation of reactive products adjusted to fit aromatic - NOx experiments as discussed with aromatic mechanism documentation. Fair fits to most p-xylene - NOx runs, though some variability in simulations of some CTC runs. Fits the one reactivity run to within the uncertainty of the data, but effect of added p-xylene too small for good mechanism evaluation. No adjustments were made. (S, MR3) (B, X)
1,2,3-Trimethyl Benzene	77		81		1	Representation of reactive products adjusted to fit aromatic - NOx experiments as discussed with aromatic mechanism documentation. Good fits to most 123-TMB - NOx runs, but incremental reactivities somewhat underpredicted in MR3 experiments.. (S, MR3) (B, X)
1,2,4-Trimethyl Benzene	77		81		1	Representation of reactive products adjusted to fit aromatic - NOx experiments as discussed with aromatic mechanism documentation. Fair fits to most 124-TMB - NOx runs. (S) (B, X)
1,3,5-Trimethyl Benzene	78		81		1	Representation of reactive products adjusted to fit aromatic - NOx experiments as discussed with aromatic mechanism documentation. Good fits to most 135-TMB - NOx runs, but incremental reactivities somewhat overpredicted in the MR3 experiment. (S, MR3) (B, X)

Table 48 (continued)

Run Type	Figure no. [a] C	D	R	P	Fit [c]	Comments [d,e]
Naphthalene	82				2	Representation of reactive products adjusted to fit aromatic - NOx experiments as discussed with aromatic mechanism documentation. Unlike the alkylbenzenes, it is necessary to assume significant formation of products that react like PAN analogues in order to approximately fit the naphthalene - NOx runs. Fair fits to most runs, but peak O3 may be somewhat overpredicted in some low NOx experiments. (S) (B)
2,3-Dimethyl Naphthalene	82				1	Representation of reactive products adjusted to fit aromatic - NOx experiments as discussed with aromatic mechanism documentation. Unlike the alkylbenzenes, it is necessary to assume significant formation of products that react like PAN analogues in order to approximately fit the 2,3-dimethylnaphthalene - NOx runs. Good fits to most runs. (S) (B)
Tetralin	82				1	Representation of reactive products adjusted to fit aromatic - NOx experiments as discussed with aromatic mechanism documentation. Unlike the alkylbenzenes, it is necessary to assume significant formation of products that react like PAN analogues in order to approximately fit the tetralin - NOx runs. Fair fits to most runs, with some discrepancies but no consistent biases. (S) (B)
Styrene			83		1	Necessary to adjust the nitrate yield in the OH reaction and the radical yield in the O3 reaction to fit the chamber data. Reasonably good fits to most of the reactivity data. (MR3, MR8, R8) (X)
Toluene Diisocyanate			84		1	A highly simplified parameterized mechanism was adjusted to fit the chamber data. Reasonably good fits were obtained, with no consistent biases. (MR3, MR8, R8) (B).
Para Toluene Isocyanate			85		1	A highly simplified parameterized mechanism was adjusted to fit the chamber data. Reasonably good fits were obtained, with no consistent biases. (MR3, MR8, R8) (B).
N-Methyl-2-Pyrrolidone			86		1	The nitrate yield in the OH reaction was adjusted to fit the chamber data. Reasonably good fits to the reactivity data were obtained.
n-Propyl Bromide			87		3	Bromine chemistry is not represented in this version of the mechanism. The highly simplified "placeholder" mechanism used for all halocarbons (with the appropriate OH rate constant) somewhat overpredicted reactivity in the high NOx runs and incorrectly predicted positive reactivity in the low NOx runs, where the compound actually inhibited O3. (MR3, MR8, R8) (B)

Table 48 (continued)

Run Type	Figure no. [a] C	D	R	P	Fit [c]	Comments [d,e]
n-Butyl Bromide			87		3	Bromine chemistry is not represented in this version of the mechanism. The highly simplified "placeholder" mechanism used for all halocarbons (with the appropriate OH rate constant) approximately fit initial reactivity data in the MR3 experiments, overpredicted reactivity in the high MR8 runs by about a factor of 2, and incorrectly predicted positive reactivity in the low NOx runs, where the compound actually inhibited O3. No adjustments were made. (MR3, MR8, R8) (B)
Trichloroethylene			88		3	Chlorine chemistry is not represented in this version of the mechanism. The highly simplified "placeholder" mechanism used for all halocarbons (with the appropriate OH rate constant) gave surprisingly good fits to the reactivity data, considering the crudity of the mechanism and the fact that no adjustments were made. (MR3, MR8, R8) (B)
Mineral Spirits Samples			89		1	The compositions assumed when simulating experiments with these mixtures are given in Table C-5 in Appendix C. The Model fits the reactivity data to within the experimental uncertainties for samples "B", "C", and "D", but slightly underpredicted the reactivity of sample "A" under higher NOx conditions. Much better mechanism performance than observed previously (Carter et al, 1997f). No adjustments were made. (MR3, MR8, R8) (B)
Exxon D95® Fluid			90		1	The composition assumed when simulating experiments with this mixture is given in Table C-5 in Appendix C. The Model fits data to within the experimental uncertainty for most runs. See Carter et al (2000x) for details and a discussion of the derivation of the composition of this fluid. (MR3, MR8, R8) (B)
Exxon Isopar-M® Fluid			91		2	The composition assumed when simulating experiments with this mixture is given in Table C-5 in Appendix C. The model has a slight bias towards overpredicting d(O3-NO) inhibition in the MR8 runs, but fits data to within the experimental uncertainty for the other runs. See Carter et al (2000x) for details and a discussion of the derivation of the composition of this fluid. (MR3, MR8, R8) (B)
Exxon Exxate-1000® Fluid (Oxo-Decyl Acetate)			92		1	The composition assumed when simulating experiments with this mixture is given in Table C-5 in Appendix C. The model fits the data to within the experimental variability, with no consistent biases. See Carter et al (2000x) for details and a discussion of the derivation of the composition of this fluid. (MR3, MR8, R8) (B)
"MIX-A" Mix		93			1	Fits are variable, but the model does not have a significant bias for the group as a whole. D(O3-NO) is predicted to within +/- 40% for most runs.

Table 48 (continued)

Run Type	Figure no. [a] C	D	R	P	Fit [c]	Comments [d,e]
"SURG-4" Mix		94			3	Model has definite bias towards overpredicting O3 in these experiments, and even more towards overpredicting initial NO oxidation rate. Possible experimental problems with these low NOx runs; NOx zeros do not appear to be correct in some cases.
"SURG-7" Mix		95			2	Model has a tendency to overpredict d(O3-NO) by about 20% on the average.
"SURG-8S" Mix		96			2	Fits are highly variable for this group, with the model having a bias towards underprediction by about 20%.
"SURG-3M" Mix		97			1	Fits are variable, with overall biases being small but somewhat different in different chambers. D(O3-NO) is usually simulated to within +/- 30%.
"SURG-8M" Mix		98			1	Generally good fits with no or small overall bias. D(O3-NO) is usually simulated by +/- 20%.
"SURG-8" Mix		99			1	Generally good fits with no or small overall bias. D(O3-NO) is usually simulated by +/- 20%.
"SURG-X" Mix		100			2	Most runs are reasonably well simulated, but there are more cases where d(O3-NO) is overpredicted than underpredicted, especially in the first hour of the run.

[a] Figure types codes: C = concentration/time plots; D = distribution plots; R = reactivity data; P = product data plots.

[b] Types of experiments used to evaluate mechanisms for VOC or mixture is indicated in parentheses after comments. S = single VOC - NOx, MR3 = "MR3" reactivity, etc. (See Table 45 for reactivity experiment type codes.). Types of light source indicated in parentheses after experiment type codes. B = blacklight chambers, X = xenon arc chambers, O = outdoor chambers.

[c] Fit codes for evaluations of mechanisms of individual VOCs are as follows:

1 Model fits data to within experimental uncertainty, no consistent biases, or biases are considered not large enough to be significant. This code also used if data are not adequate to sufficiently evaluate mechanism. For mixtures, this code means no consistent biases in d(O3-NO) predictions.

2 Some poor fits or biases indicate possible mechanism problems or needs for improvement. For mixtures, this means that there are some biases in d(O3-NO) predictions.

3 The mechanism either does not satisfactorily fit the data, or is considered to be too unrepresentative of the chemistry involved to give reliable atmospheric reactivity predictions. For mixtures, this means that there are large biases in d(O3-NO) predictions.

[d] Model tends to consistently underpredict IntOH reactivities in all low NOx (e.g., R8) incremental reactivity experiment, possibly due to problems in representation of radical reactions under low NOx conditions. This is not noted in the comments for the individual VOCs.

[e] Although there are a large number of single VOC - NOx runs for n-butane and some for a few other alkanes, these are not useful for mechanism evaluation because of their large sensitivity to the chamber radical source (Carter and Lurmann, 1990).

VI. LUMPED MECHANISM FOR AIRSHED MODELS

Airshed model applications require simulations of highly complex mixtures of large numbers of VOCs, and in most cases it is not necessary or practical to represent each of them separately. For such applications, models with lumped model species that represent reactions of a large number of species with similar reaction rates and mechanisms, are generally employed. Even for VOC reactivity assessment it is only really necessary to separately represent the VOC whose reactivity is being assessed, the reactions of most of the other VOCs present in the ambient simulation can be represented using appropriate lumped model species. This was the approach that was employed in our previous reactivity studies (e.g., Carter and Atkinson, 1989a, Carter, 1994a), and continues to be the approach used in this work.

In this section, we describe the lumping approach we recommend for use when employing this mechanism in regional model simulations, which is also the approach used in the EKMA models when calculating the reactivity scales discussed in Section VII.A. Before discussing the specific approach, we briefly summarize the various types of lumping methods that can be employed, and the factors that need to be considered when determining the recommended method.

A. Summary of Lumping Approaches

As with the previous mechanism (Carter, 1988), two different approaches, referred to as lumped molecule and variable lumped parameter condensation, can be employed to represent VOCs in complex mixtures. A third approach, referred to here as fixed parameter condensation is used in condensed models such as the LCC (Lurmann et al, 1987), RADM-2 (Stockwell et al, 1990), and RACM (Stockwell et al, 1997) can also be employed, and may be appropriate or necessary in some applications. A fourth approach, referred to as lumped structure is employed in the widely-used Carbon Bond mechanism (Gery et al, 1988) and was used to represent hydroperoxides in the previous SAPRC mechanism (Carter, 1990), though it is not used in the current mechanism. These are discussed below.

1. Lumped Molecule Approach

The lumped molecule approach involves representing the VOC by a model species in the base mechanism, on a molecule-for-molecule basis. This is the same as the approach used to represent most of the product species in the various VOC reactions, as discussed above in Section II.C.1. For example, the lumped higher aldehyde species, RCHO, can be used to represent all aldehydes present in emissions or other complex mixtures, if it is not necessary to represent them explicitly for the purpose of estimating their reactivities. Although this is less accurate than the lumped or fixed parameter approaches discussed below, it is appropriate for classes of compounds that are believed to react very similarly, or are not sufficiently important in the emissions to justify more complex approaches.

2. Variable Lumped Parameter Approach

The variable lumped parameter approach representing a group of VOCs that react with similar rate constants with model species whose kinetic and product yield parameters are weighted averages of the mixture of VOCs they are being used to represent. This is potentially the most accurate lumping method, permitting lumping of species with quite different mechanisms, provided that they react with the same species with similar rate constants, or at least have similar kinetic reactivities (fractions reacted) in

the model scenarios (Carter, 1988). Two weighting methods can be used when deriving the parameter values given the mixture of emitted or ambient VOCs being represented.

In reactivity weighting, the contribution of a given VOC to the parameters derived for the lumped model species is proportional to the amount of the VOC that is estimated to react in the scenario, which, if the VOC reacts only with OH radicals, is given by

$$\text{Amount Reacted} = \text{Amount Emitted} \cdot \text{Fraction Reacted} \qquad \text{(XXXII)}$$

where

$$\text{Fraction Reacted} = \text{Kinetic Reactivity} \approx (1 - e^{-kOH \cdot IntOH}) \qquad \text{(XXXIII)}$$

and kOH is the OH radical rate constant and IntOH is an effective integrated OH radical rate constant that is characteristic of the type of model scenario (Carter, 1988; Middleton et al, 1990), which is estimated to be ~110 ppt-min for regional model applications (Middleton et al, 1990). This is most appropriate when lumping VOCs with widely varying kinetic reactivities, as is necessary when lumping slowly reacting VOCs into a single group. However, this has the disadvantage that the number of moles of model species is different from the number of moles of compounds being represented, which detracts from the chemical realism of the mechanism. In addition, the value of IntOH appropriate for a single day urban or EKMA simulation will not be appropriate for a multi-day regional simulation, and vise-versa.

In molar weighting, the contribution of a given VOC to the parameters of the lumped model species is simply proportional to the amount of VOC emitted or input into the scenario. This is appropriate if the VOCs being lumped have similar kinetic reactivities, as is generally the case for rapidly reacting VOCs[21]. This lumping is also more chemically realistic because it preserves moles, and does not depend on any aspect of the scenario other than the emissions.

Note that a variant of the lumped parameter approach is used when representing the individual VOCs for the purpose of evaluating the mechanism against chamber data or calculating its atmospheric reactivity. However, in this case there is no lumping involved, one model species, with parameters set equal to those of the compound being represented, is used for each VOC whose mechanism is being evaluated or whose reactivity is being calculated. The one exception is model simulations of experiments or reactivities of complex mixtures (such as mineral spirits or vehicle exhausts), where species in the mixtures are lumped in the same way as recommended for regional model simulations.

Although potentially the most accurate, the lumped parameter approach has the disadvantages that nature of the model species depends on the emissions, and requires special emissions processing procedures that involves software that is not available on most modeling systems. In addition, emissions speciation is often highly uncertain, and model simulations using scenario-specific parameters for the lumped species may not necessarily be significantly more accurate than those using parameters derived using a "typical" or "representative" ambient mixture or emissions profile.

3. Fixed Parameter Approach

The fixed parameter approach is a variant of the lumped parameter approach where the parameters for the lumped species are derived using a typical or representative ambient mixture or emissions profile, and then used in all subsequent model applications regardless of the actual emissions

---

[21] VOCs with OH rate constants $\geq 10^{-11}$ cm^3 $molec^{-1}$ s^{-1} have kinetic reactivities greater than 80% for IntOH = 110 ppt-min. Since kinetic reactivities can be no greater than 100%, this means that kinetic reactivities of VOCs with this or higher rate constants are all within ± 20%.

involved. This is the approach that was used in the RADM-2 mechanism (Stockwell et al, 1990), where the parameters for the lumped alkane, alkene, and aromatic species were derived based on the RADM-2 emissions inventory, and then held fixed for all model applications using that mechanism (Carter and Lurmann, 1990). This greatly simplifies mechanism implementation and emissions processing, and is potentially as accurate as the variable lumped parameter approach if the emissions composition is uncertain or reasonably well represented by the composition used when deriving the mechanism.

In this work we present a fixed parameter version of this mechanism that can be used to permit implementation of this mechanism in modeling systems that do not support the emissions processing needed for implementing the variable parameter approach. This is discussed in Section VI.B, below. It is based on the ambient mixture of VOCs obtained from analysis of air quality data (Jeffries et al, 1989; Carter, 1994a,b) which was used to represent the base case reactive organic gas (ROG) mixture in the previous (e.g., Carter, 1994a,b) and current (see Section VII) reactivity scale calculation.

However, it is recommended that the variable parameter approach be used in model applications where it is believed that the composition of the initial and/or emitted VOC species are known with reasonable accuracy. In particular, it should be used in applications where the composition of the emitted or ambient species is believed to be significantly different from that of the base ROG mixture used to derive the lumped parameters in the fixed parameter mechanism.

4. Lumped Structure Approach

The widely-used Carbon Bond IV mechanism uses the "lumped structure" approach, where different parts of the molecule are treated as if they react independently (Gery et al, 1988). This permits representation of a large number of compounds with a relatively small number of model species, and performs reasonably well in simulating experiments with complex mixtures that are representative of those used when the mechanism was developed (Gery et al, 1988). However, as seen from the detailed mechanistic discussion given above in Section III, different parts of molecules actually do not react independently. Examples of where the lumped structure approximation break down include the dependence of nitrate yields on the size of the peroxy radicals (Section III.I) the importance of internal isomerization and rearrangement reactions undergone by larger alkoxy radicals (Section III.J). For that reason, this approximation is not used in the current version of the mechanism.

B. Recommended Lumping for Regional Model Applications

1. Lumping Approach

The optimum lumping approach in terms of minimizing the number of model species without introducing nonnegligible approximations depends on the model application and type of scenario employed. The use of the variable parameter approach permits a high degree of lumping with very little approximation in single box or EKMA model scenarios, which involve only a single day simulation with all the VOCs being introduced together (Carter, 1988). However, the requirements of multi-cell and multi-day regional models are more demanding. This is because different compositions of VOCs can be emitted at different times and locations, so no single parameterization may represent the emissions profile in all locations at all times. In addition, representing slowly reacting VOCs with more rapidly reacting model species using reactivity weighting may not appropriately represent these VOCs in multi-day simulations, since they would persist longer than the model species used to represent them. More lumped classes are therefore needed to minimize the time and space variation of the reactivity characteristics of

the VOCs represented by any given lumped species, and to permit the slowly reacting species to be more appropriately represented in multi-day scenarios.

The approach adopted in this work is to recommend a lumping approach that addresses the requirements of regional, multi-cell, multi-day model applications. Since that is the most demanding requirement, this will then give a mechanism that should be appropriate for most applications, albeit with more species than may be necessary for some applications such as EKMA. This permits use of a consistent mechanism and degree of condensation, regardless of the application.

Table 49 gives a summary of the lumped classes recommended for use with regional models. The lumping for the more reactive classes of compounds are similar to that used in other mechanisms such as the RADM-2 (Stockwell et al. 1990) and RACM (Stockwell et al, 1997) mechanisms, and condensed versions of the SAPRC-90 mechanism (Lurmann et al, 1991; Kumar et al, 1995). However, there is a larger number of slowly reacting "alkane and others" classes, to allow for appropriate representations of compounds such as ethane and propane in regional model simulations. Separate classes are used for ethane and propane and compounds with similar reactivities, with non-methane organics that react slower than half that of ethane being treated as inert. The dividing lines in terms of OH rate constants are somewhat arbitrary in the case of the alkane classes, but are chosen in the recommended lumping to be consistent with those used in the RADM-2 emissions processing system, as discussed by Middleton et al (1990). This permits the mechanism to be used in models with emissions data processed for the RADM-2 mechanism, as discussed in the following section.

Biogenic compounds are represented in separate classes because their emissions can have significantly different spatial and temporal profiles than anthropogenic emissions, and their reactivity characteristics are quite different from those of the anthropogenic alkenes they otherwise would be lumped with. Isoprene, which is the dominant biogenic in many U.S. scenarios, is represented explicitly, and a separate lumped class is used is used for terpenes.

Note that the lumped molecule assignments takes advantage of the fact that this version of the mechanism uses a relatively large number of model species represent reactive products, compared to previous mechanisms. This permits, for example, unsaturated aldehydes and ketones to be represented using isoprene product species whose mechanisms are probably closer to the compounds being represented than the generic higher saturated aldehyde or ketone species used in most mechanisms. Although the saturated higher aldehydes and ketones could be represented using the lumped parameter approach since explicit mechanisms for such compounds can be generated, the lumped molecule approach is employed because they are not sufficiently important in emissions or ambient air masses to justify using separate model species for them.

Table 49 shows that that the lumping approach for representing most oxygenated species when present in mixtures is the same as used when representing them when formed as products in the oxidations of other VOCs, as discussed above in Sections II.C.1 and II.C.2. The major exceptions are oxygenated compounds that react only with OH radicals, such as esters, acids, etc. These are represented using the appropriate lumped alkane class (ALK1, ... ALK5) depending on their OH rate constant when they are primary VOCs, but are represented by MEK, PROD2, or (for acids) RCO-OH if they are formed as reactive products of other VOCs. This is because in principle the use of lumped parameter species can permit a more accurate representation of the impacts of these compounds when present in complex mixtures, if the parameters are derived to take the contributions of these species into account. The MEK and PROD2 model species are only used to represent ketones, whose photolysis reactions cannot be represented using lumped alkane classes.

Table 49. Summary of lumped classes and lumped molecule representations recommended for representing complex mixtures in ambient model applications.

Model Species	Description
Emitted Compounds Represented Explicitly	
CH4	Methane
ETHENE	Ethene
ISOPRENE	Isoprene
HCHO	Formaldehyde
ACET	Acetone
MEOH	Methanol
PHEN	Phenol
Lumped Molecule Groups	
CCHO	Acetaldehyde and Glycolaldehyde
RCHO	Lumped C3+ Aldehydes
MEK	Ketones that react with OH radicals slower than 5×10^{-12} cm^3 $molec^{-2}$ sec^{-1}.
PROD2	Ketones that react with OH radicals faster than 5×10^{-12} cm^3 $molec^{-2}$ sec^{-1}.
CRES	Cresols
BALD	Aromatic aldehydes (e.g., benzaldehyde)
METHACRO	Methacrolein and acrolein
ISOPROD	Unsaturated aldehydes other than acrolein and methacrolein.
MVK	Unsaturated ketones
Unreactive Compounds	
INERT	Compounds other than CO or methane that do not react, or react only with OH with a rate constant less than approximately half that of ethane, or ~2×10^2 ppm-1 min-1.
Lumped Parameter Groups (Lumped using molar weighting except as indicated)	
ALK1	Alkanes and other non-aromatic compounds that are react only with OH, and have an OH rate constant (kOH) between 2×10^2 and 5×10^2 ppm-1 min-1. (Primarily ethane)
ALK2	Alkanes and other non-aromatic compounds that react only with OH, and have kOH between 5×10^2 and 2.5×10^3 ppm-1 min-1. (Primarily propane and acetylene)
ALK3	Alkanes and other non-aromatic compounds that react only with OH, and have kOH between 2.5×10^3 and 5×10^3 ppm-1 min-1.
ALK4	Alkanes and other non-aromatic compounds that react only with OH, and have kOH between 5×10^3 and 1×10^4 ppm-1 min-1.
ALK5	Alkanes and other non-aromatic compounds that react only with OH, and have kOH greater than 1×10^4 ppm-1 min-1.
ARO1	Aromatics with kOH < 2×10^4 ppm-1 min-1. (Primarily toluene and other monoalkyl benzenes.) Benzene and slower reacting aromatics such as halobenzens are lumped with reactivity weighting based on their OH rate constant relative to that of toluene, all others are lumped using molar weighting. Group given kOH of toluene.
ARO2	Aromatics with kOH > 2×10^4 ppm-1 min-1. (Primarily xylenes and polyalkyl benzenes)
OLE1	Alkenes (other than ethene) with kOH < 7×10^4 ppm-1 min-1. (Primarily terminal alkenes)
OLE2	Alkenes with kOH > 7×10^4 ppm-1 min-1. (Primarily internal or disubstituted alkenes)
TRP1	Biogenic alkenes other than isoprene (primarily terpenes)

The mechanisms for the model species ALK_n, ARO_n, OLE_n, and TRP1 are derived depending on the mixture of VOCs they are being used to represent, which depends on the emissions or initial VOCs in the model simulation. To conserve moles and for greater chemical realism, it is recommended that molar weighting rather than reactivity weighting be used in most cases. Note that for the lowest reactivity "alkane and others" class, ALK1, this means that compounds reacting much slower than the rate constant for the class should not be lumped with the class. For this reason, compounds with OH rate constants lower than about half that of ethane are treated as "inert", i.e., not lumped with ALK1. (The one exception is methane, which, because of the relatively large amount present, is represented explicitly.) Although these slowly reacting compounds, such as HCFC's, etc., may eventually react to some extent in multi-day regional episodes, the amounts emitted and therefore the amounts reacted are very small, and would have negligible effect. Of course, if the reactivities or persistence of these compounds are of interest, then separate model species should be used to represent them.

The one area where it is recommended that reactivity weighting be used concerns the representation of benzene and other slowly reacting aromatics. Because they are emitted in relatively small amounts and contribute relatively little to the overall reactivity of the mixture, it is not considered worthwhile to represent them separately, so they are represented using the ARO1 group, which is dominated by toluene and the alkylbenzenes. However, benzene has a kinetic reactivity which is less than 1/3 that of toluene, so representing it using a group that represents primarily monoalkylbenzenes would not be appropriate. For that reason, the recommended approach is to use reactivity weighting for benzene and other slowly reacting when being represented by the ARO1 group, but use molar weighting for toluene and the alkylbenzenes, and give the group the OH rate constant of toluene. If an IntOH of 110 ppt-min, as used for the RADM-2 mechanism (Middleton et al, 1990), this means that one mole of benzene would be represented by 0.295 moles of ARO1. Of course, if calculations of the persistence or role of benzene are of particular interest, then a separate model species should be used for this purpose.

The mechanisms for the model species ALK_n, ARO_n, OLE_n, and TRP1 can be derived from the emissions inventory as discussed by Carter (1988). This requires assigning all the emissions classes in the emissions inventory to detailed model species in the present mechanism, which is beyond the scope of this report. However, they can also be derived using the mixture of reactive organic measured in ambient air, as discussed in the following section.

2. Fixed Parameter Mechanism

Although state-of-the-art modeling systems should include the ability to derive the most appropriate parameters for the model species from the VOC emissions data, in practice very few modeling systems presently support this capability. In addition, use of variable parameter mechanism to represent ambient or emitted VOCs may not be necessary or appropriate in all cases. These include model applications where the compositions of the emissions input are uncertain or highly variable, or model applications that employ idealized scenarios representing a wide distribution of conditions are employed. The latter includes developing general reactivity scales such as the Carter (1994a) scales that are updated in this work. Therefore, a fixed parameter version of this mechanism is derived to address these needs, as discussed in this section.

The base case model scenarios used to derive the Carter (1994a) reactivity scales use a standard mixture of hydrocarbons and oxygenates to represent the reactive VOCs that are emitted or initially present in the scenarios. The composition of this mixture, which is given in Table 50, was derived from an analysis of hydrocarbons in urban atmospheres in the United States (Jeffries et al, 1998) and from

Table 50. Composition of the base ROG mixture used in the reactivity simulations and to derive the lumped parameters in the fixed parameter mechanism.

VOC Name	Moles VOC / Mole C Mix	Represented By	Lumped with
Ethane	0.01685	ETHANE	ALK1
Propane	0.01413	PROPANE	ALK2
n-Butane	0.01807	N-C4	ALK3
n-Pentane	0.00613	N-C5	ALK4
n-Hexane	0.00132	N-C6	ALK4
n-Heptane	0.00120	N-C7	ALK5
n-Octane	0.00074	N-C8	ALK5
n-Nonane	0.00074	N-C9	ALK5
n-Decane	0.00184	N-C10	ALK5
n-Undecane	0.00016	N-C11	ALK5
n-Dodecane	0.00033	N-C12	ALK5
n-Tridecane	0.00001	N-C13	ALK5
Isobutane	0.00788	2-ME-C3	ALK3
Iso-Pentane	0.01516	2-ME-C4	ALK4
2-Methyl Pentane	0.00355	2-ME-C5	ALK4
3-Methylpentane	0.00253	3-ME-C5	ALK4
2,2-Dimethyl Butane	0.00046	22-DM-C4	ALK3
2,3-Dimethyl Butane	0.00095	23-DM-C4	ALK4
2,4-Dimethyl Pentane	0.00060	24-DM-C5	ALK4
3-Methyl Hexane	0.00127	3-ME-C6	ALK5
2,3-Dimethyl Pentane	0.00112	23-DM-C5	ALK5
Cyclopentane	0.00071	CYCC5	ALK4
Methylcyclopentane	0.00161	ME-CYCC5	ALK4
Cyclohexane	0.00068	CYCC6	ALK5
Methylcyclohexane	0.00068	ME-CYCC6	ALK5
Ethylcyclohexane	0.00018	ET-CYCC6	ALK5
Branched C6 Alkanes	0.00024	0.5 23-DM-C4 + 0.25 3-ME-C5 + 0.25 2-ME-C5	ALK4
Branched C7 Alkanes	0.00209	0.5 24-DM-C5 + 0.25 3-ME-C6 + 0.25 2-ME-C6	0.5 ALK4 + 0.5 ALK5
Branched C8 Alkanes	0.00403	0.5 24-DM-C6 + 0.25 4-ME-C7 + 0.25 2-ME-C7	ALK5
Branched C9 Alkanes	0.00171	0.5 24-DM-C7 + 0.25 4-ME-C8 + 0.25 2-ME-C8	ALK5
Branched C10 Alkanes	0.00156	0.5 26DM-C8 + 0.25 4-ME-C9 + 0.25 2-ME-C9	ALK5
Branched C11 alkanes	0.00016	0.5 26DM-C9 + 0.25 4-ME-C10 + 0.25 3-ME-C10	ALK5
Branched C12 Alkanes	0.00033	0.5 36DM-C10 + 0.25 5-ME-C11 + 0.25 3-ME-C11	ALK5
Branched C13 Alkanes	0.00001	0.5 36DM-C11 + 0.25 5-ME-C12 + 0.25 3-ME-C12	ALK5
C7 Cycloalkanes	0.00012	ME-CYCC6	ALK5
Ethene	0.01346	ETHENE	ETHE
Propene	0.00318	PROPENE	OLE1
1-Butene	0.00115	1-BUTENE	OLE1
C4 Terminal Alkenes	0.00014	1-BUTENE	OLE1
3-Methyl-1-Butene	0.00032	3M-1-BUT	OLE1

Table 50 (continued)

VOC Name	Moles VOC / Mole C Mix	Represented By	Lumped with
1-Pentene	0.00080	1-PENTEN	OLE1
1-Hexene	0.00033	1-HEXENE	OLE1
Isobutene	0.00115	ISOBUTEN	OLE2
2-Methyl-1-Butene	0.00092	2M-1-BUT	OLE2
trans-2-Butene	0.00115	T-2-BUTE	OLE2
cis-2-Butene	0.00091	C-2-BUTE	OLE2
2-Methyl-2-Butene	0.00052	2M-2-BUT	OLE2
1,3-Butadiene	0.00062	13-BUTDE	OLE2
Isoprene	0.00130	ISOPRENE	ISOP
Cyclohexene	0.00018	CYC-HEXE	OLE2
C5 Terminal Alkenes	0.00044	1-PENTEN	OLE1
C6 Terminal Alkenes	0.00223	1-HEXENE	OLE1
C7 Terminal Alkenes	0.00119	1-HEPTEN	OLE1
C8 Terminal Alkenes	0.00024	1-OCTENE	OLE1
C9 Terminal Alkenes	0.00052	1-C9E	OLE1
C10 Terminal Alkenes	0.00010	1-C10E	OLE1
C11 Terminal Alkenes	0.00019	1-C11E	OLE1
C4 Internal Alkenes	0.00014	0.5 T-2-BUTE + 0.5 C-2-BUTE	OLE2
C5 Internal Alkenes	0.00317	0.5 C-2-PENT + 0.5 T-2-PENT	OLE2
C6 Internal Alkenes	0.00100	0.5 C-2-C6E + 0.5 T-2-C6E	OLE2
C7 Internal Alkenes	0.00044	T-3-C7E	OLE2
C8 Internal Alkenes	0.00021	T-4-C8E	OLE2
C9 Internal Alkenes	0.00024	T-4-C9E	OLE2
C10 Internal Alkenes	0.00010	T-4-C10E	OLE2
C11 Internal Alkenes	0.00019	T-5-C11E	OLE2
C7 Cyclic or di-olefins	0.00019	T-2-C7E	OLE2
a-Pinene	0.00051	A-PINENE	TRP1
3-Carene	0.00019	3-CARENE	TRP1
C9 Styrenes	0.00048	STYRENE	ARO2
C10 Styrenes	0.00036	STYRENE	ARO2
Benzene	0.00329	BENZENE	0.295 ARO1
Toluene	0.00923	TOLUENE	ARO1
Ethyl Benzene	0.00128	C2-BENZ	ARO1
n-Propyl Benzene	0.00036	N-C3-BEN	ARO1
Isopropyl Benzene (cumene)	0.00019	I-C3-BEN	ARO1
C9 Monosub. Benzenes	0.00016	N-C3-BEN	ARO1
s-Butyl Benzene	0.00023	S-C4-BEN	ARO1
C10 Monosub. Benzenes	0.00018	N-C3-BEN	ARO1
C11 Monosub. Benzenes	0.00065	N-C3-BEN	ARO1
C12 Monosub. Benzenes	0.00002	N-C3-BEN	ARO1
o-Xylene	0.00183	O-XYLENE	ARO2
p-Xylene	0.00218	P-XYLENE	ARO2
m-Xylene	0.00218	M-XYLENE	ARO2
C9 Disub. Benzenes	0.00247	0.34 M-XYLENE + 0.33 O-XYLENE + 0.33 P-XYLENE	ARO2
C10 Disub. Benzenes	0.00154	0.34 M-XYLENE + 0.33 O-XYLENE + 0.33 P-XYLENE	ARO2
C11 Disub. Benzenes	0.00010	0.34 M-XYLENE + 0.33 O-XYLENE + 0.33 P-XYLENE	ARO2

Table 50 (continued)

VOC Name	Moles VOC / Mole C Mix	Represented By	Lumped with
C12 Disub. Benzenes	0.00009	0.34 M-XYLENE + 0.33 O-XYLENE + 0.33 P-XYLENE	ARO2
1,3,5-Trimethyl Benzene	0.00072	135-TMB	ARO2
1,2,3-Trimethyl Benzene	0.00075	123-TMB	ARO2
C9 Trisub. Benzenes	0.00236	0.34 135-TMB + 0.33 123-TMB + 0.33 124-TMB	ARO2
C10 Trisub. Benzenes	0.00160	0.34 135-TMB + 0.33 123-TMB + 0.33 124-TMB	ARO2
C11 Trisub. Benzenes	0.00010	0.34 135-TMB + 0.33 123-TMB + 0.33 124-TMB	ARO2
C12 Trisub. Benzenes	0.00009	0.34 135-TMB + 0.33 123-TMB + 0.33 124-TMB	ARO2
C10 Tetrasub. Benzenes	0.00042	0.34 135-TMB + 0.33 123-TMB + 0.33 124-TMB	ARO2
Acetylene	0.00974	ACETYLEN	ALK2
Formaldehyde	0.00792	FORMALD	HCHO
Acetaldehyde	0.00477	ACETALD	CCHO
Propionaldehyde	0.00070	PROPALD	RCHO
C4 aldehydes	0.00031	1C4RCHO	RCHO
C5 Aldehydes	0.00107	1C5RCHO	RCHO
C6 Aldehydes	0.00073	1C6RCHO	RCHO
Benzaldehyde	0.00016	BENZALD	BALD
Acetone	0.00309	ACETONE	ACET
Methyl Ethyl Ketone	0.00110	MEK	MEK

oxygenate measurements in the California South Coast Air Basin (Carter, 1994a,b and references therein). Table 50 also shows the detailed model species used to represent each of measured components in the mixture, and groups used to represent them in the lumped mechanism. Since this mixture is based on VOC measurements in a variety of urban areas, it serves as an appropriate basis for deriving parameters for those lumped species that represent anthropogenic emissions.

This base ROG mixture cannot serve as a basis for deriving the parameters for the biogenic terpene (TRP1) group, since that mixture represents purely ambient VOCs. For this we use the estimated annual North American biogenic terpene emissions rates summarized by Guenther et al (2000), where the five most abundant terpenes are as follows:

Terpene	Tg C/year
α-Pinene	4.3
β-Pinene	3.1
Δ^3 O_3	1.9
Sabinene	1.1
d-Limonene	1.0

Although other terpenes listed by Guenther et al (2000) total more than 3 Tg C/year and other classes of compounds, such as alcohols and aldehydes, are also important in the biogenic inventory, this profile is used as the basis for deriving the recommended parameters for the TRP1 lumped group for the present

mechanism. Note that since the appropriate lumped group used for anthropogenic species can be used to represent the biogenic alcohols and aldehydes, the contributions of these compounds to the biogenic emissions do not affect the parameters derived for TRP1.

Table 51 gives a summary of the compounds used to derive the mechanism for each of the lumped model species in the fixed parameter mechanism. The relative contributions of the species to the parameters of each group are also shown. Except for benzene (see discussion above) the relative contributions were determined by the mole fractions of the compounds in the mixtures.

The rate constants and mechanisms for the reactions for these lumped species that are derived using this set of anthropogenic base ROG and biogenic terpene mixtures are given in Table A-3 in Appendix A. The reactions of ethene and isoprene that are used for these explicitly represented species are also shown on that table. These explicit and lumped primary VOC reactions are added to the base mechanism to constitute the full fixed parameter SAPRC-99 mechanism for use in ambient simulations. This mechanism is used in the base case simulations in the incremental reactivity calculations discussed in Section VII.

It should be emphasized, however, that for model applications where the emissions inventory is known, or where the effects of changing the composition of the inventory is being assessed, the parameters should be derived using the specific inventories used in the simulations. This is particularly true if the inventories indicate significant contributions of classes of compounds that are not in the base ROG mixture used to derive the current fixed parameter mechanism. In particular, the base ROG mixture consists primarily of the hydrocarbons of the type found in gasoline vehicle exhausts, and the parameters derived using this mixture may not be appropriate if sources involving emissions of other types of VOCs, such as glycols or alcohols, are important.

Table 51. Summary of compounds used to derive mechanisms for lumped parameter groups in the fixed parameter mechanism.

Compound	Cont'n	Compound	Cont'n	Compound	Cont'n
ALK1		ALK5		ARO1	
Ethane	100%	2,4-Dimethyl Hexane	11%	Toluene	70%
		n-Decane	10%	n-Propyl Benzene	10%
ALK2		3-Methyl Hexane	10%	Ethyl Benzene	10%
Propane	59%	n-Heptane	7%	Benzene [a]	7%
Acetylene	41%	2,3-Dimethyl Pentane	6%	s-Butyl Benzene	2%
		2-Methyl Heptane	6%	Isopropyl Benzene	1%
ALK3		4-Methyl Heptane	6%		
n-Butane	68%	2,4-Dimethyl Heptane	5%	ARO2	
Isobutane	30%	Methylcyclohexane	4%	m-Xylene	22%
2,2-Dimethyl Butane	2%	2,6-Dimethyl Octane	4%	p-Xylene	22%
		n-Nonane	4%	o-Xylene	20%
ALK4		n-Octane	4%	1,3,5-Trimethyl Benzene	14%
Iso-Pentane	45%	Cyclohexane	4%	1,2,3-Trimethyl Benzene	14%
n-Pentane	18%	2-Methyl Hexane	3%	1,2,4-Trimethyl Benzene	9%
2-Methyl Pentane	11%	4-Methyl Octane	2%		
3-Methylpentane	8%	2-Methyl Octane	2%		
2,4-Dimethyl Pentane	5%	4-Methyl Nonane	2%		
Methylcyclopentane	5%	2-Methyl Nonane	2%		
n-Hexane	4%	n-Dodecane	2%		
2,3-Dimethyl Butane	3%	Ethylcyclohexane	1%		
Cyclopentane	2%	n-Undecane	1%		
		3,6-Dimethyl Decane	1%		

[a] Reactivity weighting factor of 0.295 used for benzene. See text.

VII. ATMOSPHERIC REACTIVITY ESTIMATES

To estimate the effects of VOC emissions on ozone formation under conditions more representative of polluted urban atmospheres, incremental reactivities were calculated for all VOCs that are represented in the current mechanism. This includes not only the VOCs whose mechanisms were derived or estimated as discussed in the previous sections, but also VOCs, or mixtures of isomeric VOCs, that are represented by other VOCs using the "lumped molecule" approach. In addition to "best estimate" reactivity estimates that were derived using the mechanisms discussed above, upper limit reactivity estimates were made for the purpose of estimating maximum likely ozone impacts. The latter may be useful in some regulatory approaches as a means to take uncertainties into account. Qualitative uncertainty classifications are given for all VOCs to aid the use of uncertainty information in regulatory applications, and for determining where further studies are most needed.

Atmospheric reactivities are derived for the Maximum Incremental Reactivity (MIR) and other scales, with ozone impacts quantified in terms of both effects on peak O_3 concentration and 8-hour averages. However, the emphasis in this work is on the MIR scale because this is the scale used in the California vehicle emissions regulations (CARB, 1993), and being considered for use in consumer product regulations (CARB, 1999). Because of this, upper limit reactivity estimates are made only for the MIR scale, though an analogous approach could be applied for other scales.

A. Atmospheric Reactivity Modeling Methods

The modeling approach and scenarios used for estimating atmospheric reactivities of VOCs is generally the same as used by Carter (1994a) when developing the MIR and other scales with the SAPRC-90 mechanism. The only modification made in this work is that the MIR and other "adjusted NO_x" scales were derived by averaging the incremental reactivities of the individual adjusted NO_x scenarios (rather than by separately averaging the kinetic and mechanistic reactivities), and that reactivities are calculated for 8-hour averages rather than integrated ozone. Since the general methods and scenarios are the same as described in detail previously (Carter et al, 1994a,b), they are only briefly summarized here.

1. Scenarios Used for Reactivity Assessment

Base Case Scenarios. The scenarios employed were those used by Carter (1994a,b) to develop various reactivity scales to quantify impacts of VOCs on ozone formation in various environments. These were based on a series of single-day EKMA box model scenarios (EPA, 1984) derived by the EPA for assessing how various ROG and NO_x control strategies would affect ozone nonattainment in various areas of the country (Baugues, 1990). The characteristics of these scenarios and the methods used to derive their input data are described in more detail elsewhere (Baugues, 1990; Carter, 1994b). Briefly, 39 urban areas in the United States were selected based on geographical representativeness of ozone nonattainment areas and data availability, and a representative high ozone episode was selected for each. The initial non-methane organic carbon (NMOC) and NO_x concentrations, the aloft O_3 concentrations, and the mixing height inputs were based on measurement data for the various areas, the hourly emissions in the scenarios were obtained from the National Acid Precipitation Assessment Program emissions inventory (Baugues, 1990), and biogenic emissions were also included. Table 52 gives a summary of the urban areas represented and other selected characteristics of the scenarios.

Table 52. Summary of the conditions of the scenarios used for atmospheric reactivity assessment.

	Scenario	Max O_3 (ppb)	Max 8-Hr Avg O_3 (ppb)	ROG / NOx	NO_x / MOIR NO_x	Height (kM)	Init.and Emit. ROG (m.mol m^{-2})	O_3 aloft (ppb)	Integrated OH (ppt-min)
Avg. Cond.	Max React (MIR)	187	119	3.1	1.5	1.8	15	70	128
	Max O_3 (MOIR)	239	165	4.5	1.0	1.8	15	70	209
	Equal Benefit (EBIR)	227	172	6.4	0.7	1.8	15	70	210
Base Case	Atlanta, GA	179	132	7.3	0.7	2.1	12	63	200
	Austin, TX	175	144	9.3	0.5	2.1	11	85	179
	Baltimore, MD	334	215	5.2	1.1	1.2	17	84	186
	Baton Rouge, LA	241	173	6.8	0.9	1.0	11	62	186
	Birmingham, AL	244	202	6.9	0.5	1.8	13	81	208
	Boston, MA	197	167	6.5	0.6	2.6	14	105	262
	Charlotte, NC	143	126	7.8	0.3	3.0	7	92	212
	Chicago, IL	278	226	11.6	0.5	1.4	25	40	164
	Cincinnati, OH	205	153	6.4	0.7	2.8	17	70	220
	Cleveland, OH	252	179	6.6	0.9	1.7	16	89	187
	Dallas, TX	208	141	4.7	1.2	2.3	18	75	176
	Denver, CO	204	139	6.3	1.1	3.4	29	57	143
	Detroit, MI	246	177	6.8	0.7	1.8	17	68	235
	El Paso, TX	182	135	6.6	1.0	2.0	12	65	138
	Hartford, CT	172	144	8.4	0.5	2.3	11	78	220
	Houston, TX	312	217	6.1	0.9	1.7	25	65	225
	Indianapolis, IN	212	148	6.6	0.9	1.7	12	52	211
	Jacksonville, FL	155	115	7.6	0.6	1.5	8	40	206
	Kansas City, MO	159	126	7.1	0.6	2.2	9	65	233
	Lake Charles, LA	286	209	7.4	0.6	0.5	7	40	233
	Los Angeles, CA	568	406	7.6	1.0	0.5	23	100	134
	Louisville, KY	212	155	5.5	0.8	2.5	14	75	260
	Memphis, TN	229	180	6.8	0.6	1.8	15	58	249
	Miami, FL	132	111	9.6	0.4	2.7	9	57	181
	Nashville, TN	167	138	8.0	0.4	1.6	7	50	225
	New York, NY	365	294	8.1	0.7	1.5	39	103	159
	Philadelphia, PA	247	169	6.2	0.9	1.8	19	53	227
	Phoenix, AZ	277	193	7.6	1.0	3.3	40	60	153
	Portland, OR	166	126	6.5	0.7	1.6	6	66	233
	Richmond, VA	242	172	6.2	0.8	1.9	16	64	217
	Sacramento, CA	204	142	6.6	0.8	1.1	7	60	209
	St Louis, MO	324	209	6.1	1.1	1.6	26	82	176
	Salt Lake City, UT	186	150	8.5	0.6	2.2	11	85	182
	San Antonio, TX	133	98	3.9	1.0	2.3	6	60	192
	San Diego, CA	193	150	7.1	0.9	0.9	8	90	146
	San Francisco, CA	229	126	4.8	1.8	0.7	25	70	61
	Tampa, FL	230	153	4.4	1.0	1.0	8	68	211
	Tulsa, OK	231	160	5.3	0.9	1.8	15	70	264
	Washington, DC	283	209	5.3	0.8	1.4	13	99	239

Several changes to the scenario inputs were made based on discussions with the California ARB staff and others (Carter, 1994b). Two percent of the initial NOx and 0.1% of the emitted NO_x in all the scenarios was assumed to be in the form of HONO. The photolysis rates were calculated using solar light intensities and spectra calculated by Jeffries (1991) for 640 meters, the approximate mid-point of the mixed layer during daylight hours. The composition of the VOCs entrained from aloft was based on the analysis of Jeffries et al. (1989).

The composition of the initial and emitted reactive organics (referred to as the "base ROG" mixture) is given on Table 50, above. It is derived from the "all city average" mixture derived by Jeffries et al (1989) from analysis of air quality data, with minor modifications as discussed by Carter (1994a,b). Note that this same mixture is used to derive the parameters for the lumped parameter products (RNO3 and PROD2) in the base mechanism, and for the lumped species in the recommended fixed parameter condensed mechanism (see Sections II.C.2 and VI.B.2, respectively).

Complete listings of the input data for the scenarios are given elsewhere (Carter, 1994b).These are referred to as "base case" scenarios, to distinguish them from those where NOx inputs are adjusted as discussed below.

Adjusted NO_x Scenarios. In addition to these 39 base case scenarios, adjusted NO_x scenarios were developed to represent different conditions of NOx availability. NO_x levels were found to be the most important factor affecting differences in relative ozone impacts among most VOCs (Carter and Atkinson, 1989a; Carter, 1994a). Because of this, separate scales were derived to represent different conditions of NO_x availability, as follows:

- In the "Maximum Incremental Reactivity" (MIR) scenarios, the NO_x inputs for each of the 39 base case scenarios are adjusted such that the final O_3 level is most sensitive to changes in VOC emissions. This represents relatively high NO_x conditions where VOC control is the most effective means to reduce ozone formation. Note that the MIR NO_x levels vary from scenario to scenario, so it is not correct to say that there is a characteristic ROG/NO_x ratio that corresponds to MIR conditions.
- In the "Maximum Ozone Incremental Reactivity" (MOIR) scenarios the NOx inputs are adjusted to yield the highest maximum O_3 concentration. This represents conditions that are optimum for ozone formation. This represents moderate NO_x conditions where O_3 formation is just starting to become NO_x limited. Generally, NO_x levels of MOIR scenarios are about 70% of those of MIR conditions (Carter, 1994a). Although O_3 formation is also sensitive to VOC control under these conditions, it is less sensitive than in the higher NO_x MIR scenarios.
- In the "Equal Benefit Incremental Reactivity" (EBIR) scenarios, the NOx inputs are adjusted such that relative changes in VOC and NOx emissions had equal effect on ozone formation. This represents conditions where O_3 formation is NO_x limited to such an extent, but not to such a large extent that VOC controls are ineffective. Generally, NO_x levels in EBIR scenarios are about 70% those of MOIR scenarios, and about half those of MIR scenarios.

As discussed by Carter (1994a), there represent respectively the high, medium and low ranges of NO_x conditions that are of relevance when assessing VOC control strategies for reducing ozone. Although lower NO_x conditions than EBIR occur in many areas (especially non-urban areas), O_3 formation under such conditions is primarily sensitive to NO_x emissions, and VOC control is not as important as NO_x control under those conditions.

Averaged Conditions Scenarios. In addition to the above, "averaged conditions" MIR, MOIR, and EBIR scenarios were developed for use for screening or sensitivity calculations. This consists of developing a scenario whose inputs are based on averaging those representing the 39 urban areas, with NO_x inputs adjusted to yield MIR, MOIR, or EBIR conditions as discussed above (Carter, 1994a,b). These scenarios are also summarized on Table 52.

2. Quantification of Atmospheric Reactivity

The reactivity of a VOC in an airshed scenario is measured by its incremental reactivity. For ambient scenarios, this is defined as the change in ozone caused by adding the VOC to the emissions, divided by the amount of VOC added, calculated for sufficiently small amounts of added VOC that the incremental reactivity is independent of the amount added[22].

$$IR(VOC, Scenario) = \lim_{VOC \to 0} \left[\frac{O_3(\text{Scenario with VOC}) - O_3(\text{Base Scenario})}{\text{Amount of VOC Added}} \right] \quad \text{(XXXIV)}$$

The specific calculation procedure is discussed in detail elsewhere (Carter, 1994a,b).

Incremental reactivities derived as given above tend to vary from scenario to scenario because they differ in their overall sensitivity of O_3 formation to VOCs. These differences can be factored out to some extent by using "relative reactivities", which are defined as ratios of incremental reactivities to the incremental reactivity of the base ROG mixture.

$$RR(VOC, Scenario) = \frac{IR(VOC, Scenario)}{IR\ (Base\ ROG, Scenario)} \quad \text{(XXXV)}$$

These relative reactivities can also be thought of as the relative effect on O3 of controlling emissions of the particular VOC by itself, compared to controlling emissions from all VOC sources equally. Thus, they are more meaningful in terms of control strategy assessment than absolute reactivities, which can vary greatly depending on the episode and local meteorology.

In addition to depending on the VOC and the scenario, the incremental and relative reactivities depend on how the amounts of VOC added and amounts of ozone formed are quantified. In this work, the amount of added VOC is quantified on a mass basis, since this is how VOCs are regulated, and generally approximates how VOC substitutions are made in practice. Note that relative reactivities will be different if they are quantified on a molar basis, with VOCs with higher molecular weight having higher reactivities on a mole basis than a gram basis.

Relative reactivities can also depend significantly on how ozone impacts are quantified (Carter, 1994a). Two different ozone quantification methods are used in this work, as follows:

- "Ozone Yield" incremental reactivities measure the effect of the VOC on the total amount of ozone formed in the scenario at the time of its maximum concentration. Incremental reactivities are quantified as grams O_3 formed per gram VOC added. Most previous recent studies of incremental reactivity (Dodge, 1984; Carter and Atkinson, 1987, 1989a, Chang and Rudy, 1990;

[22] Note that this differs from how the term "incremental reactivity" is used in the context of chamber experiments. In that case, the incremental reactivity refers to the relative change observed in the individual experiments, which in general depends on the amount added.

Jeffries and Crouse, 1991) have been based on this quantification method. The MIR, MOIR, and EBIR scales of Carter (1994a) also use this quantification.

- "Max 8 Hour Average" incremental measure the effect of the VOC on the average ozone concentration during the 8-hour period when the average ozone concentration was the greatest, which in these one-day scenarios was the last 8 hours of the simulation. This provides a measure of ozone impact that is more closely related to the new Federal ozone standard that is given in terms of an 8 hour average. This quantification is used for relative reactivities in this work.

In previous reports, we have reported reactivities in terms of integrated O_3 over a standard concentration of 0.09 or 0.12 ppm. This provides a measure of the effect of the VOC on exposure to unacceptable levels of ozone. This is replaced by the Max 8 Hour Average reactivities because it is more representative of the new Federal ozone standard and because reactivities relative to integrated O_3 over a standard tend to be between those relative to ozone yield and those relative to 8-hour averages. Therefore, presenting both ozone yield and maximum 8-hour average relative reactivities should be sufficient to provide information on how relative reactivities vary with ozone quantification method. Incremental reactivities are quantified as ppm O_3 per milligram VOC emitted per square meter.

If a reactivity scale is developed based on incremental reactivities in more than one scenario, then the method used to derive the scale from the reactivities in the individual scenarios will also affect the scale. Although as discussed by Carter (1994a) a number of aggregation methods can be used, in this work we use only simple averaging of incremental or relative reactivities, as discussed below. Note that this differs somewhat from the method used by Carter (1994a) to derive the MIR and other adjusted NO_x scales, where averages of kinetic and mechanistic reactivities were used.

Based on these considerations, reactivities in the following scales were derived in this work, as follows:

- The MIR scale consists of averages of the incremental reactivities in the 39 MIR scenarios (i.e., the 39 base case scenarios with NO_x adjusted to represent MIR conditions), with O_3 quantified by ozone yields, and VOCs quantified by mass. The units are grams O_3 formed per gram VOC added.
- The MOIR and EBIR scales are derived from averages of the ozone yield incremental reactivities in the 39 MOIR or EBIR scenarios, in a manner analogous to the derivation of the MIR scale.
- The Averaged Conditions MIR, MOIR, and EBIR scales are the ozone yield incremental reactivities in the corresponding averaged conditions scenario. For most VOCs, the averaged conditions reactivities are very close to those derived from the 39 adjusted NO_x scales as discussed above.
- The Base Case O_3 Yield Scales are O_3 yield incremental and relative reactivities in the 39 base case scenarios. Thus there are 39 such scales, one for each of the 39 urban areas. Averages and standard deviations of the relative reactivities are also presented.
- The Base Case Maximum 8-Hour Average Scales are relative reactivities based on effects of the VOCs on the maximum 8-hour average ozone in the 39 base case scenarios. Averages and standard deviations of the relative reactivities in these 39 scales are also presented.

Note that the MIR scale is the one recommended by Carter (1994a) for regulatory applications requiring use of a single scale, and is preferred by the California ARB for regulatory use (e.g., CARB, 1993, 1998). This is because MIR reactivities reflect conditions that are most sensitive to VOC controls,

and serve as an appropriate complement to NO_x controls in a comprehensive control strategy. Relative reactivities in the MIR scale also correspond reasonably well to integrated O_3 reactivities in lower NO_x scenarios, because both are strongly influenced by factors of a VOCs mechanism that affect O_3 formation rates (Carter, 1994a). However, relative reactivities can differ depending on the scenarios or quantification method used, and regulatory applications that do not require use of a single scale should be based on considerations of reactivities in multiple scales.

3. Chemical Mechanism Used

The chemical mechanism employed in the atmospheric reactivity simulations consisted of the lumped mechanism discussed in Section VI with reactions added as needed to represent the VOC or mixture whose reactivity is being assessed. The lumped mechanism, which consists of the base mechanism listed in Table A-1 and the mechanism for the lumped species listed in Table A-3 is used in the "base case" simulations without the added VOCs. No lumping was employed when representing an individual VOC for calculating its reactivity, and Table A-6 in Appendix A gives the reactions used for those VOCs that are not in the base mechanism[19]. When calculating reactivities of complex mixtures (e.g., MS-A or the base ROG mixture), the components were lumped using the approach recommended in Table 49, with the parameters for the lumped model species being derived based on the specific mixtures being represented. The compositions of the mixtures whose reactivities were calculated are given in Table C-5 in Appendix C. Note that separate model species were used to represent components whose reactivities were being assessed than used to represent VOCs in the base mixture in the reactivity calculations, except for components that are already represented explicitly in the mechanism.

B. VOC Classes and Uncertainty Classifications

Atmospheric reactivity estimates were made for all VOC classes that can be used to represent emitted VOCs in the current mechanism. These classes, which are also referred to as "detailed model species", can represent either a single compound or a mixture of isomers that are assumed to have similar mechanisms, or whose detailed compositions are unknown. The individual compounds include compounds whose reactions are represented explicitly, and compounds represented by other compounds using the lumped molecule approach. The mixtures of isomers are represented by one or more compounds that are assumed to be representative of the types of compounds in the mixtures.

Table C-1 in Appendix C lists all the detailed model species used in the current version of the mechanism (including some for which mechanistic and therefore reactivity estimates have not been made), and gives other summary information concerning these species. This includes the following:

- Name. Each detailed model species has a 2-8 character detailed model species name that is used to identify it in the modeling system. Note that this name is the primary means to identify these species in some of the tabulations in this report, so can be used to identify what the name represents if this is not obvious.
- Description. The name of the VOC or the group of the VOCs that are represented by this class.
- Molecular Weight (Mwt). Because each detailed model species refers to either a single compound or set of isomeric compounds, each has a unique molecular weight associated with it. The molecular weight is used when processing mass-based emissions data, or when computing impacts of compounds on a weight basis.
- The uncertainty code (Unc) assigned to the mechanism for this model species. These codes, which are defined in Table C-2, indicate the author's subjective opinion of the likelihood that the mechanism,

and the ozone impact predictions resulting from using the mechanism, will change significantly in the future as new data become available. Note a higher number means a higher uncertainty (with 6 being the highest), and it is recommended that any reactivity-based regulation use uncertainty adjustments for those VOCs whose uncertainty classifications are greater than 4.

- The experimental data availability code (Exp.). These codes, which are defined in Table C-3, indicate the extent to which the mechanism for the compound has been or can be experimentally evaluated. Reference is also made in some cases to the availability of data to test the mechanism under MIR conditions; this refers to experiments testing the effects of the compounds on O_3 formation in surrogates representing relatively high NO_x conditions. Note that a code of "-" means there are no data available to evaluate the mechanism. The evaluation of mechanism is discussed in Section V (see also Appendix B).
- Additional information and comments (Notes). These footnotes, which are defined in Table C-4, give additional information about the representation of the detailed model species and the status of its evaluation. For example, note "1" indicates the mechanism is considered to be reasonably well established, "2" means the evaluation of mechanism for this species is discussed in this report, "4" means that the mechanism was adjusted to improve fits to chamber data, "7" means that the appropriateness of the lumped molecule representation used is uncertain, etc.
- The method used to represent the chemical reactions of the compound in the model. This could be one of the following:
  - Explicit in the base mechanism (Expl). This means that reactions of this model species are part of the base mechanism because it is used, in part, to represent organic oxidation products. The mechanisms for the organic product species in the base mechanism are discussed in Section II.C
  - Mechanism Generated (Gen'd). This means that the mechanism was generated using the mechanism estimation and generation system that is discussed in Section III. The structure that was used when generating the mechanism (see Section III.B) is also shown.
  - Assigned Parameters (Asn'd). This means that the mechanism for this compound was derived or estimated as discussed in Section IV. This includes aromatics, terpenes, and other compounds for which the mechanism generation system cannot be used.
  - Lumped Molecule (L.Mol). This means that this detailed model species is represented in the model by another model species (or mixture thereof), on a mole for mole basis. The model species or mixture used to represent it is also shown. Note that mixtures are used for detailed model species that refer to an unspecified mixture of isomers that have different reactivity. Because of analytical limitations, such unspecified mixture classes tend to occur in many speciation profiles in emissions inventories.
  - Not in model (-). The current version of the mechanism does not have mechanistic assignments for this class of compounds. It is included in the list because it occurs in speciated emissions inventories. The molecular weight and carbon number information can be used when determining an approximate representation of the compound in model applications when mixtures containing these species are emitted.
  - Mixture (Mix). This is a complex mixture. This is not strictly a detailed model species, but is included in the tabulation of reactivity results for comparison purposes, or because their reactivities are of particular interest or have been studied for other projects. These include the mixture used to represent the Base ROG in the reactivity calculations, several mixtures used by the California Air Resources Board to represent exhausts from transitional low emissions vehicles

(TLEVs) or low emissions vehicles (LEVs), several mineral spirits commercial hydrocarbon mixtures studied for Safety-Kleen (Carter et al, 1997f) or Exxon corporation (Carter et al, 2000g), and commercial ortho-acetate solvents also studied for Exxon corporation (Carter et al, 2000g). The compositions of the mixtures whose reactivities have been tabulated are given in Table C-5.

- Lumped Group. This is the lumped or explicit model species that is used in the condensed mechanism when representing the representing the detailed model species when present in mixtures, or in lumped model simulations when its reactivity is not being assessed. The footnote indicates abbreviations that are used.

C. Reactivity Results

The results of the reactivity calculations in the different scales are given in various tables in Appendix C. The incremental reactivity in the MIR scale is given in Table C-1, along with the estimated upper limit MIR, derived as discussed in the following section. Table C-6 gives reactivity data in various scales, including MIR, MOIR, EBIR, and averages, standard deviations, minima, and maxima in the O_3 yield and maximum 8-hour average relative reactivities calculated for the various scales. The incremental reactivities calculated for all the individual scenarios are given in Table C-7 and Table C-8, where Table C-7 gives the data for the ozone yield reactivities, and Table C-8 gives the data for the maximum 8-hour average reactivities. Because of their size, the latter tables are not included with the printed version of this report, but are included with the electronic version, which can be downloaded from http://cert.ucr.edu/~carter/reactdat.htm[23].

It can be seen that there have been changes in the incremental and relative reactivities for a number of VOCs, relative to previous versions. The largest changes are for the VOCs whose mechanisms have been changed because of new data or revised estimates, but other changes have resulted from changes in the base mechanism and treatment of reactive products. For example, MIR's for some high molecular weight species whose mechanisms have not otherwise changed increased because of the use or PROD2 rather than the less reactive MEK to represent reactive ketone or other non-aldehyde oxygenated products. A complete analysis of the changes to the reactivity scale due to the mechanism updates has not been carried out, but may give useful insights concerning the effects of chemical mechanism uncertainties on incremental reactivity scales.

As indicated on Table C-6, the mechanisms for some VOCs are considered to be highly uncertain, and it is recommended that any regulations that use incremental reactivity data take these uncertainties into account. In particular, it is recommended that appropriate uncertainty adjustments be used for those VOCs that are given an uncertainty code of "4" or greater. A discussion of exactly what constitutes an appropriate uncertainty adjustment is beyond the scope of this work. However, at the request of the CARB, the author developed a means to estimate "upper limit" MIR's for VOCs, given available information concerning the reaction rates and chemical type of the VOC, and the calculated MIRs for VOCs with known or estimated mechanisms (Carter, 1997). These upper limit estimates were updated for the current version of the mechanism, and the results are included on Table C-1. The methods and data used to derive these upper limit estimates are given in Appendix D to this report.

[23] This site may contain updated information when the mechanism and reactivity scale are updated in the future. However, it is expected that links and files will be retained so the version of the tables discussed in this report can still be downloaded.

VIII. REFERENCES

Alcock, W. G. and B. Mile (1975): "The Gas-Phase Reactions of Alkylperoxy Radicals Generated by a Photochemical Technique," Combust. Flame 24, 125.

Alvaro A., E. C. Tuazon, S. M. Aschmann, J. Arey and R. Atkinson (1999): "Products and mechanisms of the gas-phase reactions of OH radicals and O_3 with 2-methyl-3-buten-2-ol," Atmos. Environ. 33, 2893-2905.

Arey, J. , S. M. Aschmann, E. S. C. Kwok, and R. Atkinson (2000) Alkyl nitrate, hydroxyalkyl nitrate, and hydroxycarbonyl formation from the NO_x-air photooxidations of C_5-C_8 n-alkanes. J. Phys. Chem. A, to be submitted for publication.

Aschmann, S. M., A. A. Chew, J. Arey and R. Atkinson (1997): "Products of the Gas-Phase Reaction of OH Radicals with Cyclohexane: Reactions of the Cyclohexyl Radical," J. Phys. Chem. A, 101, 8042-8048.

Aschmann, S. M. and R. Atkinson (1998): "Kinetics of the Gas-Phase Reactions of the OH Radical with Selected Glycol Ehters, Glycols, and Alcohols," Int. J. Chem. Kinet, 30, 533-540.

Aschmann, S. M. and R. Atkinson (1999): "Products of the Gas-Phase Reactions of the OH Radical with Methyl n-Butyl Ether and 2-Isopropoxyethanol: Reactions of ROC(O·)< Radicals," Int. J. Chem. Kinet, 31, 501-513.

Atkinson, R. (1987): "A Structure-Activity Relationship for the Estimation of Rate Constants for the Gas-Phase Reactions of OH Radicals with Organic Compounds," Int. J. Chem. Kinet., 19, 799-828.

Atkinson, R. (1989): "Kinetics and Mechanisms of the Gas-Phase Reactions of the Hydroxyl Radical with Organic Compounds," J. Phys. Chem. Ref. Data, Monograph no 1.

Atkinson, R. (1990): "Gas-Phase Tropospheric Chemistry of Organic Compounds: A Review," Atmos. Environ., 24A, 1-24.

Atkinson, R. (1991): "Kinetics and Mechanisms of the Gas-Phase Reactions of the NO_3 Radical with Organic Compounds," J. Phys. Chem. Ref. Data, 20, 459-507.

Atkinson, R. (1994): "Gas-Phase Tropospheric Chemistry of Organic Compounds," J. Phys. Chem. Ref. Data, Monograph No. 2.

Atkinson, R. (1997a): "Gas Phase Tropospheric Chemistry of Volatile Organic Compounds: 1. Alkanes and Alkenes," J. Phys. Chem. Ref. Data, 26, 215-290.

Atkinson, R. (1997b): "Atmospheric Reactions of Alkoxy and Beta-Hydroxyalkoxy Radicals," Int. J. Chem. Kinet., 29, 99-111.

Atkinson, R. (2000): "Atmospheric Chemistry of VOCs and NO_x," Atmospheric Environment, 34, 2063-2101.

Atkinson, R., R.A. Perry, and J. N. Pitts, Jr. (1978): "Rate Constants for the reactions of the OH radical with $(CH_3)_2NH$, $(CH_3)_3N$, and $C_2H_5NH_2$ over the temperature range 298-426 °K," J. Chem. Phys. 68, 1850.

Atkinson, R., S. M. Aschmann, W. P. L. Carter and J. N. Pitts, Jr. (1982): "Rate constants for the Gas-Phase Reaction of OH Radicals with a Series of Ketones at 299±2 K," Int J. Chem. Kinet. 14, 839, 1982.

Atkinson, R., S. M. Aschmann, W. P. L. Carter, A. M. Winer and J. N. Pitts, Jr. (1982b): "Alkyl Nitrate Formation from the NO_x-Air Photooxidations of C_2-C_8 n-Alkanes," J. Phys. Chem. 86, 4562-4569.

Atkinson, R., S. M. Aschmann and J. N. Pitts, Jr. (1983): "Kinetics of the Gas-Phase Reactions of OH Radicals with a Series of α,β-Unsaturated Carbonyls at 299±2 K," Int. J. Chem. Kinet. 15, 75.

Atkinson, R., W. P. L. Carter, and A. M. Winer (1983b): "Effects of Temperature and Pressure on Alkyl Nitrate Yields in the NO_x Photooxidations of n-pentane and n-heptane" J. Phys. Chem. 87, 2012-2018.

Atkinson, R. and W. P. L. Carter (1984): "Kinetics and Mechanisms of the Gas-Phase Reactions of Ozone with Organic Compounds under Atmospheric Conditions," Chem. Rev. 84, 437-470.

Atkinson, R. and A. C. Lloyd (1984): "Evaluation of Kinetic and Mechanistic Data for Modeling of Photochemical Smog," J. Phys. Chem. Ref. Data 13, 315.

Atkinson, R., S. M. Aschmann, W. P. L. Carter, A. M. and Winer (1984): "Formation of Alkyl Nitrates from the Reaction of Branched and Cyclic Alkyl Peroxy Radicals with NO," Int. J. Chem. Kinet., 16, 1085-1101.

Atkinson, R., S. M. Aschmann, A. M. Winer and J. N. Pitts, Jr. (1985): "Atmospheric Gas Phase Loss Processes for Chlorobenzene, Benzotrifluoride, and 4-Chlorobenzotrifluoride, and Generalization of Predictive Techniques for Atmospheric Lifetimes of Aromatic Compounds," Arch Environ. Contamin. Toxicol. 14, 417.

Atkinson, R. and S. M. Aschmann (1986): "Kinetics of the Reactions of Naphthalene, 2-Methylnaphthalene, and 2,3-Dimethylnaphthalene with OH Radicals and with O_3 at 295±1 K," Int J. Chem. Kinet. 18, 569.

Atkinson, R. and S. M. Aschmann (1987): "Kinetics of the Gas-Phase Reactions of Alkylnaphthalenes with O_3, N_2O_5 and OH Radicals at 298±2 K," Atmos. Environ. 21, 2323.

Atkinson, R., S. M. Aschmann, and M. A. Goodman (1987): "Kinetics of the Gas-Phase Reactions NO_3 Radicals with a Series of Alkynes, Haloalkenes, and α,β-Unsaturated Aldehydes," Int. J. Chem. Kinet., 19, 299.

Atkinson, R. and S. M. Aschmann (1988a): "Kinetics of the Reactions of Acenaphthalene and Acenaphthylene and Structurally-Related Aromatic Compounds with OH and NO_3 Radicals, N_2O_5 and O_3 at 296±2 K," Int J. Chem. Kinet. 20, 513.

Atkinson, R., and S. M. Aschmann (1988b): "Rate Constant for the Reaction of OH Radicals with Isopropylcyclopropane at 298+/-2-k - Effects of Ring Strain on Substituted Cycloalkanes," Int. J. Chem. Kinet. 20, (4) 339-342.

Atkinson, R., S. M. Aschmann, J. Arey and W. P. L. Carter (1989): "Formation of Ring-Retaining Products from the OH Radical-Initiated Reactions of Benzene and Toluene," Int. J. Chem. Kinet. 21, 801.

Atkinson, R., S. M. Aschmann, and J. Arey (1991): "Formation of Ring-Retaining Products from the OH Radical-Initiated Reactions of o-, m-, and p-Xylene," Int. J. Chem. Kinet. 23, 77.

Atkinson, R., D. L. Baulch, R. A. Cox, R. F. Hampson, Jr., J. A. Kerr, and J. Troe (1992): "Evaluated Kinetic and Photochemical Data for Atmospheric Chemistry. Supplement IV (IUPAC)," J. Phys. Chem. Ref. Data 21, 1125-1568.

Atkinson, R., and W. P. L. Carter (1995): "Measurement of OH Radical Reaction Rate Constants for Purasolv ELS and Purasolv ML and Calculation of Ozone Formation Potentials," Final Report to Purac America, Inc., June.

Atkinson, R., E. S. C. Kwok, J. Arey and S. M. Aschmann (1995): "Reactions of Alkoxyl Radicals in the Atmosphere," Faraday Discuss. 100, 23.

Atkinson, R., D. L. Baulch, R. A. Cox, R. F. Hampson, Jr., J. A. Kerr, M. J. Rossi, and J. Troe (1997): "Evaluated Kinetic, Photochemical and Heterogeneous Data for Atmospheric Chemistry: Supplement V and VI, IUPAC Subcommittee on Gas Kinetic Data Evaluation for Atmospheric Chemistry," Phys. Chem. Ref. Data, 26, 521-1011 (Supplement V) and 1329-1499 (Supplement VI).

Atkinson, R., E. C. Tuazon, and S. M. Aschmann (1998): "Products of the Gas-Phase Reaction of the OH Radical with 3-Methyl-1-Butene in the Presence of NO," Int. J. Chem. Kinet., 30, 577-587.

Atkinson, R., D. L. Baulch, R. A. Cox, R. F. Hampson, Jr., J. A. Kerr, M. J. Rossi, and J. Troe (1999): "Evaluated Kinetic, Photochemical and Heterogeneous Data for Atmospheric Chemistry: Supplement VII, Organic Species (IUPAC)," J. Phys. Chem. Ref. Data, 28, 191-393.

Atkinson, R. et al. (2000a) Manuscript on OH rate constants for branched alkanes. In preparation.

Atkinson, R., E. C. Tuazon and S. M. Aschmann (2000b): "Atmospheric Chemistry of 2-pentanone and 2-heptanone," Environ. Sci. Technol., 34, 623-631.

Baldwin, A. C., J. R. Barker, D. M. Golden and G. G. Hendry (1977): "Photochemical Smog. Rate Parameter Estimates and Computer Simulations," J. Phys. Chem. 81, 2483.

Batt and Robinson (1987): "Decomposition of the t-Butoxy Radical – I. Studies over the Temperature Range 402-443 K," Int. J. Chem. Kinet. 19, 391.

Baugues, K. (1990): "Preliminary Planning Information for Updating the Ozone Regulatory Impact Analysis Version of EKMA," Draft Document, Source Receptor Analysis Branch, Technical Support Division, U. S. Environmental Protection Agency, Research Triangle Park, NC, January.

Baxley, J. S., M. V. Henley and J. R. Wells (1997). "The Hydroxyl Radical Reaction Rate Constant and Products of Ethyl 3-Ethoxypropionate," Int. J. Chem. Kinet., 29, 637-644.

Becker, K. H., V. Bastian, and Th. Klein (1988): "The Reactions of OH Radicals with Toluene Diisocyanate, Toluenediamine and Methylenedianiline Under Simulated Atmospheric Conditions," J. Photochem. Photobiol A., 45 195-205.

Bennett, P. J. and J. A. Kerr (1989): "Kinetics of the Reactions of Hydroxyi Radicais with Aliphatic Esters Studied Under Simulated Atmospheric Conditions," J. Atmos. Chem. 8, 87.

Benson, S. W. (1976): "Thermochemical Kinetics, 2nd Ed.", John Wiley and Sons, New York.

Bierbach A., Barnes I., Becker K.H. and Wiesen E. (1994) Atmospheric chemistry of unsaturated carbonyls: Butenedial, 4-oxo-2-pentenal, 3-hexene-2,5-dione, maleic anhydride, 3H-furan-2-one, and 5-methyl-3H-furan-2-one. Environ. Sci. Technol., 28, 715-729.

Baulch, D. L., I. M. Campbell, S. M. Saunders, and P. K. K. Louie (1989): "Rate Constants for the Reactions of the Hydroxyl Radical with Indane, Indene and Styrene," J. Chem. Soc. Faraday. Trans. 2, 85, 1819.

Bridier, I., H. Caralp, R. Loirat, B. Lesclaux and B. Veyret (1991): "Kinetic and Theoretical Studies of the Reactions of CH3C(O)O2 + NO2 + M <=> CH3C(O)O2NO2 + M between 248 and 393 K and between 30 and 760 Torr," J. Phys. Chem. 95, 3594-3600.

CARB (1993): "Proposed Regulations for Low-Emission Vehicles and Clean Fuels -- Staff Report and Technical Support Document," California Air Resources Board, Sacramento, CA, August 13, 1990. See also Appendix VIII of "California Exhaust Emission Standards and Test Procedures for 1988 and Subsequent Model Passenger Cars, Light Duty Trucks and Medium Duty Vehicles," as last amended September 22, 1993. Incorporated by reference in Section 1960.

CARB (1999) California Air Resources Board, Proposed Regulation for Title 17, California Code of Regulations, Division 3, Chapter 1, Subchapter 8.5, Article 3.1, sections 94560- 94539.

Calvert, J. G., and J. N. Pitts, Jr. (1966): "Photochemistry," John Wiley and Sons, New York.

Canosa-Mass et al (1996): "Is the reaction between $CH_3C(O)O_2$ and NO_3 important in the night-time troposphere?," J. Chem. Soc. Faraday Trans. 92, 2211.

Carter, W. P. L. (1987): "An Experimental and Modeling Study of the Photochemical Reactivity of Heatset Printing Oils," Report #2 on U. S. EPA Cooperative Agreement No. CR810214-01.

Carter, W. P. L. (1988): "Development and Implementation of an Up-To-Date Photochemical Mechanism for Use in Airshed Modeling," Final Report for California Air Resources Board Contract No. A5-122-32, October.

Carter, W. P. L. (1990): "A Detailed Mechanism for the Gas-Phase Atmospheric Reactions of Organic Compounds," Atmos. Environ., 24A, 481-518.

Carter, W. P. L. (1994a): "Development of Ozone Reactivity Scales for Volatile Organic Compounds," J. Air & Waste Manage. Assoc., 44, 881-899.

Carter, W. P. L. (1994b): "Calculation of Reactivity Scales Using an Updated Carbon Bond IV Mechanism," Report Prepared for Systems Applications International Under Funding from the Auto/Oil Air Quality Improvement Research Program, April 12.

Carter, W. P. L. (1995): "Computer Modeling of Environmental Chamber Measurements of Maximum Incremental Reactivities of Volatile Organic Compounds," Atmos. Environ., 29, 2513-2517.

Carter, W. P. L. (1996): "Condensed Atmospheric Photooxidation Mechanisms for Isoprene," Atmos. Environ., 30, 4275-4290.

Carter, W. P. L. (1997). "Estimation of Upper Limit Maximum Incremental Reactivities of VOCs," Prepared for California Air Resources Board Reactivity Research Advisory Committee, July 16. Available at http://www.cert.ucr.edu/~carter/absts.htm#maxmir.

Carter, W. P. L (1998):. "Estimation of Atmospheric Reactivity Ranges for Parachlorobenzotrifluoride and Benzotriflouride," Report to Occidental Chemical Corporation, March.

Carter, W. P. L., K. R. Darnall, A. C. Lloyd, A. M. Winer and J. N. Pitts, Jr. (1976): "Evidence for Alkoxy Radical Isomerizaiton in Photooxidations of C4-C6 Alkanes Under Simulated Atmospheric Conditions", Chem. Phys. Lett 42, 22-27.

Carter, W. P. L., A. C. Lloyd, J. L. Sprung, and J. N. Pitts, Jr. (1979): "Computer Modeling of Smog Chamber Data: Progress in Validation of a Detailed Mechanism for the Photooxidation of Propene and n-Butane in Photochemical Smog", Int. J. Chem. Kinet, 11, 45.

Carter, W. P. L., P. S. Ripley, C. G. Smith, and J. N. Pitts, Jr. (1981): "Atmospheric Chemistry of Hydrocarbon Fuels: Vol I, Experiments, Results and Discussion," Final report to the U. S. Air Force, ESL-TR-81-53, November.

Carter, W. P. L., and R. Atkinson (1985): "Atmospheric Chemistry of Alkanes", J. Atmos. Chem., 3, 377-405, 1985.

Carter, W. P. L. and R. Atkinson (1987): "An Experimental Study of Incremental Hydrocarbon Reactivity," Environ. Sci. Technol., 21, 670-679

Carter, W. P. L., A. M. Winer, R. Atkinson, S. E. Heffron, M. P. Poe, and M. A. Goodman (1987): "Atmospheric Photochemical Modeling of Turbine Engine Fuels. Phase II. Computer Model Development," Report on USAF Contract no. F08635-83-0278, Engineering and Services Laboratory, Air Force Engineering and Services Center, Tyndall Air Force Base, Florida, August.

Carter, W. P. L. and R. Atkinson (1996): "Development and Evaluation of a Detailed Mechanism for the Atmospheric Reactions of Isoprene and NOx," Int. J. Chem. Kinet., 28, 497-530.

Carter, W. P. L. and R. Atkinson (1989a): "A Computer Modeling Study of Incremental Hydrocarbon Reactivity", Environ. Sci. Technol., 23, 864.

Carter, W. P. L. and R. Atkinson (1989b): "Alkyl Nitrate Formation from the Atmospheric Photooxidation of Alkanes; a Revised Estimation Method," J. Atm. Chem. 8, 165-173.

Carter, W. P. L., and F. W. Lurmann (1990): "Evaluation of the RADM Gas-Phase Chemical Mechanism," Final Report, EPA-600/3-90-001.

Carter, W. P. L. and F. W. Lurmann (1991): "Evaluation of a Detailed Gas-Phase Atmospheric Reaction Mechanism using Environmental Chamber Data," Atm. Environ. 25A, 2771-2806.

Carter, W. P. L., F. W. Lurmann, R. Atkinson, and A. C. Lloyd (1986): "Development and Testing of a Surrogate Species Chemical Reaction Mechanism," EPA-600/3-86-031, August.

Carter, W. P. L., R. Atkinson, A. M. Winer, and J. N. Pitts, Jr. (1982): "Experimental Investigation of Chamber-Dependent Radical Sources," Int. J. Chem. Kinet., 14, 1071.

Carter, W. P. L., Winer, A. M., Atkinson, R., Dodd, M. C. and Aschmann, S. A. (1984a): Atmospheric Photochemical Modeling of Turbine Engine Fuels. Phase I. Experimental studies. Final Report to the USAF, ESL-TR-84-32, September.

Carter, W. P. L., Dodd, M. C., Long, W. D. and Atkinson, R. (1984b): Outdoor Chamber Study to Test Multi-Day Effects. Volume I: Results and Discussion. Final report, EPA-600/3-84-115.

Carter, W. P. L., A. M. Winer, R. Atkinson, S. E. Heffron, M. P. Poe, and M. A. Goodman (1987): "Atmospheric Photochemical Modeling of Turbine Engine Fuels. Phase II. Computer Model Development," Report on USAF Contract no. F08635-83-0278.

Carter, W. P. L., J. A. Pierce, I. L. Malkina, and D. Luo (1992): "Investigation of the Ozone Formation Potential of Selected Volatile Silicone Compounds," Final Report to Dow Corning Corporation, Midland, MI, November.

Carter, W. P. L., J. A. Pierce, I. L. Malkina, D. Luo and W. D. Long (1993a): "Environmental Chamber Studies of Maximum Incremental Reactivities of Volatile Organic Compounds," Report to Coordinating Research Council, Project No. ME-9, California Air Resources Board Contract No. A032-0692; South Coast Air Quality Management District Contract No. C91323, United States Environmental Protection Agency Cooperative Agreement No. CR-814396-01-0, University Corporation for Atmospheric Research Contract No. 59166, and Dow Corning Corporation. April 1.

Carter, W. P. L, D. Luo, I. L. Malkina, and J. A. Pierce (1993b): "An Experimental and Modeling Study of the Photochemical Ozone Reactivity of Acetone," Final Report to Chemical Manufacturers Association Contract No. KET-ACE-CRC-2.0. December 10.

Carter, W. P. L., D. Luo, I. L. Malkina, and J. A. Pierce (1994): "Environmental Chamber Studies of Atmospheric Ozone Formation from Selected Biogenic Compounds" Presented at the 207th ACS National Meeting, March 13-17, San Diego, CA.

Carter, W. P. L., J. A. Pierce, D. Luo, and I. L. Malkina (1995a): "Environmental Chamber Studies of Maximum Incremental Reactivities of Volatile Organic Compounds," Atmos. Environ. 29, 2499-2511.

Carter, W. P. L., D. Luo, I. L. Malkina, and J. A. Pierce (1995b): "Environmental Chamber Studies of Atmospheric Reactivities of Volatile Organic Compounds. Effects of Varying ROG Surrogate and NO_x," Final report to Coordinating Research Council, Inc., Project ME-9, California Air Resources Board, Contract A032-0692, and South Coast Air Quality Management District, Contract C91323. March 24.

Carter, W. P. L., D. Luo, I. L. Malkina, and J. A. Pierce (1995c): "Environmental Chamber Studies of Atmospheric Reactivities of Volatile Organic Compounds. Effects of Varying Chamber and Light Source," Final report to National Renewable Energy Laboratory, Contract XZ-2-12075, Coordinating Research Council, Inc., Project M-9, California Air Resources Board, Contract A032-0692, and South Coast Air Quality Management District, Contract C91323, March 26.

Carter, W. P. L., D. Luo, I. L. Malkina, and D. Fitz (1995d): "The University of California, Riverside Environmental Chamber Data Base for Evaluating Oxidant Mechanism. Indoor Chamber Experiments through 1993," Report submitted to the U. S. Environmental Protection Agency, EPA/AREAL, Research Triangle Park, NC., March 20..

Carter, W. P. L., D. Luo, and I. L. Malkina (1996a): "Investigation of Atmospheric Ozone Formation Potentials of C12 - C16 n-Alkanes," Report to the Aluminum Association, October 28.

Carter, W. P. L., D. Luo, and I. L. Malkina (1996b): "Investigation of the Atmospheric Ozone Impact of Methyl Acetate," Report to Eastman Chemical Company, July.

Carter, W. P. L., D. Luo, and I. L. Malkina (1996c): "Investigation of the Atmospheric Ozone Formation Potential of t-Butyl Alcohol, N-Methyl Pyrrolidinone and Propylene Carbonate," Report to ARCO Chemical Corporation, July 8.

Carter, W. P. L., D. Luo, and I. L. Malkina (1996d): "Investigation of the Atmospheric Ozone Formation Potential of Trichloroethylene," Report to the Halogenated Solvents Industry Alliance, August.

Carter, W. P. L., D. Luo, and I. L. Malkina (1997a): "Environmental Chamber Studies for Development of an Updated Photochemical Mechanism for VOC Reactivity Assessment," Final report to the California Air Resources Board, the Coordinating Research Council, and the National Renewable Energy Laboratory, November 26.

Carter, W. P. L., D. Luo, and I. L. Malkina (1997b): "Investigation of the Atmospheric Ozone Formation Potential of Propylene Glycol," Report to Philip Morris, USA, May 2.

Carter, W. P. L., D. Luo, and I. L. Malkina (1997c): "Investigation of the Atmospheric Ozone Formation Potential of Acetylene," Report to Carbind Graphite Corp., April 1.

Carter, W. P. L., D. Luo, and I. L. Malkina (1997d): "Investigation of the Atmospheric Ozone Formation Potential of Selected Alkyl Bromides," Report to Albemarle Corporation, November 10.

Carter, W. P. L., D. Luo, I. L. Malkina, S. M. Aschmann and R. Atkinson (1997e): "Investigation of the Atmospheric Ozone Formation Potentials of Selected Dibasic Esters," Report to the Dibasic Esters Group, SOCMA, August 29.

Carter, W. P. L., D. Luo, and I. L. Malkina (1997f): "Investigation of the Atmospheric Ozone Formation Potentials of Selected Mineral Spirits Mixtures," Report to Safety-Kleen Corporation, July 25.

Carter, W. P. L., D. Luo, and I. L. Malkina (1997g): "Investigation of the Atmospheric Ozone Formation Potential of t-Butyl Acetate," Report to ARCO Chemical Corporation, July 2.

Carter, W. P. L., D. Luo and I. L. Malkina (1997h): "Investigation of that Atmospheric Reactions of Chloropicrin," Atmos. Environ. 31, 1425-1439.; Report to the Chloropicrin Manufacturers Task Group, May 19.

Carter, W. P. L., D. Luo, and I. L. Malkina (1997i): "Investigation of the Atmospheric Ozone Formation Potential of Toluene Diisocyanate," Report to Society of the Plastics Industry, December.

Carter, W. P. L., D. Luo, and I. L. Malkina (1999a): "Investigation of the Atmospheric Ozone Formation Potential of Para Toluene Isocyanate and Methylene Diphenylene Diisocyanate," Report to the Chemical Manufacturers Association Diisocyanates Panel, March.

Carter, W. P. L., D. Luo, and I. L. Malkina (1999b): 'Investigation of the Atmospheric Impacts and Ozone Formation Potential of Styrene," Report to the Styrene Information and Research Center. March 10.

Carter, W. P. L., M. Smith, D. Luo, I. L. Malkina, T. J. Truex, and J. M. Norbeck (1999c): "Experimental Evaluation of Ozone Forming Potentials of Motor Vehicle Emissions", Final Report to California Air Resources Board Contract No. 95-903, and South Coast Air Quality Management District Contract No 95073/Project 4, Phase 2, May 14.

Carter. W. P. L. D. Luo, and I. L. Malkina (2000a): "Investigation of Atmospheric Reactivities of Selected Consumer Product VOCs," Draft Report to California Air Resources Board, Contract 95-308, April 29.

Carter, W. P. L., D. Luo, and I. L. Malkina (2000b): "Investigation of the Atmospheric Impacts and Ozone Formation Potentials of Selected Branched Alkanes," Report to the Safety-Kleen Corporation, in preparation.

Carter, W. P. L., et al. (2000c), "An Experimental and Modeling Study of the Photochemical Reactivity of Selected C12+ Cycloalkanes," Report to the Aluminum Association, in preparation.

Carter, W. P. L., D. Luo, and I. L. Malkina (2000d): "Investigation of the Atmospheric Ozone Formation Potentials of Selected Compounds," Report to Exxon Chemical Company, in preparation..

Carter, W. P. L. et. al (2000e): "Investigation of the Atmospheric Ozone Formation Potentials of Selected Solvents," report to Eastman Chemical Company, in preparation.

Carter, W. P. L., et. al. (2000f): "Investigation of the Atmospheric Ozone Formation Potentials of Selected Glycol Ethers," Report to the Chemical Manufacturers Association Glycol Ethers Panel, in preparation.

Carter, W. P. L., D. Luo, and I. L. Malkina (2000g): "Investigation of the Atmospheric Ozone Formation Potentials of Selected Commercial Mixtures," Report to Exxon Chemical Company, in preparation.

Chang, T. Y. and S. J. Rudy (1990): "Ozone-Forming Potential of Organic Emissions from Alternative-Fueled Vehicles," Atmos. Environ., 24A, 2421-2430.

Christensen, L. K., T. J. Wallington, A. Guschin, and M. D. Hurley (1999): "Atmospheric Degradation Mechanism of CF_3OCH_3," J. Phys. Chem A, 4202-4208.

Christensen, L. K., J. C. Ball and T. J. Wallington (2000): "Atmospheric Oxidation Mechanism of Methyl Acetate," J. Phys. Chem. A, 104, 345-351.

Cox, R. A., K. F. Patrick, and S. A. Chang (1981): "Mechanism of Atmospheric Photooxidation of Organic Compounds. Reactions of Alkoxy Radicals in Oxidation of n-Butane and Simple Ketones," Environ. Sci. Technol. 15, 587.

Croes, B., California Air Resources Board Research Division, personal communication.

Dagaut, P. T. J. Wallington, R. Liu and M. J. Kurylo (1988a): 22nd International Symposium on Combustion, Seattle, August 14-19.

Dagaut, P., T. J. Wallington, R. Liu and J. J. Kurylo (1988b): "A Kinetics Investigation of the Gas-Phase Reactions of OH Radicals with Cyclic Ketones and Diones: Mechanistic Insights," J. Phys. Chem. 92, 4375.

Dimitriades, B. (1999): "Scientific Basis of an Improved EPA Policy on Control of Organic Emissions for Ambient Ozone Reduction," J. Air & Waste Manage. Assoc. 49, 831-838

Dodge, M. C. (1984): "Combined effects of organic reactivity and NMHC/NOx ratio on photochemical oxidant formation -- a modeling study," Atmos. Environ., 18, 1657.

Donaghy, T., I. Shanahan, M. Hande and S. Fitzpatrick (1993): "Rate Constant and Atmospheric Lifetimes for the Reactions of OH Radicals and Cl Atoms with Haloalkanes," Int. J. Chem. Kinet, 25, (4) 273-284.

Donahue, N. M. M. K. Dubey, R. Mohrschaldt, K. L. Demerjian, and J. G. Anderson (1997): "High Pressure Flow Study of the Reactions $OH+NO_x$ -> $HONO_x$: Errors in the Falloff Region," J. Geophys. Res.-Atmos.102, (D5) 6159-6168.

Eberhard, J. C. Muller, D. W. Stocker, and J. A. Kerr (1993): "The Photo-Oxidation of Diethyl Ether in Smog Chamber Experiments Simulating Tropospheric Conditions: Product Studies and Proposed Mechanism," Int. J. Chem. Kinet. 25, 630-649.

Eberhard, J., C. Muller, D. W. Stocker and J. A. Kerr (1995): "Isomerization of Alkoxy Radicals under Atmospheric Conditions," Environ. Sci. Technol. 29, 232.

EPA (1984): "Guideline for Using the Carbon Bond Mechanism in City-Specific EKMA," EPA-450/4-84-005, February.

Fantechi G, NR Jensen, J Hjorth, and J Peeters (1998): "Determination of the Rate Constants for the Gas-Phase Reactions of Methyl Butenol with OH Radicals, Ozone, NO_3 radicals, and Cl Atoms," Int. J. Chem. Kinet. 30, (8) 589-594.

Forster, R., M. Frost, D. Fulle, H. F. Hamann, H. Hippler, A. Schlepegrell, and J. Troe (1995): "High-Pressure Range of the Addition of HO to HO, NO, NO_2, and CO .1. Saturated Laser-Induced Fluorescence Measurements at 298 K," J. Chem. Phys. 103, (8) 2949-2958.

Ferronato C, Orlando JJ, and Tyndall GS (1998): "Rate Mechanism of the Reaction of OH and Cl with 2-Methyl-3-Buten-2-ol," J. Geophys. Res.-Atoms. 103, (8) 25579-25586

Gardner, E. P., P. D. Sperry, and J. G. Calvert (1987): "Photodecomposition of Acrolein in O_2-N_2 Mixtures," J. Phys. Chem. 91, 1922.

Gery, M. W., D. L. Fox, R. M. Kamens, and L. Stockburger (1987): "Investigation of Hydroxyl Radical Reactions with o-Xylene and m-Xylene in a Continuous Stirred Tank Reactor," Environ. Sci. Technol. 21, 339.

Gery, M. W., G. Z. Whitten, and J. P. Killus (1988): "Development and Testing of the CBM-IV For Urban and Regional Modeling,", EPA-600/ 3-88-012, January.

Grosjean and Grosjean (1994): Int. J. Chem. Kinet. 26, 1185.

Guenther, A., C. Geron, T.Pierce, B. Lamb, P. Harley, and R.Fall (2000): "Natural emissions of non-methane volatile organic compounds, carbon monoxide, and oxides of nitrogen from North America" Atmospheric Environment, 34, 2205-2230.

Hartmann, D., A. Gedra, D. Rhasa, and R. Zellner (1986): Proceedings, 4th European Symposium on the Physico-Chemical Behavior of Atmospheric Pollutants, 1986; D. Riedel Publishing Co., Dordrecht, Holland, 1987, p. 225.

Hatakeyama, S., N. Washida, and H. Akimoto, (1986): "Rate Constants and Mechanisms for the Reaction of OH (OD) Radicals with Acetylene, Propyne, and 2-Butyne in Air at 297 +/- 2 K," J. Phys Chem. 90, 173-178.

Jeffries, H. E., K. G. Sexton, J. R. Arnold, and T. L. Kale (1989): "Validation Testing of New Mechanisms with Outdoor Chamber Data. Volume 2: Analysis of VOC Data for the CB4 and CAL Photochemical Mechanisms," Final Report, EPA-600/3-89-010b.

Jeffries, H. E. (1991): "UNC Solar Radiation Models," unpublished draft report for EPA Cooperative Agreements CR813107, CR813964 and CR815779".

Jeffries, H. E. and R. Crouse (1991): "Scientific and Technical Issues Related to the Application of Incremental Reactivity. Part II: Explaining Mechanism Differences," Report prepared for Western States Petroleum Association, Glendale, CA, October.

Jenkin, M. E., R. A. Cox, M. Emrich and G. K. Moortgat (1993): "Mechanisms for the Cl-atom-initiated Oxidation of Acetone and Hydroxyacetone in Air," J. Chem. Soc. Faraday Trans. 89, 2983-2991.

Kelly, N. and J. Heicken (1978): "Rate Coefficient for the Reaction of CH3O with CH3CHO at 25° C," J. Photochem. 8, 83.

Kircher, C. C. and S. P. Sander (1984): "Kinetics and Mechanism of HO_2 and DO_2 Disproportionations" J. Phys. Chem. 88, (19) 2082-2091.

Kirchner, F. and W. R. Stockwell (1996): "Effect of Peroxy Radical Reactions on the Predicted Concentrations of Ozone, Nitrogenous Compounds, and Radicals," J. Geophys. Res. 101, 21,007-21,022.

Kirchner, F., F. Zabel and K. H. Becker (1992): "Kinetic Behavior of Benzoylperoxy Radicals in the Presence of NO and NO2," Chem. Phys. Lett. 191, 169-174.

Kirchner, F., L. P. Thüner, I. Barnes, K. H. Becker, B. Donner, and F. Zabel (1997): Environ. Sci. Technol. 31, 1801.

Kwok, E. S. C., and R. Atkinson (1995): "Estimation of Hydroxyl Radical Reaction Rate Constants for Gas-Phase Organic Compounds Using a Structure-Reactivity Relationship: An Update," Atmos. Environ 29, 1685-1695.

Kwok, E. S. C., R. Atkinson, and J. Arey (1995): "Observation of Hydrocarbonyls from the OH Radical-Initiated Reaction of Isoprene," Envrion. Sci. Technol. 29, 2467.

Kwok, E. S. C., S. Aschmann, and R. Atkinson (1996): "Rate Constants for the Gas-Phase Reactions of the OH Radical with Selected Carbamates and Lactates," Environ. Sci. Technol 30, 329-334.

Kumar, N., F. W. Lurmann, and W. P. L. Carter (1995), "Development of the Flexible Chemical Mechanism Version of the Urban Airshed Model," Report to California Air Resources Board, Agreement no. 93-716. Document No. STI-94470-1508-FR, Sonoma Technology, Inc. Santa Rosa, CA, August.

Langford, A. O, and C. B. Moore (1984): "Collision complex formation in the reactions of formyl radicals with nitric oxide and oxygen," J. Chem. Phys. 80, 4211.

Langer, S., E. Jjungstrom, I Wangberg, T. J. Wallington, M. D. Hurley and O. J. Nielsen (1995): "Atmospheric Chemistry of Di-tert-Butyl Ether: Rates and Products of the Reactions with Chlorine Atoms, Hydroxyl Radicals, and Nitrate Radicals, "Int. J. Chem. Kinet., 28, 299-306.

Lurmann, F. W., W. P. L. Carter, and R. A. Coyner (1987): "A Surrogate Species Chemical Reaction Mechanism for Urban-Scale Air Quality Simulation Models. Volume I - Adaptation of the Mechanism," EPA-600/3-87-014a.

Lurmann, F. W., M. Gery, and W. P. L. Carter (1991): "Implementation of the 1990 SAPRC Chemical Mechanism in the Urban Airshed Model," Final Report to the California South Coast Air Quality Management District, Sonoma Technology, Inc. Report STI-99290-1164-FR, Santa Rosa, CA.

Magnotta, F. and H. S. Johnston (1980): "Photo-Dissociation Quantum Yields for the NO_3 Free-Radical," Geophys. Res. Lett. 7, (10) 769-772.

Mellouki, A., R. K. Talukdar, A. M. R. P. Bopegedera, and C. J. Howard (1993): " Study of the Kinetics of the Reactions of NO_3 with HO_2 and OH," Int. J. Chem. Kinet. 25, (1) 25-39.

Majer, Naman, and Robb (1969): "Photolysis of Aromatic Aldehydes," Trans. Faraday Soc, 65 1846.

Mentel T.F., D. Bleilebens. and A. Wahner (1996): "A study of nighttime nitrogen oxide oxidation in a large reaction chamber - the fate of NO_2 , N_2O_5 , HNO_3 , and O_3 at different humidities." Atmos. Environ., 30, 4007-4020.

Middleton, P., W. R. Stockwell, and W. P. L. Carter (1990): "Aggregation and Analysis of Volatile Organic Compound Emissions for Regional Modeling," Atmos. Environ., 24A, 1107-1133.

Mineshos, G., and S. Glavas (1992): "Thermal Decomposition of Peroxypropionyl Nitrate –Kinetics of the Formation of Nitrogenous Products," React. Kinet. Catal. Lett. 45, (2) 305-312.

Muthuramu, K., P. B. Shepson and J. M. O'Brien (1993): "Preparation, Analysis, and Atmospheric Production of Multifunctional Nitrates," Environ. Sci. Technol. 27, 1117.

NASA (1994): "Chemical Kinetics and Photochemical Data for Use in Stratospheric Modeling, Evaluation Number 11," JPL Publication 94-26, Jet Propulsion Laboratory, Pasadena, California, December.

NASA (1997): "Chemical Kinetics and Photochemical Data for Use in Stratospheric Modeling, Evaluation Number 12," JPL Publication 97-4, Jet Propulsion Laboratory, Pasadena, California, January.

H. Niki, P. D. Maker, C. M. Savage, and L. P. Breitenback (1985): "An FTIR Study of the Cl-Atom-Initiated Reaction of Glyoxal," Int. J. Chem. Kinet. 17, 347.

NIST (1994): "NIST Standard Reference Database 25. Structures and Properties, Version 2.01," National Institute of Standards and Technology, Gaithersburg, MD 20899.

NIST (1998): "The NIST Chemical Kinetics Database, NIST Standard Reference Database 17 - 2Q98," National Institute of Standards and Technology, Gaithersburg, MD 20899.

Paulson, S. E., J. J. Orlando, G. S. Tyndall, and J. G. Calvert (1995): "Rate Coefficients for the Reactions of $O(^3P)$ with Selected Biogenic Hydrocarbons," Int. J. Chem. Kinet. 27, 997.

Pitts, J. N., Jr., K. Darnall, W. P. L. Carter, A. M. Winer, and R. Atkinson (1979): "Mechanisms of Photochemical Reactions in Urban Air," EPA-600/ 3-79-110, November.

Pitts, J. N., Jr., E. Sanhueza, R. Atkinson, W. P. L. Carter, A. M. Winer, G. W. Harris, and C. N. Plum (1984): "An Investigation of the Dark Formation of Nitrous Acid in Environmental Chambers," Int. J. Chem. Kinet., 16, 919-939.

Plum, C. N., Sanhuesa, E., Atkinson, R., Carter W. P. L. and Pitts, J. N., Jr. (1983): "OH Radical Rate Constants and Photolysis Rates of alpha-Dicarbonyls," Environ. Sci. Technol. 17, 479-484.

Porter, E., G. Locke, J. Platz, J. Treacy, H. Sidebottom, W. Mellouki, S. Teton, and G. LeBras. (1995): "Kinetics and Mechanisms for the OH Radical Initiated Oxidation of Oxygenated Organic Compounds," Workshop on Chemical Mechanisms Describing Oxidation Processes in the Troposphere, Valencia, Spain, April 25-28.

Roberts, J. M. and S. B. Bertman (1992): "The Thermal Decomposition of PeroxyAcetic Nitric Anhydride (PAN) and Peroxymethacrylic Nitric Anhydride (MPAN)," Int J. Chem. Kinet. 24, 297.

Rudich Y, R Talukdar, JB Burkholder, and AR Ravishankara (1995): "Reactions of Methylbutenol with Hydroxyl Radical – Mechanism and Atmospheric Implications," J. Phys. Chem. 99, (32) 12188-12194.

Rudich Y, RK Talukdar, RW Fox, and AR Ravishankara (1996): "Rate Coefficients for Reactions of NO_3 with a few Olefins and Oxygenated Olefins," J. Phys. Chem. 100, (13) 5374-5381.

Saunders, S. M., D. L. Baulch, K. M. Cooke, M. J. Pilling, and P. I. Smurthwaite (1994): "Kinetics and mechanisms of the reactions of OH with some oxygenated compounds of importance in tropospheric chemistry," Int. J. Chem. Kinet., 26, 113-130.

Schurath, U. and V. Wipprecht (1980): "Reactions of peroxiacycl radicals." Proc. 1st European Symp. On the Physico-Chemical Behavior of Atmospheric Pollutants, pp. 157-166. Commiss. European Commun.

Seefeld, S. and J. A. Kerr (1997): "Kinetics of the Reactions of Propionylperoxy Radicals with NO and NO_2: Peroxypropionyl Nitrate Formation under Laboratory Conditions Related to the Troposphere," Environ. Sci. Technol. 31, (10) 2949-2953

Shepson, P. B., E. O. Edney, and E. W. Corse (1984): "Ring Fragmentation Reactions on the Photooxidations of Toluene and o-Xylene," J. Phys. Chem. 88, 4122.

Shepson, P. B., E. O. Edney, T. E. Kleindienst, G. R. Namie and L. T. Cupitt (1985): "The Production of Organic Nitrates from Hydroxyl and Nitrate Radical Reaction with Propylene," Environ Sci. Technol., 19, 849.

Sidebottom, H. W., G. LeBras, K. H. Becker, J. Wegner, E. Porter, S. O'Donnell, J. Morarity, E. Collins, A. Mellouki, S. Le Calve, I. Barnes, C. Sauer, K. Wirtz, M. Martin-Revejo, L. Theuner and J. Bea (1997): "Kinetics and Mechanisms for the Reaction of Hydroxyl Radicals with $CH_3OCH_2OCH_3$ and Related Compounds," Final Report to Lambiotte & Cie, S.A., September.

Slagle, I. R., J.-Y. Park, and D. Gutman (1984): "Kinetics of polyatomic free radicals produced by laser photolysis. 3. Reactions of vinyl radicals with molecular oxygen," J. Mm. Chem. Soc. 106, 4356-4361.

Smith, D. F, T. E. Kleindienst, E. E. Hudgens, C. D. McIver and J. J. Bufalini (1991): "The Photooxidation of Methyl Tertiary Butyl Ether," Int. J. Chem. Kinet. 23, 907-924.

Smith, D. F, T. E. Kleindienst, E. E. Hudgens, C. D. McIver and J. J. Bufalini (1992): "Kinetics and Mechanism of the Atmospheric Oxidation of Ethyl Tertiary Butyl Ether," Int. J. Chem. Kinet. 24, 199-215.

Stemmler, K. D. J. Kinnison and J. A. Kerr (1996): "Room Temperature Coefficients for the Reactions of OH Radicals with Some Monoethylene Glycol Monoalkyl Ethers," J. Phys. Chem, 100, 2114.

Stemmler, K., W. Mengon and J. A. Kerr (1996): "OH Radical Initiated Photooxidation of 2-Ethoxyethanol under Laboratory Conditions Related to the Troposphere: Product Studies and Proposed Mechanism," Environ. Sci. Technol. 30, 3385-3391.

Stemmler, K. , Mengon, W. and J. A. Kerr (1997a): "Hydroxyl-Radical-Initiated Oxidation of Isobutyl Isopropyl Ether Under Laboratory Conditions Related to the Troposphere: Product Studies and Proposed Mechanism," J. Chem. Soc., Faraday Trans. 93, 2865-2875.

Stemmler, K. W. Mengon, D. A. Kinnison, and J. A. Kerr (1997b): "OH Radical Initiated Photooxidation of 2-Butoxyethanol under Laboratory Conditions Related to the Troposphere: Product Studies and Proposed Mechanism," Environ. Sci. Technol. 31, 1496-1504.

Stockwell, W.R. and J.G. Calvert (1983): "The Mechanism of the HO-SO_2 Reaction," Atmos. Envir., 17, 2231 - 2235.

Stockwell, W. R., P. Middleton, J. S. Chang, and X. Tang (1990): "The Second Generation Regional Acid Deposition Model Chemical Mechanism for Regional Air Quality Modeling," J. Geophys. Res. 95, 16343- 16376.

Stockwell, W.R., F. Kirchner, M. Kuhn, and S. Seefeld (1997): "A new mechanism for regional atmospheric chemistry modeling," J. Geophys. Res., 102, 25847-25880.

Takagi, H., N. Washida, H. Akimoto, K. Nagasawa, Y. Usui, and M. Okuda (1980): "Photooxidation of o-Xylene in the NO-H_2O-Air System," J. Phys. Chem. 84, 478.

Tsang, W.; and R. F. Hampson (1986): "Chemical kinetic data base for combustion chemistry. Part I. Methane and related compounds," J. Phys. Chem. Ref. Data 15, 1087.

Tsang, W (1987): "Chemical kinetic data base for combustion chemistry. Part 2. Methanol," J. Phys. Chem. Ref. Data 16, 471.

Tsang, W (1988): "Chemical kinetic data base for combustion chemistry. Part 3. Propane," J. Phys. Chem. Ref. Data 17, 887.

Tuazon, E. C., R. Atkinson, C. N. Plum, A. M. Winer, and J. N. Pitts, Jr. (1983): "The Reaction of Gas-Phase N_2O_5 with Water Vapor," Geophys. Res. Lett. 10, 953-956.

Tuazon E.C., R. Atkinson R. and W. P. L. Carter W.P.L. (1985): "Atmospheric Chemistry of cis- and trans-3-Hexene-2,5-dione,". Environ. Sci. Technol., 19, 265-269.

Tuazon, E. C., H. MacLeod, R. Atkinson, and W. P. L. Carter (1986): "Alpha-Dicarbonyl yields from the NO_x-air photooxidations of a series of aromatic-hydrocarbons in air," Environ. Sci. Technol. 20, (4) 383-387

Tuazon, E. C. and R. Atkinson (1989): "A Product Study of the Gas-Phase Reaction of Methacrolein with the OH Radical in the Presence of NO_x," Int. J. Chem. Kinet. 22, 591-602.

Tuazon, E. C., and R. Atkinson (1990): "Formation of 3-Methylfuran from the Gas-Phase Reaction of OH Radicals with Isoprene and the Rate Constant for its Reaction with the OH Radical," Int. J. Chem. Kinet., 22, 591.

Tuazon, E. C., W. P. L. Carter and R. Atkinson (1991a): "Thermal Decomposition of Peroxyacetyl Nitrate and Reactions of Acetyl Peroxy Radicals with NO and NO_2 Over the Temperature Range 283-313 K," J. Phys. Chem., in 95, 2434.

Tuazon, E. C., W. P. L. Carter, S. M. Aschmann, and R. Atkinson (1991b): "Products of the Gas-Phase Reaction of Methyl tert-Butyl Ether with the OH Radical in the Presence of NO_x," Int. J. Chem. Kinet., 23, 1003-1015.

Tuazon, E. C., S. M. Aschmann and R. Atkinson (1998a): "Products of the Gas-Phase Reactions of the OH radical with 1-Methoxy-2-Propanol and 2-Butoxyethanol," Environ. Sci. Technol., 32, 3336-3345.

Tuazon, E. C., S. M. Aschmann, R. Atkinson, and W. P. L. Carter (1998b): "The reactions of Selected Acetates with the OH radical in the Presence of NO: Novel Rearrangement of Alkoxy Radicals of Structure RC(O)OCH(O.)R"', J. Phys. Chem A 102, 2316-2321.

Tuazon, E., C., S. M. Aschmann, and R. Atkinson (1999): "Products of the Gas-Phase Reaction of the OH Radical with the Dibasic Ester $CH_3OC(O)CH_2CH_2CH_2C(O)OCH_3$," Environ. Sci. Technol., 33, 2885-2890.

Veillerot, M., P. Foster, R. Guillermo, and J. C. Galloo (1995): "Gas-Phase Reaction of n-Butyl Acetate with the Hydroxyl Radical under Simulated Tropospheric Conditions: Relative Rate Constant and Product Study," Int. J. Chem. Kinet. 28, 233-243.

Wallington, T. J. and M. J. Kurylo (1987): "Flash Photolysis Resonance Fluorescence Investigation of the Gas-Phase Reactions of OH Radicals with a Series of Aliphatic Ketones over the Temperature Range 240-440 K," J. Phys. Chem 91, 5050.

Wallington, T. J., P. Dagaut, R. Liu and M. J. Kurylo (1988a): "Rate Constants for the Gas Phase Reactions of OH with C_5 through C_7 Aliphatic Alcohols and Ethers: Predicted and Experimental Values," Int. J. Chem. Kinet. 20, 541.

Wallington, T. J., R. Liu, P. Dagaut, and M. J. Kurylo (1988b): "The Gas-Phase Reactions of Hydroxyl Radicals with a Series of Aliphatic Ethers over the Temperature Range 240-440 K," Int. J. Chem. Kinet. 20, 41.

Wallington, T. J., P. Dagaut and M. J. Kurylo (1988c): "Correlation between Gas-Phase and Solution-Phase Reactivities of Hydroxyl Radicals toward Saturated Organic Compounds," J. Phys. Chem. 92, 5024.

Wallington, T. J., P. Dagaut, R. Liu, and M. J. Kurylo (1988d): "The Gas Phase Reactions of Hydroxyl Radicals with a Series of Esters Over the Temperature Range 240-440 K," Int. J. Chem. Kinet. 20, 177.

Wallington, T., J., W. O. Siegl, R. Liu, Z. Zhang, R. E. Huie, and M. J. Kurylo (1990): "The Atmospheric Reactivity of à-Methyltetrahydrofuran," Env. Sci. Technol. 24, 1568-1599.

Wallington, T. J. and S. M. Japar (1991): "Atmospheric Chemistry of Diethyl Ether and Ethyl tert-Butyl Ether," Environ. Sci. Technol. 25, 410-415.

Wallington, T. J., J. M. Andino, A. R. Potts, S. J. Rudy, W. O. Siegl, Z. Zhang, M. J. Kurylo and R. H. Huie (1993): "Atmospheric Chemistry of Automotive Fuel Additives: Diisopropyl Ether," Environ. Sci. Technol. 27, 98.

Wallington, T. J., M. D. Hurley, J. C. Ball, A. M. Straccia, J. Platz, L. K. Christensen, J. Schested, and O. J. Nielsen (1997): "Atmospheric Chemistry of Dimethoxymethane ($CH_3OCH_2OCH_3$): Kinetics and Mechanism of Its Reaction with OH Radicals and Fate of the Alkoxy Radicals $CH_3CHO(\cdot)OCH_3$ and $CH_3OCH_2OCH_2O(\cdot)$," J. Phys. Chem. A, 101, 5302-5308.

Weaver, J.; J. Meagher, R. Shortridge, and J. Heicklen (1975): "The Oxidation of Acetyl Radicals," J. Photochem. 4, 341.

Wells, J. R., F. L. Wiseman, D. C. Williams, J. S. Baxley, and D. F. Smith (1996): "The Products of the Reaction of the Hydroxyl Radical with 2-Ethoxyethyl Acetate," Int. J. Chem. Kinet., 28, 475-480.

Wyatt, S. E., J. S. Baxley and J. R. Wells (1999), "The Hydroxyl Radical Reaction Rate Constant and Products of Methyl Isobutyrate," Int. J. Chem. Kinet. 31, 551-557.